Springer Theses
Recognizing Outstanding Ph.D. Research

Rosario Ruggieri

Speleological and Speleogenetic Aspects of the Monti di Capo San Vito (Sicily)

Influence of Morphotectonic Evolution

Springer

Springer Theses

Recognizing Outstanding Ph.D. Research

Aims and Scope

The series "Springer Theses" brings together a selection of the very best Ph.D. theses from around the world and across the physical sciences. Nominated and endorsed by two recognized specialists, each published volume has been selected for its scientific excellence and the high impact of its contents for the pertinent field of research. For greater accessibility to non-specialists, the published versions include an extended introduction, as well as a foreword by the student's supervisor explaining the special relevance of the work for the field. As a whole, the series will provide a valuable resource both for newcomers to the research fields described, and for other scientists seeking detailed background information on special questions. Finally, it provides an accredited documentation of the valuable contributions made by today's younger generation of scientists.

Theses are accepted into the series by invited nomination only and must fulfill all of the following criteria

- They must be written in good English.
- The topic should fall within the confines of Chemistry, Physics, Earth Sciences, Engineering and related interdisciplinary fields such as Materials, Nanoscience, Chemical Engineering, Complex Systems and Biophysics.
- The work reported in the thesis must represent a significant scientific advance.
- If the thesis includes previously published material, permission to reproduce this must be gained from the respective copyright holder.
- They must have been examined and passed during the 12 months prior to nomination.
- Each thesis should include a foreword by the supervisor outlining the significance of its content.
- The theses should have a clearly defined structure including an introduction accessible to scientists not expert in that particular field.

More information about this series at http://www.springer.com/series/8790

Rosario Ruggieri

Speleological and Speleogenetic Aspects of the Monti di Capo San Vito (Sicily)

Influence of Morphotectonic Evolution

Doctoral Thesis accepted by
the University of Nova Gorica, Slovenia

Springer

Author
Dr. Rosario Ruggieri
Alumni Club
University of Nova Gorica
Nova Gorica
Slovenia

Supervisor
Prof. Martin Knez
Karst Research lnstitute ZRC SAZU
University of Nova Gorica
Postojna
Slovenia

ISSN 2190-5053 ISSN 2190-5061 (electronic)
Springer Theses
ISBN 978-3-319-21719-2 ISBN 978-3-319-21720-8 (eBook)
DOI 10.1007/978-3-319-21720-8

Library of Congress Control Number: 2015946587

Springer Cham Heidelberg New York Dordrecht London

Printed on acid-free paper

Springer International Publishing AG Switzerland is part of Springer Science+Business Media
(www.springer.com)

Parts of this thesis have been published in the following journal articles:

Ruggieri R. Messina Panfalone D., Antonioli F., Rosso A., Sanfilippo R., Maniscalco R. 2012. The Rumena flank margin cave and its implication in support of the evolution of the Monti di Capo San Vito (North-western Sicily). *Rend. Online Soc. Geol. It*., Vol. 21 (2012), pp. 632–633, 3 figs.

Rosario Ruggieri, Giuseppe Napoli, Pietro Renda, 2013. Influence of the Plio-Pleistocene Tectonics on the evolution of the Purgatorio Polje (North-western Sicily). 2013 ICS Proceedings, Vol. 3, pp. 402–407.

Ilaria Maria D'Angeli, Joe De Waele, Rosario Ruggieri, Laura Sanna, 2013. Pleistocene sea level changes as revealed by flank margin caves in telogenetic limestones in Sicily and Sardinia (Italy). 2013 ICS Proceedings Vol. 3, pp. 29–33.

Rosso A., Sanfilippo R., Ruggieri R., Maniscalco R. and Vertino A., 2014. Exceptional record of submarine cave communities from the Pleistocene of Sicily (Italy). DOI 10.1111/let.12094 © 2014 Lethaia Foundation. Published by John Wiley & Sons Ltd.

Ruggieri R. & De Waele J., 2014. Lower to Middle Pleistocene Flank Margin Caves at Custonaci (Trapani, NW Sicily) and their relation with past sea levels. Acta Carsologica 43/1, 11–22, Postojna 2014.

I dedicate this work to my wife Iolanda who has been walking with me the inscrutable paths of this life, sharing the passion for the magic world of the caves, and also for encouraging me to carry out the karst story here presented.

I also want to dedicate it to my small always smiling grandchild Rosario hoping that one day he might like to go across the exciting underground world.

Supervisor's Foreword

Initially this study started with the aims of seeking the relationship between the tectonic evolution and the karst processes in the Trapani mountains, in the extreme north-west of Sicily, an exceptional karst context for the unique variety and richness of forms, both surface and underground. Then this study underwent an unexpected surge, well ahead of expected expectations, with the results of two important discoveries that have allowed it to extend the framework of knowledge on the speleogenesis of the study area and its interaction with the paleoclimatic factors.

The discovery of caves considered of marine origin, present along the relict paleo-cliffs of the study area, which originated with *flank margin cave* mechanisms, was the first element that has expanded the geographical presence of this speleogenetic phenomenology, found and studied in tropical environments, but so far detected in the Mediterranean only in some conglomeratic formations in Croatia. These morphologies, certainly interesting, for the "hypogenic connotations", as described by the author, are more directly related to ancient marine levels, than to the epigenic caves. But this element, although important, alone would definitely not have added more insights into the evolution of the karst processes along the coastal belt, unless in this research the second and most important discovery concerning the extraordinary fossil content of marine organisms and of speleothems had not happened with evidence of different stages of ingression and regression of the sea, in the *flank margin caves* Grotta Rumena.

With this further element the scientific findings of this study have embraced a broader Mediterranean context than the study area of the Capo San Vito Mountains, for different aspects of research related to the elements encountered, and the paleoclimate implications and of change of sea level during the Pleistocene age.

Therefore, this research and its discoveries will surely activate, as indeed in some respects has already happened, a whole series of paleontological and paleoecologycal investigations on the communities of submerged caves, for the widespread deposits of marine fossils, and on the paleogeography linked to the paleoclimatic and sea levels changes, as well as the tectonic implications, during the Pleistocene in the central Mediterranean. Remarkable changes etched on the walls and speleothems in the Grotta Rumena, thanks to this study, have been protected and established as a geosite of worldwide importance.

Postojna, Slovenia
July 2015

Associate Professor Martin Knez
univ. grad. eng. geology

Acknowledgments

I would like to thank Prof. Dr. Andrej Kranjc, Prof. Dr. Martin Knez and Prof. Dr. Tadej Slabe, head of the Karst Research Institute of the Scientific Research Centre at the Slovene Academy of Sciences and Arts, who have given me the opportunity to write this thesis.

My mentors were Prof. Dr. Stanka Šebela and Prof. Dr. Ugo Sauro. I thank both of them for their constructive suggestions during the field excursions carried out in the study area, their support and supervision of the thesis.

I thank Prof. Jo De Waele, for his suggestions during some field excursions in the area of study and in some caves, and for his supervision of the work.

Finaly, I thank geom. Davide Messina Panfalone member of CIRS, my caving association, for his help on the topographic survey of several caves considered in this study.

This doctoral study is partly co-financed by the European Union and by the European Social Fund respectively. The co-financing is carried out within the Human resources development operational programme for the years 2007–2013, 1. developmental priorities: Encouraging entrepreneurship and adaptation; preferential directives 1.3: scholarship schemes.

Photos of the present study were made by the author with the exception of photos Fig. 6.47 taken by Prof. Ugo Sauro, Figs. 6.68, 6.237, 6.239, 6.253, 6.328, 8.6 and 8.7 taken by Davide Messina Panfalone.

Contents

Chapter 1
Introduction

1.1 Importance of the Study Area

The area of research is in the extreme north-west of the island of Sicily (Fig. 1.1) and forms part of the mountain range of Trapani. It is bound, to the north, by the Tyrrhenian Sea, to the west, by the Gulf of Cofano, to the east, by the Gulf of Castellammare and to the south by the Guidaloca and Forgia streams.

The orography of the area, which is predominantly mountainous, consists of a system of ridges, usually ranged NW-SE, separated by structural depressions. Along the sea, the study area is characterized by narrow to medium coastal extension strips. From a geological point of view, this territory displays evidence of a complex morpho-structural context, derived from deformations and overthrusting induced during the Sicilian-Appennine-Maghrebian orogenesis. The latter began in the Upper Oligocene period, and endured through successive Plio-Pleistocene extensional transcurrent neotectonic phases linked to the evolution of the southern Tyrrhenian margin.

The prevalently carbonatic nature of the area and the structural discontinuities present due to the diverse orogenic and neotectonic phases that the area has undergone, have all favoured, guided and controlled the development of widespread and important karst phenomena. These can be observed on the surface in an extremely variegated range of morphologies ranging from micro to macro in dimension, and underground in the form of numerous caves, mostly vertical, all of which are decorated by diffuse calcite deposits.

The study area comprehends two municipalities: San Vito Lo Capo and Custonaci. The latter community is the centre of the second most important Italian marble industry (after Carrara, in Tuscany). This commercial activity, which has had deleterious effects on the general environment, has also negatively affected the karst phenomena of the area. The numerous quarries have not only already destroyed many areas but also threaten caves of particular scientific and aesthetic interest in neighbouring exploitation zones. Hence, there is an urgent need to

R. Ruggieri, *Speleological and Speleogenetic Aspects of the Monti di Capo San Vito (Sicily)*, Springer Theses, DOI 10.1007/978-3-319-21720-8_1

Fig. 1.1 Location of the study area

protect the surface and underground karst morphologies both from physical degradation and, particularly, from the problems related to pollution of the aquifers. The latter are especially vulnerable to waste generated by these quarries together with other contaminating material.

In this context, it is imperative to stress the conservation value of these carbonate formations. Especially those morphologies that originate from erosive/corrosive processes and that evolve inside peculiar geostructural context. In view of this, the study and analysis of certain karst morphologies (e.g. vadose/phreatic, sea paleo-notch, speleothems with lihtophagic holes, paleokarst fillings), can provide information on past geological and paleogeographical contexts, such as orogenic deformative phases and neotectonic and eustatic events.

1.2 Goals of the Thesis

The objective of this study is to encompass the karst processes that have developed in the Monti di Capo San Vito in the context of the morpho-tectonic evolution of the area. The aim is to understand the possible relation between the Plio-Pleistocene and present tectonic phases and the karst morphogenetic and speleogenetic processes that have evolved in this particular area of the Apenninic-Maghrebian chain.

As a result, the goals of the present research have been to establish the following:

1. Characterization of the karst morphologies (surface and underground)
2. Tectonic structural control in the karstification process
3. Influence of morpho-tectonic evolution and climate change on the speleogenesis.

1.3 Methodology

The research that is presented in the following thesis has been structured in two main sections:

(a) The first part describes the main physical, geomorphological, hydrographic, geological and hydrogeological characteristics of the research area.
(b) The second part has been divided in a number of subsections, mainly:

- *Karst geomorphological features*
  This chapter is subdivided in two main parts:
  The main surface karst morphologies classified according to both genetic and morphological criteria are presented in the first part while in the second part the main caves that have been explored and surveyed in the study area by the author are described from a structural and morphological point of view.
- *Structural geological analysis of the karst surface*
  In this chapter the structural surveys carried out in the research area are described and analyzed. The aim is to define the tectonic controls on the speleogenetic processes mentioned before. In this context, the structural data and kinematic evidence surveyed at the surface are compared with those obtained from the various caves. From this comparison, the main tectonic deformations are correlated to the caves located in the four zones in which the area of study has been sub-divided.
- *Results and discussion*
  In this last chapter, based on the structural and morphological karst data analyzed, a model of the speleogenetic evolution of the main karst structures in the study area is formulated and presented. These structures are represented in the coastal zone by the karst caves Grotta del Fantasma and Grotta Rumena, and, inland, by the karst system Polje di Purgatorio-Dolina della Bufara. The model shows evidence of the influence of the morpho-tectonic evolution on the speleogenesis of the above mentioned karst system during the Plio-Pleistocene.

In conclusion, the main outcomes of this research, which have enabled a better understanding of the geological and paleoclimatic characteristics of the study area, are illustrated.

Chapter 2
Research Area

2.1 Physical Geography

The area under study is situated in the northern part of the Monti di Trapani in the extreme north-west of Sicily: it is bordered to the south by the hills enclosing the towns of Trapani and Castellammare del Golfo and, to the east and west, by the Tyrrhenian Sea (Fig. 2.1). The territory is predominantly mountainous and its orographic profile is characterized by the following system of reliefs:

(a) the Mt. Sparagio ridge mainly oriented WNW-ESE, which, at 1,110 m asl, is the highest point in the Monti di Trapani;
(b) the NW-SE ridges of Mt. Palatimone–Mt. San Giovanni with their respective maximum peaks of 595 and 455 m asl and Mt. Cofano, which reaches an altitude of 657 m; and
(c) the Mt. Monaco–Mt. Speziale ridges, oriented towards the N-S and with peaks of 532 and 943 m asl respectively.

There are also some separate elevations within the Mt. Sparagio mountain system: the Prima Colma (1,007 m asl), the Colma di Mezzo (1,001 m asl), the Pizzo Bufala (861 m asl) and the Pizzo di Giacolamaro (791 m asl). Lesser elevations worth noting are the NW-SE Pizzo Corvo–Cozzo Pignatello, with peaks of 334 and 295 m asl; the complex of Rocca Rumena–Monte Bufara (323 m asl)—Mt. Zimmaria (315 m asl), which is elongated in the direction of NE-SW and the small isolated elevation of Cozzo Cataruccia (279 m asl). There are areas of plain or semi-plain land in the more extended Purgatorio plain, where heights above sea level range from 240 to 290 m. Similar topography is also to be found in: (a) the areas of Piano Zubbia–Scaletta–Assieni–Piano dei Tribli, with elevations from 180 to 240 m asl; (b) the Cornino plain in the stretch of land from 0 to 100 m asl and bordered to the S-W by the Forgia stream, to the N-E by the slopes of Mt. Cofano, to the east by the rocky cliffs of Scurati–Cerriolo–Rocca Rumena and to the west by

R. Ruggieri, *Speleological and Speleogenetic Aspects of the Monti di Capo San Vito (Sicily)*, Springer Theses, DOI 10.1007/978-3-319-21720-8_2

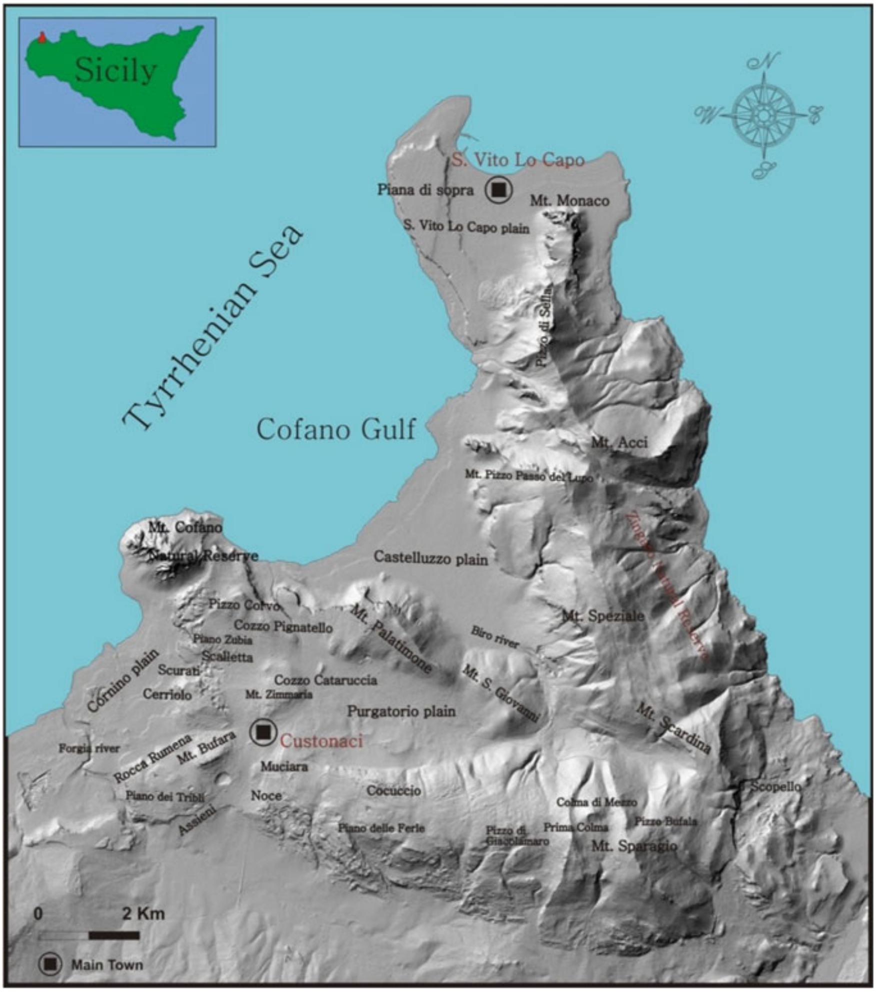

Fig. 2.1 General map of the study area Mt. di Capo San Vito (*Hillshade map from* DEM Regione Siciliana 2007–2008)

the sea; (c) the Castelluzzo plain, situated along a strip of terrain ranging from 0 to 130 m asl; and (d) the Piana di Sopra di San Vito, in the northernmost sector of the area, having altitudes ranging from 60 to 80 m asl. Plain-like zones or mildly undulating topography, less extensive than the ones described above, are also found in the Mt. Sparagio mountain system, in the Le Colme locality (920–900 m asl), Giacolamaro, Piano delle Ferle, Coccuccio and Muciara–Noce areas. From an environmental point of view the discussed territory is of extreme importance both for its natural beauty and for the biodiversity of its flora and fauna. This is further demonstrated by the fact that this area includes two of the most important Sicilian

Nature Reserves: (i) The Riserva Naturale Orientata dello Zingaro and (ii) the Riserva di Monte Cofano. However, the zone also includes the second most important marble quarrying industry in Italy, located at Custonaci which, although providing welcome local employment, has certainly brought about a general and serious degradation of the natural environment, as well as interfering with the karst features located in the quarried area.

2.2 Geomorphological Features

The main karst features, the focus of this research, are a constituent part of the general geomorphological context of the territory and traceable to different morphogenetic processes. In particular, six major areas of different landforms were recognized (Agnesi et al. 2002), all of which are described in the next chapters (Fig. 2.1).

2.2.1 Coastal Areas

These areas (Cornino, Castelluzzo and S. Vito Lo Capo plains) are characterized by a series of marine terraces, consisting of platforms at different levels, and formed by the abrasion of sea water. The terraces are, sometimes covered by continental or marine deposits and separated from each other by modestly sized banks and irregular cliffs. They have been carved by sea-notches, or more frequently, by shelters and caves, both of marine and karst in origin and reworked by hyperkarst marine processes (Antonioli et al. 1993; Antonioli and Ruggieri 2000; Ruggieri 2009; Ruggieri and Messina Panfalone 2011). Altogether seven orders of marine terraces have been observed at altitudes between about 95–105 m (I order) and 1–5 m (VII order) (Di Maggio et al. 1999).

At higher levels (200–225 m asl) the presence of other marine platforms in the Triassic-Liassic substrate has been observed. As far as the dating is concerned, the succession of the terraces has been formed after the Late Lower Pleistocene since the features are cut into deposits attributable to that period, whereas those at higher levels are, as a result, coeval or older than the Lower Pleistocene. The VI order terrace is datable to the Euthyrrhenian because of the presence of *Strombus bubonius* deposits, while the VII order terrace was cut into the previous order and is therefore younger and should presumably be considered ‘Neotyrrhenian’. The presence of faunal remains relating to the *Elephas falconeri* type in the sedimentary deposits of the order II terrace, bears witness to a date older than 250 or 350 thousand years, but probably earlier than 750 or 850 thousand. The changes of levels of the inner margins belonging to the same terrace order, show differential movements in the different sectors, with a range of uplift of about 0.11–0.14 m/kyr for the Middle to Late Pleistocene and 0.01–0.1 m/kyr for the post Eutyrrhenian period (Di Maggio et al. 1999; Antonioli et al. 1999a, b, 2002).

2.2.2 The Mt. Sparagio Ridge

Monte Sparagio is a ridge formation of Mesozoic carbonate rocks that develops in a WNW-ESE direction and reaches a peak of 1,110 m asl, the highest point in the Capo San Vito mountain system. Along the northern face, a large fault slope is visible, while the southern side is characterized by an eastern sector exhibiting structural slopes and a western sector constituted by an upper slope and by numerous other fault scarps. The summit areas (situated at altitudes from 190 to 900 m asl) consist of steps of more or less flat surfaces, probably formed by erosion during the ‘planation’ in the continental phase. Both the flat areas and the slopes, as will be described in the sections to follow, are of particular interest for their various karst morphologies, such as karren, dry valleys and deep fluviokarst canyons.

2.2.3 The Mt. Palatimone Ridge

This ridge constitutes a *cuesta* monocline relief of Mesozoic dolomite extending NW-SE and with a southern side that links up with a structural slope. In its northernmost sector the slope was eroded by the Pleistocene sea and a cliff was created. Along its southern parts, the structural slope seems to have come apart and retreated back due to phenomena of both erosion and karst corrosion caused by the flooding phases of the Purgatorio polje described hereunder. This area shows a vast amount of surface karst morphologies, particularly along the southern structural slope together with numerous vertical caves located on both sides of the ridge.

2.2.4 The Purgatorio Plain

This area consists of a large depression, including a relict polje. This landform was formed, not only due to selective processes resulting from the presence of clay and karst soluble terrains in the area between the carbonate outcroppings of Mt. Sparagio and Mt. Palatimone but also as a result of tectonic processes pointed out by systems of faults. To the south-west of Mt. Palatimone small monocline and relict relief features are to be found, all resulting from karst processes. This depression, which is opened with a deep fluviokarst gorge along its north-west margin, is particularly karstified with surface and underground morphologies, many of which are among the most interesting in the area.

2.2.5 The Mt. Acci–Pizzo di Sella Ridge

The Pizzo di Sella-Mt. Acci ridge extends as a large anticline, of which the fold-back axis plunges first N-S at Pizzo di Sella, then progressively verges NW-SE and finally E-W towards Mt. Acci. The eastern flank of this ridge/anticline consists of a large fault slope, while the western flank is made up of a series of recumbent folds, the partial erosion of which has brought to light an alternation of hard and soft rocks. In this area the enormous energy involved in uplifting has led to selective erosion processes with carbonate rock scarps affected by collapses, and clay denudation surfaces ruined by landslides.

2.2.6 The Mt. Speziale–Mt. Scardina Ridge

These areas are prevalently made up of Upper Triassic dolomitic rocks and are essentially characterized by two types of landscape: (a) the summit areas where ancient relict forms have been preserved and (b) the slopes where the processes of degradation and denudation predominate.

The area between Mt. Speziale and Mt. Scardina is dominated by some depressions, which extend NNW-SSE at altitudes between 600 and 900 m asl. These surfaces have been initially dislocated by tectonic movements (responsible for the formation of scarps and faults) and afterwards been karstified forming uvala landforms. This area, particularly on the eastern slope, is marked by deep canyons, which have originated during the tectonic uplift (with block-faults) and with the consequential lowering of the erosional base level.

2.2.7 The Mt. Cofano Area

The Mt. Cofano relief is surrounded by extensive fault slopes and abandoned cliffs along its southwestern side. The latter have been intensely subject to processes of physical rock disintegration with the accumulation of modern and ancient debris.

2.2.8 The Scopello Area

The overlapping of carbonate rocks (display a fragile behavior) onto pelagic deposits (have a plastic behavior) allowed for the genesis of deep-seated gravitational slope deformations (DPGV) (Agnesi et al. 1984, 1987, 1989, 1995, 2000, 2002), which are particularly evident in the Scopello area (Agnesi et al. 1987). The result of these processes is an extremely jagged landscape with extensive detached scarps subject to collapse or overturning, large unattached blocks prone to movement and deep trenches, sometimes open and sometimes filled with detritus.

References

Agnesi V, Macaluso T, Monteleone S, Pipitone G (1984) Fenomeni di deformazione gravitativa profonda (deep-seated gravitational slope deformations) osservati nella Sicilia occidentale. Boll Soc Geol It 103:671–679

Agnesi V, Macaluso T, Pipitone G (1987) Ruolo delle deformazioni gravitative profonde nell'evoluzione geomorfologica dell'area di Scopello (Trapani). Boll Soc Geol It 106:231–238

Agnesi V, Macaluso T, Monteleone S, Pipitone G, Sorriso-Salvo M (1989) Tipi e dinamica delle deformazioni gravitative profonde in relazione alle strutture geologiche. I casi di Monte Genuardo e di Scopello (Sicilia occidentale). Boll Soc Geol It 108:379–389

Agnesi V, Di Maggio C, Macaluso T (1995) Deformazioni gravitative profonde e superficiali nella penisola di Capo San Vito (Sicilia occidentale). Mem Soc Geol It 50:11–21

Agnesi V, Di Maggio C, Macaluso T, Rotigliano E (2000) Genesis and evolution of Deep Seated Gravitational Slope Deformation phenomena in Western and Central Sicily. Mem Soc Geol It 55:363–371

Agnesi V, Di Maggio C, Macaluso T, Madonia G, Rotigliano E (2002) Schema geomorfologico della Penisola di Capo San Vito (Sicilia nord-occidentale). Speleologia Iblea 10:37–47

Antonioli F, Ferranti L, Sottosanti G (1993) Le grotte sommerse della Riserva dello Zingaro. Speleologia n. 29:36–42

Antonioli F, Cremona G, Immordino F, Puglisi C, Romagnoli C, Silenzi S, Valpreda E, Verrubbi V (1999a) Quaternary and Holocene differential movements in a mediterranean coastal area (San Vito Lo Capo, Sicily-Italy). Phys Chem Earth 68

Antonioli F, Cremona G, Puglisi C, Silenzi S, Valpreda E, Verrubbi V (1999b) Quantitative assessment of post Tyrrenian differential crustal movements in a Mediterranean coastal area (San Vito Lo Capo, Sicily-Italy). Phys Chem Earth (A) 24(4):343–347

Antonioli F, Cremona G, Immordino F, Puglisi C, Romagnoli C, Silenzi S, Valpreda E, Verrubbi V (2002) New data on the Holocenic sea-level rise in NW Sicily (Central Mediterranean Sea). Glob Planet Change 34:121–140

Antonioli F, Ruggieri R (2000) Geomorfologia e speleogenesi nell'area carsica di Monte Palatimone (Custonaci Tp) ed interconnessioni con il livello di base marino. Speleologia Iblea 8:213–223

DEM Regione Siciliana. Modello digitale del terreno passo 2 m derivato da dati LIDAR volo ATA 2007–2008 in UTM-WGS84 fuso 33 N

Di Maggio C, Incandela A, Masini F, Petruso D, Renda P, Simonelli C, Boschian G (1999) Oscillazioni eustatiche, biocronologia dei depositi continentali quaternari e neotettonica nella Sicilia nord-occidentale (Penisola di San Vito Lo Capo - Trapani). Il Quaternario 12(1):25–49

Ruggieri R (2009) Karst Itinerary and cave discovery in the Zingaro Reserve. Azienda Foreste Demaniali. Priulla, Palermo, pp 207

Ruggieri R, Messina Panfalone D (2011) Dentro e fuori la montagna. Priulla, Palermo, pp 182 www.google.com/intl/it/earth/index.html

Chapter 3
Hydrographic Aspects

3.1 Climatic Aspects

The climatic conditions that characterize the area under study can be deduced from the general situation determined for the whole territory of the Province of Trapani. These have been based on the statistical elaboration of rainfall and temperature data referring to the years 1965–1994 (AA 1998) and collected at meteorological stations (Fig. 3.1). As far as temperature data is concerned the observations that were carried out made it possible to distinguish two large distinct areas: (a) a coastal area including those internal zones closest to it with an average annual temperatures of 18–19 °C; and (b) another comprising the more hilly parts with an average annual temperature of 17 °C. With regard to rainfall, the overall average annual precipitation for the Province of Trapani was 545 mm. Within the area, three macro areas can be further distinguished: (i) a coastal area with an average annual rainfall between 450 and 500 mm; (ii) an intermediate zone with values of 500–600 mm; and (iii) an internal hilly area and the coastal highlands with average annual rainfall ranging between 600 and 680 mm. If the climatic classification indices of De Martonne (1926) and Thornthawaite (1948) were to be applied, the territory under study would be classified as a temperate-hot/dry sub-humid area/region for the internal hilly areas, and semi-arid for the remaining areas (AA 1998).

3.2 Elements of Hydrology

3.2.1 Streams

There are two streams that cut through the research area both in the central part and also its southern side (Fig. 3.2). The former is the Biro stream whose basin is limited, in its intial stages of flow, by a superficial watershed passing through Piano

R. Ruggieri, *Speleological and Speleogenetic Aspects of the Monti di Capo San Vito (Sicily)*, Springer Theses, DOI 10.1007/978-3-319-21720-8_3

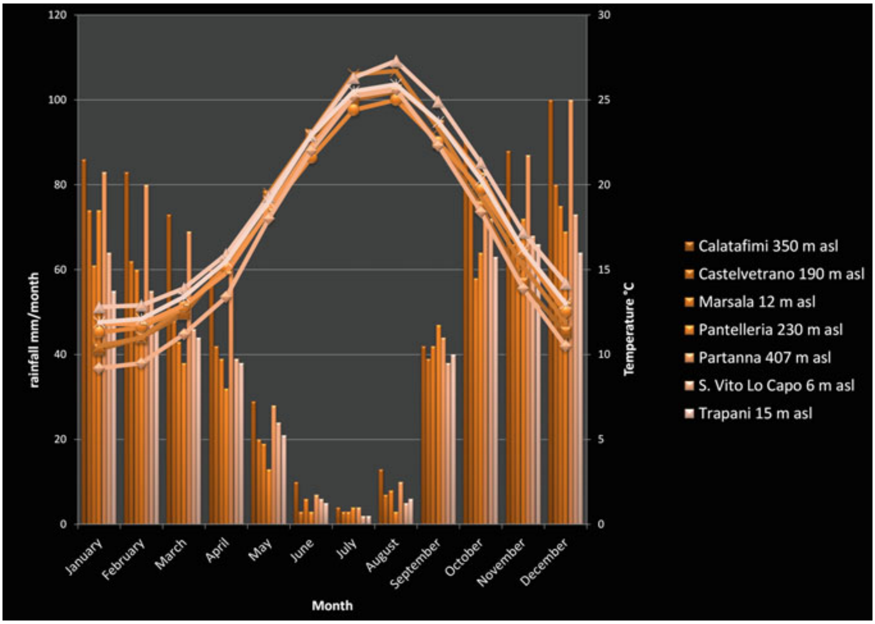

Fig. 3.1 Diagram of the average monthly rainfall—temperatures (1965–1994) of the metereological stations sited in the Trapani province (AA 1998)

dell'Arena. This is a linking sector between the aforementioned ridges, which flows, on average, from the east-south-east to the west-north-west along the southern sector of the Castelluzzo plain until it meets the Golfo di Cofano. The Biro flows and cuts, for approximately half of its length (about 8 km), through the Mesozoic carbonate series. For its remaining course reaching the sea, it cuts into the Lower Pleistocene calcarenites of the Castelluzzo plain. The fact that it flows parallel to the fault slope of the Mt. Palatimone ridge brings into question whether a certain control has been exercised by this structure on its development. The evolution of the stream, in any case tied to the depression of the Castelluzzo plain, has been affected by regular tectonic upliftings and by eustatic phases that have interested the plain beginning from the end of the Lower Pleistocene. The second, the Forgia stream, runs from SE to NW for about 15 km reaching the Tyrrhenian sea. It borders the southern part of the study area, for most of its length, into Tortonian clay terrains. In other areas, the Forgia stream cuts into outcroppings that are initialy basaltic then change to limestones (Mesozoic) in the final part along of the Cornino plain.

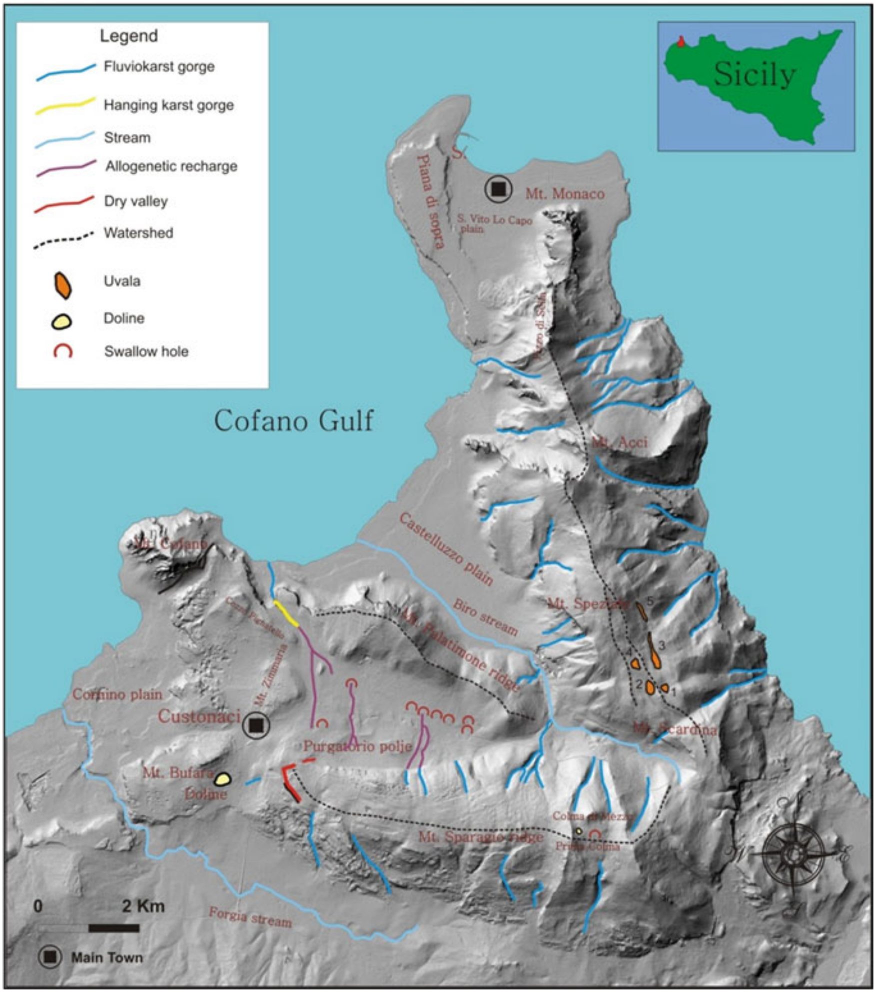

Fig. 3.2 Map of the study area with the main hydrographic features (*Hillshade map from* DEM Regione Siciliana 2007–2008)

3.2.2 Springs

The vast majority of springs located in the study area led back to sources that emerge along the coastal belt, the only exception being a small discharge spring sited in the upper part of the basin of the Biro stream. Some springs of limited discharge are present along the shoreline of the Cornino coastal belt, drained from the biocalcarenites of the Lower Pleistocene, which constitute a shallow porous aquifer whose action is tied to the state of the seasonal rains. A certain number of submerged marine springs, present along the coastal belt of the Zingaro Reserve, are of greater importance in terms of discharge. These drain deep karst aquifers in the dolomite and dolomitic limestones of the Upper Triassic–Lower Liassic and are characterized by flow in conduits and karst caves sited at variable depth from a few meters to about 30 m below sea level (Cassinis 1967; Cassa per il Mezzogiorno 1976; Bartolomei et al. 1983).

3.3 Hydrographic Network

The landforms that characterize the hydrographic network in the research area can be subdivided into the following categories:

1. Fluviokarstic canyons
2. Fluviokarstic gorges
3. Dry valleys
4. Poljes
5. Uvalas
6. Dolines
7. Swallow holes

3.3.1 Fluviokarstic Canyons

The canyons present in the study area are located on the slopes of the mountain ridges and can be clearly seen as deep cuts in the landscape. These usually trending NNW-ENE, E-W and NE-SW on the eastern slopes of the Mt. Monaco-Speziale-Scardina ridges (Figs. 3.2 and 3.3–4) with lengths extending from 800 m to 2,600 m and slopes ranging in interval of 20–40 %. The NNE-SSW, NNW-SSE and N-S orientations on the slopes of Mt. Sparagio (Figs. 3.2 and 3.3–4), have lengths varying between 300 and 1,000 m and slopes ranging in the interval of 25–35 %. The above mentioned canyons, cut into Mesozoic dolomite and dolomitic limestone terrains, are mainly aligned along fault lines. The evolution of these deep cuttings has been tied to the deformation tectonic phases and to the uplifting of the ridges, which started at the end of the Miocene and is still active up to the present day.

3.3.2 Fluviokarstic Gorges

A deep narrow gorge cutting into the Upper Jurassic–Lower Cretaceous calcarenites along a tectonic structure oriented NNW-SSE, is located in the extreme north-western sector of the Purgatorio plain, in the Cipollazzo area. The gorge

Figs. 3.3–4 Canyons in the Zingaro Reserve (*left photo*) and in the Sparagio north-eastern slope (*right photo*) (from Google Earth)

develops for about 550 m with an average topographic slope of about 22 %, a width ranging from 4 to 8 m and by vertical walls of about 20–30 m in height. Along its longitudinal axis several morphological steps and swallow holes are present, with giant potholes at the bottom. In particular, about half way down on the right bank, a sink cave known as the "Abisso delle Gole" opens up a few meters above the bed. According to the records, this cave has been explored to a depth of about 140 m. The gorge constitutes the only outlet of the polje, with a spectacular 2 m opening downflow hanging about 40 m above the Castelluzzo plain (Figs. 3.2, 3.5 and 3.6).

Fig. 3.5–6 Cipollazzo gorge outlet (*left photo*) of the Purgatorio polje (from Google Earth) and its final downflow part 40 m above the Castelluzzo plain (*right photo*)

3.3.3 Dry Valleys

These are present in the westernmost part of the Purgatorio polje, in the Muciara area and sited in two contiguous sectors separated by a structural high (Figs. 3.2 and 3.7). The paleovalley located in the western sector is made up of two branches, both separated by a structural high. The longest, with altitudes varying between 314 and 345 m asl, is about 720 m long and with an average width of 90 m. It stretches in a NNW-SSE direction and is bordered by sub-vertical carbonate walls that are 10 m high on the eastern side and about 5 m high on the western side. The minor branch, with an elevation ranging from 354 and 357 m asl, is about 390 m long and 50 m wide. This ancillary branch is bordered by lower slopes approximately 5 m in height and stretches in a NW-SE direction. Basaltic terrains outcrop on the bed of both of the depressions. The paleovalley located along the eastern sector is about 400 m long and has a width of about 90 m in its initial stages, which decreases to

Fig. 3.7 Dry valleys in the High Muciara sector (from Google Earth)

approximately 50 m towards its higher end. It is bordered by rocky slopes reaching, on average, 5 m in height, with outcrops of clay terrains on the bed. The valley ranges in elevation 340 and 360 m and follows a WSW-ENE direction.

As will be discussed in the subsequent chapters, the aforementioned landforms show a genesis and evolution strictly controlled by the Pleistocene wrench tectonics accompanied by karstification processes.

3.3.4 Poljes

A large polje type depression occupies the Purgatorio plain in the western sector of the study area. It is located between the Mt. Palatimone–Mt. S. Giovanni ridge to the north, and Mt. Sparagio to the south (Fig. 3.2). It extends for 4 km over a triangle shape of about 6.4 km^2. The polje has a perimeter of c. 16 km and an average width of 800 m with a maximum width of 1,700 m on its eastern side and an elevation of 225–300 m asl.

The hydrographic network in the depression is somewhat limited as a result of the diffuse karstification present, especially, in the polje sector. In this case, during the phases of seasonal full flow, the concentrated runoff that starts from the canyons on the northern slopes of the Mt. Sparagio ridge, is captured by numerous swallow holes sited in a narrow strip at the contact between the Lower Pliocene calcarenite outcrops and the Mesozoic limestones outcropping in the area of the polje and of the contiguous pediment. This hydrographic network is therefore principally entirely constituted of three shallow cuts, with lengths ranging between 1 and 1.5 km, and running from south to north on Tortonian clay terrains. A fourth shorter cut, about 500 m in length, runs from south-east to north-west in direction of the aforesaid gorge.

3.3.5 Uvalas

The depressions classified as uvalas in this study (Čalić 2011; Sauro 2012) (even if the dimensions are in general smaller than the typical uvalas) and whose genesis is described in Sect. 6.1, are present in the summital part of the Mt. Speziale ridge, in the Pianello area. They extend in a NNW-SSE direction and are bordered by slope faults which are probably linked to deep-seated gravitational slope deformations (DPGV) (Agnesi et al. 1984, 1989, 1995), and subsequent karst solution processes. These depressions can be described as follows (Figs. 3.2 and 3.8).

- Uvala N. 1 of sub-triangular shape has an area of 17,085 m^2 and extended along a N 326° direction. It stretches for about 170 m and is approximately 133 m width. The elevation of the bottom is 581 m and maximum elevation along the western slope reaches 616 m while that of the eastern slope is 688 m.

Fig. 3.8 Uvala landforms in the Pianello area of the Zingaro Reserve (from Google Earth)

The altitude along the northern slope reaches a maximum of 611 whereas that of the southern slope is 595 m.

- Uvala N. 2 is located to the west of the Uvala N. 1 and has a fusoidal shape with an area equal to 24,540 m^2. It extends in N 345° direction with length of about 320 m and width of about 140 m in its southern sector. The bottom elevation is 580 m asl with the maximum elevation of the western slope reaching 633 m. The eastern slope is 616 m, the northern slope attains a height of 617 while the southern slope has an altitude of 581 m. In the central part of the depression, a sub-circular artificial excavation has been completed in the terra rossa filling terrain. The excavation attains an area of 2,060 m^2 and has a diameter of 40 m and is generally full of water in the rainy season.

- Uvala N. 3 can be subdivided in two branches. The southern one of ellipsoidal shape has an area of 43,000 m^2, with its main axes reaching 410 m. It extends in a N 350° direction and has a secondary axes of about 165 m. The elevation of the bottom is 587 m, with a maximum elevation of 627 m attained along its western slope. The eastern slope reaches a height of 658 m while the southern slope 598 m in altitude. The narrower northern sector has an area of 23,100 m^2 with length totaling to about 150 m and width of 55 m. It extends in a N 350° direction with bottom elevations between 589 and 604 m and maximum elevations of the slopes of 832 and 656 m, respectively to the west and east.
- Uvala N. 4 is situated to the west of the N. 3, is of irregular rectangular shape and has an area of about 16,500 m^2. Uvala N. 4 extends in a N 336° direction with its principal side equal to about 250 m in length and its secondary side being 170 m long. The elevation of the bottom ranges between 624 and 636 m asl.
- Uvala N. 5 extends to about 230 m in a N-S direction. It is narrower than Uvala N. 4 and has an area of 6,300 m^2. It is approximately 20 m wide and has an elevation of the bottom, which varies between 636 and 646 m.

3.3.6 Dolines

A collapse doline bordered by steep to vertical walls and with a flat bottom is present in the Mt. Bufara area. The shape is almost sub-elliptical, with its eastern side larger than the western one and with an area of 55,360 m^2. Its main axis is about 300 m long and extends in a NE-SW direction while the secondary axis is about 230 m long and extends in NW-SE direction. The doline bottom stands at 142 m asl while the summital part of the walls vary between 180 m, in the southern sector, and 202 m in the northern sector. The latter exhibits a sub-vertical cliff, which reaches a maximum height of 35 m (Figs. 3.2 and 3.9).

A solution doline is, on the other hand, present in the Mt. Sparagio ridge, between the Colma di Mezzo and Prima Colma. It has a sub-elliptical shape and an area of 1,000 m^2. Its main axis is 50 m long and extends in a NNW-SSE direction while the secondary axis is 25 m long. The bottom of the doline has elevations ranging between 905 and 909 m asl and is occupied by a dense vegetation consisting mainly of trees (Figs. 3.2 and 3.10).

3.3.7 Swallow Holes

A number of swallow holes are present in the Purgatorio polje. These are small depressions partially occluded by debris, which capture the runoff of the plain. Other swallow holes are present along the Cipollazzo gorge and on the Mt. Sparagio ridge between Colma di Mezzo and Prima Colma (Figs. 3.2, 3.10 and 3.11).

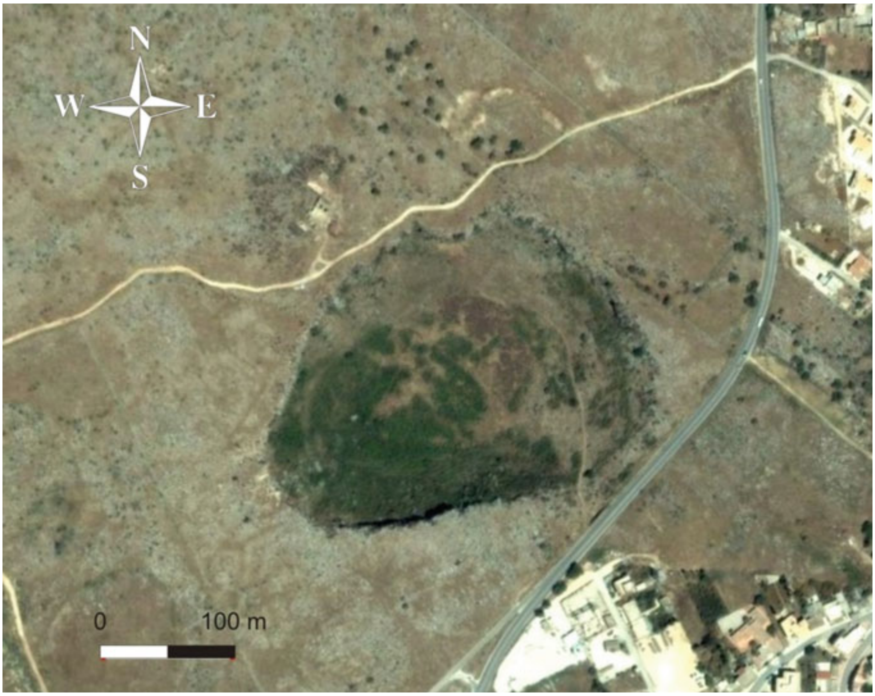

Fig. 3.9 Bufara doline (from Google Earth)

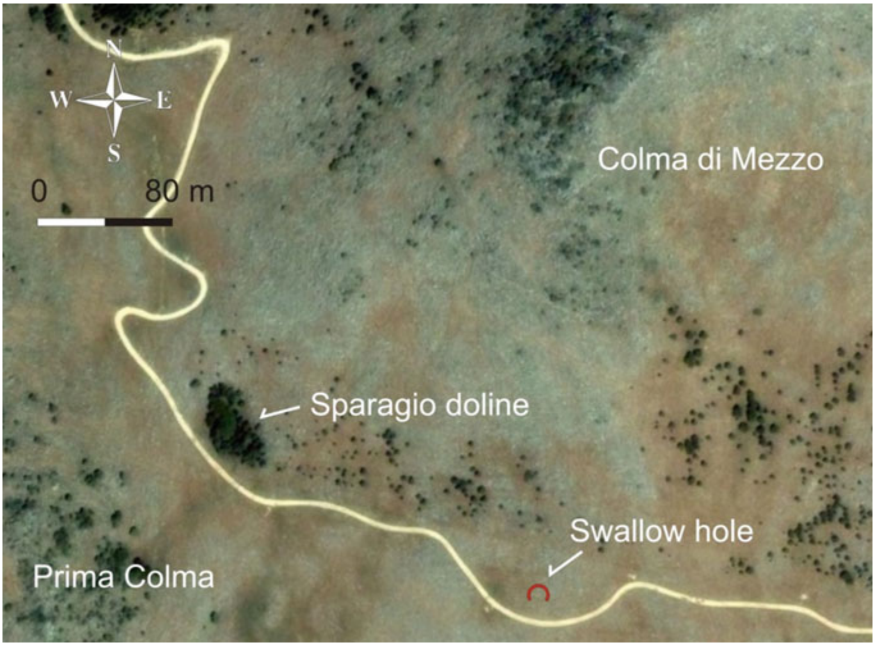

Fig. 3.10 Sparagio doline (from Google Earth)

Fig. 3.11 Map of the Purgatorio polje with the locations of the surveyed swallow holes (from Google Earth)

References

AA VV (1998) Climatologia della Sicilia a cura dell'Ass. Agr. e Foreste, Regione Siciliana

Agnesi V, Macaluso T, Monteleone S, Pipitone G (1984) Fenomeni di deformazione gravitativa profonda (deep-seated gravitational slope deformations) osservati nella Sicilia occidentale. Boll Soc Geol It 103:671–679

Agnesi V, Macaluso T, Monteleone S, Pipitone G, Sorriso-Salvo M (1989) Tipi e dinamica delle deformazioni gravitative profonde in relazione alle strutture geologiche. I casi di Monte Genuardo e di Scopello (Sicilia occidentale). Boll Soc Geol It 108:379–389

Agnesi V, Di Maggio C, Macaluso T (1995) Deformazioni gravitative profonde e superficiali nella penisola di Capo San Vito (Sicilia occidentale). Mem Soc Geol It 50:11–21

Bartolomei C, Celico P, Pecoraro A (1983) Schema idrogeologico della Sicilia nord-occidentale. Boll Soc Geol It 102:329–354, 9 ff

Čalić J (2011) Karstic uvala revisited: toward a redefinition of the term. Geomorphology 134 (2011):32–42

Cassa per il Mezzogiorno (1976) Rilievo aereo multispettrale su alcuni tratti di costa siciliana. Rip. Progetti idrici (Div. 3) - Idrotecneco (Studio inedito)

Cassinis R (1967) Preliminari su una ricerca degli efflussi d'acqua dolce lungo le coste siciliane mediante misure di salinità in mare. Boll Geof Teor Appl 9:34, Trieste

DEM Regione Siciliana. Modello digitale del terreno passo 2 m derivato da dati LIDAR volo ATA 2007–2008 in UTM-WGS84 fuso 33 N

De Martonne EM (1926) Un nouvelle fonction climatologique: l'indice de aridité. La météorologie. pp. 449–458, Paris

Sauro U (2012) Closed depression in karst area. In: Encyclopedia of Caves. Elsevier Inc.

Thornthawaite CW (1948) An approach towards a rational classification of climate. Geogr Rev Americ Geoph Soc 55–94

www.google.com/intl/it/earth/index.html

Chapter 4
Geological Framework

4.1 Regional Geological Context

In the Central Mediterranean region the Appenninic-Maghrebian Orogen originated during the Tertiary by the convergence between the European and the Africa-Adria Plates. In Sicily this orogen, corresponding to a thrust belt-foredeep-foreland system (Ogniben 1960; Broquet and Mascle 1972; Catalano and D'Argenio 1978, 1982), extends with dominant E-W trend from the Trapani Mts. to the Peloritani Mts. and is formed by a stack of imbricate foreland-verging folds and related thrust sheets (Bianchi et al. 1987; Roure et al. 1990; Catalano et al. 2000).

The tectonic units were piled along thrusts and were transported southwards during the construction of the Neogene Appenninic-Maghrebian fold-thrust system. The syn-tectonic deposits lying on the stacked chain units are progressively younger toward the foreland, and were affected by contractional deformations acquired during the southwards migration of the thrust front (Caire 1960; Roure et al. 1990).

4.1.1 Structural Domains in the Central Mediterranean

In the central Mediterranean the structural domains are: the *Foreland Domain*, the *Orogenic Domain* and the *Hinterland Domain* (Ben Avraham et al. 1990; Roure et al. 1990; Lentini et al. 1994; Finetti et al. 1996) (Fig. 4.1).

The *Hinterland Domain* is represented by the Corsica-Sardinia Block and the Tyrrhenian Basin. The latter is characterized by an oceanic crust, and its opening started since Serravallian time (Lentini et al. 1995a, b).

The *Foreland Domain* includes the relatively deformed (by extensional tectonics) continental areas of the Africa plate, represented by the Pelagian Block and the Adria (Apulian Block), which have been separated, during Jurassic or earlier times, by the growing oceanic crust of the Ionian Basin (Grasso 2001 and references therein).

R. Ruggieri, *Speleological and Speleogenetic Aspects of the Monti di Capo San Vito (Sicily)*, Springer Theses, DOI 10.1007/978-3-319-21720-8_4

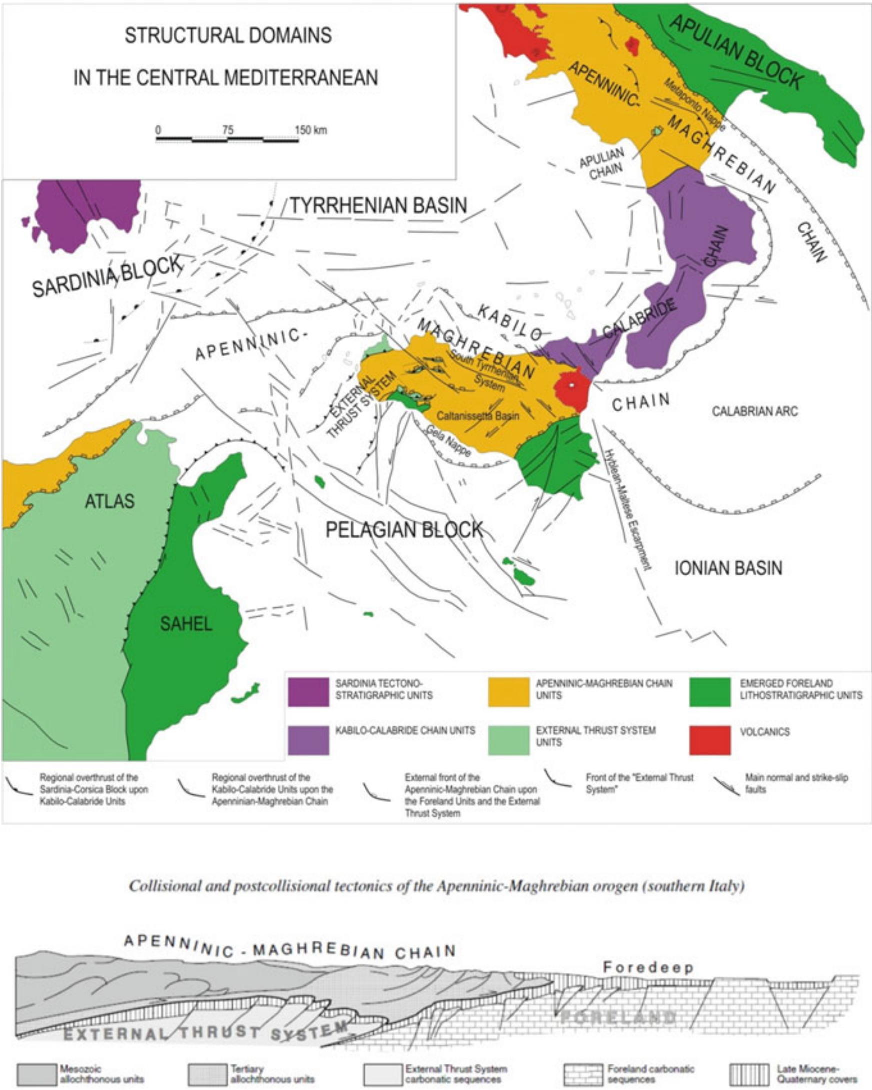

Fig. 4.1 Structural domains of the Appenninic-Maghrebian orogen and their geometry along a southwest-northeast-oriented schematic cross-section of the southern Appennines. The orogenic belt shows a regional duplex geometry. The footwall is represented by the external thrust system (the Apulian thrust in the southern Apennines). The Appenninic-Maghrebian chain consists of an allochthonous roof thrust system in which the Mesozoic and the Tertiary sequences are mostly decoupled (Lentini et al. 2006)

In Sicily, the Foreland Domain, represented by the Hyblean Plateau and the Sciacca platform of western Sicily, is the emerged part of the Pelagian Block, a wide platform extending off-shore in the Sicily Channel and emerging in correspondence with the Lampedusa Island and the Maltese Archipelago (Finetti 1982; Reuther and Eisbacher 1985; Burollet et al. 1987; Grasso 2001) and in the Sahel region of Tunisia.

The Pelagian Block is characterized by a 25–35 km thick crystalline basement (Cassinis et al. 1979; Scarascia et al. 2000) overlaid by a 6–7 km thick Mesozoic-Cenozoic shallow-water to basin carbonate sedimentary succession, with repeated intercalations of volcanic rocks. The Pelagian block represents an E-W segment of the Africa continental margin (Dewey et al. 1989) flexured to the north beneath the orogenic belt.

The *Orogenic Domain* is composed of three superimposed tectonic belts, the External Thrust System (ETS), the Appenninic-Maghrebian Chain (AMC) and the Calabride Chain (CC) derived, respectively, from the detachment of the internal sedimentary cover of the flexure sector of the continental foreland, by the imbrications of the sedimentary sequences belonging to both the oceanic crust-type sectors (Tethys and Ionian basins) and the continental-type crust sector (inner carbonate platforms) and by the delamination of the European margin.

The Pelagian-Sicilian Thrust Belt (PSTB) originated from the detachment of the sedimentary covers of the inner margin of the Pelagian Block. It is mainly buried below the unrooted nappes of the Appenninic-Maghrebian chain. The PSTB is exposed in western Sicily, at the Monte Kumeta and Rocca Busambra ridges and in the Trapani Mountains.

Data from the deep exploration of the Central Mediterranean (CROP Project, Finetti et al. 2005a, b), showed that the Foreland Blocks are in collision with a continental crust, named "Panormide crust" (Lentini et al. 2006) recognized in the Tyrrhenian offshore of Sicily and the Southern Appennines respectively.

The expression of the continental collision that, from Tortonian times, involved the Africa margin (Lentini et al. 1994, 1995a, b) is represented by structures of the South Tyrrhenian System (Finetti and Del Ben 1986; Finetti et al. 1996). These structures represent the kinematic junction to the progressive southeastward advance of the Calabria-Peloritani Arc, related to the northwestward subduction of the oceanic Ionian crust (Finetti 1982; Finetti and Del Ben 1986; Maliverno and Ryan 1986; Patacca and Scandone 1989; Mantovani 2005). Since the Late Pliocene the northern Sicilian margin was involved in the Tyrrhenian tectonic collapse, as testified by the transtensive structures that affect the Plio-Pleistocene sediments (Del Ben and Guarnieri 2000; Guarnieri 2004).

4.2 Geological Setting of the Study Area

4.2.1 Previous Studies

The area of research has been an object of study and controversy since the beginning of the twentieth century. Baldacci (1886), Lugeon and Argand (1906), Fabiani and Trevisan (1940) were the first to prove the existence of thrust sheets in the Monti di Capo San Vito, Monti di Palermo and Madonie areas. Later, Broquet et al. (1984) recognized in western Sicily, different nappes derived from deformations of various domains, stacked between the end of the Tortonian and the Early Pliocene. Giunta and Liguori (1970, 1972, 1973) proposed a palaeogeographic model with the following domains from north to south: an internal zone, the Panormide Platform, the Imerese Basin, an intermediate Basin, the Trapanese Basin, the Sicanian Basin and the "External" Platform (Fig. 4.2). They also identified tectono-stratigraphic units derived from the previously described Domains, which were piled up and inclined towards the southern Trapanese domain in Middle Miocene times. Catalano and D'Argenio (1982) refered the areas of Monte Monaco, Monte Sparagio and Monte Acci to the Prepanormide Domain. Catalano et al. (1985) based on seismic analysis of the Sardinian channel and the Channel of Sicily, described the Prepanormide, Tunisian, Trapanese, Panormide and Imerese Domains and the lateral relations between them. Montanari (1987) referred the areas Monte Monaco, Monte Sparagio and Erice to the Tunisian Domain, close to the Panormide and Imerese Domains. Abate et al. (1991), on the basis of facies and structural analyses, identified six new structural units, indicating a vergence (towards east and south east). More recently, several studies on reprocessed seismic lines (Catalano et al. 2000, 2002), Finetti et al. (2005a, b) and Lentini et al. (2006) assert that the area of Monti di Capo San Vito is part (external thrust) of the Pelagian Sicilian Thrust Belt (PSTB) originated from the detachment of the sedimentary covers of the inner Pelagian Block, which is mainly buried below the unrooted nappes of the Appenninic-Maghrebian chain. In this context, some tectonic subunits have been identified and renamed, and the area of this research is assumed to belong to the Mount Inici Subunit.

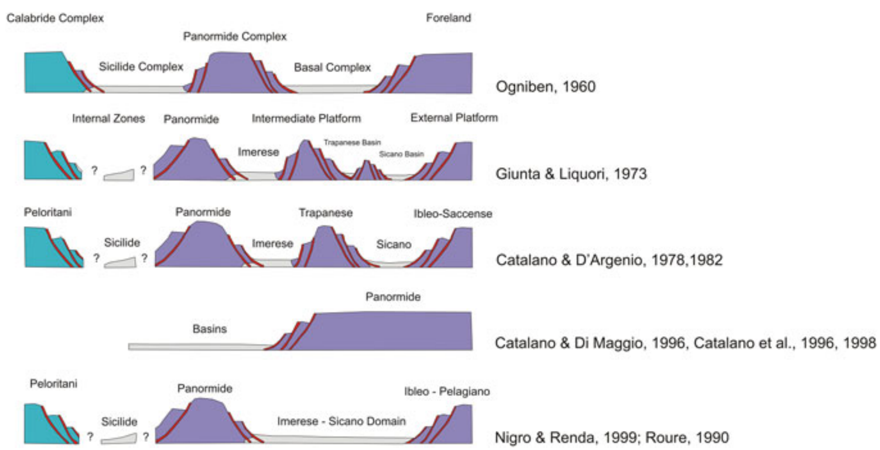

Fig. 4.2 Paleogeographic models illustrating the various domains during the Mesozoic proposed by different Authors (after Nigro et al. 2008)

4.2.2 Lithology

The sedimentary succession cropping out in the study area consists mainly of Upper Triassic to Pliocene carbonates. The carbonates show platform from open reef to basinal facies. The succession is here described from the bottom to the top (Catalano et al. 2011—Fig. 4.3):

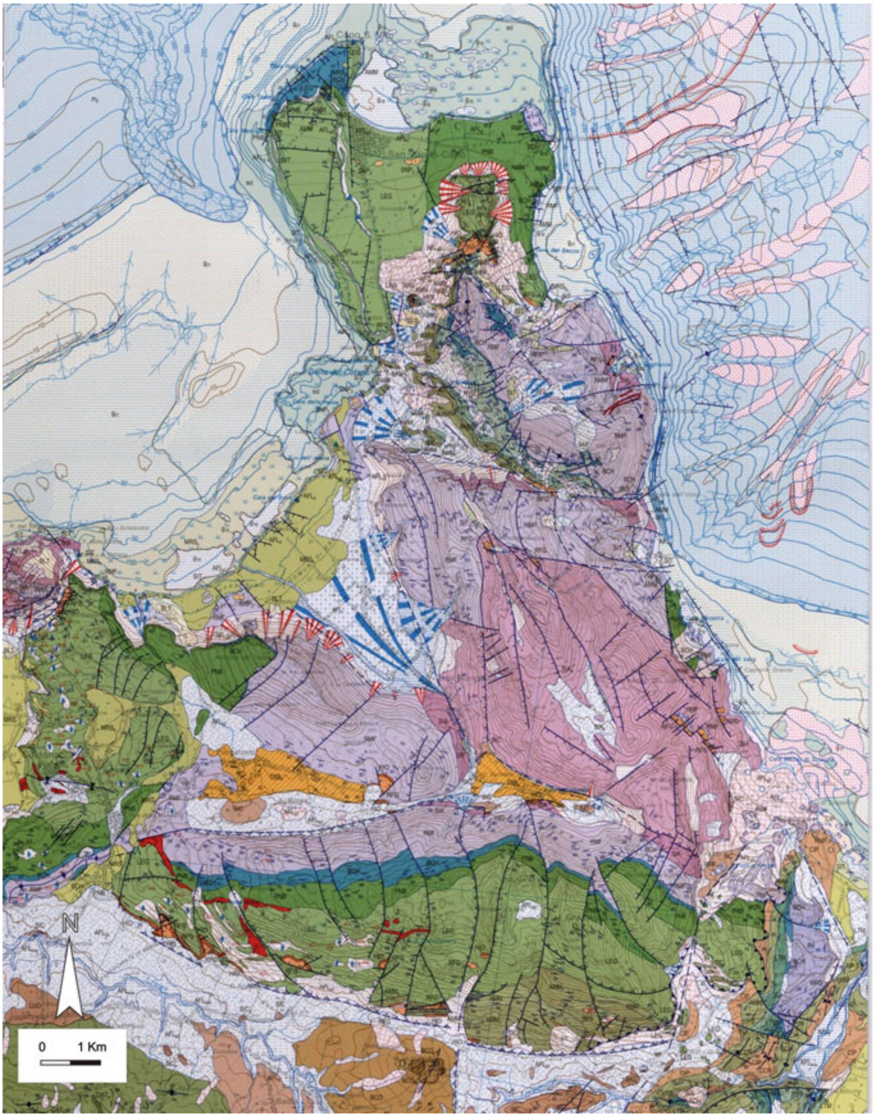

Fig. 4.3 Geological map of the Monti di Capo San Vito (from ISPRA, Servizio Geologico d'Italia—Carta Geologica d'Italia alla scala 1:50.000—Castellammare del Golfo 593—Regione Siciliana Ass. Territorio Ambiente, SistemaCART-Roma–2011)

SIA **Sciacca Formation**: massive dolostones and dolomitic breccias (Upper Triassic);

RMF **Capo Rama Formation**: Dolomitic limestones, loferitic and stromatolithic packstones, wackstones with *Megalodon* sp., with basaltic intercalations (Upper Triassic-Lower Liassic);

BCH **Buccheri Formation**: red nodular limestones with ammonites, bedded cherty horizons and "radiolarites" (Dogger-Malm);

PNB **Piano Battaglia limestones**: Calcarenites alternated with calcirudites, limestone breccias with fragments of *Ellipsactinia,* crinoide sandstones and ammonitic marls (Upper Tithonian-Lower Cretaceous);

LEG **Pellegrino Formation**: biocalcirudites, biocalcarenites, biolithites with lamellibranchia, limestones and marls with belemnites and foraminifera, radiolarites with basaltic intercalations (Upper Cretaceous);

AMM **Amerillo Formation**: marly limestones, calcarenites and marls with planctonic foraminifera and carbonatic megabreccia horizonts ("Scaglia *Auct*." Upper Cretaceous-Eocene);

HIO **Mischio**: glauconitic biocalcarenites and biocalcirudites with lamellibranchia, gastropods and algae (Burdigalian);

RFG **Torrente Foggia clays**: clay, sandy clay and marls (Upper Langhian-Lower Tortonian);

SIC **Castellana Sicula Formation**: marly clay with sandy and yellow sandstones (Upper Serravallian—Lower Tortonian);

TRV **Terravecchia Formation**: Sands, clay, sandy clay and grey marls clay marls (Upper Tortonian–Lower Messinian);

GPQ **Pasquasia Formation**: gypsum macrocrystals, and gypsum clays (Upper Messinian);

TRB **Trubi**: marls and limestone marls passing in the Purgatorio plain to calcarenites and calcirudites (Lower Pliocene);

MRS **Marsala Synthem**: calcarenites and calcirudites, sands (Lower Pleistocene);

BLT **Polisano Synthem**: Eolianites. quartzitic and/or carbonatic eolic sands with cross-bedding lamination (Middle Pleistocene);

RFR **Raffo Rosso Synthem**: cemented and stratified detritus, sandstones and eolic calcarenites (Upper Pleistocene);

AFL **Capo Plaia Synthem**: Talus, elluvial and colluvial deposits (Upper Pleistocene—Holocene)

The above sequences outcropping along the Capo S. Vito peninsula have been alternatively ascribed to different domains (e.g. Imerese, Panormide, etc. Catalano et al. 2011; Lentini et al. 2006) in the geological literature.

4.2.3 Structural Setting

According to Abate et al. (1991, 1993, 1996, 1998), six major tectonic units, crop out in this area stacked after the Middle Tortonian, with stepped ramp-flat thrust geometries (Incandela 1995), while according to Catalano et al. (2011) two main tectonic units have been observed: U.S.S. Monaco-Sparagio and U.S.S. Acci (Fig. 4.4).

During the Early Pliocene new thrusts and back-thrusts were produced (Giunta and Liguori 1972; Abate et al. 1991, 1993; Incandela 1995). The structural analysis revealed at least two fold generations. The older system is oriented N-S and NE-SW and is probably associated with Miocene thrusting. This system is reoriented by an E-W trending superimposed fold system, which is probably related to the Pliocene thrusting. The northern vergence of several large scale folds (Acci Mt., Sparagio

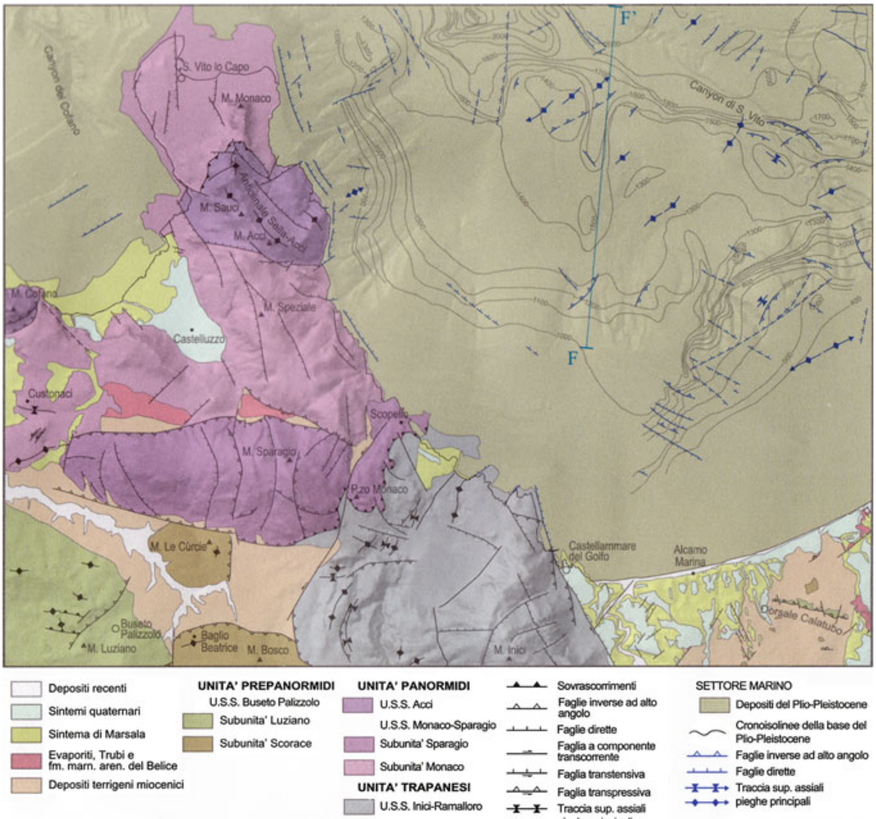

Fig. 4.4 Tectonic scheme of the study area (from ISPRA, Servizio Geologico d'Italia—Carta Geologica d'Italia alla scala 1:50.000—Castellammare del Golfo 593—Regione Siciliana Ass. Territorio Ambiente, SistemaCART—Roma—2011)

Mt., etc.) is probably associated with the Pliocene back-thrusting (Abate et al. 1991, 1993).

From the beginning of the Early Miocene, the units previously pertaining to the old Tethys margin (basins and carbonate platforms) were rotated during deformations and nappe emplacement. As a result of this orogenic phase, transpressive structures developed (Oldow et al. 1989).

Since Middle Pliocene strike-slip tectonics affected the tectonic pile resulting in a NW-SE/W-E trending dextral fault system and a N-S/NE-SW trending left-lateral fault system. These faults cut pre-existing thrust fronts and produced drag folds and minor thrust; they also produced transpressional structural highs (flower structures) and transtensional depressions (pull-apart basins) filled with Pliocene-Pleistocene deposits. The former structures linked to the dynamics of the Tyrrhenian opening, which migrated south-eastward (Abate et al. 1998; Nigro and Renda 2005) (Fig. 4.5).

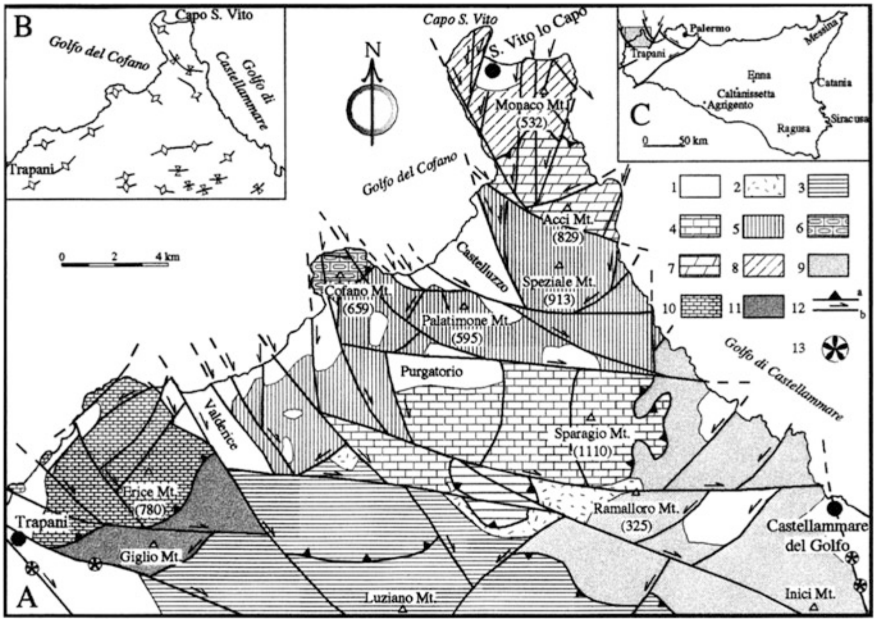

Fig. 4.5 Tectonic sketch of the Trapani Mts. *1* Plio-Pleistocene deposits; *2* Tortonian-Messinian deposits; *3* Monte Luziano Unit (*Upper* Cretaceous-*Upper* Miocene); *4* Sparagio Mt. Unit (*Upper* Triassic-Middle Tortonian); *5* Speziale-Palatimone Mts. Unit (*Upper* Triassic-Middle Tortonian); *6* Cofano Mt. Unit (*Upper* Triassic-Middle Tortonian); *7* Acci Mt. Unit (*Upper* Triassic-Middle Tortonian); *8* Monaco Mt. Unit (*Upper* Triassic-Middle Tortonian); *9* Ramalloro Mt. Unit (*Upper* Triassic-Middle Tortonian); *10* Mt. Erice Unit (*Upper* Triassic-Middle Tortonian); *11* Giglio Mt. Unit (*Upper* Triassic-Middle Tortonian); *12a* main thrusts; *12b* main strike-slip faults; *13* thermal springs. B. Plio-Pleistocene axial fold trends (Abate et al. 1998)

The flight of Pleistocene marine and continental deposits suggests the persistence of transpressive tectonic activity until the present time (Abate et al. 1998; Nigro et al. 2000; Antonioli et al. 1999a, b; Tondi 2007).

References

Abate B, di Maggio C, Incandela A, Renda P (1991) Nuovi dati sulla geologia della Penisola di Capo San Vito (Sicilia nord-occidentale)—Mem. Soc Geol It 47:15–25

Abate B, di Maggio C, Incandela A and Renda P (1993) Carta Geologica dei Monti di Capo San Vito, scala 1:25.000—Dip. Geologia e Geodesia dell'Università di Palermo

Abate B, Incandela A, Renda P, Tramutoli M (1996) Facies ed evoluzione sedimentaria del "Bacino di Trapani" (Sicilia occidentale) durante l'Oligocene-Miocene. Mem Soc Geol It 51:119–128, 6 ff

Abate B, Incandela A, Nigro F, Renda P (1998) Plio-Pleistocene strike-slip tectonics in the Trapani Mts. (NW Sicily). Boll Soc Geol It 117:555–567, 10 ff

Antonioli F, Cremona G, Immordino F, Puglisi C, Romagnoli C, Silenzi S, Valpreda E, Verrubbi V (1999a) Quaternary and holocene differential movements in a mediterranean coastal area (San Vito Lo Capo, Sicily-Italy). Physics and Chemistry of the Earth, vol 68

Antonioli F, Cremona G, Puglisi C, Silenzi S, Valpreda E, Verrubbi V (1999b) Quantitative assessment of post Tyrrenian differential crustal movements in a Mediterranean coastal area (S. Vito—Sicily—Italy). Phys Chem Earth (A), 24(4):343–347

Baldacci I (1886) Descrizione geologica dell'Isola di Sicilia. Mem Descr Carta Geol d'It 1: 3–403

Ben Avraham Z, Boccaletti M, Cello G, Grasso M, Lentini F, Torelli L, Tortorici L (1990) Principali domini strutturali originatisi dalla collisione neogenico-quaternaria nel Mediterraneo Centrale. Mem Soc Geol It 45:453–462

Bianchi F, Carbone S, Grasso M, Invernizzi G, Lentini F, Longaretti G, Merlini S, Mostardini F (1987) Sicilia orientale: profilo geologico Nebrodi-Iblei. Mem Soc Geol It 38:429–458

Broquet P, Mascle G (1972) Les grands traits stratigraphiques et structuraux de la partien septentrionale des Monts de Trapani (Sicile occidentale). Ann Soc Geol Nord, XCII 3:139–146

Broquet P, Duée G, Mascel G, Truillet R (1984) Evolution structurale alpine récente de la Sicile et sa signification géodinamique. Revue de Géol. Dynamique et de Géographie Phisique 25 (2):75–85

Burollet PF, Mugniot GM, Sweeney P (1987) The geology of the Pelagian block: the margins and basinc of southern Tunisia and Tripolitania. In: Nairn A, Kanes W, Stelhi FG (eds) The ocean basins and margins, Plenum Press, 4B:331–339

Caire A (1960) Sicily in its Mediterraneaan setting. In: Alvarez W, Gohrbandt KHA (ed) Geology and History of Sicily, Petroleum Expl Soc Libya, pp 145–170

Cassinis R, Franciosi R, Scarascia S (1979) The structure of the Earth's crust in Italy: a preliminary typology based on seismic data: Bollettino di Geofisica Teorica a Applicata, vol 21, pp 105–126

Catalano R, D'Argenio B (1978) An essay of palinspastic restoration across the western Sicily. Geol Romana 17:145–159

Catalano R and D'Argenio B (1982) Schema geologico della sicilia. In: Catalano and B. D'Argenio (eds) Guida alla geologia della Sicilia Occidentale. Soc Geol It, Palermo

Catalano R, Catalano R, D'Argenio B, Montanari L, Mortolotti E, Torelli L (1985) Marine geology of the NW Sicily offshore and its relationships with mainland structures. Boll Soc Ital 104:207–215

Catalano R, Franchino A, Merlini S, Sulli A (2000) Central western Sicily structural setting interpreted from seismic reflection profiles. Mem Soc Geol It 55:5–16

Catalano R, Merlini S, Sulli A (2002) The structure of western Sicily, central Mediterranean. Petroleum Geoscience 8:7–18

Catalano F, Agate M, Basilone L, di Maggio C, Mancuso M, Sulli A (2011) Note illustrative della Carta Geologica d'Italia alla scala 1:50.000, foglio 593 Castellammare del Golfo. ISPRA, Servizio Geologico d'Italia. Regione Siciliana Ass. Territorio Ambiente

Del Ben A, Guarnieri P (2000) Neogene Transpression in the Cefalù Basin (Southern Tyrrhenian): comparison between land and marine data. Mem Soc Geol It 55:27–33

Dewey JF, Helman ML, Turco E, Hutton DHW, Knott SD (1989) Kinematics of the Western Mediterranean In: Coward MP, Dietrich D and Park RG (eds) Alpine Tectonics Geol Soc Spec Publ, vol 45, pp 265–283

Fabiani R, Trevisan L (1940) Prove dell'esistenza di uno stile tettonico a falde di ricoprimento nei monti di Palermo. Attti R. Acc. d'Italia. Mem Cl Sc fis mat e nat 11:435–448

Finetti IR (1982) Strucure, stratigraphy and evolution of the central mediterranean. Boll Geof Teor Appl 24:247–312

Finetti IR, Del Ben A (1986) Geophysical study of the Tyrrhenian opening. Bol Geofis Teor Appl 28:75–155

Finetti IR, Lentini F, Carbone S, Catalano S, Del Ben A (1996) Il Sistema Appenninico Meridionale-ARco Calabro-Sicilia nel Mediterraneo centrale: studio geologico-geofisico. Boll Soc Geol It 115:529–559

Finetti I, Lentini F, Carbone S, Del Ben A, di Stefano, Forlin E, Guarnieri P, Pipan and Prizzon A (2005a) Geological outline of the sicily and lithospheric tectono-dynamics of its tyrrehian margin from CROP seismic data. In: Finetti IR (ed) CROP, Deep seismic exploration of the mediterranean region: spec. Elsevier chapter 15:319–376

Finetti I, Lentini F, Carbone S, Del Ben A, di Stefano, Forlin E, Guarnieri P, Pipan and Prizzon A (2005b) Crustal tectonostratigraphy and geodynamics of the southern Apennines from CROP and other integrating geophysicalgeological data. In: Finetti IR (ed.) CROP, Deep Sesmic Rxploration of the Mediterranean region: spec. vol 15, Elsevier, pp 319–376

Giunta G, Liguori V (1970) Geologia della penisola di Capo San Vito (Sicilia nord-occidentale). Lav Ist Geol Univ Palermo 9:21

Giunta G and Liguori V (1972) Geologia della estremità Nord-occidentale della Sicilia. Riv Min Sic 136–138, 165–226, Palermo

Giunta G, Liguori V (1973) Evoluzione paleotettonica della Sicilia nord-occidentale. Boll Soc Geol It 92:903–924

Grasso M (2001) The appenninic-maghrebian orogen in southern Italy, sicily and adjacent areas. In: Vai GB, Martini JP (eds) anatomy of an orogen: the apennines and adjacent mediterranean basins (eds) 255–286. Kluwer Academic Publishers

Guarnieri P (2004) Structural evidence for the deformation by block rotation in the context of transpressive tectonics, northwestern Sicily (Italy). J Struct Geol 26:207–219

Incandela A (1995) Lineamenti stratigrafico-strutturali dell'estremità nord-occidentale della Sicilia e delle isole di Favignana e Levanzo (Arcipelago delle Egadi). Tesi di Dottorato, Palermo

Lentini F, Carbone S, Catalano S (1994) Main structural domains of the central mediterranean region and their tectonic evolution. Boll geof Teor Appl 36:103–125

Lentini F, Carbone S, Catalano S, Di Stefano A, Gargano C, Romeo M, Strazzulla S, Vinci G (1995a) Sedimentary evolution of basins in mobile belts; Examples from tertiary terrigenous sequences of the Peloritani Mts (NE Sicily). Terra Nova 7:161–170

Lentini F, Carbone S, Catalano S, Grasso M (1995b) Principali lineamenti strutturali della Sicilia nord-occidentale. Vol Spec Studi Geol Camerti (1995/2), 319–329

Lentini F, Carbone S, Guarnieri P (2006) Collisional and postcollisional tectonics of the Apenninic-Maghrebian orogene (southern Italy). In: Dilek Y, Pavlides S (eds) Postcollisional tectonics and magmatism in the Mediterranean region and Asia: Geological Society of America Special Paper 409. pp 57–81

Leugeon M, Argand E (1906) Sur le grands phenomenes de charriage en Sicile. CR Ac Sc 142:966–969

Maliverno A, Ryan WBF (1986) Extension in the Tyrrhenian Sea and shortening in the apennines as a result of the arc migration driven by sinking of the lithosphere. Tectonics 5:227–245

Mantovani E (2005) Evolutionary reconstruction of the Mediterranean region: extrusion tectonics driven by plate convergence. In: Finetti IR (ed) CROP deep seismic exploration of the mediterranean region Spec. vol. Elsevier 32, 705–746

Montanari L (1987) Lineamenti stratigrafico-paleo-geografici della Sicilia durante il ciclo alpino. Mem Soc Geol It 38:361–406, 22 ff

Nigro F, Renda G (2005) Transtensional/extensional fault activity from the Mesozoic rifting to Tertiary chain building in Northern Sicily (Central Mediterranean). Geologica Carpathica 56(3):255–271

Nigro F, Renda P, Arisco G (2000) Tettonica recente nella Sicilia nord-occidentale e nelle isole Egadi. Boll Soc Geol it 119:307–319, 7 ff

Nigro F, Renda P, Selvaggio G, Favara R (2008) Evoluzione geologica della Sicilia Centro-Occidentale. Geologi di Sicilia, anno XVI, Ottobre–Dicembre 2008, n. 4

Ogniben L (1960) Nota illustrativa dello schema geologico della Sicilia nord-orientale: Riserva Mineraria Siciliana, vol 11, p 183–212

Oldow JS, Channel JET, Catalano R, D'Argenio B (1989) Contemporaneous thrusting and large-scale rotation in the Western Sicilian fold and thrust belt. Tectonics 9:661–681

Patacca E, Scandone P (1989) Post Tortonian mountain building in the Apennines. The role of the passive sinking of a relic of lithospheric slab. In: The lithosphere in Italy. In: Boriani A, Bonafede M, Piccardo GB, Vai GB (ed) Advances in Earth Science. Res Atti Conv Lincei 80:157–176

Reuther CD, Eisbacher GH (1985) Pantelleria rift-crustal extension in a convergent intraplate setting. Geolog. Rundschau 74:585–597

Roure F, Howell DG, Muller C, Moretti I (1990) Late Cenozoic subduction complex of Sicily. J Struct Geol 12(2):259–266

Scarascia S, Cassinis R, Lozej A, Nebuloni A (2000) A seismic and gravimetric model of crustal structures across the sicily channel rift zone. Boll Soc Geol It 19:213–222

Tondi E (2007) Nucleation, development and petrophysical properties of faults in carbonate grainstone: evidence from the San Vito Lo Capo peninsula (Sicily, Italy). J Struct Geol 29(2007):614–628

Chapter 5
Hydrogeological Aspects

5.1 General Framework

The geological and structural setting of the study area, characterized mainly by outcrops of Mesozoic-Cenozoic carbonates often dissected by thrust, normal and strike-slip faults, has determined the genesis of a series of both independent and interconnected hydrostructures.

Within the same basin of recharge, they are characterized by extremely variable reservoir geometries, which depends on permeability of the rocks, karstification and degree of fracturation linked with tectonic structures.

As far as the preferential directions of the underground water flow is concerned, great importance is given to the structural characteristics of the rocks such as dip direction of the layers and the systems of fractures that dissect the aquifers.

The complex network constituted by the interconnection of the above systems is also influenced by the intense karstogenesis, which has been active for a long time: both by the increase of secondary porosity connected to the dissolution of rock and also, in other cases, by the reduction of porosity because of the occlusion of various drainage conduits due to collapses or to the filling of chemical deposits.

In the area under consideration previous studies have identified one major hydrological unit (Mt. Inici–Mt. Sparagio, according to Bartolomei et al. 1983; Mt. Monaco–Mt. Sparagio, according to Cusimano et al. 2002) with homogenous hydrological conditions, bordered to the south by the clay-marl-sand complex, which makes up an efficient buffer for the base aquifer.

To the other sides the border is mainly the sea and only for a short stretch sand-gravel-calcarenite complexes (Celico 1979; Bartolomei et al. 1983). The previous authors subdivided this hydrological unit into secondary sub-units or minor hydrostructures.

R. Ruggieri, *Speleological and Speleogenetic Aspects of the Monti di Capo San Vito (Sicily)*, Springer Theses, DOI 10.1007/978-3-319-21720-8_5

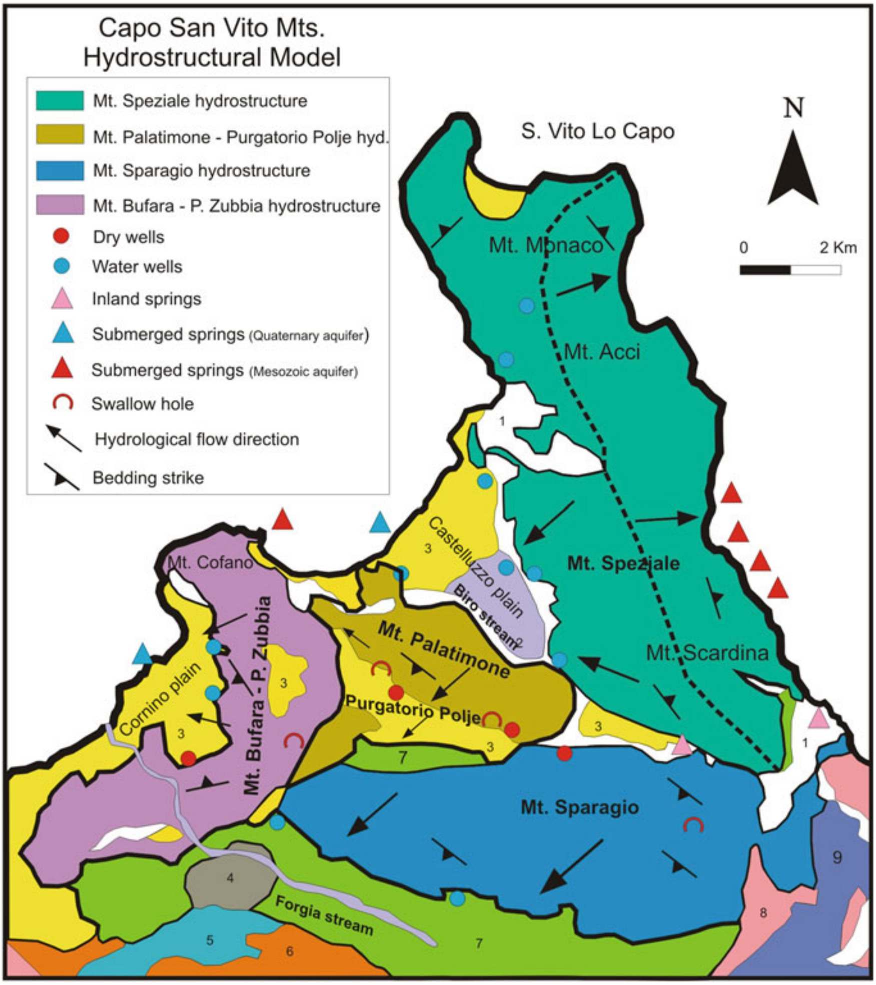

The description of the main hydrogeological features in terms of recharge area and preferential underground flow directions is based on structural and geomorphological data collected both during the speleological researches carried out in the last years (Ruggieri 1996, 2000, 2002, 2009; Ruggieri and Messina Panfalone 2011) and, in particular, during the present research.

The rough general hydrogeological framework, reconstructed during the present study, is partially different from that reported from previous authors (Fig. 5.1). It is not exhaustive and constitutes just a starting point for further studies addressed to a better knowledge of the underground hydrodynamics, watersheds and water flow directions along the coast, which is till now scarcely studied.

◀ **Fig. 5.1** Hydrostructural model of the study area. *Legend* (*1*) Talus; (*2*) Alluvium; (*3*) Bioclastic calcarenites and conglometates (Plio-Pleistocene); (*4*) Sandy clays, sandstones, sands and conglomerates (Lower Messinian-Upper Tortonian); (*5*) Clays marls and marly limestones (Upper Eocene-Upper Miocene); (*6*) Marls and marly limestones, calcilutites and marls calcisiltites, biocalcarenites and biocalcirudites (Lower Cretaceous—Middle Miocene); (*7*) Clays and sandy clays (Upper Langhian-Tortonian); (*8*) Clays and sandy clays and marls (Upper Langhian-Tortonian); (*9*) Dolostones, dolomitic limestones, stromatolithic limestones (Upper Triassic-Middle Miocene); **Mt. Speziale hydrostructure**: Dolostones and dolomitic limestones, stromatolithic limestones, loferithic breccias and sedimentary veins, nodular limestones, marls, and calcilutite marls, limestones with volcanic intercalations (Upper Triassic-Middle Miocene); **Mt. Palatimone–Purgatorio Polje hydrostructure**: Stromatolithic dolostones, dolomitic limestones, breccias and sedimentary veins, bioclastic calcarenites (Upper Triassic-Lower Pleistocene); **Mt. Sparagio hydrostructure**: Dolostones and dolomitic limestones, stromatolithic limestones, nodular limestones, marls, and calcilutite marls, limestones with volcanic intercalations (Upper Triassic-Middle Miocene); **Mt. Bufara–Piano Zubbia hydrostructure:** Stromatolithic dolostones, dolomitic limestones, loferithic breccias and sedimentary veins, nodular limestones with ammonites, calcilutites, calcarenites, calcirudites, intercalations basaltic lava with pillow, bioclastic calcarenites (Upper Triassic-Lower Pleistocene) (Geology after Cusimano et al. 2002)

5.1.1 Mt. Palatimone–Polje of Purgatorio's Hydrostructure

This structure is mainly constituted by the previously mentioned monocline, bordered in its southern part by a fault with a NW-SE trend, which separates the Mesozoic dolomites from the Lower Pliocene calcarenites of the Purgatorio plain. The strata dip to SSW, and are dissected by faults dipping towards NW.

Stratigraphic and structural analyses, underground karst morphology data together with previous data from wells obtained in the Purgatorio plain (Pratelli and Aiello 2002), give the following indications:

1. The main drainage of rainfall, which seeps in both slopes of the ridge, is directed towards the SW in the direction of the Purgatorio plain;
2. In the Purgatorio polje the drainage of the water coming from the ridge and captured by the swallow holes is towards the SW, as shown by the preferential directions of karstification of the main caves surveyed to a depth of around 200 m.
3. Finally a certain amount of epikarst water from the plain seems to be directed, controlled by a NW-SE trending structural discontinuity, towards the fluviokarst Gole di Cipolazzo which, in this respect, constitutes the underground and surface hydrological outlet of the Purgatorio polje.

5.1.2 Mt. Sparagio's Hydrostructure

This structure is basically the WNW-ESE ridge of Mt. Sparagio, with its peak of 1,110 m asl, sloping down towards the west to an elevation of 150–200 m asl in the area of Assiene.

In its northern sector, the boundary of the hydrostructure is constituted by a reverse fault, which interpose the Mesozoic dolomites with the Miocene pelites and quartzite sands that crop out in the southern sector of the Plain of Purgatorio. In the south, the Serravallian-Middle Tortonian clay and sandy marl (Marl of San Cipirello, Mt. Ramalloro Unit) are in tectonic contact with the overthrusted Mesozoic-Cretaceous carbonates.

The comparison of the structural data with the karst structures observed on the ridge provide evidence for an average direction of the underground water flow towards the south and the south-west (Figs. 5.1 and 5.2).

This underground water drainage would feed the carbonate aquifers, limited by Miocene clays, that outcrop in the plain of the basin of the Forgia stream, as has also been demonstrated by some water-wells drilled there (Pratelli and Aiello 2002).

From the northern slopes a secondary part of the rain water, drained by some canyons, feeds the Polje of Purgatorio hydrostructure, via the swallow holes.

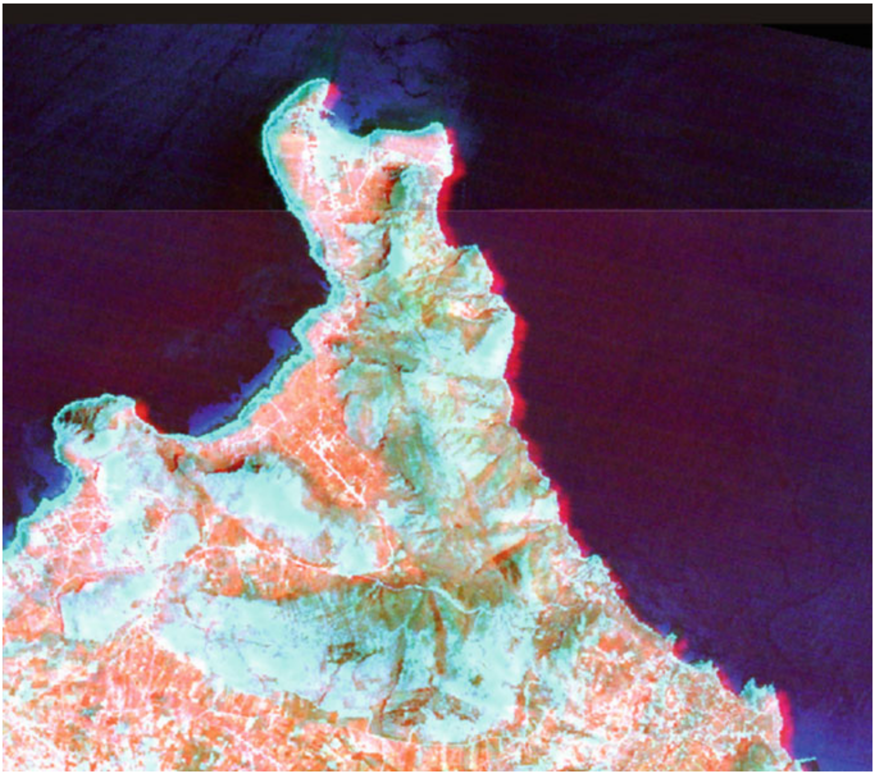

Fig. 5.2 Band 621 LANDSAT image of the study area (Cassa per il Mezzogiorno 1976)

5.1.3 Mt. Bufara–Piano Zubbia's Hydrostructure

In part fed by the hydrostructures of Mt. Palatimone–Purgatorio plain and Mt. Sparagio, this hydrostructure shows the following karstified structures: in the central-northern sector mainly NE-SW oriented structures that dip towards the SE, dissected by NW-SE structures dipping towards SW, and in the southern sector structures oriented towards the NNE-SSW.

With regard to the dip direction of the strata, towards SW in the northern sector and towards the NW in the southern sector, the underground water of the carbonate Mesozoic phreatic aquifer, overlapped by the Pleistocene calcarenites, flows towards the Cornino coast, where a series of submerged springs along the shoreline (Figs. 5.3–4) and submerged caves at a certain distance from the coast are known.

5.1.4 Mt. Monaco–Speziale–Mt. Scardina's Hydrostructure

In general terms it is constituted by the NNW-SSE trend carbonatic ridge of Mt. Monaco–Mt. Speziale–Mt. Scardina, borded by the sea to the east. It is dissected by E-W/NE-SW oriented structures on its eastern slopes and NNW-SSE on its summit and western parts.

There is a watershed in this hydrostructure, oriented N-S in the northern sector and NNW-SSE in centre-south sector, that creates conditions for an underground drainage diversification, as follows:

- towards the east, along the coast or out to sea, as has been confirmed by the presence of numerous submarine springs (Cassinis 1967), also discovered by multispectral aerial surveys (Cassa per il Mezzogiono 1976) and submerged caves explored along the coast of the Zingaro Natural Reserve (Antonioli et al. 1993; Sottosanti 1994);

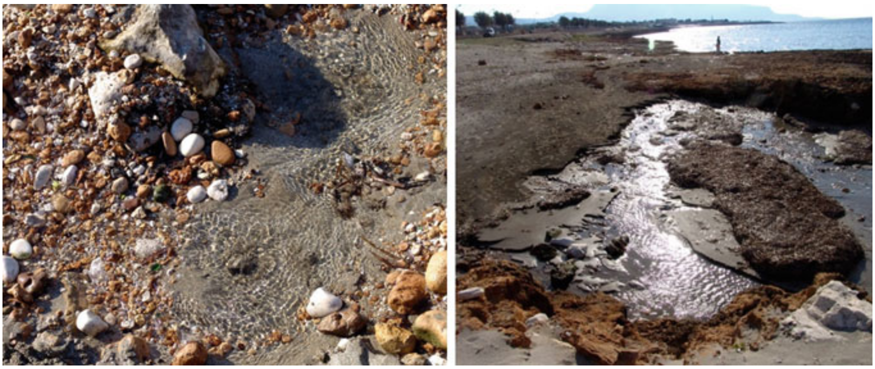

Figs. 5.3–4 Springs along the shoreline in the coastal belt of Cornino plain

- towards the NW, from Piano dell'Arena towards the upper basin of the Biro stream; and towards W/SW, respectively the Golfo di Cofano and the Piana di Castelluzzo (Pratelli and Aiello 2002) (Figs. 5.1 and 5.2).

5.2 The Coastal Strip and the Problems of the Vulnerability of the Aquifers

On the coastal zone of Cornino and Casteluzzo a *secondary reservoir* has been identified where the Pleistocene calcarenite formations are in contact with the carbonate Mesozoic formations below sea-level.

The lower grade permeability of the calcarenites, with respect to the Mesozoic limestone aquifer, slows down the intrusion of marine water. This phenomenon has already been observed by means of geochemical analyses carried out on water samples collected from wells located 4 km far from the shoreline. Water contamination due to the growing anthropic urbanization of the coastal area, has also come to light through studies carried out on the vulnerability of the aquifers and on the hydrological risk (Cimino et al. 2006).

The research carried out has revealed an extremely unacceptable quality of water analyzed, which only in some cases and only after appropriate treatment, could be re-used for various industrial purposes or for irrigation. This implies that it would be very important to prevent the pollution of the aquifers, attempting to mitigate all those factors that have a negative impact on the quality of the water supply destined for human use.

References

Antonioli F, Ferranti L, Sottosanti G (1993) Le grotte sommerse della Riserva dello Zingaro. Speleologia n. 29:36–42

Bartolomei C, Celico P, Pecoraro A (1983) Schema idrogeologico della Sicilia nord-occidentale. Boll Soc Geol It 102:329–354, 9 ff

Cassa per il Mezzogiorno (1976) Rilievo aereo multispettrale su alcuni tratti di costa siciliana. Rip. Progetti idrici (Div. 3) – Idrotecneco (Studio inedito)

Cassinis R (1967) Preliminari su una ricerca degli efflussi d'acqua dolce lungo le coste siciliane mediante misure di salinità in mare. Boll Geof Teor Appl 9:34, Trieste

Cimino A, Artico C, Orecchio S (2006) Gli acquiferi costieri del settore Bonagia-Cornino nel Trapanese: prime analisi dei processi di contaminazione in relazione con la vulnerabilità SINTACS. Thalassia Salentina 29(1):265–279

Celico P (1979) Legenda idrogeologica ragionata per i territori a prevalente componente carsica. Note Ist Geol Appl Napoli 15:54

Cusimano G, Frias F, Gatto L, Incandela A (2002) Assetto idrostrutturale dei Monti di Trapani (Sicilia nord-occidentale) e valutazioni delle risorse idriche immagazzinate. Speleologia Iblea 10:117–124

Pratelli W, Aiello MC (2002) Aspetti idrogeologici in relazione alla fenomenologia carsica dei Monti di Custonaci e San Vito Lo Capo. Speleologia Iblea 10:125–131

Ruggieri R (1996) Primo resoconto della campagna di ricerca speleologica realizzata dal C.I.R.S. a Custonaci (Tp). Atti del II Conv Reg di Spel, Catania, 1994

Ruggieri R (2000) Grotte e Carsismo. Vol. "La Riserva di Monte Cofano", coll. Sicilia foreste, a cura Foreste Demaniali Regione Siciliana

Ruggieri R (2002) Peculiarità geomorfologiche e speleologiche dell'area carsica di Custonaci (Tp). Speleologia Iblea 10:197–203

Ruggieri R (2009) Karst Itinerary and cave discovery in the Zingaro Reserve. Azienda Foreste Demaniali. Priulla, Palermo, pp 207

Ruggieri R, Messina Panfalone D (2011) Dentro e fuori la montagna. Palermo, Priulla, p 182

Sottosanti V (1994) Il patrimonio speleologico della Riserva Naturale dello "Zingaro". Boll Acc Gioenia Sci. Nat. 27(348):631–639

Chapter 6
Karst Geomorphological Features

6.1 Karst Features of the Study Area

Previously it has been noted how the main morphostructures constituting the Capo San Vito mountain ridges are expression of the phases of tectonic structuration and of the subsequent mechanical and gravitational dynamics and other denudational processes. On these main forms, and in particular on the outcropping carbonate rocks, a diverse series of solution phenomena both above and below ground has evolved, such as to confer on the whole area a quite unmistakable karst character (Ruggieri 2009; Ruggieri and Messina Panfalone 2011).

In this context, the objectives of this research have included both the survey of the surface karst morphologies, from the minor forms to those increasingly larger, being speleogenetically tightly linked to the surface forms as from these depends the diffuse or concentrate infiltration of waters, and the caves, these latters divided into karst caves and sea paleo-caves, described below.

6.2 Surface Karst Morphologies

These karst surface morphologies surveyed in the different areas of the Capo San Vito Mts. have been subdivided in elementary karren features, complex large-scale landforms and macro karst forms (see Table 6.1). The below reported description will consider both the genetic criteria, concerning the solution agent (Ginés 2009; Slabe 2009) and a morphotype criteria, which subdivided the karren forms into the following typologies: circular plan forms; linear forms hydrodynamically controlled; polygenetic forms (Perna and Sauro 1978; Ford and Williams 1989, 2007; Palmer 2007; Slabe 1995).

R. Ruggieri, *Speleological and Speleogenetic Aspects of the Monti di Capo San Vito (Sicily)*, Springer Theses, DOI 10.1007/978-3-319-21720-8_6

Table 6.1 Distribution of the main karst surface morphologies in the different outcropping limestone formations of the research area

Surface morphologies	Upper Triassic	Upper Triassic Liassic	Dogger Malm	Tithonian Lower Cretaceous	Middle Cretaceous	Upper Cretaceous Eocene	Lower Miocene
Microrills		x		x			
Rillenkarren	x	x		x	x		
Rinnenkarren	x	x	x	x	x	x	x
Wall karren	x	x	x	x	x	x	
Solution pans	x	x		x	x		
Grikes	x	x					
Subsoil forms	x	x		x	x	x	x
Boxworks		x		x			
Pinnacles forms	x	x		x	x	x	
Lim. pavements		x					x
Pendant forms					x		
Biokarstic holes		x			x		
Relict valley	x	x		x	x		
Dolines	x (collap.)				x (solution)		
Uvala	x						
Polje		x					

6.2.1 *Elementary Karren Features*

6.2.1.1 Tiny Water Films–Linear Forms Hydrodynamically Controlled

Microrills: Formed by thin water films derived from dew and driven by capillarity forces (Gomez-Pujol and Fornós 2009), the microrills usually appear as rectilinear incisions of about 1 mm wide and up to a couple of decimeters long. The grooves can also be with meandering forms as well as rectilinear and can also appear in the form of sub-parallel bunches, convergent or divergent in a fan shape. A few examples of microrills in sub-parallel bunch form is the one that was formed in the Norian-Liassic dolomitic and calcareous-dolomitic outcroppings in the Purgatorio plain (Fig. 6.1) and along the slopes of the Mt. Palatimone ridge (Fig. 6.2).

Fig. 6.1 Microrills on the Purgatorio plain

Fig. 6.2 Microrills on the limestone slopes of the Mt. Palatimone ridge

Fig. 6.3 Rainpits on limestone of the Rocca Rumena relict sea-cliff

6.2.1.2 Stormshowers–Circular Plan Forms

Rainpits–Solution pits–Boxwork forms: These are small dissolutional forms (Macaluso and Sauro 1996), defined by Ginés and Lundberg (2009), as small-scale free, single, circular hydrodynamically-controlled by droplet impact produced in a solutional environment of direct rainfall impact.

Boxwork forms are a particular type of rainpits, which occupy reasonable large, slightly inclined surfaces with a network of small polygonal enclosures separated by thin veins. The formation of these small reliefs can be attributed to selective solution processes when the presence of calcite veins turn out to be less soluble than the rock that contains them. Some examples of the above mentioned forms are observable in the biocalcarenites of the Upper Cretaceous of the Rocca Rumena relict sea-cliff (Fig. 6.3) where two genetic mechanisms, hydrodynamic and biogenic, seem to have occurred.

6.2.1.3 Direct Rainfall–Linear Forms Hydrodynamically Controlled

Solution flutes–Rillenkarren: these are the most frequent forms of solution found in the area, and are found on more or less inclined exposed surfaces not far from the watersheds of the rocky outcrops (a few centimeters or decimeters) subject to

Figs. 6.4–5 Rillenkarren in the Rocca Rumena's cliffs with ridges disturbed by different processes (case hardening by evaporation, biological actions, etc.)

Figs. 6.6–7 Rillenkarren in the Mt. Palatimone (*left*) and in the Mt. Zimmaria slopes

rainwater washing over them. The dimensions are about a centimeter wide and as long as a meter; the section is generally *U* shaped with sharp crests. Like the microrills, these morphologies can occur in bunches of sub-parallel with a convergent or divergent dendritic structure.

In the carbonate reliefs throughout the territory under study these forms of solution have been surveyed with particular frequency: on the Rocca Rumena cliff on its vertical slopes and also on its very little inclined shelf (Figs. 6.4–5), on the slopes of the Mt. Palatimone–Mt. San Giovanni ridge (Fig. 6.6), in the Mt. Zimmaria area (Fig. 6.7), in the Muciara area (Fig. 6.8), Purgatorio Plain area (Fig. 6.9), in the Bellazita area (Figs. 6.10–11), on the coastal belt of the Zingaro Reserve, between its northern entrance and Cala Tonnarella dell'Uzzo (Figs. 6.12–13, 6.14–15 and 6.16), in the Pizzo Passo del Lupo–Mt Acci (Figs. 6.17 and 6.18) and in the Piano dell'Arena-Scardina area (Figs. 6.19 and 6.20–21).

Figs. 6.8–9 Rillenkarren in the Muciara area (*left photo*); Rillenkarren in the Purgatorio plain (*right photo*)

Figs. 6.10–11 Rillenkarren in the Bellazita area

Figs. 6.12–13 Rillenkarren in the coastal slopes of the Zingaro Natural Reserve

Figs. 6.14–15 Rillenkarren in the coastal slopes of the Zingaro Natural Reserve

Figs. 6.16–17 Rillenkarren in the Zingaro area (*left photo*); Rillenkarren in the Mt. Acci slopes (*right photo*)

Figs. 6.18–19 Rillenkarren in the Mt. Acci area (*left photo*); Rillenkarren in Mt. Scardina area (*right photo*)

Figs. 6.20–21 Rillenkarren in Mt. Scardina area

6.2.1.4 Channelled Waterflow–Linear Forms Hydrodynamically Controlled

Solution runnels–Rinnenkarren: those solution karren appear in widths and depths of various centimeters and they can be many meters long. They can be rectilinear or assume a meandering form where the surface is less steep. More frequently found than the rillenkarren, they have been observed in the following areas: Via Madonna–Sciarotta (Fig. 6.22); Muciara area (Fig. 6.23); on Mt. Palatimone slopes (Figs. 6.24–25 and 6.26–27); on the coastal strip of the Zingaro Reserve between its northern entrance and Cala Tonarella dell'Uzzo (Fig. 6.28); on the slopes of the Rocca Rumena cliffs (Fig. 6.29).

Figs. 6.22–23 Rinnenkarren in the Madonna area (*left photo*); Rinnenkarren in the Muciara area (*right photo*)

Figs. 6.24–25 Rinnenkarren in the Mt. Palatimone ridge

Figs. 6.26–27 Rinnenkarren in the Mt. Palatimone slopes

Figs. 6.28–29 Rinnenkarren in the Zingaro coast (*left photo*); Rinnenkarren in the Rocca Rumena cliffs (*right photo*)

Figs. 6.30–31 Wall karren in the Rocca Rumena cliffs

Wall solutional runnels–Wandkarren: furrows, which develop on sub-vertical outcrops are present in several sectors of the area due to both sheet water and rivulets flowing down the bearing slope, the former called half-pipe wandkarren, the latter grike-like wandkarren (Verres 2009). Examples of these forms are present in the area of Rumena cliffs (Figs. 6.30–31), Sella Cofano (Fig. 6.32), in the area of Mt. Zimmaria (Fig. 6.33), in the Mt. Acci area (Fig. 6.34), in Noce area slopes (Figs. 6.35, 6.36, 6.37–38 and 6.39), in the Zingaro Natural Reserve coastal belt (Fig. 6.40).

Figs. 6.32–33 Wall karren in the Sella Cofano area (*left photo*); Wall karren in the Mt. Zimmaria area (*right photo*)

Figs. 6.34 Wall karren in the slopes of Mt. Acci (Zingaro Natural Reserve)

Fig. 6.35 Wall karren in the slopes of Noce area (Mt. Sparagio ridge)

Fig. 6.36 Wall karren in the Noce area

Figs. 6.37–38 Wall karren in the Noce area (*left photo*); Wall karren in the Noce area with hollows

Figs. 6.39–40 Wall karren in the Noce area (*left photo*); Wall karren in the Zingaro coastal area (*right photo*)

6.2.1.5 Standing Water–Circular Plan Forms

Kamenitzas–Solution pans–Phytokarst solution pans: morphologies, which collect meteoric water, with flat bottom and sub-circular or elliptical section, in diameter from a few centimeters to some meters, floored by a thin layer of soil, vegetation or algal remains, which cause dissolution. These solution forms (some of which with linear or meandering runnel outlet) have been observed in the following areas: Bufara (Figs. 6.41–42), Mt. Palatimone–Mt. San Giovanni (Figs. 6.43–44, 6.45–46 and 6.47), Rocca Rumena (Figs. 6.48 and 6.49), Tribli (Fig. 6.50), Sella di Cofano (Figs. 6.51–52), Purgatorio plain (Figs. 6.53, 6.54–55 and 6.56), Mt. Sparagio (Fig. 6.57), coastal belt, between the north entrance and the Cala Tonnarella dell'Uzzo of the "Riserva dello Zingaro" (Fig. 6.58), Noce area (Fig. 6.59), Muciara area (Figs. 6.60–61 and 6.62) and Piano dell'Arena area (Fig. 6.63).

Figs. 6.41–42 Solution pans in the Mt. Bufara area

Figs. 6.43–44 Solution pans in the pediment of Mt. Palatimone ridge

Figs. 6.45–46 Solution pans in the Mt. Palatimone area (*left photo*); Solution pans in the Mt. San Giovanni area (*right photo*)

Figs. 6.47 Large solution pan with micro-notch in the pediment of Mt. Palatimone ridge

Fig. 6.48 Solution pan in the Rocca Rumena

Fig. 6.49 Solution pan with micro-notch in the Rocca Rumena slope

Fig. 6.50 Solution pan in the Tribli area

Figs. 6.51–52 Solution pans in the Sella Cofano area

Figs. 6.53 Large solution pan in the Purgatorio polje

Figs. 6.54–55 Solution pans in the Purgatorio polje

Figs. 6.56–57 Solution pans with micro-notch in the Purgatorio polje (*left photo*); Solution pan in the Mt. Sparagio ridge (*right photo*)

Figs. 6.58–59 Relict of a solution pan partly destroyed by weathering in the Zingaro coastal belt (*left photo*); Solution pans with outlets in the Noce area (*right photo*)

Figs. 6.60–61 Solution pans with meandering runnels in the Muciara area (Mt. Sparagio ridge)

Figs. 6.62–63 Solution pan with outlet runnel in the Muciara area (*left photo*); Solution pan in the Piano dell'Arena area (*right photo*)

6.2.1.6 Sheet Wash Waterflow

Solution ripples: these wave-like forms, transverse to the downward water movement (Ginés 2009), were observed in the Upper Triassic–Lower Liassic dolomitic limestones outcropping in the Purgatorio plain (Figs. 6.64 and 6.65).

Fig. 6.64 Solution ripples in the dolomitic limestone of Purgatorio polje

Fig. 6.65 Close up of transitional forms between solution ripples and alveolar hollows

6.2.1.7 Infiltration–Linear Forms Fracture Controlled

Grikes/karst channels (*cleft*): these are fissures of even quite notable dimensions imposed on fractures or faults. A distinction can be made between 'trench-like grikes' if the bottom lies on a bedding plane or 'diaclase grike' if they tend to close down along the plane of the fracture (Sauro 1979). These morphologies are particularly common in certain areas of Mt. Palatimone slopes and pediment, reaching lengths of up to ten meters, widths from 1 to 3 m and depths from 2 to about 8 m (Figs. 6.66–67, 6.68–69, 6.70–71 and 6.72) and also in the Noce area of Mt. Sparagio ridge (Figs. 6.73–74 and 6.75).

Figs. 6.66–67 Diaclase grikes in the Mt. Palatimone slopes

Figs. 6.68–69 Trench-like grikes in the Mt. Palatimone ridge (bogaz)

Figs. 6.70–71 Wide grikes (bogaz) in the slopes of Mt. Palatimone ridge

Fig. 6.72 Bogaz type depression (karst corridor) closed with walls to obtain a water reservoir for grazing animals in the Mt. Palatimone pediment

Figs. 6.73–74 Diaclase grikes in the Noce area (Mt. Sparagio ridge)

Fig. 6.75 Crossing of diaclase grikes in the Noce area (Mt. Sparagio ridge)

6.3 The Epikarst Pattern and Its Subcutaneous Rock Forms

Thanks to the presence of the numerous quarry scars, it has been possible to observe the structure of the epikarst that is present in the upper parts of the limestone outcrops, both in the Mt. Palatimone ridge and that of Mt. Sparagio. In most cases it is possible to observe, starting from the surface, variable thickness of epikarst characterized by subsoil morphologies ranging from a few meters to tens of meters followed by a vadose zone with shafts located along faults or fractures.

In particular, it is possible to observe an epikarst zone, which is highly karstified and fractured, made from a range of forms, which will be described further down, and a vadose zone from, which shafts open with blind terminations at their tops (Fig. 6.76). The passage from the epikarst zone to the vadose zone is not linked to lithological changes but to the decreasing number of fractures.

The hydrological situation also changes from one of high hydraulic conductivity in the epikarst zone to a concentrated flow present in the vadose zone, which is responsible for the presence of the numerous shafts (Klimchouk et al. 1996). The main epikarstic features characterizing such a hydrologic zone will be discussed in the next chapters.

Fig. 6.76 Blind head of a shaft (Zubbia Cocuccio) opened up at the base of a cut-wall of a quarry in the Mt. Sparagio ridge

6.3.1 Soil Percolation Rock Forms

Rock forms due to the percolation of water through the soil or sediments, or to the flow of water at the contact between the rock and soil have been observed in the area of research. In this regard, according to Perna and Sauro (1978), Ginés (2009), Zseni (2009) and Slabe and Liu (2009), these forms have been classified as follows:

Subsoil karren of micro-cuestas type: these forms, outcropping from the soil with the heads of the layers linked to the dip of the bedding planes, are diffusely present in the area of Giacolamaro of Mt. Sparagio ridge (Figs. 6.77–78).

Figs. 6.77–78 Micro-cuestas type subsoil karren in the Giacolamaro area (Mt. Sparagio ridge)

Rundkarren–Rounded runnels: furrows with smoothed ribs and/or rounded cross-sections are present in the Zimmaria–Gnarosa area (Figs. 6.79–80); in the Noce area (Fig. 6.81); in the Giacolamaro area (Fig. 6.82); in the Purgatorio polje (Fig. 6.83) and in the Palatimone slopes (Fig. 6.84).

Smooth surface–Subcutaneous karren forms: smooth rock surfaces related to subsoil corrosion are present in the Mt. Acci area of the Zingaro Reserve (Fig. 6.85), in the Bellazita area (Fig. 6.86) and in the Noce area (Fig. 6.87).

Subsoil pinnacles: deltoid forms delimited by cutters or grikes filled with soil were observed on the cut-walls of the quarries in the Noce area (Figs. 6.88 and 6.89).

Subsoil cups: circular or elongated forms arranged in steps in a rounded limestone outcrop, are present in the Mt. Zimmaria area (Fig. 6.90) probably due to the soil percolation water.

Subsoil scallops: shallow forms in overhanging surfaces due to the flow of water along the permeable contact of the rock with the soil (Slabe and Liu 2009) were observed in the Noce area (Fig. 6.91).

Figs. 6.79–80 Rundkarren with wallkarren in the Zimmaria—Gnarosa area

Figs. 6.81–82 Rundkarren in the Noce area (*left photo*); Rundkarren in the Giacolamaro (Mt. Sparagio) (*right photo*)


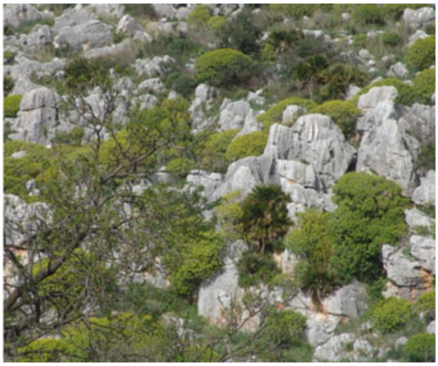

Figs. 6.83–84 Rundkarren in the Purgatorio plain (*left photo*); Rundkarren in the Mt. Palatimone slopes (*right photo*)


Figs. 6.85–86 Smooth surface in the Mt. Acci area (*left photo*); Smooth clint surface in the Bellazita area (*right photo*)


Figs. 6.87–88 Smooth surface below rillenkarren in the the Noce area (*left photo*); Subsoil pinnacles in the Noce area (*right photo*)

Figs. 6.89–90 Subsoil pinnacles in the Noce area (*left photo*); Subsoil cups in the Mt. Zimmaria area (*right photo*)

Figs. 6.91–92 Subsoil scallops in the slopes of Noce area (*left photo*); Cutter, pipes and tubes in a quarry of Mt. Palatimone ridge (*right photo*)

Cutters: great vertical forms like grikes but larger than 1 m filled with soil, were observed in the cut wall of a quarry in the Mt. Palatimone ridge (Fig. 6.92).

Subsoil pipes: vertical holes with depth/wide > 2 (Zseni 2009) were observed in the Tribli area (Fig. 6.93) and in the Cocuccio area (Fig. 6.94).

Subsoil tubes: Subcutaneous inclined pipes (Zseni 2009) are present in the Cocuccio area (Figs. 6.95–96).

Subsoil hollows–Subcutaneous cavernous karren: These can be defined as openings, with dimensions from a few centimeters to a couple of decimeters, generally with sub-circular or sub-elliptical sections, more or less elongated and having the origin following a fissure. More articulated forms can occur through the


Figs. 6.93–94 Subsoil Pipes in the epikarst of Tribli area (*left photo*); Subsoil pipe in the Cocuccio area (*right photo*)


Figs. 6.95–96 Subcutaneous tubes and pipes in the epikarst of Cocuccio area Mt. Sparagio ridge

anastomosis of contiguous holes due to the progressive corrosion of their walls. Examples of these morphologies have been observed in the Portella di Baida area (Mt. Sparagio ridge) (Fig. 6.97) and in the Mt. Palatimone slopes (Fig. 6.98).

Subsoil spongework forms: These morphologies show variously vacuolated or sponge-like forms, and result from selective weathering or karst corrosion, or both, on carbonates characterized by a different degree of cementation. Typical examples in the area are those that can be seen in Zingaro coastal slope (Fig. 6.99) and in the Giacolamaro areas (Fig. 6.100). Similar morphologies can be observed in the Mt. Speziale and Pianello area: they are connected to selective erosion and corrosion of the Upper Triassic floury dolomites.

Subsoil notches: notches probably due to the corrosion of a steep rock surface along a long-lasting level of sediment surrounding (Slabe 2009) have been observed in the Mt. Passo del Lupo slope (Figs. 6.101–102).

Figs. 6.97–98 Subcutaneous hollows in Portella di Baida area (*left photo*); subsoil cavernous karren in the Mt. Palatimone slopes (*right photo*)

Figs. 6.99–100 Subsoil spongework in the Zingaro Natural Reserve (*left photo*); subsoil spongework in the Giacolamaro areas, Mt. Sparagio (*right photo*)

Figs. 6.101–102 Subcutaneous notches in the Mt. Passo del Lupo slopes

6.4 Complex Processes–Polygenetic Forms

Pinnacles–Spitzkarren–Pinnacle karrenfield: these morphologies are residual forms (Zseni 2009), whether they are single examples or in groups, in the form of towers, peaks (pinnacles) and spires of various dimensions reaching diverse meters height. They are the result of selective erosion and phenomena of karst solution. In this regard, while harsh, furrowed morphologies and sharp crests bear evidence to erosive processes intervening in a more general context of the planation of surfaces, rounded forms, on the contrary, manifest corrosive processes at work in *covered karst* conditions, initiated in a situation of a rock surface mantled by an eluvial cover, subsequently removed by erosion. On the inclined surface of these larger forms *karren* of various forms and dimensions can be found (microrills, rillenkarst and rinnenkarst), as well as solution pans in the sub-flat parts and biokarst honeycomb formations, such as those described in the previous chapters.

A classic example of covered karst morphology can be seen in Noce area, where the excavation of a quarry allows one to observe the fragmentation of the apical portion of the massive rocky structure covered by soil, which was caused by karst corrosion working at the rock-soil contact. This action of dissolution has, on the one hand, enlarged the part of the fracture nearest to the surface and, on the other, acting in a uniform manner on the rock walls, has modeled out a general bevelled, rounded morphology. The pinnacles and spires on top of the front of the quarry are, on the other hand, expression of a past condition of covered karst, which evolved into uncovered karst by the fact that the soil has been eroded, with the consequent formation of both *karren*, corrosion holes and selective erosion morphologies. Of this latter morphology the zones of pinnacles and spires are found at Noce area (Figs. 6.103–104), Mt. Palatimone (Figs. 6.105–106 and 6.107), Mt. Zimmaria (Fig. 6.108), Ferle area in the Mt. Sparagio ridge (Figs. 6.109–110 and 6.111) and in the Zingaro Natural Reserve (Figs. 6.112–113, 6.114–115, 6.116–117, 6.118 and 6.119).

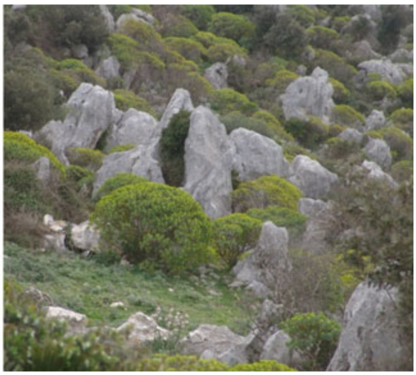

Figs. 6.103–104 Pinnacles rising up from subsoil in the Noce area (Mt. Sparagio ridge)

Figs. 6.105–106 Pinnacles in the Mt. Palatimone slopes

Figs. 6.107–108 Pinnacles in the Mt. Palatimone slope (*left photo*); Pinnacles in the Mt. Zimmaria slope (*right photo*)

Figs. 6.109–110 Pinnacles in the Mt. Sparagio area (*left photo*); Pinnacles–Stone forest area in the Ferle area (*right photo*)

Figs. 6.111 Pinnacles–Stone forest in the Ferle area (Mt. Sparagio ridge)

Figs. 6.112–113 Pinnacles and spires in the Pianello area (Zingaro Natural Reserve)

Figs. 6.114–115 Pinnacles in the Pianello area (*left photo*); Pinnacles in the Mt. Speziale slope (*right photo*)

Figs. 6.116–117 Pinnacles in the Monte Passo del Lupo (*left photo*); Pinnacles in the Sughero area (Zingaro Natural Reserve) (*right photo*)

Figs. 6.118 Pinnacles in the Zingaro Natural Reserve

There is a very particular, and in many ways a most enchanting, mesostructure in the Portella San Giovanni (Zingaro Natural Reserve) half a kilometer long, called the *Dragon*, derived by selective erosion/corrosion processes (Fig. 6.120).

Limestone pavements: these morphologies generally consist of a complex of flat rock surfaces (clints–flachkarren) delimited by a network of grikes and sculptured by different types of forms created by the solution of running water. They usually cover surfaces of several square meters sometimes channeled along pre-existent micro fractures. In the study area examples of *limestone pavements* have been

Figs. 6.119–120 Pinnacle and spires in the Pizzo Passo del Lupo area, Zingaro Natural Reserve (*left photo*); Ridge in the Portella San Giovanni of Zingaro Natural Reserve (*right photo*)

observed in some sectors of Tribli area (Fig. 6.121), in the Palatimone dolostones (Fig. 6.122), in the Noce area (Figs. 6.123–124), in the Purgatorio plain (Fig. 6.125), in the biocalcirudite outcrops of Bellazita area (Fig. 6.126), in the

Figs. 6.121–122 Limestone pavement in the Tribli area (*left photo*); Limestone pavement in the Mt. Palatimone slopes area (*right photo*)

Figs. 6.123–124 Limestone pavement in the Noce area (Mt. Sparagio ridge)

Figs. 6.125–126 Limestone pavement in the Purgatorio polje (*left photo*); Limestone pavement in the Bellazita area (*right photo*)

Muciara area (Fig. 6.127), on the southern foothill sector of Mt. Acci in the Zingaro Reserve (Figs. 6.128, 6.129), in the Piano dell'Arena–Mt. Scardina area (Fig. 6.130).

Pendants/cloud forms and bowls: hemispheric cloud-type forms, about a decimeter in size, and bowls, the former originated by selective erosion and solution processes along a bedding plane parting. These morphologies are present on the small folded strata of the Tribli cliff (Figs. 6.131 and 6.132).

Fig. 6.127 Limestone pavement in the Muciara area (Mt. Sparagio ridge)

Fig. 6.128 Limestone pavement in the Mt. Acci area (Zingaro Natural Reserve)

Figs. 6.129–130 Limestone pavement in the Mt. Acci area (*left photo*); Limestone pavement in the Piano dell'Arena–Mt. Scardina area (*right photo*)

Fig. 6.131 Pendants and bowls in the bedding plane and layers of the Tribli cliff

Fig. 6.132 Close up of biokarst bowls on the limestone layers of Tribli cliff

6.4.1 Biokarstic Borings and Lichen Karren

Biokarst holes and honeycomb forms: these are small cylindrical or hemispherical cavities, only a few centimeters wide, that appear on calcareous walls usually clustered together or intersected with each other forming honeycombed structures. The phenomenon of their construction, called "saxicavismo", has been attributed to the secretion of certain acids by a gastropod mollusc [the *pulmonata stylommatophora*] (Sacchi 1955) often observed nesting in these honeycomb formations. In the karst area being studied, biokarst holes and honeycombed morphologies have been observed just about everywhere.

They are particularly apparent on Noce area (Figs. 6.133–134 and 6.135–136), on the Purgatorio plain (Fig. 6.137), on the slopes of the Rumena cliff (Fig. 6.138), in the Sella Cofano area (Fig. 6.139), in the area of Mt. Zimmaria (Fig. 6.140), in the area of Portella di Baida (Fig. 6.141), on Mt. Palatimone.slopes (Figs. 6.142 and 6.143), in Cocuccio area (Fig. 6.144), in the coastal slopes (Figs. 6.145, 6.146 and 6.147–148) and in the Canalone of Mastro Peppe Siino of the Zingaro Natural Reserve (Fig. 6.149).

Biokarst borings and lichen micro-karren: these morphological type, in which the term 'karren' is used in the widest sense, has been observed as micro-pit and phyto-crusts on the Lower Miocene biocalcarenite outcrops in the Purgatorio plain (Fig. 6.150) and in the form of a labyrinthine design of a network of sinuous lichen canalicula, divided by rounded borders, in the Portella San Giovanni ridge (Fig. 6.151).

Figs. 6.133–134 Alveolar hollows on the limestone slopes of Noce area (Mt. Sparagio ridge)


Figs. 6.135–136 Alveolar hollows probably caused by karst solution along flutes (*left photo*); Borings in the Noce area (*right photo*)


Figs. 6.137–138 Alveolar hollows on the dolomitc limestone of Purgatorio plain (*left photo*); Cluster of borings in the Rocca Rumena cliff (*right photo*)


Figs. 6.139–140 Cluster of borings in the Sella Cofano area (*left photo*); Cluster of borings in the Mt. Zimmaria area (*right photo*)

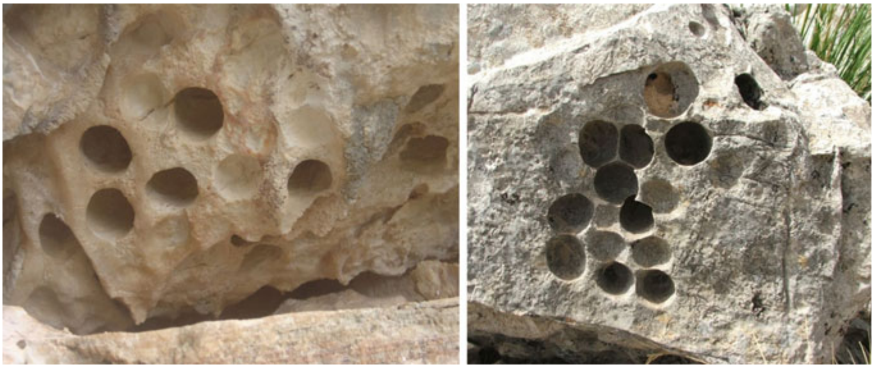

Figs. 6.141–142 Borings in the Portella di Baida area (*left photo*); Cluster of borings in the Mt. Palatimone area (*right photo*)

Fig. 6.143 Cluster of borings in the Mt. Palatimone pinnacles

Fig. 6.144 Cluster of borings in the Cocuccio area (Mt. Sparagio ridge)

Fig. 6.145 Poligenetic micro-alveolations on the limestone coastal slope of the Zingaro Natural Reserve

Fig. 6.146 Biokarstic circular bowls on a limestone layer of the Zingaro Natural Reserve

Figs. 6.147–148 Cluster of borings in the Zingaro Natural Reserve coastal area

Fig. 6.149 Cluster of borings with colonization of lichens in the Canalone di Mastro Peppe Siino (Zingaro Natural Reserve)

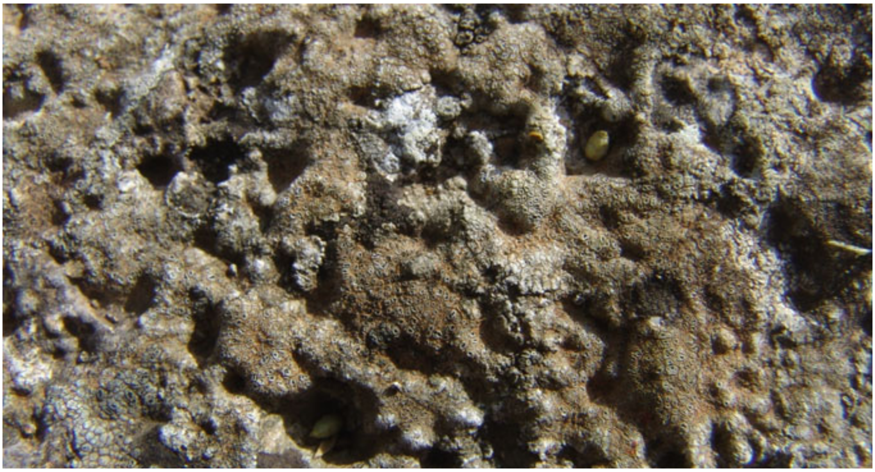

Fig. 6.150 Biokarstic borings and lichens on the biocalcarenites of Lower Miocene in the Purgatorio polje

Fig. 6.151 Lichen micro karren on the dolomitic limestone of Portella San Giovanni ridge

6.5 Macro Karst Forms

Karst Valleys/Gorges: those valleys come into this classification, which apart from having been subject to the fluvial erosive processes, also demonstrate specific karst characteristics both of the morphological (the forms of the valleys, the existence of caves, etc.) and the hydrological types (swallow holes, springs, lack of water, etc.). Relict *fluviokarst* valleys are those which, for tectonic reasons (elevations or dislocations), are no longer able to carry out any real or important function of superficial drainage, because they are no longer connected to the active hydrographic net, which covers and cuts into the surrounding territory. They represent, then, a condition of relict morphology of past fluvial erosive processes. In the study area both types of fluviokarst valleys, the active and the relict, are present.

The Cipolazzo *gorge* falls into the first morphology of fluviokarst valleys, the active one. It is located in the north-west sector of Mt. Palatimone ridge. This morphology is a classic example of a karst gorge forming a deep narrow gash a few meters wide, which runs for about 550 m along a NW-SE oriented tectonic discontinuity. Along its course there are various erosive and corrosive morphologies to be seen: giant potholes, which form large deep pools of various dimensions at the foot of the high vertical walls; segments with step-like morphologies where the layers from massive become thinner; swallow holes, sink caves and various karst

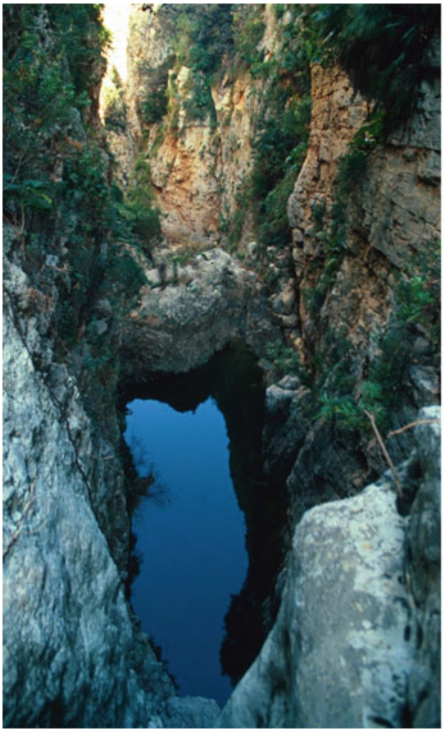

Figs. 6.152–153 Cipollazzo fluviokarstic gorge

corrosion morphologies on the walls (Fig. 6.152). The *Gole di Cipollazzo* constitute the superficial, and in part subterranean, water drainage collecting system for the Purgatorio polje directed towards the westernmost part of the Castelluzzo plain. Tectonics and the processes of karstification have also created particular morphological conditions known as a *hanging valley*, with its difference of altitude of 40 m vis à vis the plain (Fig. 6.153).

The best known large fluviokarst gully morphologies are the NE-SW and WNW-SSE orientated ones that dissect the western slopes of the Zingaro Natural Reserve channeling, with considerable kinetic energy given the high gradients involved, the water flow towards the coastal strip below (Figs. 6.154, 6.155 and 6.156).

Among the morphologies to be included in the relict *fluviokarst* valley category one should note two dry valleys in the Muciara area, separated by a structural high, one constituted by a NNW-SSE oriented depression, which extends for about 720 m and about 90 m wide, filled with basalts, the second extending for about 400 m with WSW-ENE direction and about 50–90 m wide in which eluvial and colluvial deposits *outcrop*. These depressions are surrounded by slopes about 5–10 m high, which are carved by rinnenkarren forms. The first depression constitutes a monoclinal small dry valley interested on the limestone slopes by corrosive karst processes, with a flat bottom cutting an intrusive basalt body (Fig. 6.157). Instead

Fig. 6.154 Fluviokarstic canyons along the Zingaro coastal belt

Fig. 6.155 Canyon in the coastal belt of the Zingaro Natural Reserve

Fig. 6.156 Gorge along the coastal belt of the Zingaro Natural Reserve

Fig. 6.157 Monoclinal small dry valley with flat bottom cutting an intrusive basaltic body in the Muciara area

Fig. 6.158 Relict dry fluviokarst valley with trending WSW-ENE in the Muciara area

the second, as will be discussed in the following chapters, constitutes a relict fluviokarst valley outlet of the Purgatorio polje (Fig. 6.158).

There is a third fluviokarst depression at Piano delle Ferle, which extends in a WNW-ESE direction for about 500 m and is about 35 m wide and surrounded by low slopes. These depressions owe their origin to tectonic events, which controlled the main directions in which they developed. They evolved in relation to the concurrent processes of fluvial erosion, selective erosion and karst corrosion, followed by an inactivation process caused by tectonic events, the dislocation of which modified their original hydrostructural context.

6.5.1 Closed Depressions

Swallow holes: these small closed forms of swallowing intermittent surface water flow (Bini et al. 1986) have been observed both on Mt. Sparagio in the Colma di Mezzo area (Fig. 6.159) and, in greater numbers, on the Purgatorio Plain, where they appear as small closed depressions, covered by detritus and stones (Fig. 6.160), or as impenetrable holes (Fig. 6.161), or as elongated apertures over fractures (Fig. 6.162).

Fig. 6.159 Swallow hole in the Mt. Sparagio area

Fig. 6.160 Swallow hole in the Baglio Messina area, Mt. Sparagio

Fig. 6.161 Swallow hole in the Purgatorio polje

Fig. 6.162 Swallow hole in the Purgatorio polje

Dolines: the most frequent genesis of these macro-morphologies is *normal solution* of the rock by running water attracted by centripetal movement towards an absorbent point. Another regular genesis can be the collapse of the ceilings of a cave (*collapse doline*), more or less close to the ground surface, which can make this type of morphology appear like a shaft, sometimes a deep one (Sauro 1995, 2003). This type of karst macroform is present in the study area both in *normal solution* and collapse forms. The most interesting example of collapse doline, in terms of dimensions, is the Bufara doline, which lies below the mountain of the same name: it is elliptical in form, has a major axis of 300 m, a minor one of 230 m and an average depth of 49 m (Figs. 6.163 and 6.164). This collapse depression is probably linked also with intersection of old paleokarstic features.

The *Zubbia della Ficara* in the summit area of the Zingaro Reserve is of the *collapse doline* typology (Fig. 6.165). Smaller depressions, but of the solution type, are present in the proximity of the Bufara doline in sub-circular form with a diameter of 110 m, on Mt. Sparagio at the foot of the Colma di Mezzo relief in sub-elliptical form with dimensions of 50 by 25 m (Fig. 6.166), and again on Mt. Sparagio but in the Cocuccio sector in a roughly sub-elliptical form and dimensions of about 45 by 33 m.

Fig. 6.163 Bufara doline (Mt. Bufara area)

Fig. 6.164 View of the inner part of the Bufara doline

Fig. 6.165 Ficara collapse doline in the Pianello area (Zingaro Natural Reserve)

Fig. 6.166 Colma di Mezzo solution doline in the Mt. Sparagio ridge

Uvalas: Closed depressions (Čalić 2011) which extend with trending NNW-SSE are present in the summit part of the Zingaro Natural Reserve (Pianello area) (Figs. 6.167 and 6.168). They show a flat bottom, filled with several meters of red clay (terra rossa), and are delimited by slopes of both tectonic and erosive origin, with local phenomena of surface faulting. They are probably linked to several episodes of deep-seated gravitational deformations, which affected the area in connection with strong earthquakes (Agnesi et al. 1984, 1987, 1989, 1995), with following deepening of the structural depression due to karst solution process. At this regard, they could be classified as tecto-karstic small uvalas (Sauro 2012).

Polje: part of the Purgatorio plain, because of its morphological, structural and karst characteristics, forms a large polje that extends in WNW-ESE direction for about 4 km with an area of about 6.4 km^2. This flat-surface depression is bordered to the north by the slopes of the Mt. Palatimone–Mt. San Giovanni ridge, on the south by the Mt. Sparagio ridge and on the west by the relief of Mt. Zimmaria and Mt. Bufara (Fig. 6.169). From a structural point of view, evidence of fault contact can be recognized on the northern and western side, while on the southern side an over thrusting limit has been identified by Abate et al. (1993) or a reverse fault by Catalano et al. (2011).

As far as the lithological profile is concerned the following terrains outcrop in this structure: Norian-Liassic dolostones and Tithonian-Lower Cretaceous calcirudites, breccia and calcarenites, which form a 300–500 m wide belt on the northern

Fig. 6.167 Small uvalas type depression with trending NNW-SSE in the Pianello area of the Zingaro Natural Reserve

Fig. 6.168 Small uvala type depression in the Pianello area of the Zingaro Natural Reserve

side, morphologically constituting a pediment formed by the retreat of Mt. Palatimone's slopes; Lower Pliocene bioclastic calcarenites and sands, which outcrop in the central sector of the plain, passing into lacustrine silts and sands towards the north-west; pelites and Langhian-Middle Tortonian quartzite sands outcropping in the southern sector right up to the boundary with the slopes of the Mt. Sparagio ridge.

Fig. 6.169 General view of the Purgatorio polje

From data obtained during a 264 m deep drilling for water wells on the Purgatorio polje carried out in the area of the Lower Pliocene calcarenites outcroppings, the following lithological sequence was identified: calcarenites of up to 48 m thick laying over Miocene clays, themselves about 16 m deep, in their turn covering Upper Triassic dolostones and limestones. The above mentioned stratigraphy, in the structural and stratigraphic context of the outcroppings surveyed in the plain, shows a paleogeographic condition of the Purgatorio depression, previous to the polje formation, characterized by the presence of a morpho-tectonic depression in which the calcarenites of the Lower Pliocene sediments were deposited.

As far as the surface hydrology is concerned the polje shows two shallow incisions that originate on the slopes of Mt. Sparagio and run south-north, the waters from both being captured by swallow holes. On the north-west border the deep fluviokarst *Cipollazzo gorge* is, as we have already described, the only outlet for the superficial water-flow coming from the clay and sandy terrain of the plain.

Relict fluviokarst morphologies attributable to a past drainage condition with an outlet in the Muciara area are recognizable in the south-west sector of the polje in Mocata-Cofanello sector. In this regard, it has been hypothesized that this fluviokarst inactive structure was connected in the past with the neighbouring depression of Muciara area, which is now separated because of the effects of tectonic dislocation. Given this hypothesis, which will be discussed in the Chap. 8 of this study, it would seem plausible that the formation of the Bufara doline was connected with these dry fluviokarst depressions, fed by less permeable clay part of the basin of the Purgatorio polje (Fig. 6.170). The most markedly karst character of the Purgatorio polje, however, is to be found in the north sector where there are Triassic dolostones

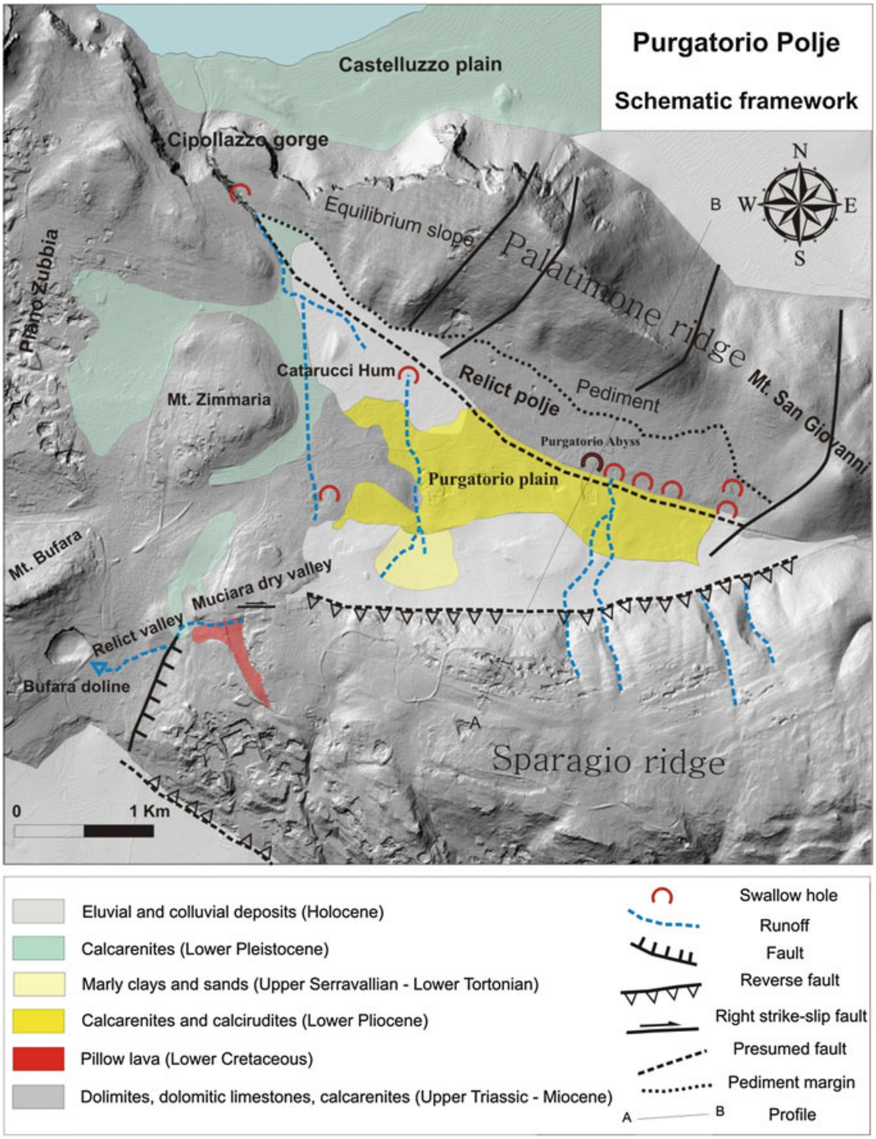

Fig. 6.170 Map of the Purgatorio polje (lithology from Catalano et al. 2011) (*Hillshade map from* DEM Regione Siciliana 2007–2008)

outcropping and a various series of both surface and subterranean morphologies. Particularly significant concerning the origin and evolution of the polje is the series of swallow holes, along a belt close to the presumed fault line between the Lower Pliocene calcarenites and the outcropping dolomites that capture both the running water coming down from the slopes of the Mt. Sparagio ridge and, also, the runoff

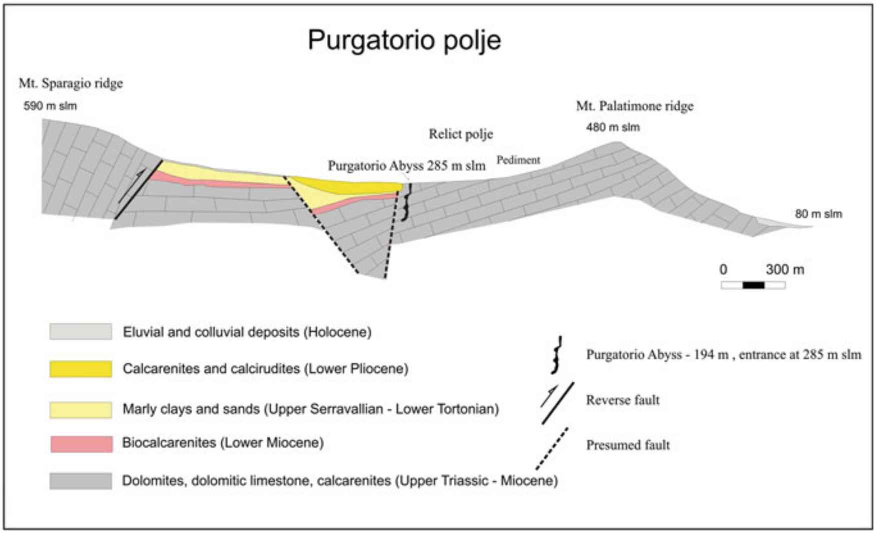

Fig. 6.171 Profile A–B of the Purgatorio polje (see map of Fig. 6.170)

accumulated on the Mt. Palatimone rocky pediment. In the general morphological context of the polje, which is constituted by ample flat surfaces, the isolated reliefs of Cozzo Cataruccia and Cofanello are singular, and constitute relict morphologies (hum type) of the previous relief worn away by the processes of erosive planation and karst corrosion.

Finally as evidence of the intense processes of karstification that have been going on the underground area of the polje, there are numerous vertical caves, some of them of considerable depths, which will be described further on (Fig. 6.171).

6.6 Karst Cave Morpho-Tectonic Structures

For the purposes of this research 40 caves were analyzed, subdivided into five areas (Sites *a*-*b*-*c*-*d*-*e*), hypothesizing in the context a certain concurrence in the principal structural, hydrological and hydrogeological lineaments that characterize the single aforementioned sites (e.g. the main structural trend, the morphological context, the aquifer area of recharge, etc.). Within these areas, where the conditions warrant it, the caves have been further subdivided into karst caves in the strict sense of the definition, i.e. those originating from dissolutional processes, and structural caves linked to only tensional/extensional tectonics.

For every cave the main characteristics have been noted with regard to their lithology, morphology (karren, deposits, etc.), hydrology (vadose, phreatic), structure (faults, joints), speleometry, so that they can be collocated in the tectonic-deformation setting that has characterized the territory under study, and also with a view to formulation of an evolutive-speleogenetic model influenced by past climatic conditions. These latter are further treated in Chap. 7 dealing with the structural control on the speleogenetic processes.

With this premise, the caves have been divided as follows:

- The caves in the Mt. Bufara–Cerriolo–Piano Zubbia areas (Site *a*)
- The caves in the Mt. Palatimone–Mt. San Giovanni ridge (Site *b*)
- The caves in the Purgatorio polje (Site *c*)
- The caves in the Mt. Sparagio ridge (Site *d*)
- The caves in the Mt. Monaco–Mt. Speziale–Mt. Scardina ridge (Site *e*)

6.6.1 The Caves in the Mt. Bufara–Cerriolo–Piano Zubbia Area (Site a*)*

In this area Upper Cretaceous carbonates outcrop (limestones, biocalcarenites and biocalcirudites) with dips generally to SW and dissected by NE-SW and E-W structures (see Fig. 4.3 of the Chap. 4). Four of the most interesting karst caves in the study area are situated in this sector of the Custonaci territory, they are: the Grotta del Fantasma, the Grotta della Clava, the Grotta Maria SS. di Custonaci and the Grotta Cerriolo (Fig. 6.172).

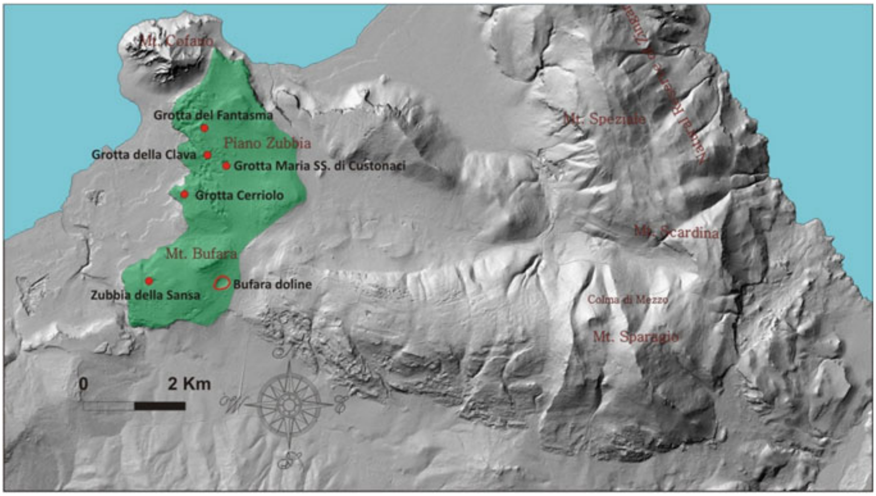

Fig. 6.172 Location of the Caves in the Mt. Bufara–Cerriolo–Piano Zubbia area (*green sector*) (*Hillshade map from* DEM Regione Siciliana 2007–2008)

The Grotta della Clava: the cave, which is situated in the Piano Zubbia area within the Municipality of Custonaci, opens at 190 m asl, extends for 759 m, and descends for a total of 89 m. It developed along a system of fractures, which dip to N 40 at 75°, and which gradually dissect at depth the bedding planes of the Upper Cretaceous limestone dipping to N 240 at 20° (see stereogram of Fig. 6.173 and Table 6.2).

This structural situation characterizes the general trend of the cave, which consequentially developed principally in a downwards direction, interrupted by sharp upward tracts where fractures have occurred, and less violent slopes caused by strata collapses at fractured intersections or bedding plane partings. Subsequent phenomena of widening and filling—connected respectively to collapse and the deposits of calcite concretions—have occurred, sometimes with results that have significantly modified the environment.

From the hydrological point of view the cave remains entirely in the vadose zone, its phreatic zone being unreachable speleologically, because of the occlusion of the vertical conduits on the fracture due to collapsing in the east part and to calcite fillings in the lower west section.

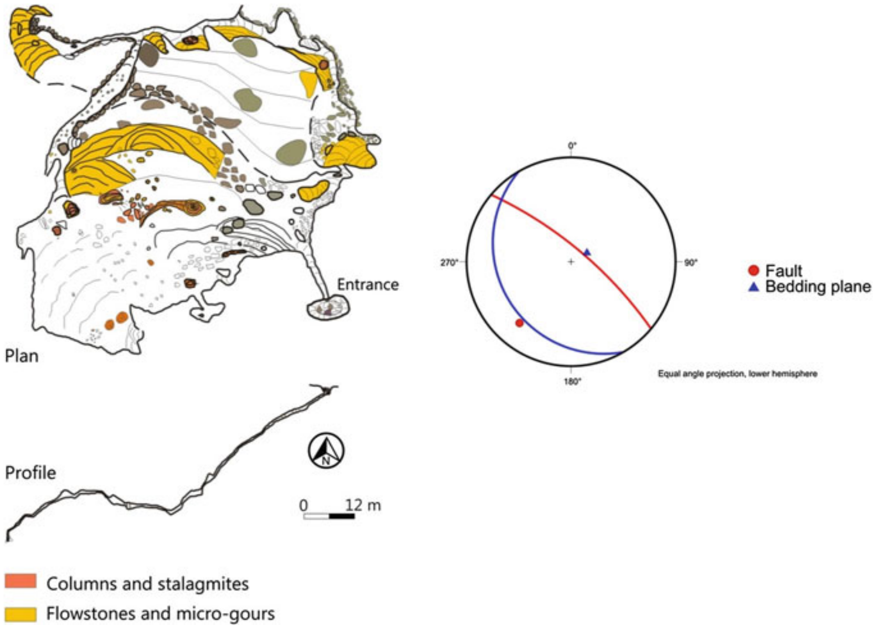

Fig. 6.173 Map of Grotta della Clava and stereogram of the main geological structures

The *Grotta della Clava* is one of the most interesting caves for the richness, variety and beauty of speleothems. In this regard, in the upper sector, very impressive and varied morphologies of calcite deposits, both in form and dimension, can be observed: groups of stalagmites, large columns, stalactites, helictites, draperies, etc. (Figs. 6.174, 6.175 and 6.176). In other parts one can also see columns broken off (Fig. 6.177) probably due to tectonic movements (Cucchi et al. 1983; Šebela 2008, 2010) and corroded calcite deposits probably caused by condensation-corrosion processes.

Fig. 6.174 Columns and speleothems in the Grotta della Clava

Fig. 6.175 Widespread flowstones

Fig. 6.176 Clava-forms speleothems

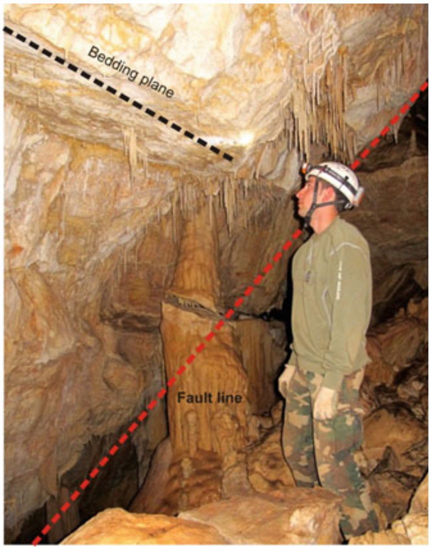

Fig. 6.177 Evidence of a fractured column and axis deviation from vertically probably due to tectonic movements along the fault

The Grotta Maria SS. di Custonaci: the cave, located in the Scaletta area in the Municipality of Custonaci, has its entrance at 152 m asl, extends for 1,321 m, and descends for a total of 90 m. The cave extends for about 1 km along a fault with dip to N 230 at 80°, reaching a depth of −90 m from the entrance. This structure dissects the bedding planes of the Upper Cretaceous limestone with dip to N 200 at 40° in the medium-upper sector and to N 225 at 50° in the medium-lower sector (Fig. 6.178 and Table 6.2). These geological structures causes steep-to-vertical descending tracts linked to less inclined tracts, where signs of collapsed rocks and deposits of calcite can be present. In the south-east sector the deepening of the cave along a geological discontinuity with dip to N 230 at 80° is evident.

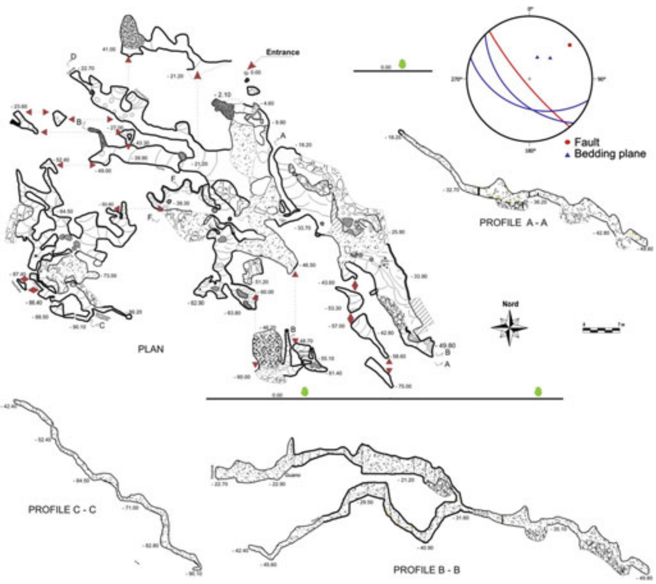

Fig. 6.178 Map and stereogram of the main geological structures of Grotta Maria SS. di Custonaci

From the hydrological point of view the cave remains mostly in the vadose zone, until a depth of about 85 m, while in the sector below phreatic corrosive morphologies are present. The cave presents various speleothems (Fig. 6.179) some of which show clear breaks probably due to tectonic movements (Figs. 6.180 and 6.181–182).

Figs. 6.179–180 Widespread flowstones (*left photo*); Broken large stalagmite columns (*right photo*)

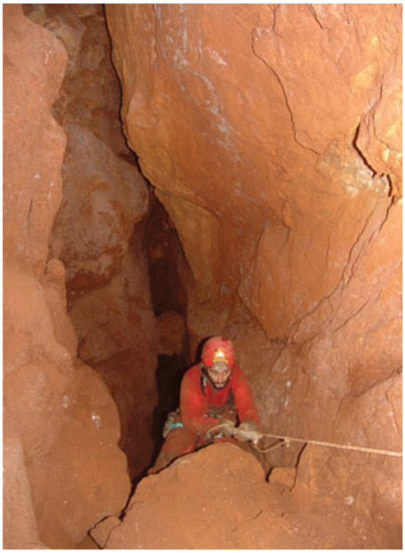

Figs. 6.181–182 Deflected and broken columns (*left photo*); Shaft along a NW-SE oriented fault (*right photo*)

The Grotta del Fantasma: The cave opens at 198 m asl in a small closed depression in the area of Piano Zubbia, intensively exploited for its "marbles" in several quarries (Ruggieri and Messina Panfalone 2011). It extends for 1,138 m, reaching a depth of 149 m. The cave developed in the Upper Cretaceous calcarenites and, from the morpho-structural point of view, can be subdivided into the following four main sectors (Fig. 6.183).

Upper-middle part: After a first part, from the entrance, developed along a bedding plane with dip to N 200 at 25°, it extends on a fault with dip to N 130–150 at 75°. The characteristics are vertical for the first 10–15 m., followed by a less steep tract full of collapsed blocks of various dimensions.

Lower-middle part: from the *Sala della Medusa* to the *Sala della Balena*: this part extends along flat strata with dip to N 140 at 36°. The general characteristics are of a slide covered by calcite crusts and occasional rock collapse.

Lower part: which corresponds to the *Sala del Fantasma*, a large collapse chamber bordered by fractures with dip to N 210–225 at 80° and also characterized by the presence of considerable calcite and detritic deposits, both of them particularly modified chemically (clay and old guano).

Terminal lower part: developing along a fault with dip to N 210 at 80° bordering the southern side of the chamber, this sector, which descends about 15 m below the *Sala del Fantasma*, constitutes for the moment the deepest part of the cave at 49 m asl.

The cave has clearly formed along two main fault systems. The first striking NE-SW with inclination of 75° towards SE, on which the first part of the cave is developed, and the second with WNW-ESE direction and dipping 80° toward the

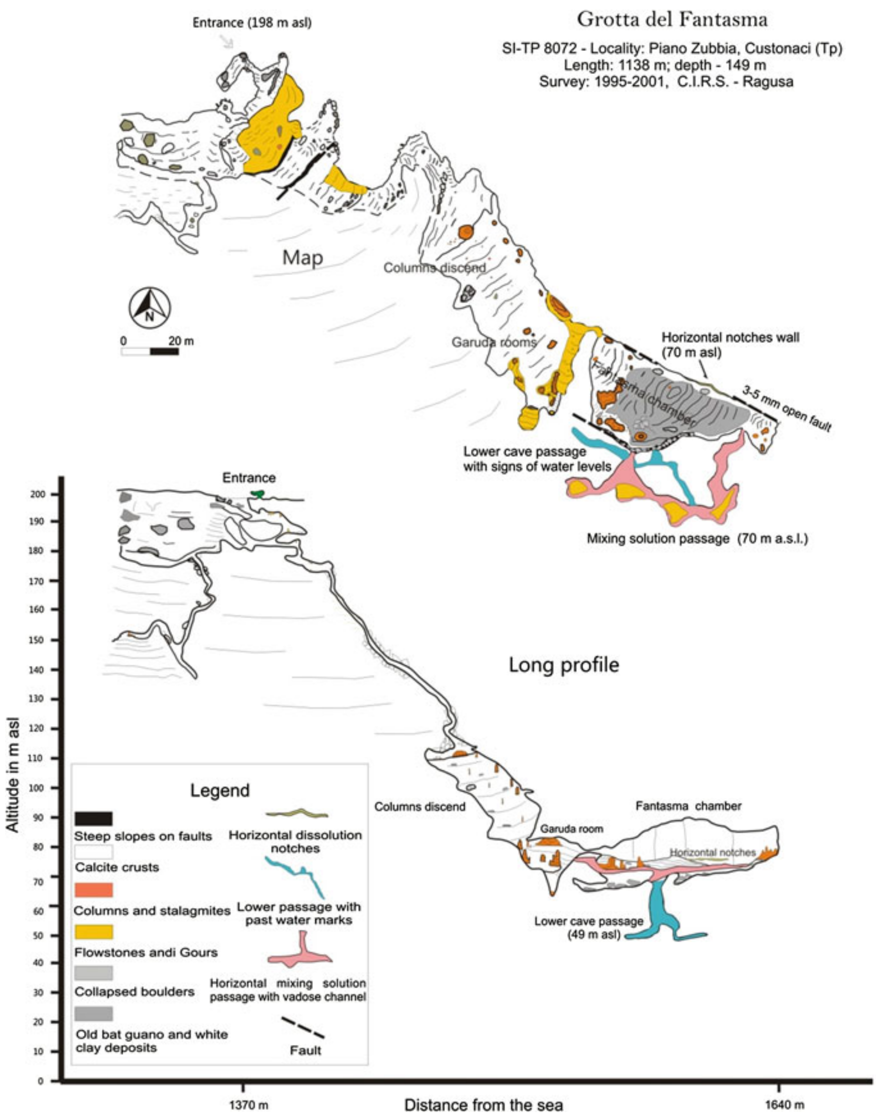

Fig. 6.183 Map of Grotta del Fantasma with main morphologies and geological structures

SSW that influences the deepest part of the cave. While the first part is characterized by narrow fissure-like voids descending rapidly and with many indices of recent tectonic activity such as broken columns and deflected stalagmites that show evidences of left lateral movements (Fig. 6.184) (Cucchi et al. 1983; Šebela 2008, 2010), at 120 m depth (around 80 m asl) the cave shows typical dissolutional features such as rounded passages and cupola ceilings. Ten meters lower these tubes end in a large room called “Sala del Fantasma”. This room has an elliptic

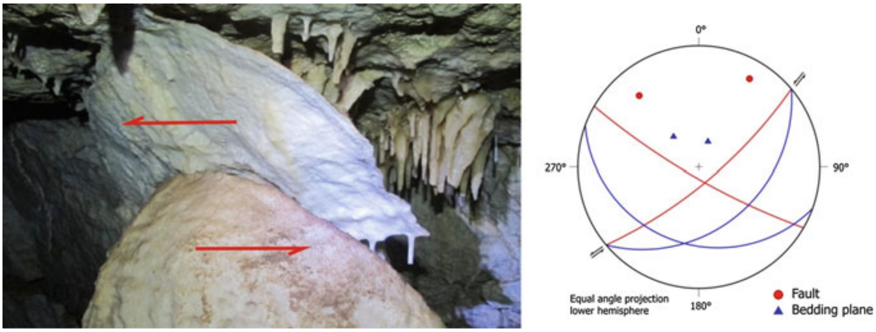

Fig. 6.184 Deflected speleothem, which evidences *left* lateral movement along the NE-SW fault; on the *right*, stereogram with projection of the main structures surveyed inside the cave

shape, is 50 m long and 25 m wide and has a height of around 6–10 m. Its centre is occupied by a large heap of old bat guano, and large white and corroded speleothems stand out on the dark background (Fig. 6.185). The northern part of this chamber is formed along a WNW-ESE fault with reddish mylonite (Fig. 6.186), creating a perfectly straight wall up to 10 m high (Fig. 6.187). In general the roof and walls have extremely well rounded shapes, and at around 70 m asl the walls are perforated by rounded tubes, forming a sort of perfectly horizontal notch (Fig. 6.188), as verified with a Suunto clinometer (Ruggieri and De Waele 2014). Several smaller rounded passages develop southeastward but return to the main chamber. Some of these passages tend to taper out toward the East. The room is decorated with large calcite speleothems such as stalagmites, columns and

Fig. 6.185 Corroded speleothems in the “Sala del Fantasma”

Fig. 6.186 South-east sector of the "Sala del Fantasma" with evidence of a WNW-ESE oriented fault

Fig. 6.187 Straight fault wall with breccia and reddish mylonite

Fig. 6.188 Sub-horizontal notches and spongework cavities on the northern wall of the "Sala del Fantasma"

stalactites. All of these are intensively corroded, and are covered with an over 1 cm thick layer of white powder or black deposits and wet clay (Figs. 6.189–190).

These corrosion phenomena are most intense at 70 m asl, corresponding to the altitude of the aforementioned notch. The corrosion is probably related to condensation water created by the slow combustion of the bat guano, although the major corrosion at 70 m asl indicates an influences of a stable water level. Apart

Figs. 6.189–190 Corroded speleothems with white deposit (moonmilk) (*left photo*); black powder and wet brown clay (*right photo*)

from extensively corroded walls and speleothem, it is also possible to observe a ceiling channel, probably due to an antigravitative phase (Pasini 1973), in a phreatic conduit on a sub-horizontal interlayer, which opens onto the great collapse chamber at 1.5 m from the ceiling (Figs. 6.191 and 6.192). One descending conduit along the

Fig. 6.191 Ceiling channel on the cave ceiling (*right side*)

Fig. 6.192 Phreatic conduit along the bedding plane at 70 m asl, with calcite deposits

Fig. 6.193 WNW-ESE wall fault descending at 49 m asl, with traces of old water level mark

WNW-ESE fault develops further 40 meters towards SSW reaching an altitude of 49 m asl (Fig. 6.193). In this passage several traces of old water levels are clearly recognized (Antonioli and Ruggieri 2000). Nowhere in the cave there are fluvial sediments, and the walls are always smooth and do not reveal any scallops or similar forms.

From the speleogenetic point of view, the Grotta del Fantasma is an enlarged (Middle Pleistocene) fault intercepted by a *flank margin cave* at 80 m asl, located at around 1500 m of the coastline, with the main level of mixing corrosion, corresponding to the longest stable position of the sea level, located at 70 m asl. Flank margin caves develop easily in young immature (eogenetic) limestones, where primary porosity facilitates the ingression of salt water and mixing with seeping fresh water. Many of these caves have been reported from carbonate islands such as the Bahamas and Bermuda (Mylroie et al. 1995), Guam (Mylroie et al. 2001), Isla de Mona (Puerto Rico) (Frank et al. 1998), and the Mariana Islands (Jenson et al. 2006), or from eolian calcarenites such as the case of Kangaroo Island, Australia (Mylroie and Mylroie 2009). In more recent times *flank margin caves* have also been found in older and mature limestones, where mixing occurs along secondary permeability pathways such as fractures and bedding planes. Good examples are described from New Zealand (Mylroie et al. 2008), and Croatia (Otoničar et al. 2010).

Where fresh water discharge on the carbonate coast is greater, caves with a ramiform pattern will form. When fresh water discharge largely overrules the salt

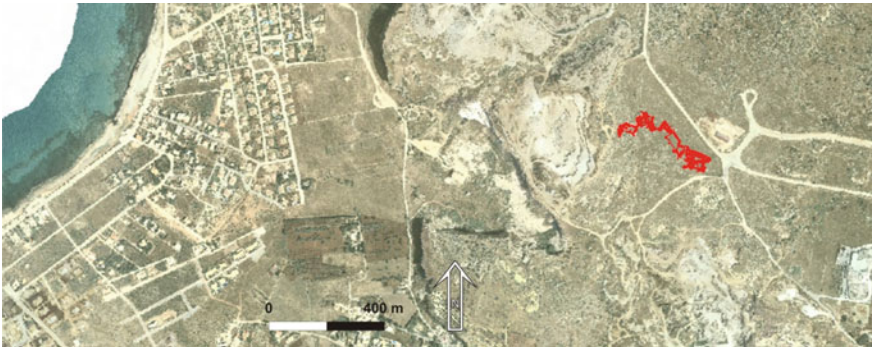

Fig. 6.194 Location of Fantasma cave with respect to the actual coastal line (1,500 m) and to the relict sea-cliff (around 500 m westwards) (*Orthophoto image from* Regione Siciliana 2007–2008)

water entering the rock mass, caves will have very extensive stream passages developing inland. In this case speleogenesis is mainly controlled by normal dissolution and erosion processes, and cave altitudes do not necessarily reflect sea levels. The influence of mixing processes is visible only in the cave passages closest to the sea, fading slowly going landwards.

Where fresh water discharge is slightly more important than salt water intrusion, ramiform caves develop, with passages modified by mixing corrosion processes also far inland. This type of caves, halfway between normal epigenic stream caves and *flank margin caves*, can be reliable sea level indicators only in their parts close to the coast (Smart et al. 2006). As above described, taking into account the actual distance from the relict sea-cliff (around 500 m) (Fig. 6.194), the presence of both dissolution morphologies due to mixtures of waters, and paragenetic phreatic features, supports for the Grotta del Fantasma an early speleogenesis, *flank margin cave* type, followed by an epigenetic speleogenesis, with conduits forming along bedding planes.

The Grotta Cerriolo: The Cerriolo cave, which is situated at about 200 m to the NW of Custonaci about 155 m asl, has its entrance inside a disused quarry in Portella del Cerriolo area, an area that has been declared a suburban park by the Municipality of Custonaci. The cave extends for about 400 m and goes 23 m below the entrance. It has its origin in the Upper Cretaceous carbonate sequence. From the morpho-structural point of view it may be subdivided into the following three sectors (Fig. 6.195).

<u>Central entrance sector</u>: a descending one oriented WNW which dips at 30°, interposed between two steps and two terraces and the western sector of the *Vano delle Lame*, formed along a bedding plane (Figs. 6.196 and 6.197–198).

<u>Right-hand eastern sector</u>: called the *Ramo della Ruota*, it has a low passage and is characterized by such morphologies as the detachment of stratum on the low

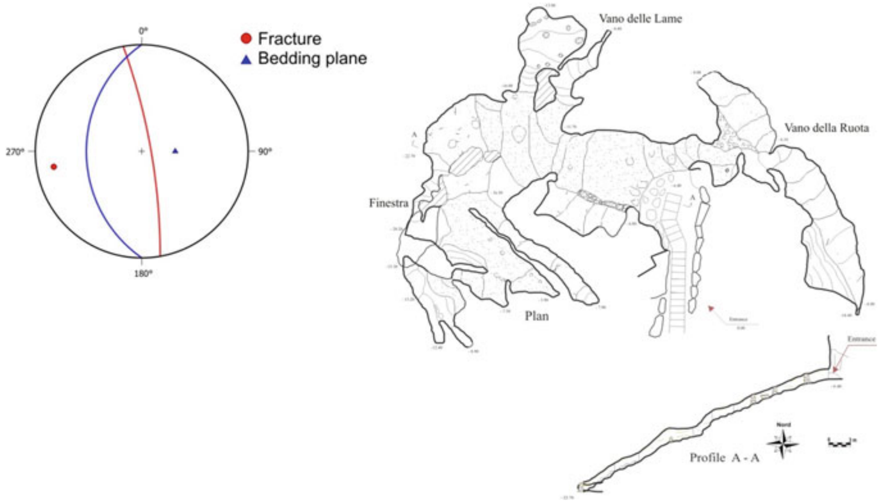

Fig. 6.195 Map and profile of Grotta Cerriolo and stereogram of the main geological structures

Fig. 6.196 Descending part of the Grotta Cerriolo along the dip of a bedding plane

Figs. 6.197–198 Sector of the Cerriolo cave with large curtain-type speleothems

ceiling and large calcite crust covering the floor. Also to be observed are low stalagmitic columns that extend between the floor and the low roof, and rimstones. As has already been mentioned the terminal part of this sector ends on a small pit placed on a fracture with dip to N 80 at 80°.

Extreme western sector: constituted by the *Ramo della Finestra* and characterized by a descending sector on a bedding plane oriented towards the south-west. In this environment numerous calcite deposits are to be found.

6.6.1.1 Structural Data

The analysis of the structural data surveyed in the above mentioned caves verifies the considerations being reported below (see Tables 6.2, 6.3, 6.4, 6.5, 6.6, 6.7 and general map of Fig. 6.302).

In the Mt. Bufara–Piano Zubbia area, the karstification processes have mainly been active along NW-SE oriented faults and, to a lesser extent, along NE-SW oriented structures. In particular, the Grotta della Clava and the Grotta Maria SS. di Custonaci both develop along NW-SE trending faults, with the first cave dipping to NE while the second one to the SW (Fig. 6.199). A major control of stratification on karst processes is clearly shown in the Grotta Cerriolo, which extends along the dip of the exposed layers of the area (see Table 6.2).

Table 6.2 Cave geological structures of the Mt. Bufara–Cerriolo–Piano Zubbia areas

Cave	Fracture/Fault		Bedding plane	Lithology	Length/Depth (m)
	Strike	Dip direction			
Grotta della Clava	N 130	N 40/75°	N 240/20°	Biocalcarenites Upper Cretaceous	759/−89
Grotta del Fantasma					
Upper sector			N 200/25°	Biocalcarenites Upper Cretaceous	1,138/−149
Middle-upper sector	N 40–60	N 130–150/75°			
Middle-lower sector			N 140/36°		
Lower sector	N 120–135	N 210–225/80°			
Final lower sector	N 120	N 210/80°			
Grotta Cerriolo	N 170	N 80/80°	N 250–290/35°	Biocalcarenites Upper Cretaceous	400/−23
Grotta Maria SS. di Custonaci				Biocalcarenites Upper Cretaceous	1,321/−90
Middle-upper sector			N 200/40°		
Middle-lower sector	N 140	N 230/80°	N 225/50°		
Zubbia della Sansa	N 135	N 225/85°	N 270/20°	Calcarenites Upper Tithonian—Lower Cretaceous	42/−7.4

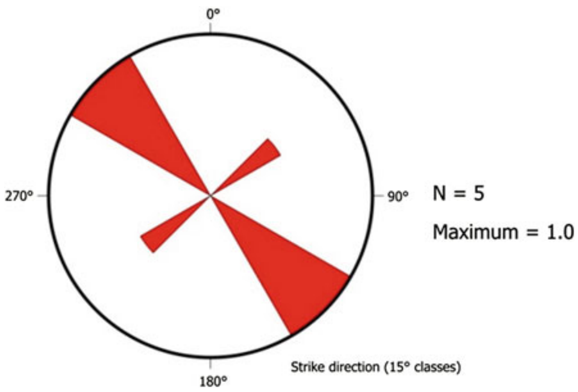

Fig. 6.199 General Rose diagram of main karstification geological structures in the Piano Zubbia-Mt. Bufara area

6.6.2 *The Caves in the Mt. Palatimone–Mt. San Giovanni Ridge (Site* **b***)*

The Mt. Palatimone ridge is made up, in its central-eastern sector, of Upper Triassic-Lower Liassic dolomitic limestone, and, in its western part, of calcarenites and calcirudites of the Upper Tithonian–Lower Cretaceous (see Fig. 4.3 of Chap. 4). The dip of the strata is mainly to SSW; the main fault system has a NNE-SSW trend with dip at WNW, while on some sectors of both slopes there are areas frequently dissected by systems of joints, on which are generated both karst caves and trench-like grikes (Sauro 1979). For descriptive purposes the caves have been subdivided into those situated on the northern slope and those situated on the southern slope of the ridge (Fig. 6.200) described below.

Zubbia ru Zu Santoru: This cave is to be found at 540 m asl; it is typically vertical, descends to −45 m with respect to the entrance level and extends in real terms for 75 m. The cave develops on a fracture with N 160 orientation, in the Norian-Liassic dolomites and dolomitic limestone, which in this sector have a dip to N 190 at 16° (see stereogram, Fig. 6.201). In this vadose environment on a fracture both gravitational detachment morphologies (blocks and large rock masses) and flowstone deposits are to be found (Fig. 6.202). These latter are particularly present in the initial sector of the second pit and also in the final part.

At the bottom there is also a thick deposit of silty-clayey detritus transported there over time by percolation water, which has contributed, together with the carbonate clasts, to the obstruction of the Zubbia at a depth of 45 m.

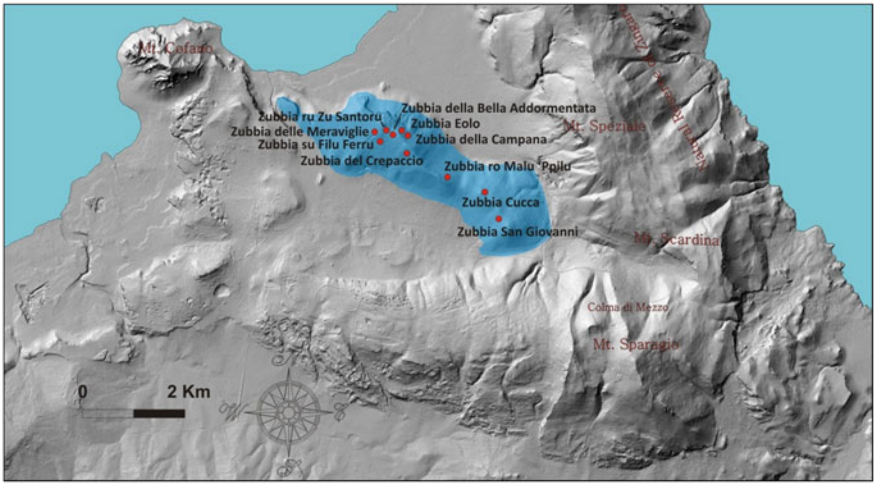

Fig. 6.200 Location of caves in the Mt. Palatimone–Mt. San Giovanni ridge (*blue sector*) (*Hillshade map from* DEM Regione Siciliana 2007–2008)

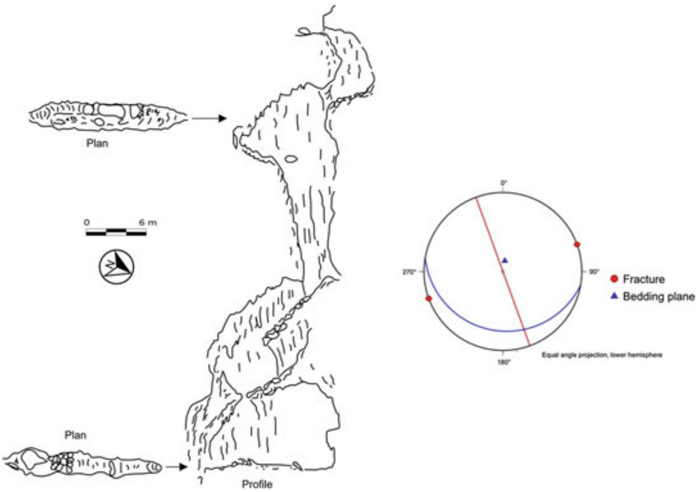

Fig. 6.201 "Zubbia ru Zu Santoro", map and stereogram of the main geological structures

Fig. 6.202 Flowstones on the fracture wall

Zubbia della Bella Addormentata: The entrance is at 540 m asl, and it descends vertically for just 11 m, along a chamber that extends for 8 m and is about 2 m wide, before closing like the preceding cave, though much higher up, due to the progressive accumulation of variously-sized bits of carbonate clast detritus in the fracture walls (Fig. 6.203). It develops along a fracture with N 160 direction, in the Norian-Liassic dolomitic formation with dip to N 190 at 16° (see stereogram, Fig. 6.204). In this vadose environment, apart from the clast deposits, some flowstones can also be observed.

Zubbia delle Meraviglie: The entrance is hidden among blocks of quarry-stone at 515 m asl: the cave is initially vertical, descends for a total of 55 m compared with the level of the entrance area and extends for about 200 m (Fig. 6.205). It develops along a fault with dip to N 60 at 60° (Figs. 6.206–207), which crosses for 50 m the Norian-Liassic dolomitic formation. This latter has a dip direction N 200 at 35°. A large part of the cave is interested by abundant calcite deposits, which have

Fig. 6.203 Shaft developed along a NNW-SSE oriented fracture

created extensive flowstones of various morphologies on the walls and the floor (Figs. 6.208–209).

Zubbia su Filu Ferru: The entrance in the form of a pit, at 490 m asl, is about 22 m deep and has a length of 62 m. The cave develops along a N 150 oriented fault, which cuts the Norian-Liassic dolomitic terrains, the strata of which outcrop locally with dip to N 200 at 23° (see stereogram, Figs. 6.210 and 6.211). As far as the calcite deposits this vadose cave contains, it offers a rich variety of speleothems deriving from percolation waters (Figs. 6.212 and 6.213).

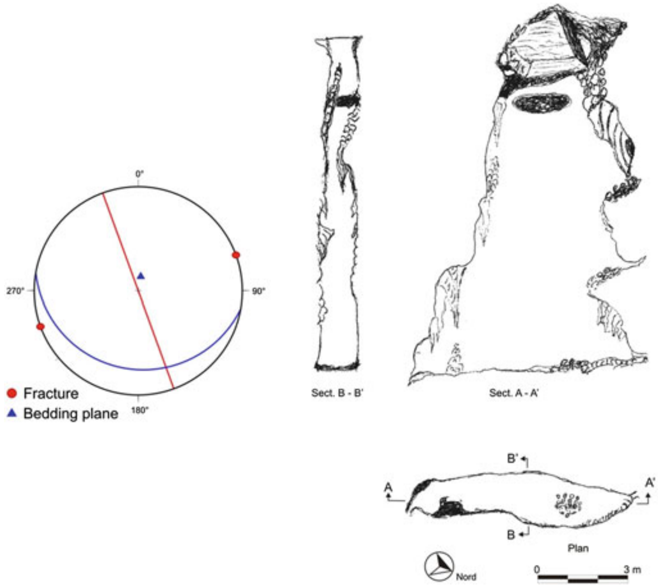

Fig. 6.204 Map of "Zubbia della Bella Addormentata" and stereogram of the main geological structures in cave

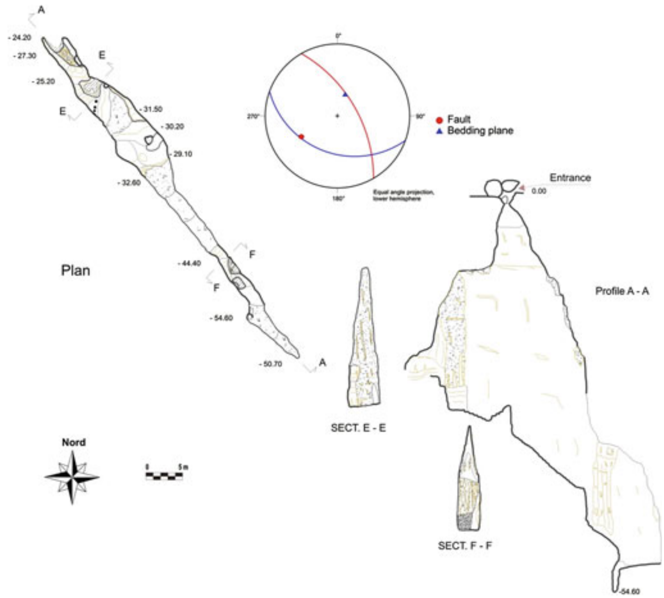

Fig. 6.205 Map of the "Zubbia delle Meraviglie" and stereogram of main geological structures in cave

Figs. 6.206–207 Shaft along a NNW-SSE trending fault

Figs. 6.208–209 Speleothems and large flowstones in the Zubbia delle Meraviglie

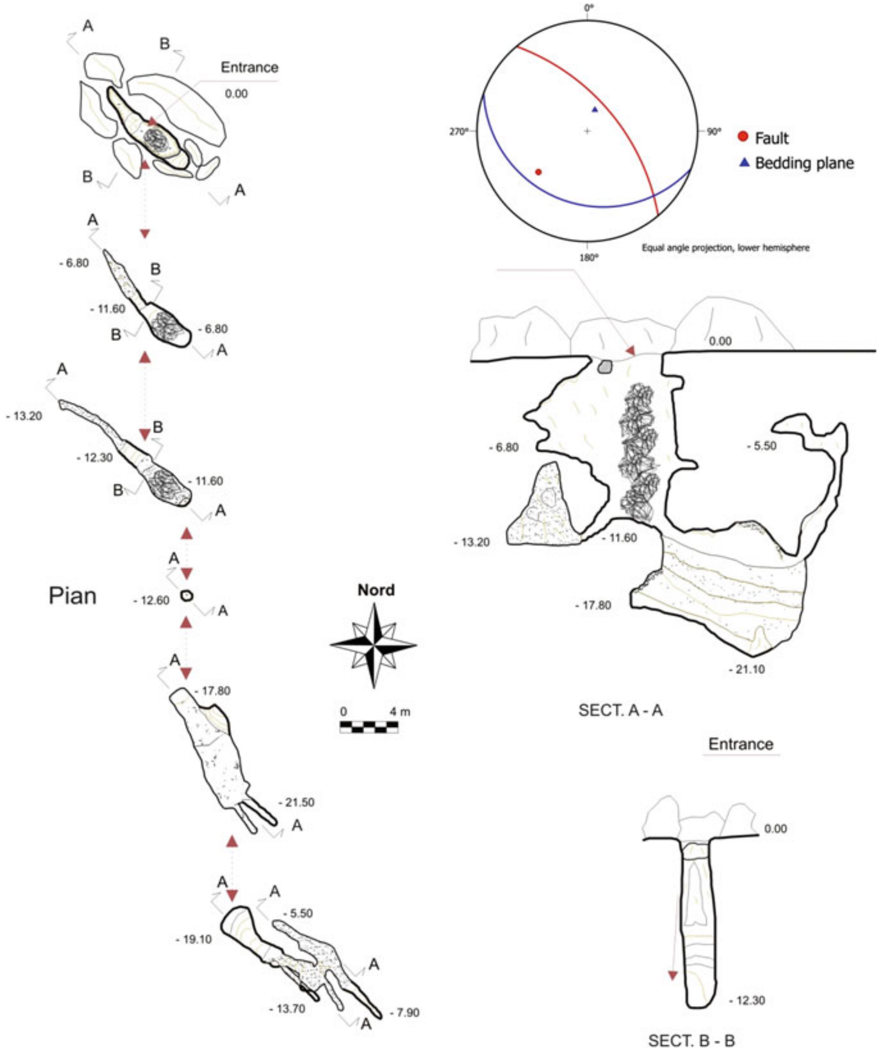

Fig. 6.210 Map of “Zubbia su Filu Ferru” and stereogram of the main geological structures in cave

Zubbia-grike: This is a cave located in the Palatimone southern slope grikes karrenfield, where a large number of gullies and trenches have evolved from the pre-existing network of fractures through the corrosive and differentially erosive action of running and infiltrative waters. The *Zubbia-grikes* is a fairly frequent case in the study area of the grike/cave mixed morphology. The opening is at 492 m asl (Fig. 6.214); it extends for about 23 m and has a depth of 5 m; it develops along a N

Fig. 6.211 Entrance shaft along a NW-SE oriented fault

Fig. 6.212 Partially corroded calcite flowstone

Fig. 6.213 Breccia and corroded calcite flowstone laminations in the "Zubbia Su Filu Ferru"

Fig. 6.214 Bottom of the Zubbia–grike with conduit

30 oriented fracture, which cuts the Norian-Liassic dolomitic terrains locally outcropping with dip N 200 at 32° (Figs. 6.215 and 6.216). In the subterranean parts of the grike there are calcite deposits on the walls and concretions.

Fig. 6.215 Map of Palatimone Zubbia–grike

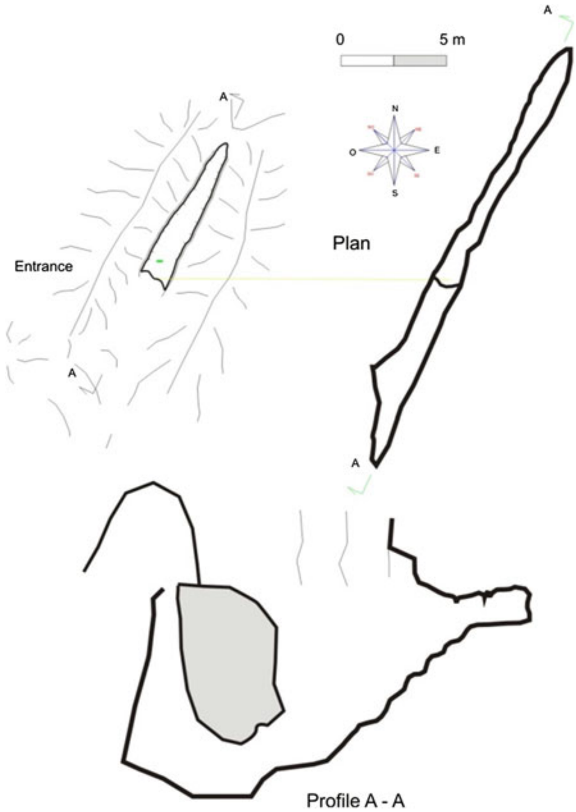

Fig. 6.216 Stereogram of the main geological structures in cave

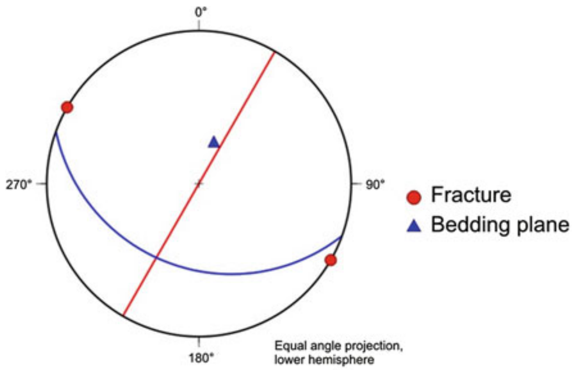

Zubbia ro Malu 'Ppilu: The vadose cave has its opening at 370 m asl on the low slope facing *Portella della Ronza*, between Mt. Palatimone and Mt. San Giovanni. It has a vertical development: a depth of −11.5 m and an extension of 14 m on a fracture oriented NNE-SSW, which dissected the Norian-Liassic dolomitic layers. These latter have a dip to N 200 at 28° (Figs. 6.217–218).

Zubbia San Giovanni: The opening of this vadose cave is at 400 m asl and develops for 47 m, going down 25 m. It extends vertically, on a fracture, with a dip to N 105 at 85°, in the dolomitic terrains of the Norian-Liassic.

This morphostructure appears to be dissected by a fracture with a dip to N 40 at 75°, while the dip direction of the layers is N 180–190/20–30° to the east of the fracture, and N 230/23° to the west (see stereogram, Fig. 6.219).

The cave is particularly rich in calcite deposits of a variety of morphologies, such as: flowstones on the walls, draperies, popcorn concretions and stalactites and stalagmites of various dimensions (Figs. 6.220–221).

Zubbia Cucca: A vadose vertical cave 34 m deep, this *zubbia* opens at 401 m asl on the summit of the Mt. San Giovanni ridge. It develops in the Norian-Liassic

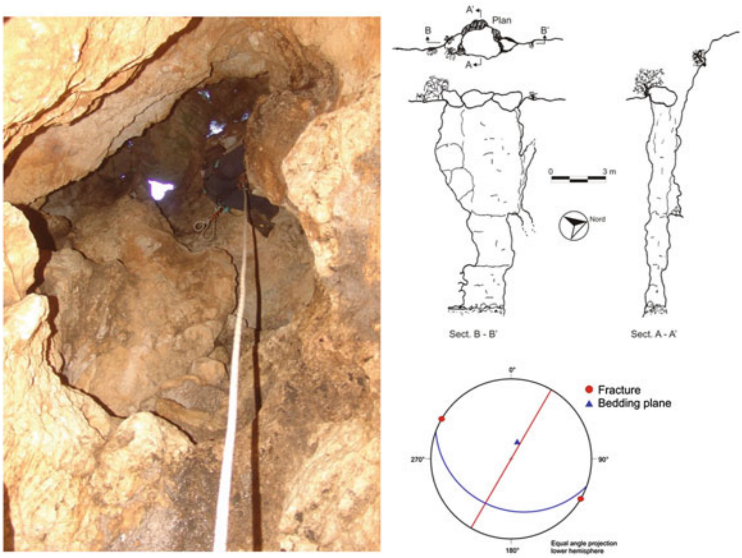

Figs. 6.217–218 Zubbia ru Malu 'Ppilu, entrance shaft (*left photo*); map and stereogram of main geological structures in cave (*right side*)

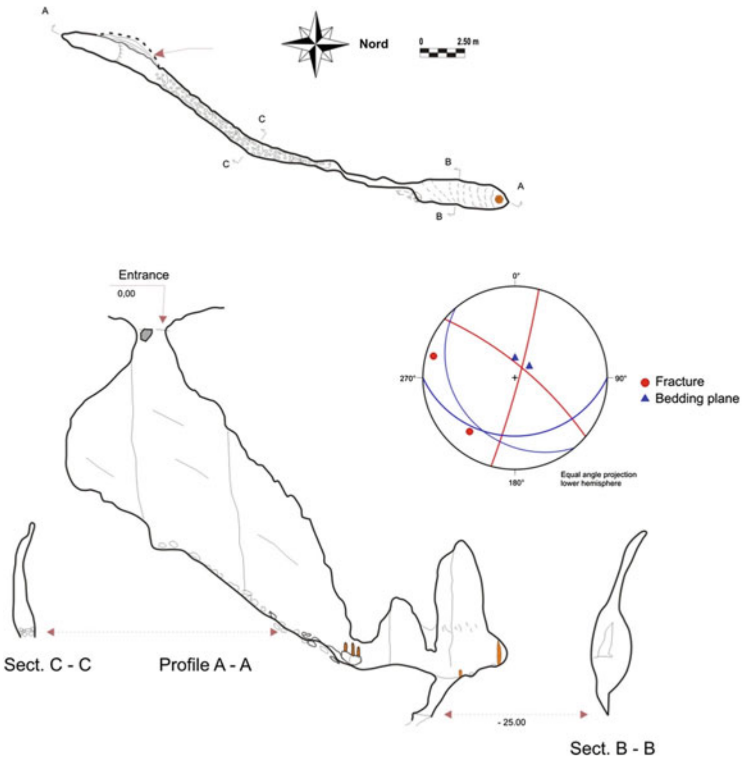

Fig. 6.219 Map of Zubbia San Giovanni and stereogram of the main geological structures in cave

Figs. 6.220–221 Flowstones on the walls of Zubbia San Giovanni

dolomite outcroppings, with dip to N 210–220 at 20°, along a fracture with dip to N 30 at 85°; this fracture is dissected by a secondary one with dip to N 310 at 85° (Figs. 6.222 and 6.223).

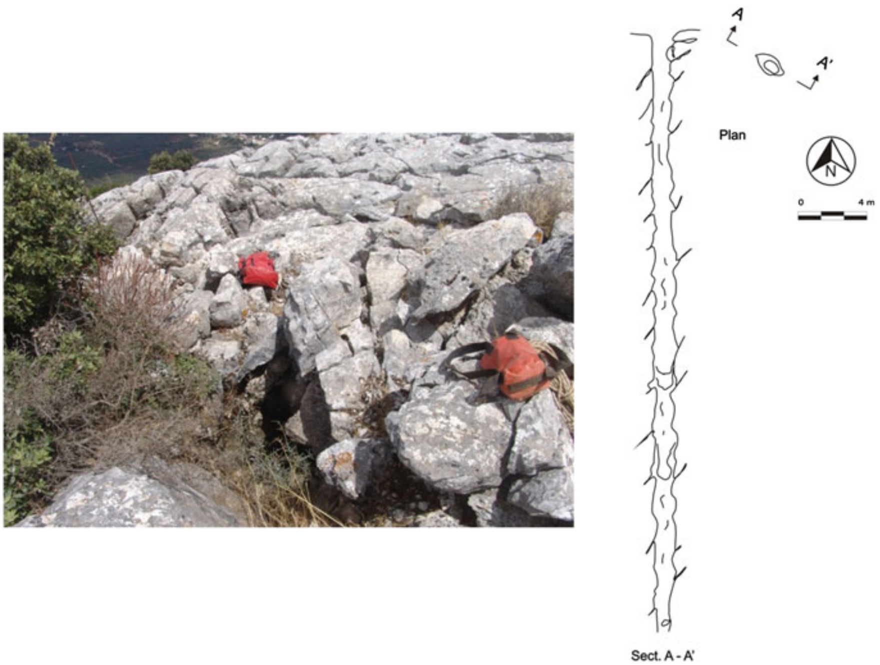

Fig. 6.222 Entrance of "Zubbia Cucca" and map (*right side*)

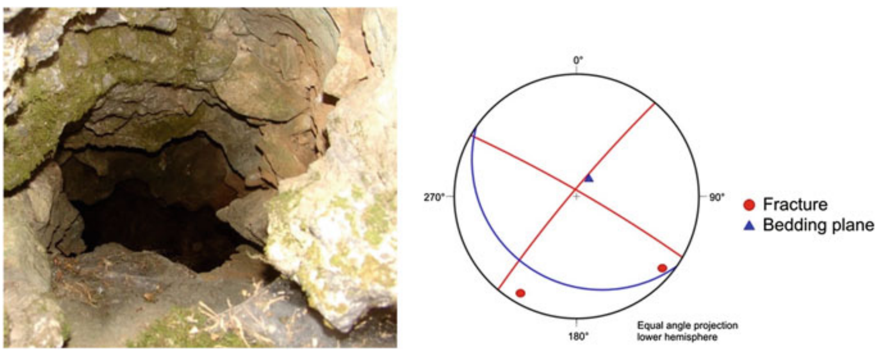

Fig. 6.223 Internal part of the shaft along a fracture with dip to N 30 at 85° and stereogram of the main geological structures in cave

Abisso Eolo: This vertical vadose cave has its entrance, through which a strong current of air flows, at 385 m asl; it descends for about 70 m and extends for 110 m. It develops in the Norian-Liassic dolomitic layers with dip to N 200 at 25°, along a NE-SW oriented fracture (see stereogram, Fig. 6.224).

Zubbia della Campana: The entrance is at 375 m asl and descends for about 47 m, with a total length of 93 m. This vadose cave develops in the dolomites and dolomitic limestone of Norian-Liassic age, with dip to N 200 at 25°, along a fault, which cuts the Mt. Palatimone ridge with NNE-SSW direction (Figs. 6.225, 6.226–227).

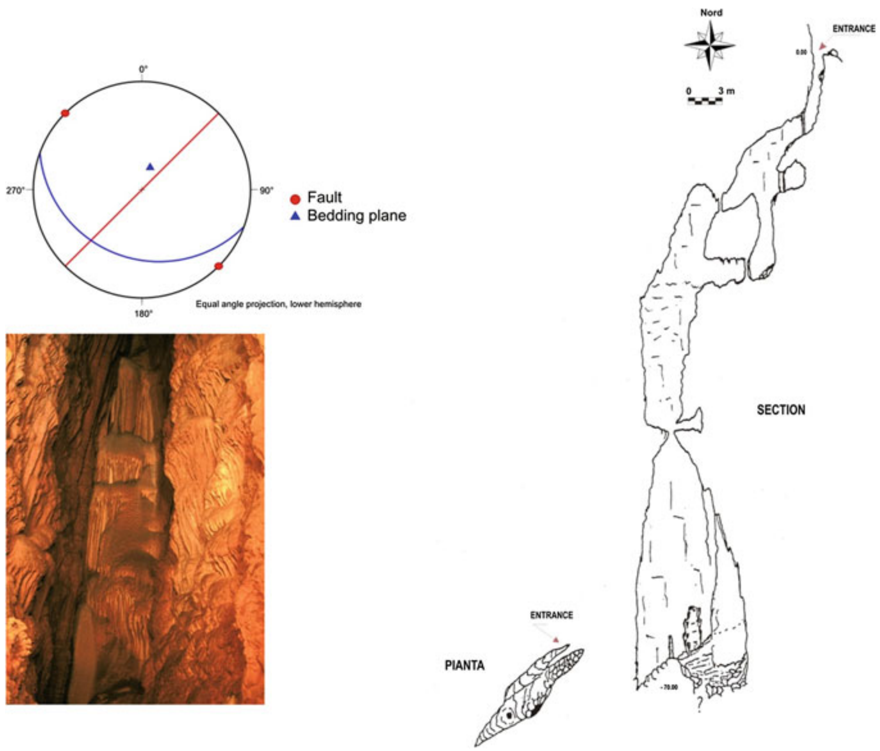

Fig. 6.224 Flowstones, map and stereogram of the main geological structures of Abisso Eolo

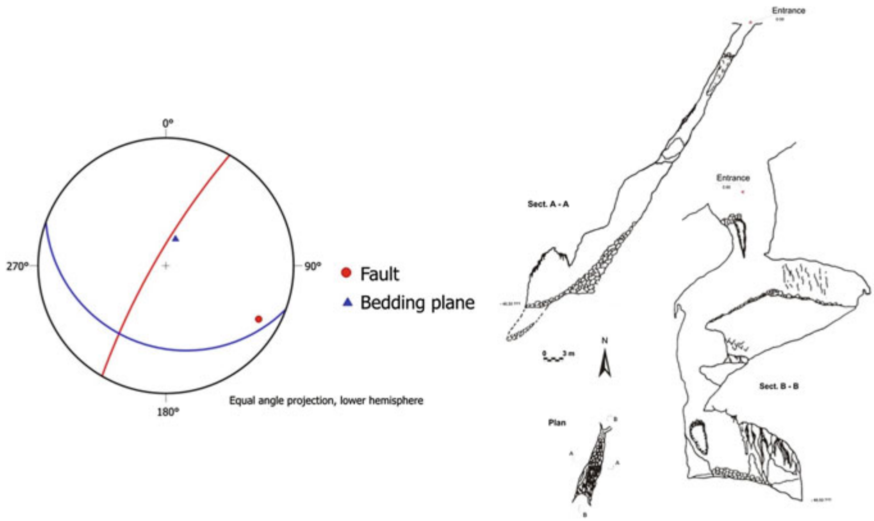

Fig. 6.225 Stereogram of the main geological structures and map of the cave

Figs. 6.226–227 Environments of the Zubbia della Campana with widespread speleothems

Table 6.3 Cave geological structures of the Mt. Palatimone–Monte San Giovanni ridge

Cave	Fracture/Fault		Bedding plane	Lithology dolomitic limestone	Length/Depth (m)
	Strike	Dip direction			
Zubbia ru Zu Santoru	N 160		N 190/16°	Norian–Liassic	75/−45
Zubbia delle Bella addormentata	N 160		N 190/16°	Norian–Liassic	8/−11
Zubbia delle Meraviglie	N 150	N 60/60°	N 200/35°	Norian–Liassic	200/−55
Zubbia su Filu Ferru	N 150	N 60/60°	N 200/23°	Norian–Liassic	108/−22
Zubbia–Grike	N 30		N 200/32°	Norian–Liassic	23/−5
Zubbia ro Malu ‘PPilu	N 30		N 200/25°	Norian–Liassic	14/−12
Zubbia Cucca					
Main fracture	N 120	N 30/85°	215/20°	Norian–Liassic	−34
Secondary fracture	N 40	N 310/85°			
Zubbia San Giovanni					
Main fracture	N 15	N 105/85°	N 230/23°	Norian–Liassic	47/−25
Secondary fracture	N 130	N 40/75°	N 185/25°		
Abisso Eolo	N 45		N 200/25°	Norian–Liassic	110/−70
Zubbia della Campana	N 30	N 300/80°	N 200/25°	Norian–Liassic	93/−47

6.6.2.1 Structural Data

The analysis of the structural data surveyed in the above mentioned caves verifies the considerations being reported below (see Tables 6.3, 6.4, 6.5, 6.6, 6.7 and general map of Fig. 6.302).

The general diagram being represented in Fig. 6.228 shows that for the whole Mt. Palatimone–Mt. San Giovanni ridge, there are two major cave karstification trends–NNW-SSE and NE-SW. The diagrams in Fig. 6.229 show the NNW-SSE main karstification direction of the western sector of the ridge and the NE-SW direction, which prevails along the eastern sector. The boundary between the two sectors has been placed, on the basis of morphostructural evidence, passing along the NNE-SSW oriented fault, which transversely cuts the whole ridge.

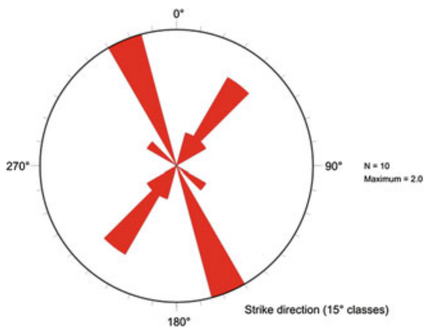

Fig. 6.228 General Rose diagram of the main directions of karstification of the Mt. Palatimone–Mt. San Giovanni ridge

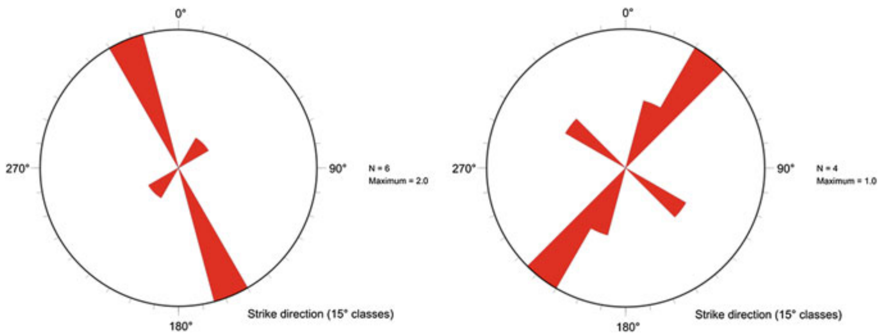

Fig. 6.229 Rose diagram of prevalent karstification of the western sector (*left side*) and eastern sectors (*right side*) of the Mt. Palatimone–Mt. San Giovanni ridge

6.6.3 *The Caves of Purgatorio Polje (Site* c*)*

The subterranean karst morphologies of the Purgatorio plain are distributed along a strip of land about 5 km long and 0.5 km wide on which the Norian-Liassic dolomitic limestones, dolomites and calcarenites outcrop. To the south of this sector of the southern slopes of the Mt. Palatimone–Mt. San Giovanni ridge there is a more tabular area, lithologically speaking, made up of Lower Pliocene calcarenite terrains (see Fig. 4.3 of the Chap. 4). On the contact between the two formations, differential erosion created a bland incisional drainage line, which runs in WNW-ESE direction.

It is significant, in this regard, that the swallow holes present in the polje are situated in the proximity of this formational contact along the aforementioned WNW-ESE line (see Fig. 6.170 of this chapter). As described before, the polje is the combined result of retreat by erosive/corrosive processes of the Mt. Palatimone-San Giovanni ridge's slope, added to the karstification—planation processes, acting both on the surface and underground, set in motion by the caves and swallow holes described below (Fig. 6.230).

Abisso del Purgatorio: the entrance of this vertical cave is at 285 m asl. It extends for 432 m and descends for 194 m, which makes it the deepest cave, and one of the most interesting, from the geomorphological and hydrological points of view, in the territory of Monti di Capo San Vito.

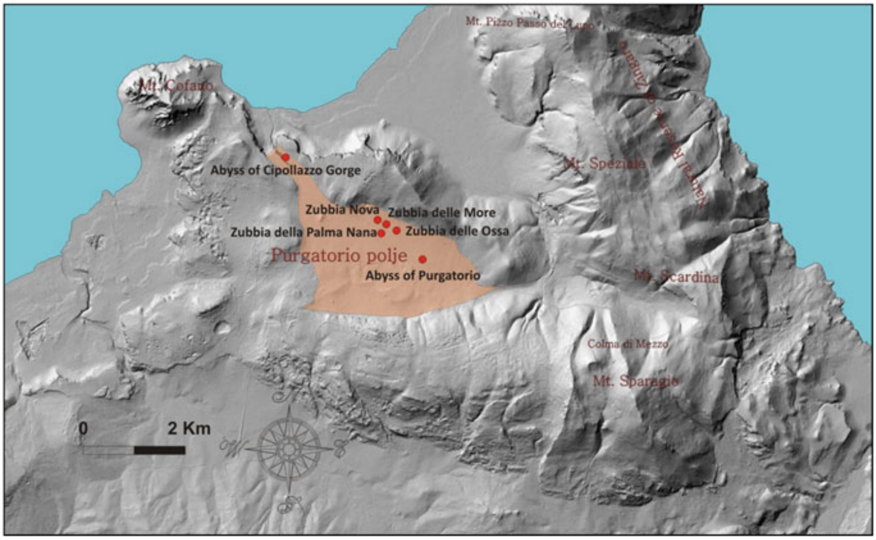

Fig. 6.230 Locations of the caves located in the Purgatorio polje (*peach colored sector*) (*Hillshade map from* DEM Regione Siciliana 2007–2008)

The cave has developed in the Norian-Liassic dolomite and dolomitic limestone terrains, which outcrop near the cave's entrance with dip to N 230 at 25°. Proceeding from the highest sector slowly downwards, one can distinguish the following hydrological and morphostructural zones described below (Fig. 6.231).

Upper vadose zone: this covers 285 m asl, the height of the entrance, down to 190 m asl, and includes the entrance pit, the successive *Pozzo della Vespa* (Figs. 6.232 and 6.233), the *Pozzo-Cascata* and the two following small pits before the *Salone dell'Abete*. This first tract is settled on a fracture N 30, that cuts the Norian-Liassic dolomitic terrains, which have a dip direction of N 220/26° and N 190/35° respectively, in the upper tract of the *Pozzo della Vespa* and in the *Pozzo-Cascata* sector. In this latter sector a sub-parallel system of fractures is also evident, with a direction of N 40–50. In this initial part of the cave, calcite deposits on the walls of the shafts and rock blocks deposits on their floors are present.

In the terminal part of the *Pozzo-Cascata* a meandering morphology can be observed, probably linked to the fractures to be found in this sector.

Median vadose zone: this sector develops between altitudes 190 and 150 m asl and includes the *Salone dell'Abete* and the *Salletta Lourdes* just below it. This part of the cave, which is made up of a vast environment dominated by cyclopic collapsed rock blocks, has assumed a 'fictitious' role of median in the context of the

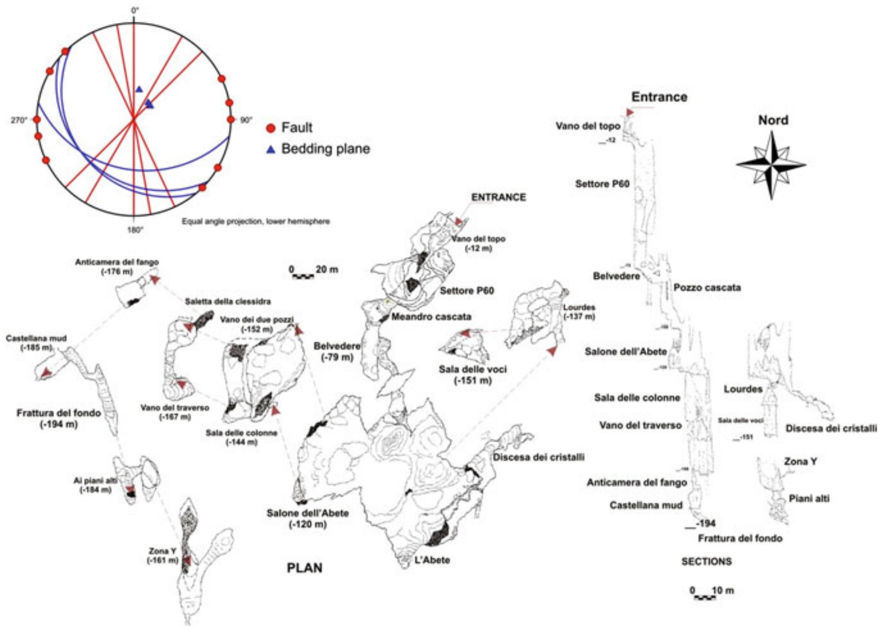

Fig. 6.231 Map, sections and stereogram of the main geological structures of Abisso del Purgatorio

Fig. 6.232 Shaft along a NNE-SSW oriented fault

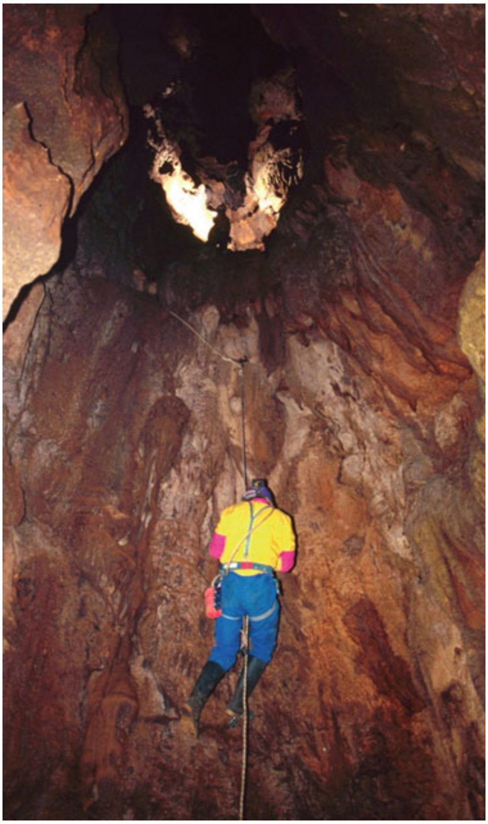

Fig. 6.233 "Pozzo della Vespa" along a NNE-SSW oriented fault

vertical vadose zoning, in virtue of a morphostructural situation controlled by a collapse gravitational morphogenesis. In this respect, it is to be noted that, within the confines of this large collapse zone, the two fracture systems N 30 and N 155 have constituted the weak structural points on which karst corrosion has come to bear and determined the present morphological conformation.

As far as the calcite deposit morphologies are concerned, a great number of speleothems are to be found in the *Salone dell'Abete* (Figs. 6.234–235), covering both the collapse masses and the walls, some of them of particular beauty: the *Abete* (or fir tree, hence the name), a fascinating, sparkling, flowstone several meters high, framed in a recess in the wall; the *Discesa dei Cristalli*, formed by a succession of *rimstones s*eparated by *flowstones*, accompanied by shining calcite crystals; the *Mensole*, a curious series of concretions towering on high; and certainly not last *La Grande Stalattite*, several meters long, hanging down from the north-east ceiling of the big chamber, and the *Medusa*, a spectacular curtain suspended from the north-west ceiling.

Lower vadose zone: Between 150 and 115 m asl this sector includes the *Sala delle Colonne*, the parallel *Sala delle Voci*, the *Vano dei due Pozzi,* the *Vano del Traverso* and the *Anticamera del Fango*. This vadose sector of the abyss is still controlled by the main N 30 fault, while on a secondary N-S oriented fracture the

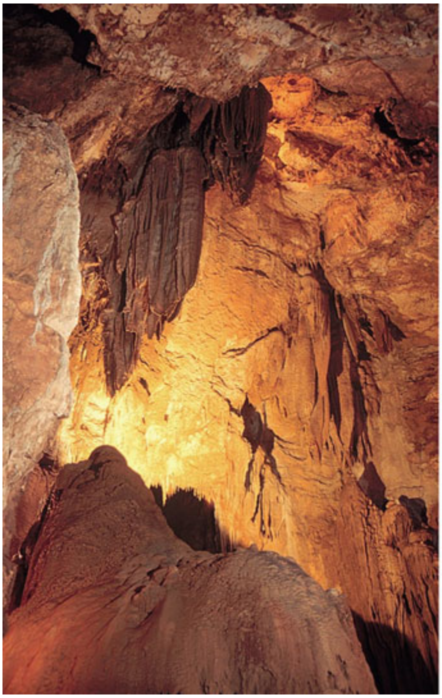

Figs. 6.234–235 Flowstones and speleothems covering the collapsed boulders in the "Salone dell'Abete"

sector of the *Vano del Traverso* developed. With regard to calcite deposit morphologies in the zone, *The Sala delle Colonne* should be noted, as well as calcite flowstones on the walls of the shafts.

Upper Epiphreatic oscillation zone: This is a sector of the cave, from 115 to 96 m asl, which shows two different hydrological functions. The first is included within the area below the pit on the *Vano del Traverso,* on a N-S fracture, and the *Castellana Mud* zone, on the N 40 oriented fracture, characterized by the considerable presence of mud on the walls and floors of both environments. It is to be noted that in the lowest part of the *Traverso pit* there is a narrow hole in the mud that fills the conduit, from which a distinct air current is emitted.

The second sector is constituted by two conduits: one is established on a N170 oriented fracture, which leads to the deepest part of the *Abyss*; the other climbs to *Ai Piani Alti* sector, on the N-S and N 40 fracture (see stereogram of Fig. 6.231). This second sector is different from the first because of the absence of mud and because in season it suffers from copious presence of water, in the form of sheet-water on the walls and dripping water. In this final part of the *Abyss* calcite deposits are present in the vertical conduit of the *Piani Alti* both as flowstones covering the walls and as various types of concretions (rimstones, stalactites, etc.).

The Abisso del Purgatorio owes its origins and extension to the capture of the running waters, that had their origin on the plain, in a concentrate form following the occurrence of meteoric events. It acted as a sink-cave for a certain period of time until, with the opening of new swallow holes at a higher level and the consequent reduction of the surface water-flow, the system's ability to capture water became progressively reduced. The present hydrological functions of the cave in the polje context are particularly clear in lowest part, by observing the deposits and morphologies there. The deep phreatic zone, not reachable except in its upper part of oscillation, appears in fact to be supplied by two different drainage systems. In this regard, the floods captured in concentrated form by the external swallow holes were conveyed, and to a lesser extent they still are, through the principal body of the cave, which descends mainly on the N 30–40 fault. This explains the massive presence of wet mud in this deep sector of the cave. This hydrological function of concentrated flow must have been much more efficient in the past before the tectonic uplifts in this area, with the opening of new fractures and the consequent opening of new swallow holes, pushed the superficial water-capturing system further back in the recharge area of the polje. On the other hand, the water coming from the *Piani Alti* sector works in a different way: through N 40 and N-S/N 170 fractures draining a surface infiltration that spreads from the overhead dendritic epikarst zone.

Zubbia delle More: the entrance is at 265 m asl and is in the form of a pit; it reaches a depth of 43 m with an effective extension of 76 m. The cave develops in the Norian-Liassic dolomites and dolomitic limestone with dip direction to N 220 at 15°. The development of this essentially vertical vadose cave is controlled by two fracture systems, as follows: in the entrance sector there is the first N-S oriented system, which dissected the second, which has a direction of N 145, on which the two successive pits develop (Figs. 6.236 and 6.237).

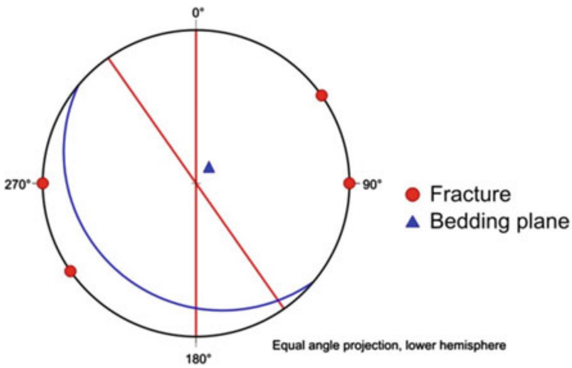

Fig. 6.236 Stereogram of the main geological structures in cave

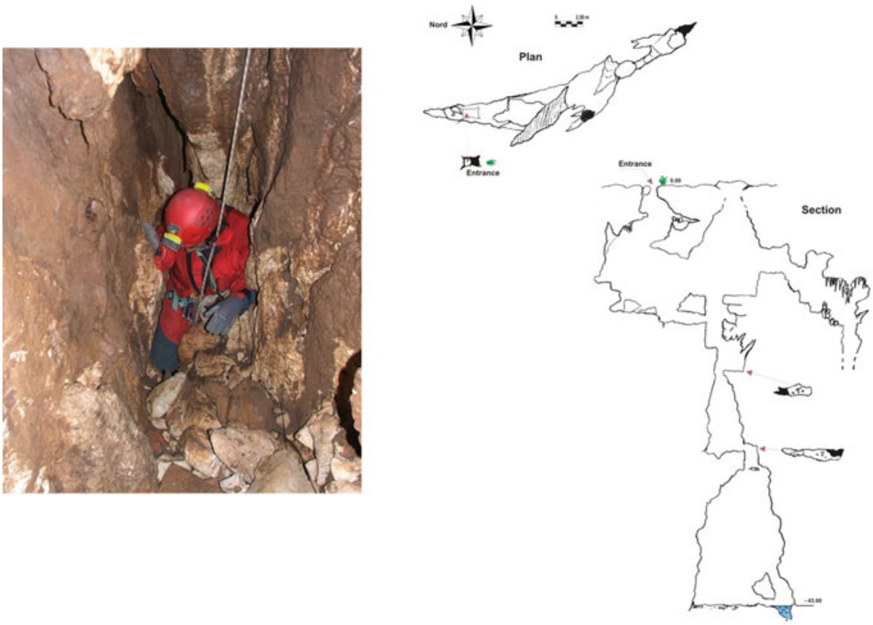

Fig. 6.237 Narrow pit along a NW-SE oriented fracture and map of the Zubbia delle More

Zubbia della Palma Nana: the entrance is at 265 m asl, the effective development is 30 m, the depth 18 m. The cave, which shows both vadose and epikarst phreatic morphologies, is mainly developed along a fracture with dip direction to N 110 at 80°. The incoming conduit, on the fracture just mentioned, follows the dip direction of the layers (N 210/25°) before being dissected, in the terminal part, by a second fracture, with a dip direction to N 200 at 80° (see stereogram, Fig. 6.238).

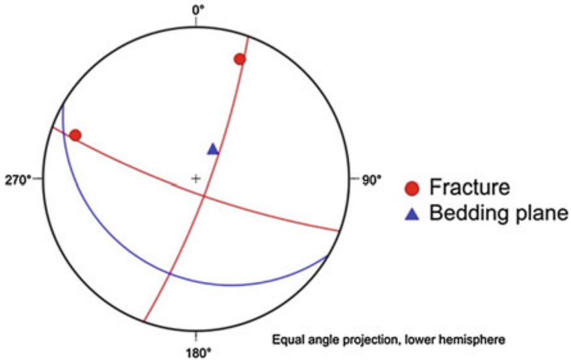

Fig. 6.238 Stereogram of the main geological structures in cave

Along the initial conduit erosion morphologies can be seen, which have cut into the fracture, and phreatic corrosion morphologies along the bedding plane. On the walls there are splash calcite deposits (Figs. 6.239–240).

Zubbia delle Ossa: with an opening at 267 m asl and, an effective development of 21 m and a depth of 24 m, this vadose morphology develops mainly on an irregular fracture with a dip to N 30 at 80° dissected by another with a N-S direction (see stereogram, Fig. 6.241). There are calcite deposits on the walls and collapse blocks in the terminal part of the descending conduit (Fig. 6.242).

Zubbia Nova: Vertical vadose cave with entrance at 265 m asl, developed along a fracture with immersion to N 280 at 85°, with a depth of 16 m. The above mentioned structure dissects the limestones of Norian–Liassic age, which show a dip to N 210 at 20°. The upper part of the cave is interested by clast collapse morphologies, while the lower one by calcite deposits on the walls (Figs. 6.243 and 6.244).

Abisso delle Gole di Cipollazzo: the opening is to be found at 180 m asl in the Cipollazzo gorge and it extends for 170 m, with a total depth of 120 m. The cave develops in the Upper Jurassic–Lower Cretaceous calcarenites and calcirudites with dip to N 290–310 at 20°. The structures surveyed inside the cave showed a fault with a dip to N 165 at 85°, which can be observed in the *Sala dei Funghi* sector, on the wall under the *Pozzo Brecciato* (Fig. 6.245), and a NW-SE trending fault in the upper part of the cave. The successive terminal conduit, developed on a N 125 oriented fracture, is characterized by a considerable presence of mud and by traces of running water (see stereogram, Fig. 6.246).

The abyss from the hydrological point of view constitutes one of the temporarily active sink-caves that capture a considerable amount of the floodwater coming from the Purgatorio polje.

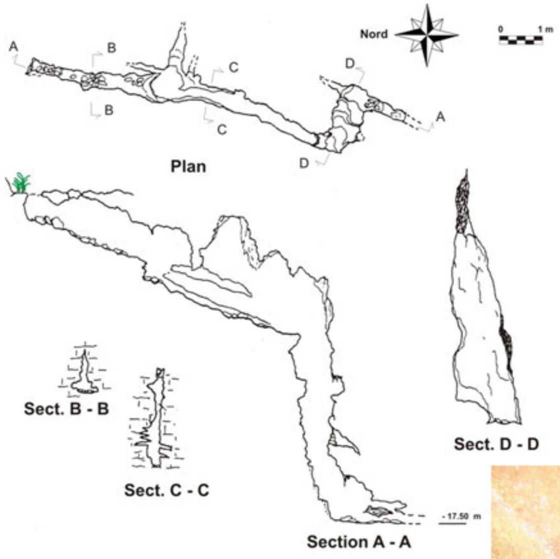

Figs. 6.239–240 Map and photos of the shaft and conduit along a WNW-ESE fracture

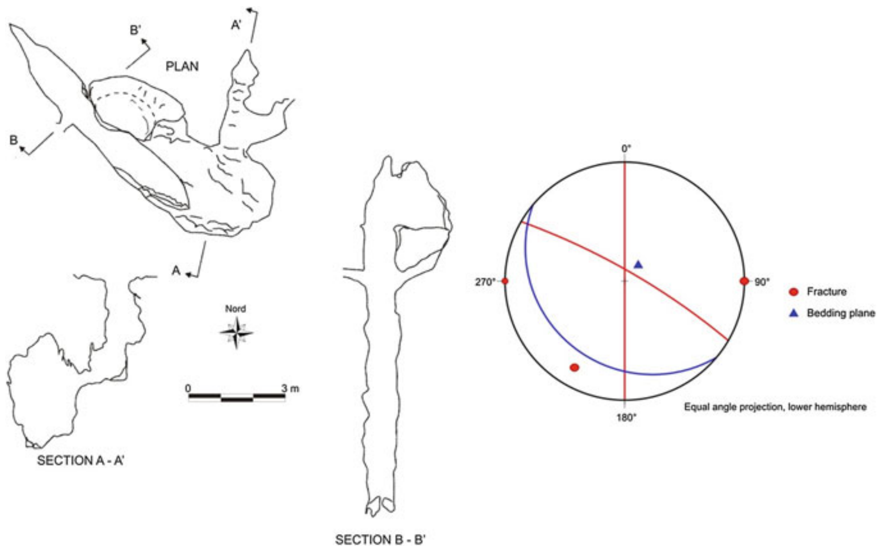

Fig. 6.241 Map and stereogram of main geological structures

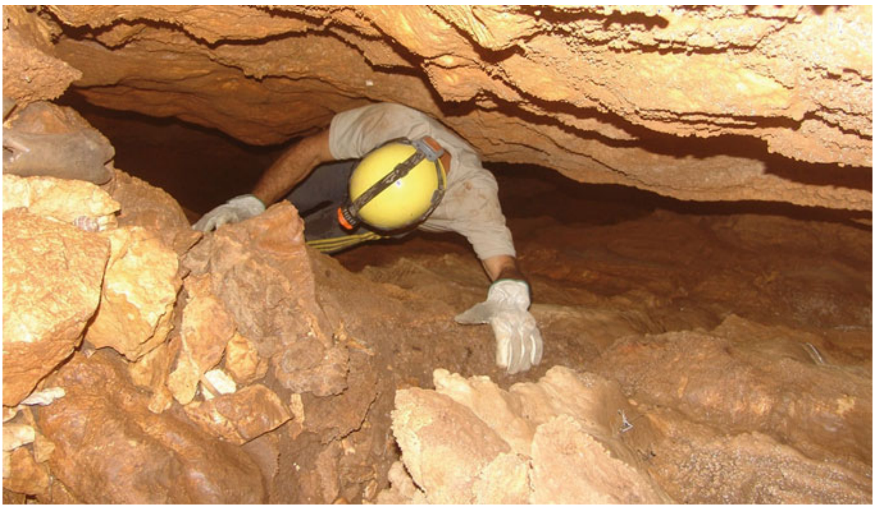

Fig. 6.242 Descending conduit along a NW-SE oriented fracture with rock block deposits

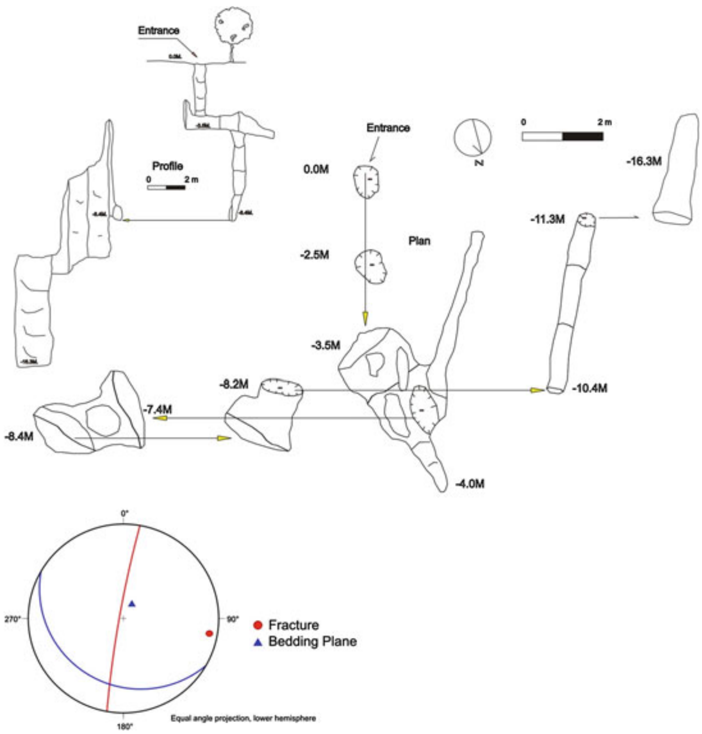

Fig. 6.243 Map and stereogram of the main geological structures in cave

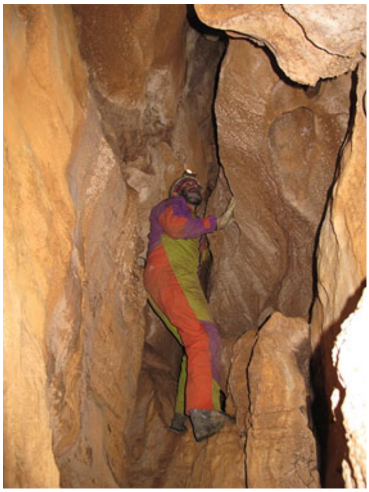

Fig. 6.244 Conduit developed along a NNE-SSW oriented fracture

Fig. 6.245 Shaft developed along a ENE-WSW oriented fault

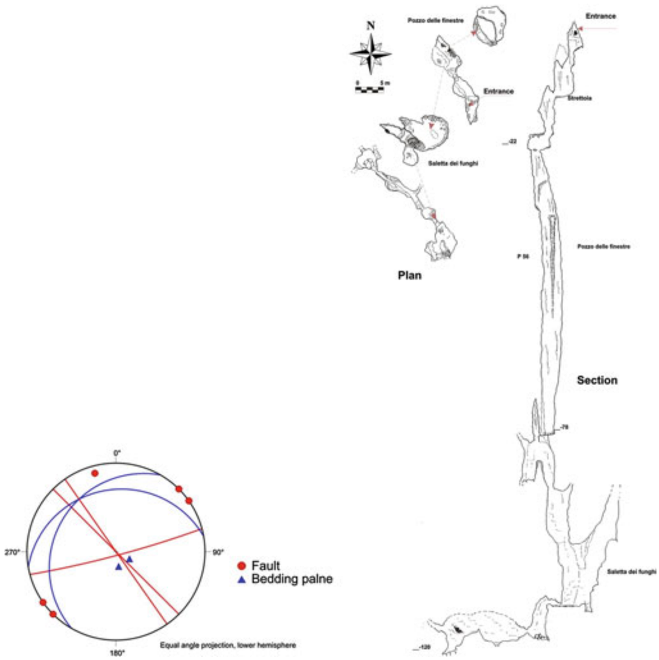

Fig. 6.246 Stereogram of the main geological structures and map of the cave

6.6.3.1 Structural Data

The analysis of the structural data surveyed in the above mentioned caves verifies the considerations being reported below (see Tables 6.4, 6.5, 6.6, 6.7 and general map of Fig. 6.302).

The karstification processes developed in the polje have mainly affected NNE-SSW oriented structures, and, to a lesser extent, NE-SW and NW-SE trending structures (Fig. 6.247).

The analysis also shows the different trend between the western sector, with NW-SE and E-W main directions (Fig. 6.248), and the central and eastern sector of the polje, with prevalent directions extending NNE-SSW (Fig. 6.249) and NE-SW respectively (Fig. 6.250).

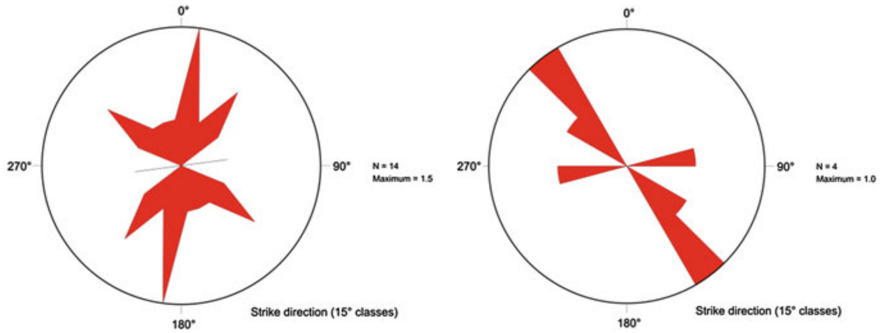

Figs. 6.247–248 Polje general Rose diagram of karstification (*left*) and cave karstified geological structures in the polje western sector (*right side*)

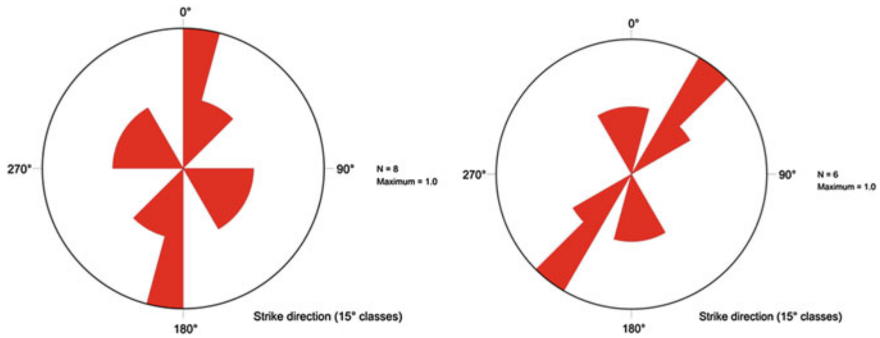

Figs. 6.249–250 Rose diagram of the cave karstified geological structures of the central (*left side*) and eastern sector (*right side*) of the polje

Table 6.4 Cave geological structures of the Purgatorio polje

Cave/Sectors	Fracture/Fault		Bedding plane	Lithology	Length/Depth (m)
	Strike	Dip direction			
Abisso del Purgatorio					
Upper vadose zone	N 30		N 230/25°	Dolomitic limestone Norian–Liassic	432/−194
Pozzo Vespa					
Belvedere	N 40–50		N 220/26°		
Middle vadose zone	N 155/N 30		N 190/35°		
Salone Abete					
Upper Epiphreatic oscillation zone	N-S/N 170/N 40				
Bottom					
Zubbia delle More					
Main fracture	N 145		N 220/15°	Dolomitic limestone Norian–Liassic	76/−43
Secondary fracture	N-S				
Zubbia della Palma Nana					
Main fracture	N 20	N 110/80°	N 210/25°	Dolomitic limestone Norian–Liassic	30/−18
Bottom sector	N 110	N 200/80°			
Zubbia delle Ossa					
Main fracture	N 120	N 30/80°	N 220/20°	Dolomitic limestone Norian–Liassic	21/−24
Secondary fracture	N-S				
Zubbia Nova	N 10	N 280/85°	N 210/20°	Dolomitic limestone Norian–Liassic	34/−16
Abisso delle Gole				Calcarenites Upper Jurassic–Lower Cretaceous	170/−120
Pozzo brecciato	N 135		N 300/20°		
Sala dei Funghi	N 75	N 165/85°			
Bottom	N 125		N 350/20°		

6.6.4 *The Caves in the Mt. Sparagio Ridge (Site* d*)*

The karst caves surveyed on the Monte Sparagio ridge are mainly to be found in its northern sector, which is characterized by the outcropping of the Norian-Liassic dolomites and dolomitic limestones. These terrains are covered, as one proceeds to higher ground and stratigraphic positions, by the Dogger-Malm red nodular limestones, calcarenites and calcilutites, the so-called *Rosso Ammonitico*, which in their turn are superseded by the calcirudites, calcarenites and calcilutites of the Upper Titonian-Lower Cretaceous age, followed by the biocalcarenites and biocalcirudites with basaltic intercalations of the Upper Cretaceous (see Fig. 4.3 of the Chap. 4). The surveyed caves are described below (Fig. 6.251).

Zubbia delle Tre Corna: the opening appears at 765 m asl, the effective extension is measured at 81 m, and, at 51 m, this cave is the deepest one yet surveyed on the Mt. Sparagio ridge. This vertical and vadose cave developed in the Norian-Liassic dolomite and dolomitic limestone carbonate terrains, with dip to N 155 at 35°. From a structural point of view there are two fracture systems: one with an N 145 direction and another, which intersects with the first, with N 50 (Figs. 6.252 and 6.253).

Grotta delle Eccentriche: at 605 m asl, the entrance on the left hand side of the Mt. Sparagio road, the cave extends for about 12 m and descends, with respect to the ground level at the entrance, for 3 m. Having its origins in the Norian-Liassic dolomites, it is developed on a sub-parallel system of fractures, with 40–50 cm spacing, with dip to N 65 at 75°.

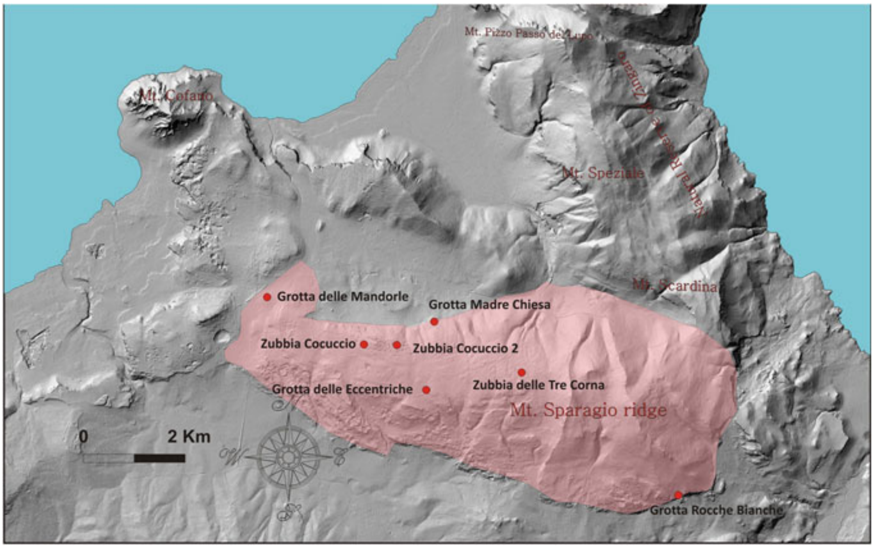

Fig. 6.251 Location of caves in the Mt. Sparagio ridge (*Hillshade map from* DEM Regione Siciliana 2007–2008)

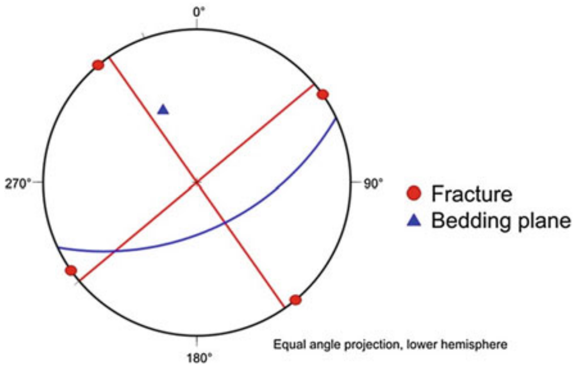

Fig. 6.252 Stereogram of the main geological structures in cave

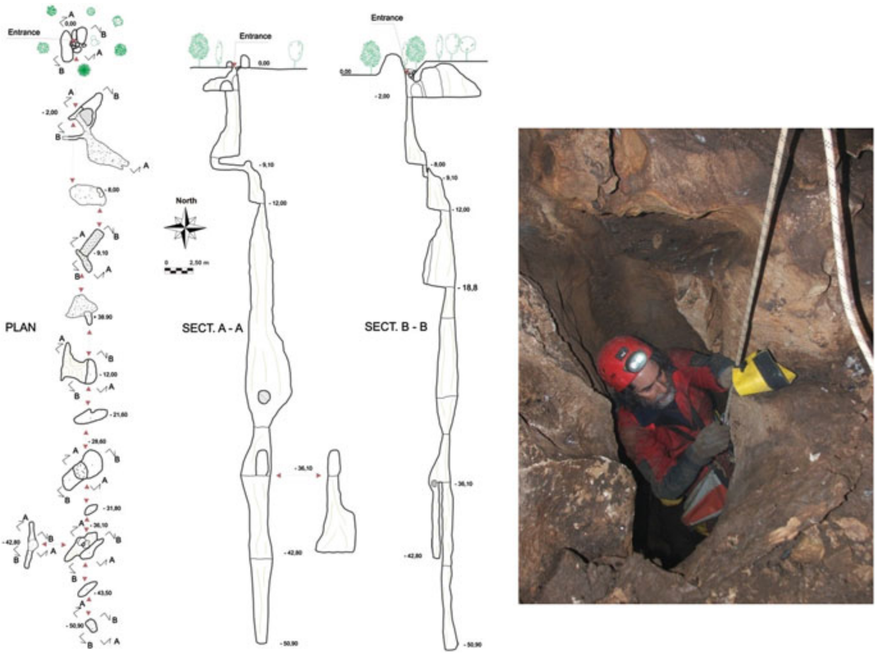

Fig. 6.253 Map of the cave and photo of shaft along a NW-SE oriented fracture

This system is intersected by a second system with a dip to N 270 at 85° (see stereogram, Fig. 6.254). The particularity of this small cave is that it contains in its terminal section a wall, and part of the roof, richly covered by spectacular helictite concretions (Fig. 6.255), while on the floor underneath bunches of coralloid splash concretions seem to grow out of the ground.

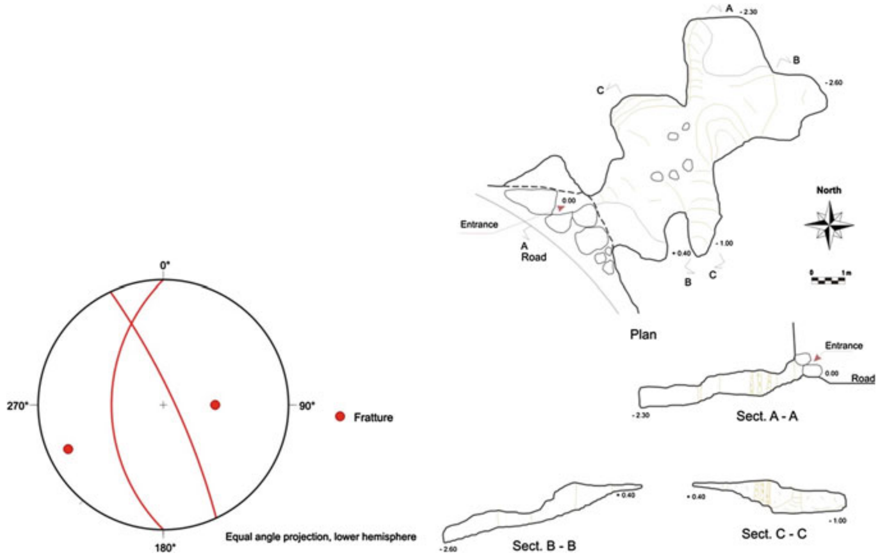

Fig. 6.254 Stereogram of the main geological structures and map of the cave

Fig. 6.255 Helictites

Zubbia Cocuccio 1: a vertical cave with its opening at 520 m asl situated in one of the disused quarries in the Cocuccio area on Mt. Sparagio, it extends for about 62 m, and descends for 42 m compared with the entrance ground level. The cave develops on the Norian-Liassic dolomites and dolomitic limestone, which have a dip to N 100 at 70°. The first part of the cave, which consists of the pit and the descending passage, develops along a fracture with dip to N 100 at 80°.

The second and last part, on the other hand, are respectively developed on a fracture with a dip to N 160 at 40° and on a fracture of the same above mentioned system N100/80° (Figs. 6.256 and 6.257). Inside the cave, which is of the vadose type, there are widespread calcite deposits, some particularly beautiful such as: extended petrified flowstones, large draperies and columns.

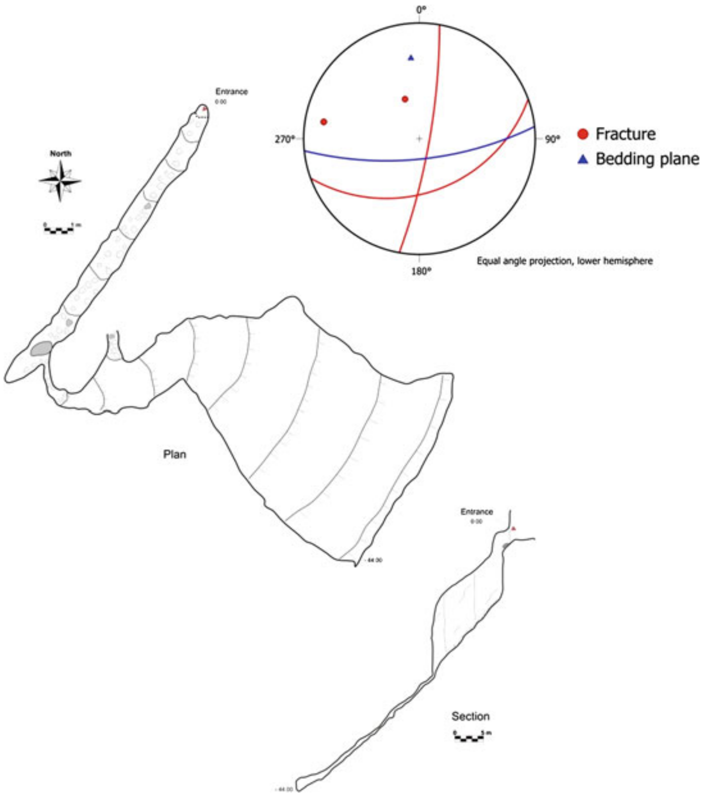

Fig. 6.256 Map and stereogram of the main geological structures in cave

Fig. 6.257 Grotta Cocuccio 1, shaft along a NE-SW oriented fracture

Grotta delle Mandorle: the opening of the cave is at 240 m asl; it extends for about 33 m and drops 12 m with respect to the entrance. It develops, in the Norian-Liassic dolomites and dolomitic limestone outcropping in the area with dip to N 105 at 30°, along a main fracture with dip to N 220–230 at 75°. This latter is dissected, in the terminal part of the main chamber, by a secondary fracture with a dip to N 190 at 85° (see stereogram, Fig. 6.258). In the terminal chamber collapse morphologies can be observed and in the ceiling there is a large rocky wedge bordered by fractures. Calcite deposits are also present both in the initial conduit, in the form of flowstones, and particularly in the terminal chamber with morphologies such as columns and stalagmites of various dimensions (Fig. 6.259).

Zubbia Cocuccio 2: the entrance, at the altitude of 559 m asl, is located inside a disused quarry; it extends essentially vertically and reaches a depth of 12.5 m. This vadose cave, which has its origins in the Norian-Liassic dolomites, develops on a fracture with a dip to N 150 at 80°. Outside the cave the following has also been surveyed: a fracture with a dip direction to N 60 at 70–75°, which intersects both

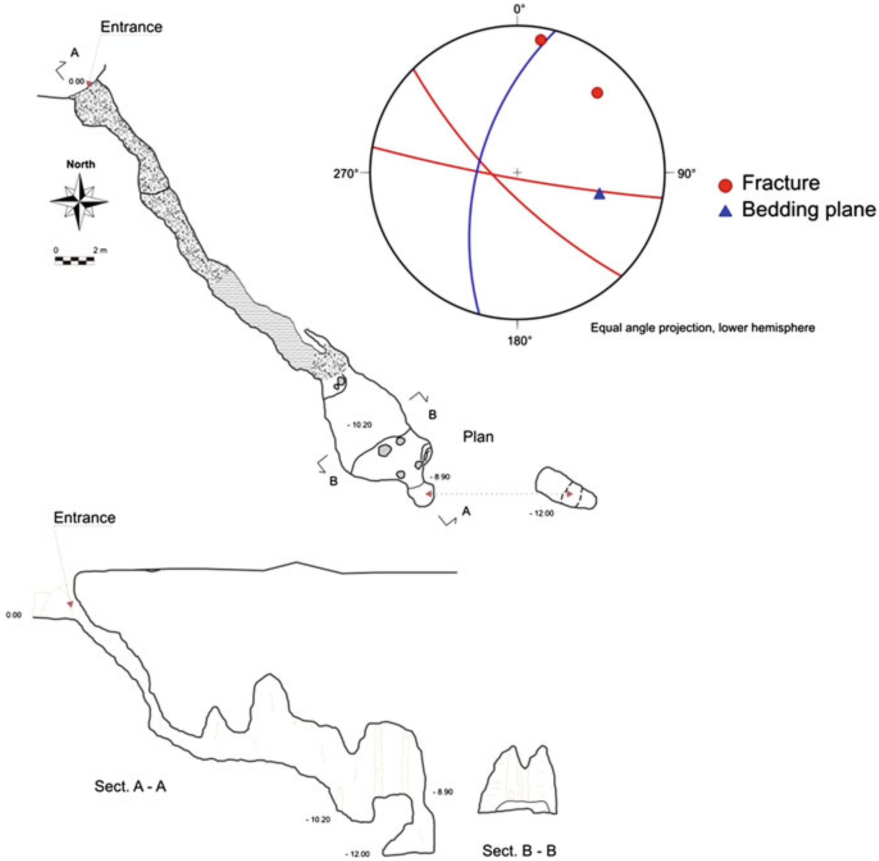

Fig. 6.258 Map and stereogram of the main geological structures in cave

the aforementioned fracture of the cave, and the layer bedding planes, this latter with a dip to N 180 at 70–75° (Figs. 6.260 and 6.261).

Grotta Rocche Bianche: this cave is situated, at an altitude of 361 m asl, on the southern side of the Mt. Sparagio ridge in Rocche Bianche area: it extends for 94 m and in an upwards direction for a total of 21 m. The cave, which develops in intercalations of carbonate megabreccia of Upper Cretaceous–Eocene age, owes its genesis to tectonic processes linked to deformation phases and to successive collapse phenomena, which in time have amplified the section. Concerning this aspect, on the east wall of the cave one can observe a NW-SE oriented fault wall, which is marked by striation (Figs. 6.262 and 6.263).

Grotta Madre Chiesa: this cave is located along the northern slope in the foothill of Mt. Sparagio ridge at an altitude of 378 m asl. It extends for 44 m, with a 3 m positive difference in level and presents typical structural morphologies such as collapsed block debris and elongated conduits developed along faults dipping to N 340 at 80° and to N 180 at 80° (Figs. 6.264 and 6.265).

Fig. 6.259 Columns and speleothems in the cave

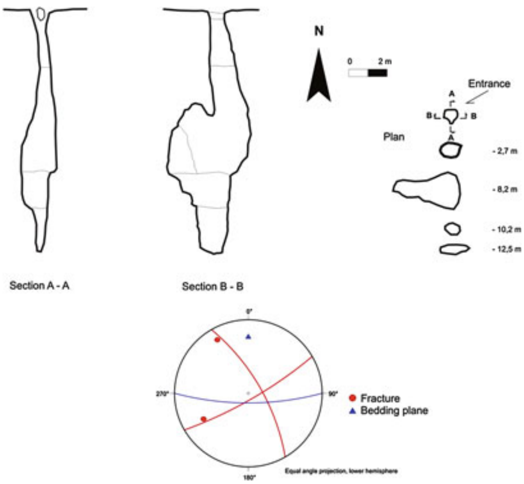

Fig. 6.260 Map and stereogram of the main geological structures in cave

Fig. 6.261 Speleothems on the wall of Zubbia Cocuccio 2

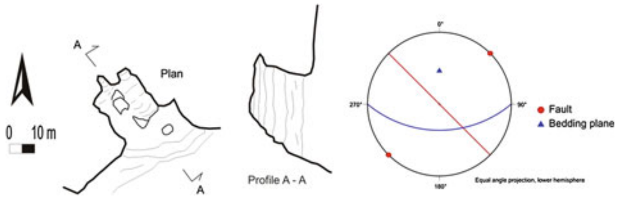

Fig. 6.262 Map and stereogram of the main geological structures

Fig. 6.263 Wall fault of the cave with striation

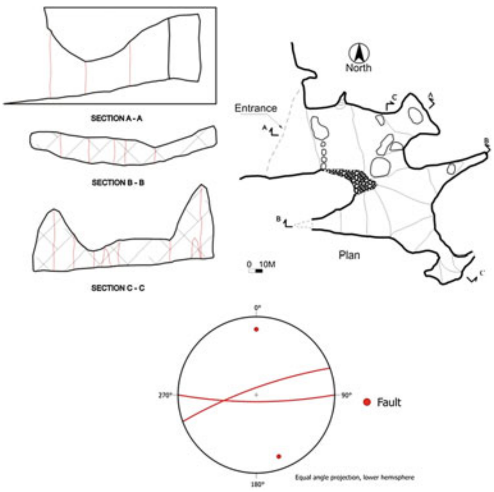

Fig. 6.264 Map and stereogram of the main geological structures

Fig. 6.265 Structural morphologies along a fault

6.6.4.1 Structural Data

The analysis of the structural data surveyed in the above mentioned caves verifies the considerations being reported below (see Tables 6.5, 6.6 and 6.7 and general map of Fig. 6.302).

On the Mt. Sparagio ridge, the main karstified structures that have been surveyed in caves present an ESE-WSW and NNW-SSE trend (Fig. 6.266). The same structural trends have also been surveyed in the tectonic caves *Rocche Bianche* and *Madre Chiesa* (Fig. 6.267).

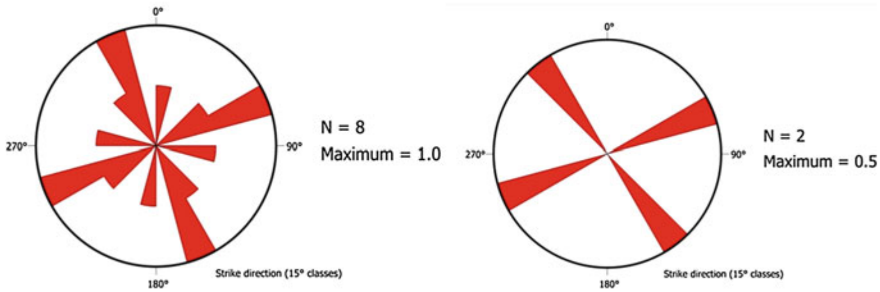

Figs. 6.266–267 Rose diagram of the main karstified structures surveyed in the caves (*left side*) and of the main structures surveyed in tectonic caves (*right side*)

Table 6.5 Cave geological structures of the Mt. Sparagio ridge

Cave/Sectors	Fracture/Fault		Bedding plane	Lithology	Length/Depth (m)
	Strike	Dip direction			
Zubbia delle 3 Corna					
Fracture 1	N 160	N 70/70°	N 160/35°	Dolomitic limestone Norian–Liassic	81/−51
Fracture 2	N 50	N 320/75°			
	N 135	N 40–50/88°			
Grotta delle Eccentriche	N 155	N 65/80°		Dolomitic limestone Norian–Liassic	40/−3
	N 180	N 270/45°			
Zubbia Cocuccio 1			N 174/70°	Dolomitic limestone Norian–Liassic	62/−44
Upper sector	N 10	N 100/80°			
Lower sector	N 70	N 160/40°			
	N 10	N 100/80°			
Zubbia Cocuccio 2			N 180/75°	Dolomitic limestone Norian–Liassic	−12.5
Main fracture	N 60	N 150/80°			
Outside fracture	N 150	N 60/70°			
Grotta delle Mandorle					
Main fracture	N 135	N 225/75°	N 105/30°	Calcarenites	40/−12
Secondary fracture	N 100	N 190/85°		Upper Jurassic–Lower Cretaceous	
Grotta Rocche Bianche	NW-SE with striations	N 225/80°	N 180/50°	Calcilutites Upper Cretaceous–Eocene	94/21
Grotta Madre Chiesa		N 340/80°		Dolomitic limestone Norian–Liassic	44/3
		N 180/80°			

6.6.5 *The Caves in the Mt. Monaco–Mt. Speziale–Mt. Scardina Ridge (Site* e*)*

The caves surveyed in the Mt. Monaco–Mt. Speziale–Mt. Scardina ridge are mainly located in its eastern sector, characterized by the outcropping of the stromatolithic limestone and the dolomitic limestone of the Norian-Liassic age (see Fig. 4.3 of Chap. 4). The caves surveyed for their morphostructural aspects are below synthetically described (Fig. 6.268).

Fig. 6.268 Location of the caves in the Mt. Monaco–Mt. Speziale–Mt. Scardina ridge (*yellow part*) (*Hillshade map from* DEM Regione Siciliana 2007–2008)

Grotta del Sughero: this cave, situated in Sughero area at 239 m asl of the Zingaro Natural Reserve, extends for 527 m with a depth of −22 m. It is made up of various chambers and develops in the Norian-Liassic dolostones on two levels along a NNW-SSE system of fractures. The cave shows numerous speleothems of various genesis and morphologies (Figs. 6.269 and 6.270–271).

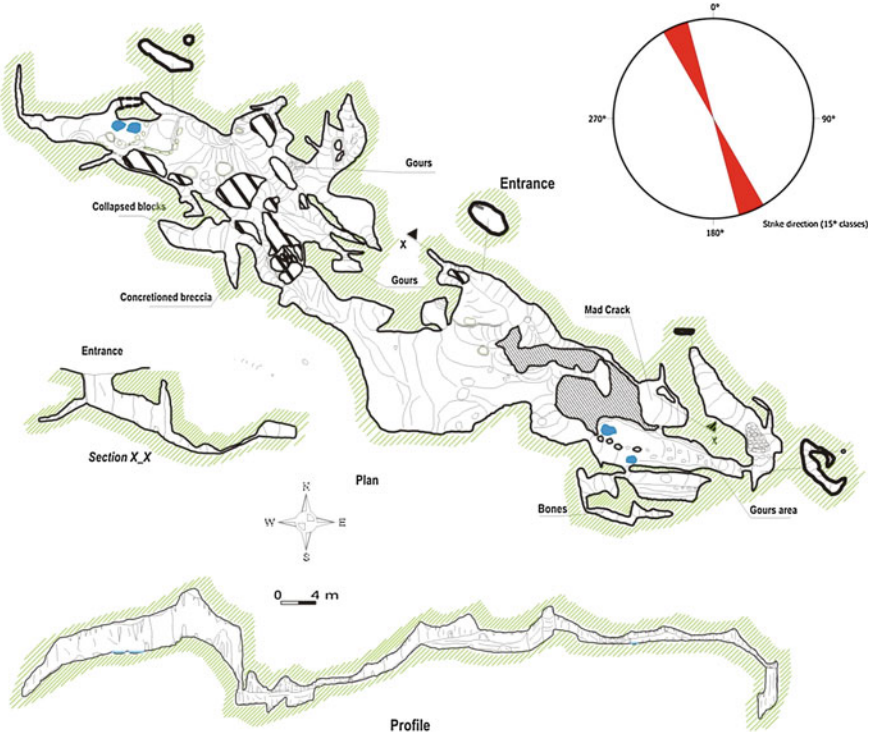

Fig. 6.269 Map of the cave and Rose diagram of the main geological structures

Figs. 6.270–271 Flowstones and helictites (*right photo*) in the Sughero cave

Zubbia dei Coralli: a vertical vadose cave in Cusenza area at 369 m asl. It extends for about 153 m, to a depth of −55 m below the entrance level. It develops in the Norian-Liassic dolostones, along a fracture oriented NE-SW (Fig. 6.272). Internally numerous speleothems of various genesis and morphology are present (Figs. 6.273 and 6.274).

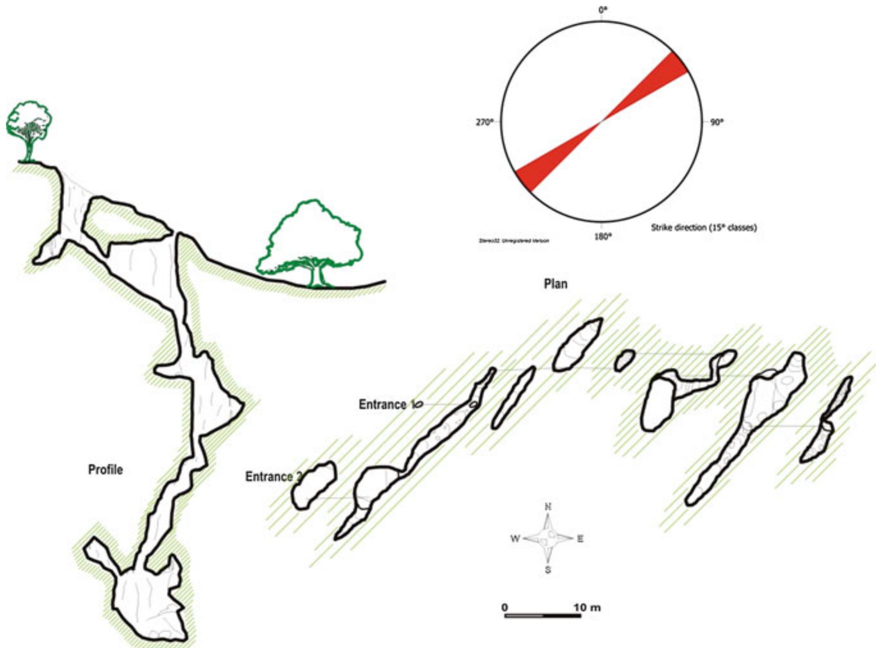

Fig. 6.272 Map and Rose diagram of structures in cave

Fig. 6.273 Widespread flowstones in the cave

Fig. 6.274 Shaft on a NE-SW oriented fracture

Zubbia delle Lame: a vertical vadose cave in Cusenza area: the entrance is at 409 m asl; it extends in the Norian-Liassic dolomites for about 50 m, descending for 15 m, on two fractures oriented N-S and NE-SW (Fig. 6.275). There are a great number of calcite concretions of a variety of morphologies (Figs. 6.276–277).

Zubbia del Corno: a vertical vadose cave at 375 m asl in Cusenza area. It also develops in the Norian-Liassic dolomites, and extends for about 50 m, but only descends for 10 m, on two fractures, the main one oriented NW-SE and the secondary one N-S (Fig. 6.278). This cave also contains many calcite fillings of various morphologies (Figs. 6.279–280).

Zubbbia della Ficara: a collapse doline-cave with its entrance at 637 m asl in the Pianello area: it has a lenght of 31 m and reaches a depth of 11 m. It develops in the Upper Triassic doloarenites, along a N-S oriented fracture (Fig. 6.281). Large flowstones and speleothems are present (Figs. 6.282–283).

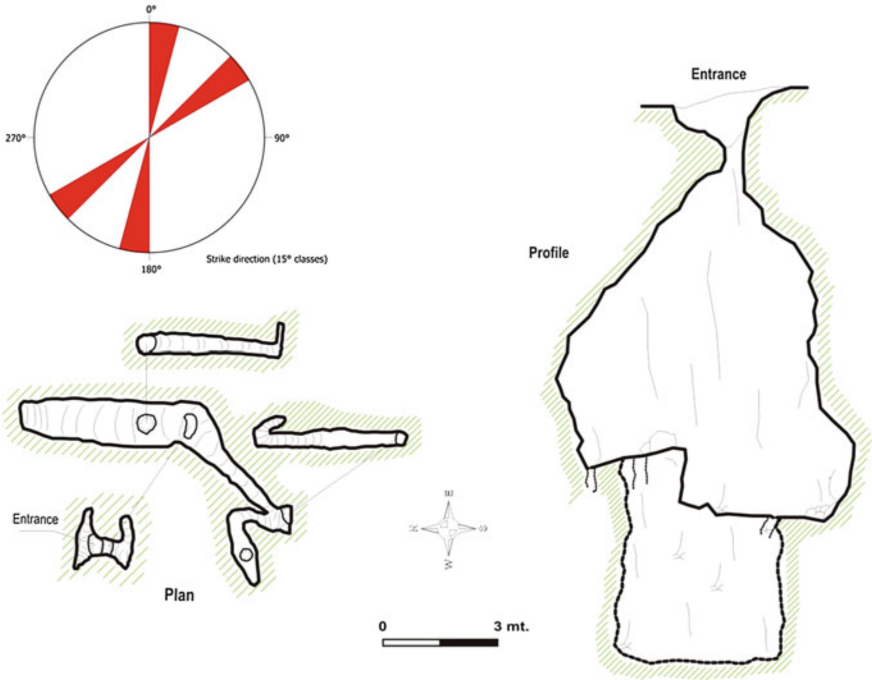

Fig. 6.275 Map and Rose diagram of the Zubbia delle Lame

Figs. 6.276–277 Entrance shaft along a NW-SE oriented fracture and wall flowstones

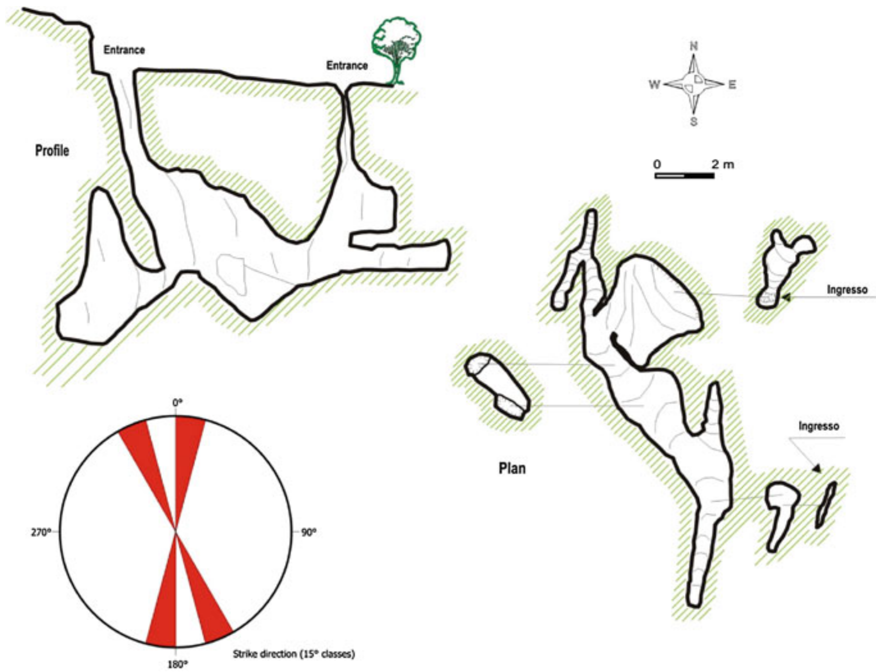

Fig. 6.278 Map and Rose diagram of the Zubbia del Corno

Figs. 6.279–280 Entrance along a NW-SE oriented fracture (*left photo*); Wide flowstones inside the cave (*right photo*)

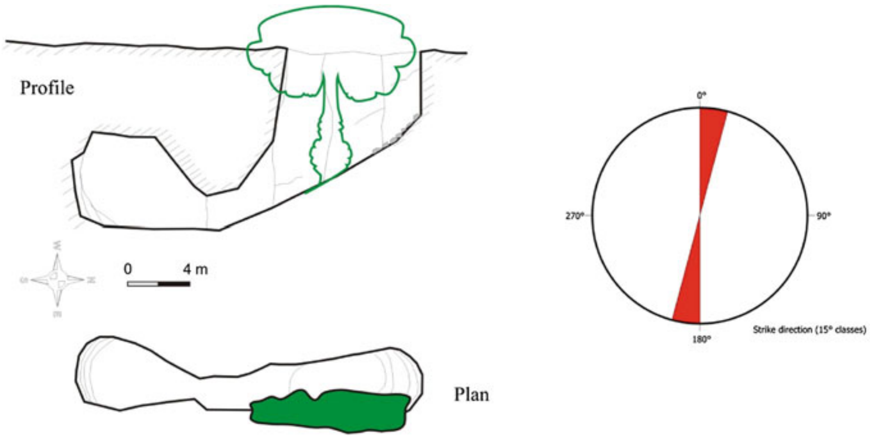

Fig. 6.281 Map and Rose diagram of Zubbia delle Ficara

Figs. 6.282–283 Bottom of the Zubbia and speleothems

Zubbia di Monte Scardina: this vertical vadose cave is to be found in the Mt. Scardina area at an altitude of 577 m asl. It develops in the Norian-Liassic dolostones, extending for about 166 m with a depth of 66 m, on a NW-SE oriented fault (Fig. 6.284). Speleothems of different forms and genesis are present in the cave (Figs. 6.285–286).

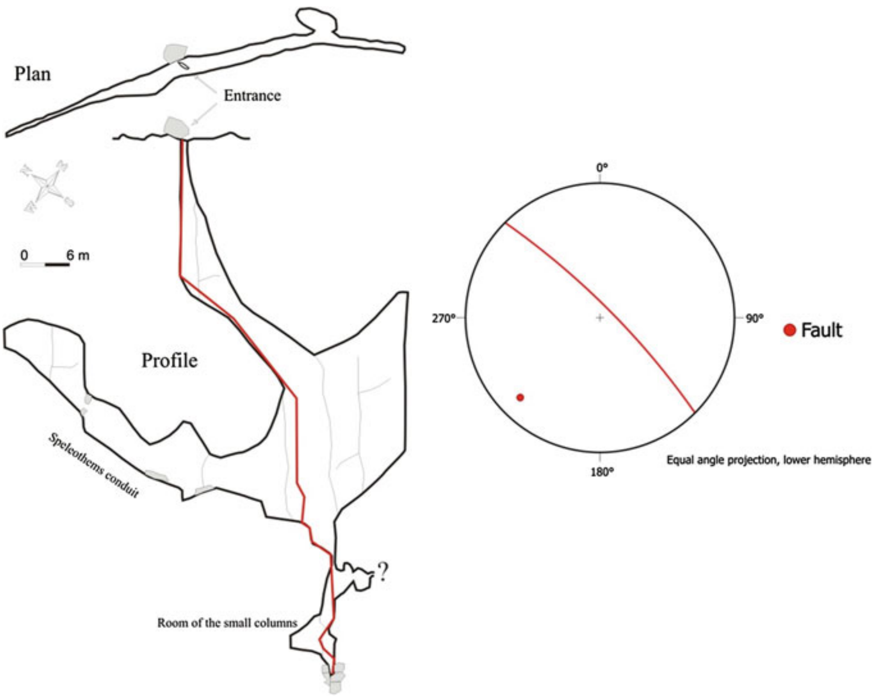

Fig. 6.284 Map and Rose diagram of Zubbia Scardina structures in cave

Figs. 6.285–286 Shaft on a NW-SE oriented fault and speleothems in the Zubbia di Monte Scardina (*right photo*)

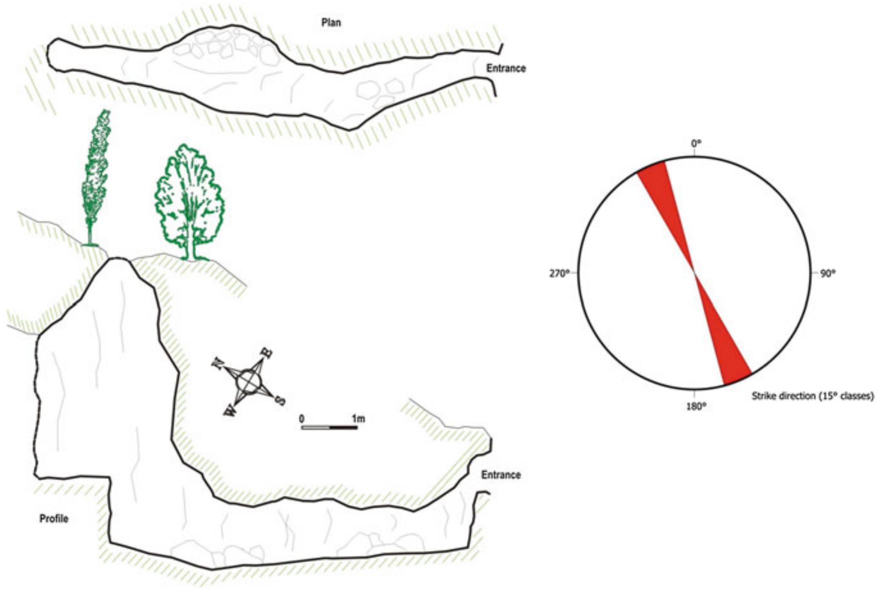

Fig. 6.287 Map and Rose diagram of the main geological structures in cave

Grotta di Mt. Speziale: an extensional tectonic cave with its entrance at 739 m asl. It develops in the Norian-Liassic dolostones for about 20 m, with an upward trend of 3 m, along a NNW-SSE fracture (Fig. 6.287). On the wall of the cave calcite deposits are present (Figs. 6.288 and 6.289).

Grotta 1 and 2 of Mt. Scardina: structural caves, linked to the deep-seated gravitational slope deformations, which have affected the eastern sector of the ridge (Agnesi et al. 1987, 1995), found at 577 m asl in the Monte Scardina relief. They extend for 407 m, descending 42, developing in the Norian-Liassic dolostones, along an extensional fault oriented NNW-SSE (Figs. 6.290, 6.291 and 6.292).

Grotta del Riccio: this cave is located on the western slope of the Mt. Monaco-Mt. Speziale-Mt. Scardina ridge in the Cocuzzo Mondello area at an altitude of 246 m asl. It is about 103 m long, with a depth of 8 m, and develops in the Upper Cretaceous limestone. The cave opens up in two conduits: the first one developed along a fracture dipping to N 190 at 80°, the second along a NE-SW trending fracture (refer to stereogram in Fig. 6.293). The cave presents, especially in the latter conduit, a rich variety of speleothems including large flowstones and microgours (Fig. 6.294).

Grotta della Volpe: this cave is located on the western slope of the Mt. Monaco-Mt. Speziale-Mt. Scardina ridge in the Cocuzzo Mondello area, close to the Riccio cave, at a higher altitude of 270 m asl. It is about 110 m long, with a positive altitude difference of 18.5 m, and develops in the Upper Cretaceous limestone.

Fig. 6.288 Conduit along a fracture

Fig. 6.289 Calcite deposits on the wall of the cave

Fig. 6.290 Fault of Mt. Scardina

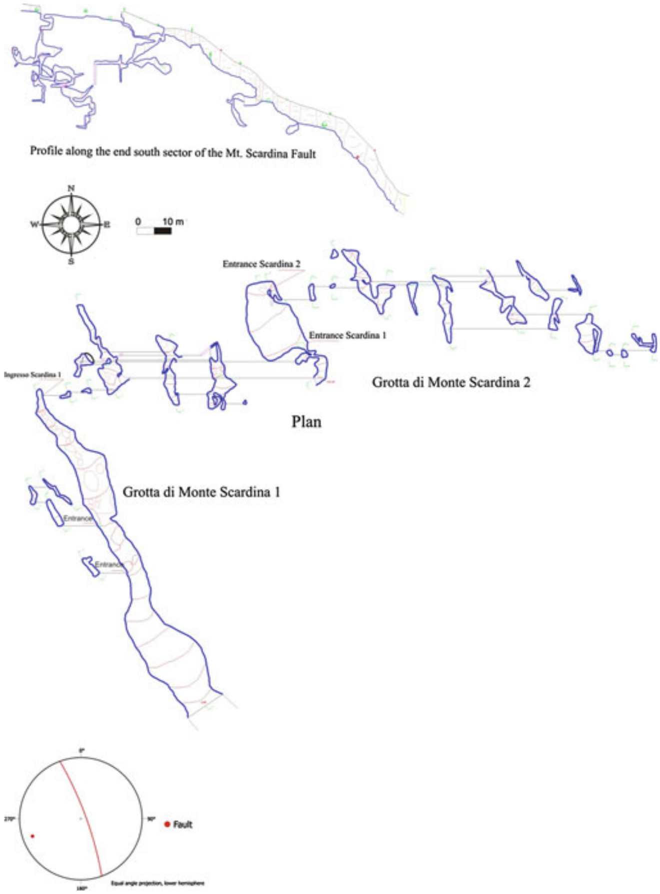

Fig. 6.291 Map and stereogram of the main geological structures

Fig. 6.292 View of the fault with block material

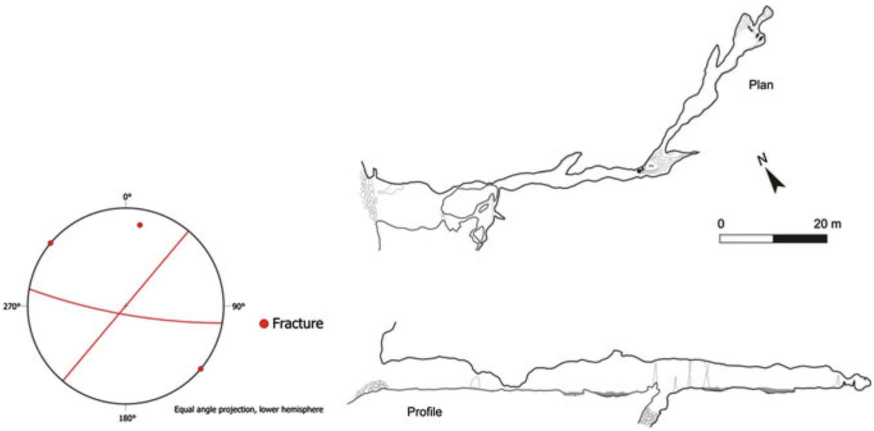

Fig. 6.293 Map and stereogram of the main geological structures of the Grotta del Riccio

Fig. 6.294 Widespread flowstones in the Grotta del Riccio

The cave develops with an ascending conduit for about 80 m, and later starts to descend until it closes with a narrow conduit. The main conduit develops along a fracture with dip to N 170 at 80°, which cuts the limestone layers dipping to N 330 at 55° (Figs. 6.295 and 6.296–297). The cave presents a rich variety of speleothems including large flowstones and microgours.

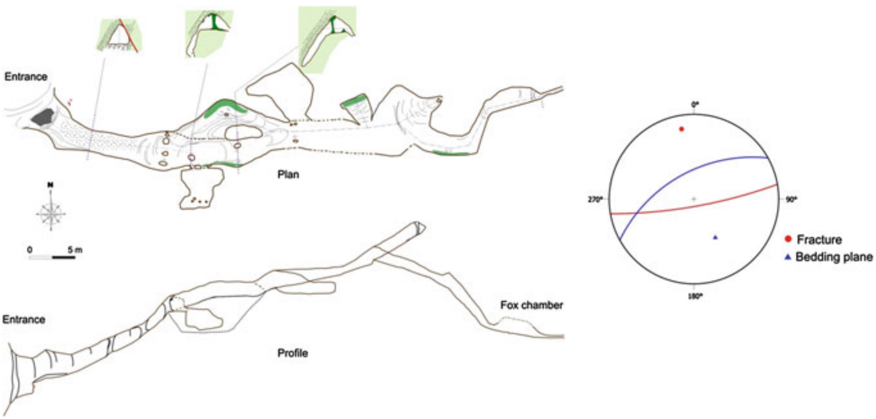

Fig. 6.295 Map and stereogram of the main geological structures in cave

Figs. 6.296–297 Cave wall dissected by a dipping ESE-WNW fracture (*left photo*); conduit along a bedding plane layers dipping to N 330 at 55° (*right photo*)

6.6.5.1 Structural Data

The analysis of the structural data surveyed in the above mentioned caves verifies the considerations being reported below (see Tables 6.6 and 6.7 and general map of Fig. 6.302).

The major karstified cave structures surveyed in the Mt. Monaco–Mt. Speziale-Mt. Scardina ridge indicate a principal NNW-SSE trend and a secondary ESE-WSW/NNE-SSW trend (Fig. 6.298). In particular, in the northern segment an E-W trend prevails (Fig. 6.299), in the central part an NE-SW trend is dominant (Fig. 6.300), while in the southern sector a NNW-SSE trend prevails (Fig. 6.301).

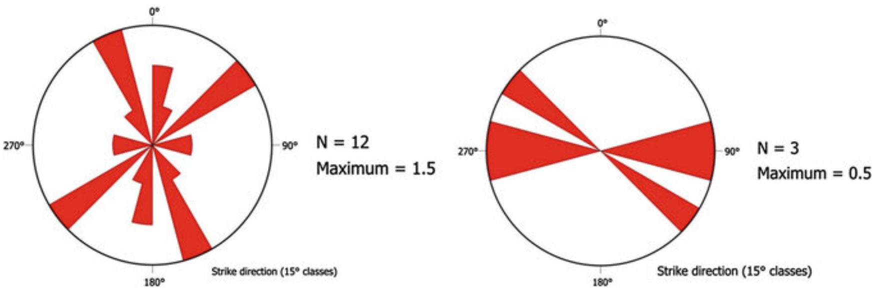

Figs. 6.298–299 General Rose diagram of the main karstified structures surveyed in the caves present in the ridge (*left side*);—Rose diagram of the northern sector of the ridge (*right side*)

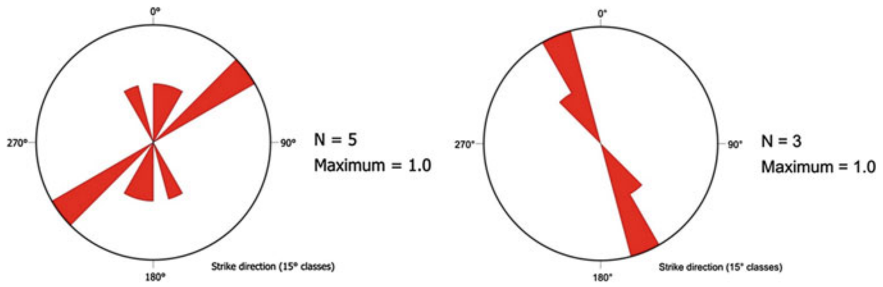

Figs. 6.300–301 Rose diagram of the central (*left side*) and southern (*right side*) sector of the Mt. Monaco–Mt. Speziale–Mt. Scardina ridge

Table 6.6 Cave geological structures of the Mt. Monaco–Mt. Speziale–Mt. Scardina ridge

Cave/Sectors	Fracture/Fault		Bedding plane	Lithology	Length/Depth (m)
	Strike	Dip direction			
Zubbia dei Coralli	N 45			Dolomitic limestone Norian–Liassic	153/−55
Zubbia delle Lame				Dolomitic limestone Norian–Liassic	50/−15
Fracture 1	N-S				
Fracture 2	N 45				
Zubbia del Corno				Dolomitic limestone Norian–Liassic	50/−10
Main fracture	160				
Secondary fracture	N 20				
Grotta Mt. Speziale	N 160			Dolomitic limestone Norian–Liassic	20/3
Grotta 1 Mt. Scardina	N 160	N 70/80°		Dolomitic limestone Norian–Liassic	177/−24
Grotta 2 Mt. Scardina	N 160	N 70/80°		Dolomitic limestone Norian–Liassic	230/−42
Zubbia Mt. Scardina	N 135	N 45/80°		Dolomitic limestone Norian–Liassic	166/−66
Grotta del Sughero	N 160			Dolomitic limestone Norian–Liassic	527/−22
Zubbia della Ficara	N-S			Dolostone Upper Triassic	31/−11
Zubbia di Pizzo Candela				Dolomitic limestone Norian–Liassic	9/−5
	N 250				
	N 100				
Grotta del Riccio				Biocalcarenites Upper Cretaceous	103/−8
Fracture 1	N 100	N 190/80°			
Fracture 2	NE-SW				
Grotta della Volpe				Biocalcarenites Upper Cretaceous	110/18.5
	N 80	N 170/80°	N 330/55°		

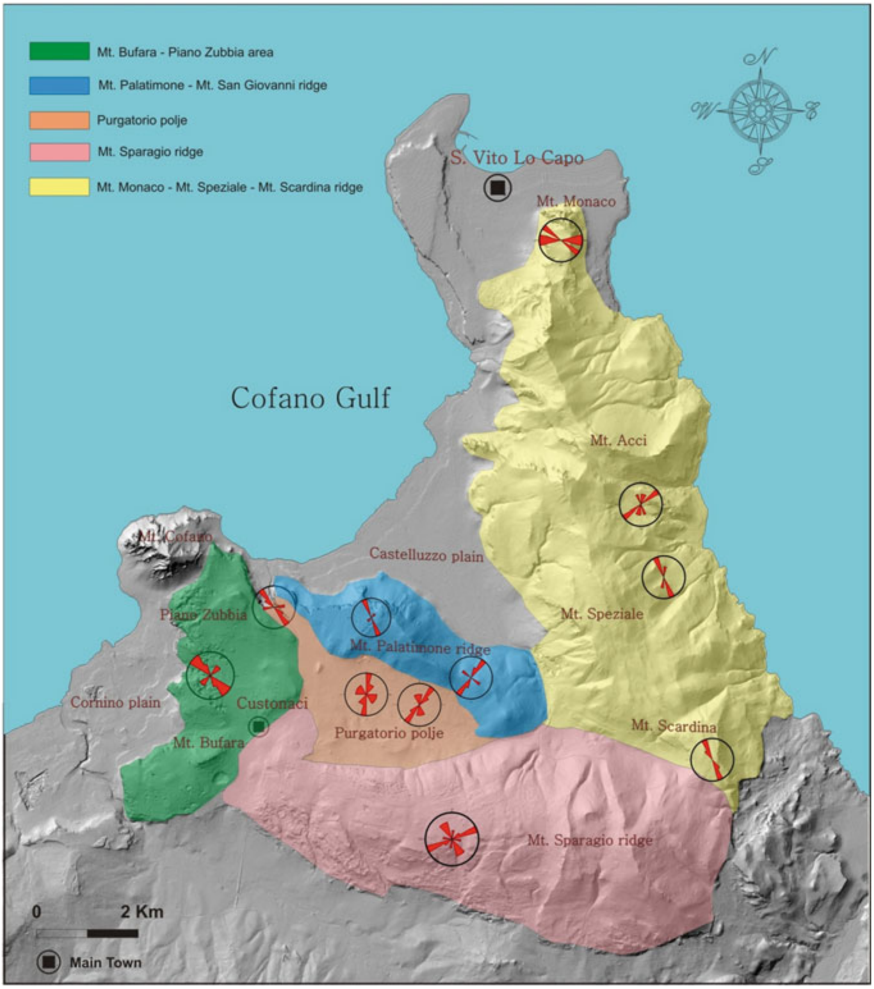

Fig. 6.302 Map with Rose diagrams of the main karstified cave geological structures surveyed in the study area (*Hillshade map from* DEM Regione Siciliana 2007–2008)

Table 6.7 Synoptic table of the main and secondary cave karstified geological structures in the selected areas of study

Karst area	Fault/Fracture	
	Main	Secondary
Mt. Bufara–Cerriolo–Piano Zubbia	NW-SE	NE-SW
Mt. Palatimone–Mt. S. Giovanni	NNW-SSE	NE-SW
Purgatorio polje	NNE-SSW	NW-SE
Mt. Sparagio ridge	ENE-WSW	NW-SE
Mt. Monaco-Speziale-Scardina ridge	NNW-SSE	NNE-SSW

6.7 The Sea Caves and Coastal Karren in the Relict Sea-Cliffs

Near the coastal belt of the studied territory close to the relict marine cliffs some morphologies are present, whose origin in some cases is due to the erosive/corrosive sea actions in other cases to biokarst erosion. The actual position of these marine forms close to the coast line is due to negative eustatic changes happened in the Pleistocene age and to the tectonic uplift, which have affected in different way the area of research (Antonioli et al. 1999a, b; Di Maggio et al. 1999). The survey carried out along these relict cliffs made possible to distinguish the following morphologies:

- *Erosional notches*, coastal karren due to intense biogenic activity, combined or not with abrasion, hydraulic action and dissolutional processes, in the intertidal zone of the cliffs (Viles 1984; Lundberg 2009);
- *Sea paleo-forms gorge-types*, characterized by short length, narrow width and with a general morphology of a karstified tapering fracture;
- *Structural caves*, small-medium caves along fractures or bedding planes widened by rock collapses and in some cases by karst dissolution;
- *Sea caves* (*littoral caves*), due to the prevalent sea erosion with or without karst solution processes originated along bedding planes and fractures;
- *Flank margin caves* formed at the top and at the bottom of the freshwater lens in coastal areas by mixing dissolution (Mylroie and Carew1990). This very special type of caves has been reported especially in eogenetic limestones of carbonate islands such as the Bahamas and Bermuda (Mylroie et al. 1995), Guam (Mylroie et al. 2001), and the Mariana Islands (Jenson et al. 2006), but also in mature limestones of New Zealand (Mylroie et al. 2008), in brecciated limestones on the Island of Cres in Croatia (Otoničar et al. 2010) and in eolian calcarenites of Kangaroo Island, Australia (Mylroie and Mylroie 2009).

The aforementioned forms have been surveyed in the relict cliffs present in the area of research and described below.

6.7.1 The Mt. Cofano–Mt. Palatimone Relict Sea-Cliff Features

A total number of six sea caves were surveyed along the relict cliffs of Monte Cofano and south-western areas (Figs. 6.303, 6.304, 6.305 and Table 6.8), five of which were developed on fractures while one developed along a bedding plane.

The structural data collected from the above mentioned caves and shown in the diagram of Fig. 6.306, indicates a main NW-SE trend and a NE-SW secondary trend. The Grotta del Crocifisso, which has an archeological importance, is

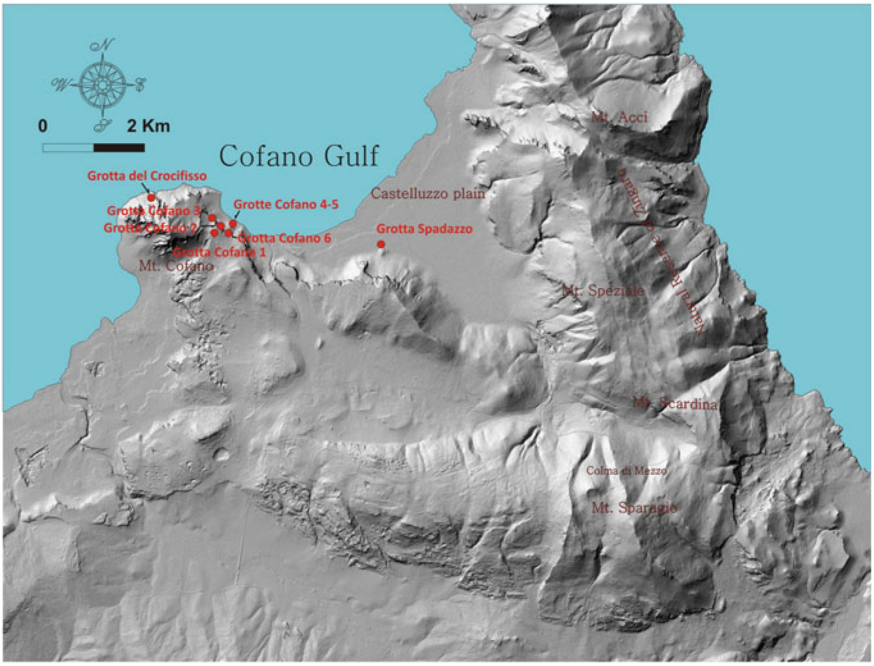

Fig. 6.303 Location of the sea caves and karst forms in the Mt. Cofano and in the northern slope of Mt. Palatimone relict sea-cliffs (*Hillshade map from* DEM Regione Siciliana 2007–2008)

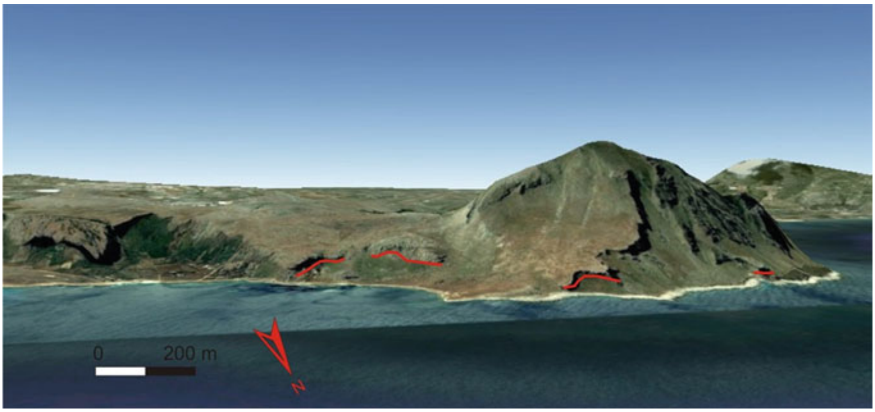

Fig. 6.304 Mt. Cofano–Mt. Palatimone coastal belt and relict sea-cliffs (*red lines*) (from Google Earth)

Table 6.8 Caves and coastal karren in the Mt. Cofano–Mt. Palatimone relict sea-cliffs

Morphology	Elevations m asl	Structure		Lithology	Cave type/Deposits
		Fracture	Bedding plane		
Grotta del Crocifisso	60	N 250/80°		Dolomites Upper Triassic	**Sea cave**—archaeological deposits
Grotta Cofano 1	184	NNE-SSW		Calcarenites Upper Jurassic–Valanginian	**Sea cave**
Grotta Cofano 2	158	N 40		Calcarenites Upper Jurassic–Valanginian	**Sea cave**—phreatic morphologies
Grotta Cofano 3	105	N 130		Calcarenites Upper Jurassic–Valanginian	**Sea cave**—rock shelter sea-fossils and paleo-notches
Grotta Cofano 4	44			Calcarenites Upper Jurassic–Valanginian	**Sea cave**—bedding plane chimney conduit
Grotta Cofano 5	43	N 145		Calcarenites Upper Jurassic–Valanginian	**Sea cave**—notches
Grotta Cofano 6	133			Calcarenites Upper Jurassic–Valanginian	**Flank margin cave**—bedding plane
Grotta Spadazzo	50			Eolianites Lower Pleistocene	**Flank margin cave**—flowstones

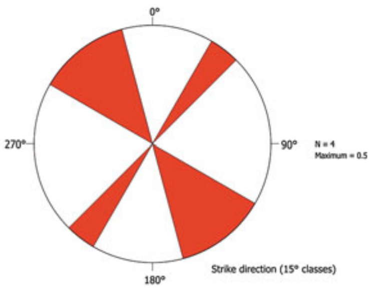

Figs. 6.305–306 Mt. Cofano–Mt. Palatimone relict sea-cliffs (*left photo*); Caves Rose diagram of geological structures in caves (*right side*)

Figs. 6.307–308 Grotta del Crocifisso at 60 m asl (*left photo*); Grotta Cofano 3 with notch in the cliff (*right photo*)

Fig. 6.309 Grotta Cofano 5 with notch in the cliff

developed in Upper Triassic dolostones (Fig. 6.307), the others on calcarenites of Upper Jurassic-Lower Cretaceous.

The cave present in eolianites of the Lower Pleistocene of Spadazzo area, at the foot of the northern slopes of Monte Palatimone (Fig. 6.308) and the Grotta Cofano

Fig. 6.310 Grotta Spadazzo in the eogenetic eolianites (*flank margin cave*)

Fig. 6.311 *Flank margin cave*—Grotta Cofano 6, along a bedding plane

6 (Fig. 6.309) have been classified, for all their morphologies, as *flank margin caves*. The former originated in eogenetic porous diagenetically immature calcarenites (Fig. 6.310), the latter in a telogenetic mature limestone (Fig. 6.311).

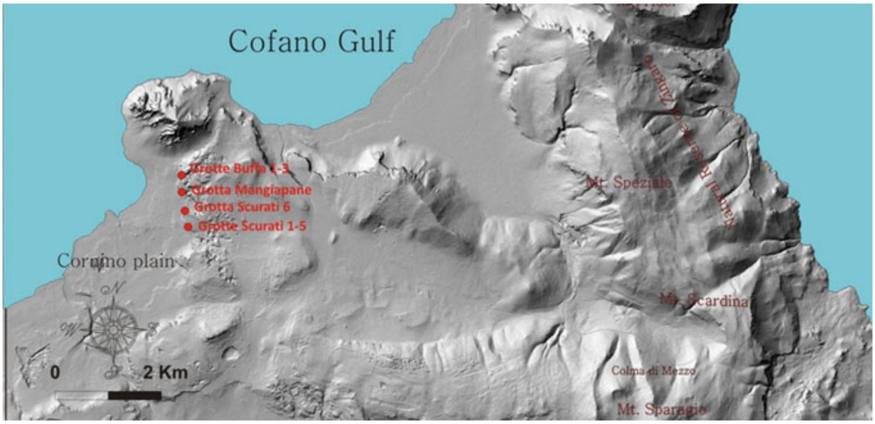

Fig. 6.312 Location of the sea caves and coastal karren in the Scurati–Cerriolo relict sea-cliffs (*Hillshade map from* DEM Regione Siciliana 2007–2008)

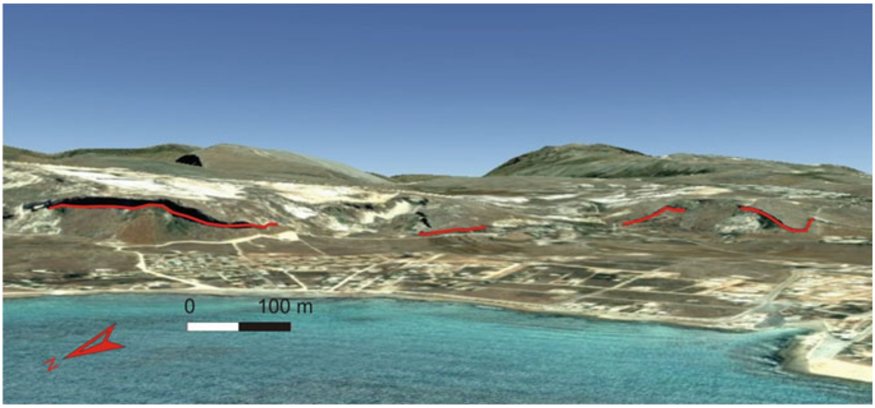

Fig. 6.313 Cornino coastal belt and Scurati–Cerriolo relict sea-cliffs (*red lines*) (from Google Earth)

6.7.2 The Scurati–Cerriolo Relict Sea-Cliff Features

Along the relict sea-cliffs of Scurati-Cerriolo area, surrounding the coastal plain of Cornino, a total of 16 karst morphologies were detected (Figs. 6.312, 6.313, Table 6.9), of which twelve are caves and four paleo-notches (Figs. 6.324–325, 6.326–327 and 6.328–329). Of these caves, six have been classified as sea caves (Fig. 6.315), two as structural caves, four as *flank margin caves* developed in a telogenetic limestone of the Upper Cretaceous (Figs. 6.316–317, 6.318–319, 6.320–321 and 6.322–323).

The structural data collected, shown in the Rose diagram of Fig. 6.314, indicates a main N-S trend.

Table 6.9 Caves and coastal karren in the Scurati–Cerriolo relict sea-cliffs

Morphology	Elevation m asl	Structure		Lithology	Cave type/Deposits
		Fracture	Bedding plane		
Grotta Mangiapane	62	N 170		Upper Cretaceous limestone	**Sea cave**—lithophaga borings
Grotta Buffa 1	59	N 260/80°		Upper Cretaceous limestone	**Sea cave**—lithofaga borings–sea shells
Grotta Buffa 2	52	N 235/80°		Upper Cretaceous limestone	**Sea cave**
Grotta Buffa 3	71			Upper Cretaceous limestone	**Flank margin cave**—bedding plane
Grotta Scurati 1	66	N 10		Upper Cretaceous limestone	**Flank margin cave**—bedding plane/sea deposits
Grotta Scurati 2	66			Upper Cretaceous limestone	**Flank margin cave**
Grotta Scurati 3	71	N-S		Upper Cretaceous limestone	**Sea cave**—sea deposits
Grotta Scurati 4	72	N-S		Upper Cretaceous limestone	**Sea cave**—deposits/notch and ceiling channel
Grotta Scurati 5	72	N-S		Upper Cretaceous limestone	**Sea cave**—fracture/bedding plane
Grotta Scurati 6	67			Upper Cretaceous limestone	**Flank margin cave**—bedding plane
Grotta CerrioloVolpe	110			Upper Cretaceous limestone	**Structural cave**—bedding plane
Grotta Caruso	138	N 160	N 160/20°	Upper Cretaceous limestone	**Structural cave**
Notch Scurati 4	71			Upper Cretaceous limestone	Biogenic form

(continued)

Table 6.9 (continued)

Morphology	Elevation m asl	Structure		Lithology	Cave type/Deposits
		Fracture	Bedding plane		
Notch Scurati 5	71				Biogenic form
Notch Volpe	109			Upper Cretaceous limestone	Biogenic form
Notches Cerriolo	81			Upper Cretaceous limestone	Biogenic form faulted notch

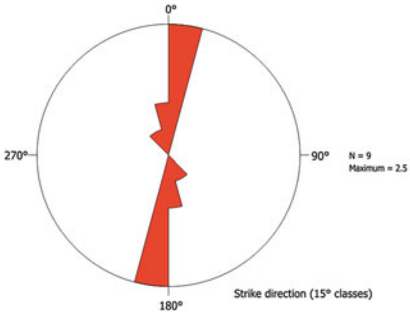

Figs. 6.314–315 General Rose diagram of the main geological structures in caves (*left side*); The sea cave Grotta Mangiapane (*right side*)

Figs. 6.316–317 *Flank margin cave* Grotta Buffa 3 (*left photo*); *Flank margin caves* along the Scurati relict sea-cliff (*right photo*)

Figs. 6.318–319 *Flank margin cave* Grotta Scurati 1 (*left photo*) along a bedding plane (*right photo*)

Figs. 6.320–321 Sea sediments in the Grotta Scurati 1 (*left photo*); Rock pillars in the *flank margin cave* Grotta Scurati 2 (*right photo*)

Figs. 6.322–323 Grotta Scurati 6 in the relict sea-cliff (*left photo*); Rock pillars in the *flank margin cave* Grotta Scurati 6 (*right photo*)

Figs. 6.324–325 Paleo-notch 4 at 72 m asl in the Scurati relict sea-cliff (*left photo*); Paleo-notch 5 at 72 m asl (Scurati relict sea-cliff) (*right photo*)

Figs. 6.326–327 Cerriolo relict sea-cliff with sea paleo-notch (*left photo*); Faulted paleo-notch in the Cerriolo cliff (*right photo*)

Figs. 6.328–329 Cerriolo paleo-notch at 81 m asl (*left photo*); Volpe paleo-notch at 109 m asl (*right photo*)

6.7.3 The Rocca Rumena Relict Sea-Cliff Features

Along the relict cliff of Rocca Rumena, bound to the south-east by the plain of Cornino, a total of 14 karst morphologies were identified (Figs. 6.330, 6.331 and Table 6.10), of which: six are sea caves (Figs. 6.333 and 6.334–335), one is a structural cave, two are micro-gorge type forms and one is a paleo-notch. The sea caves together with the two small gorge forms are set along fractures, while another two caves, together with a flat morphology, are made of anastomosed solution voids (Fig. 6.336), developed along bedding planes, hence, considered of *flank margin caves* genesis (Fig. 6.337). The structural data collected (shown in Fig. 6.332) indicates a main NNW-SSE trend and an E-W secondary trend.

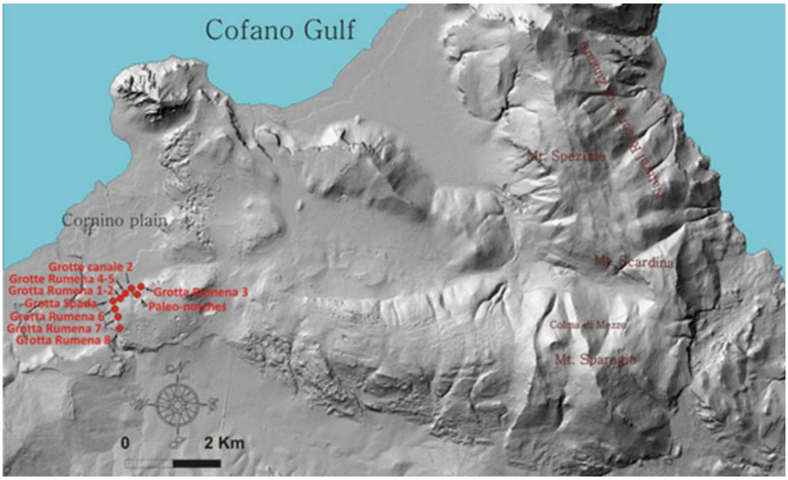

Fig. 6.330 Location of the sea caves and coastal karren surveyed in the Rocca Rumena relict sea-cliffs (*Hillshade map from* DEM Regione Siciliana 2007–2008)

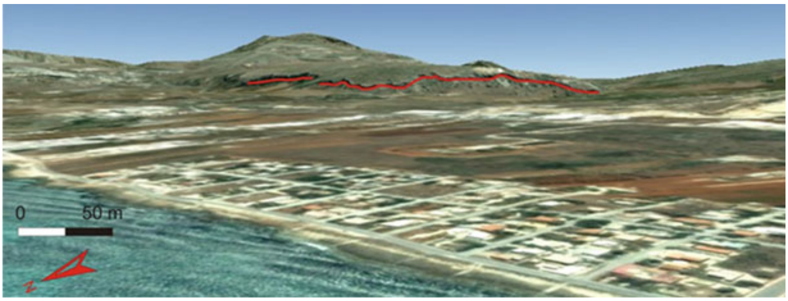

Fig. 6.331 Cornino coastal belt and Rocca Rumena relict sea-cliffs (*red lines*) (from Google Earth)

Table 6.10 Sea caves and coastal karren in the Rocca Rumena relict sea-cliffs

Morphology	Elevation m asl	Structure		Lithology	Cave type/Deposits
		Fracture	Bedding plane		
Grotta Rumena 1	95	N 230/85°	N 260/27°	Calcarenites Upper Cretaceous	**Flank margin cave**—Sea organogenic crusts and lithopaga borings
Grotta Rumena 2	110	N 250/75°		Calcarenites Upper Cretaceous	**Sea cave**—with notches
Grotta Rumena 3	130	N 60/85°		Calcarenites Upper Cretaceous	**Sea cave**
Grotta Rumena 4	111	N-S		Calcarenites Upper Cretaceous	**Sea cave**—and wall notch
Grotta Rumena 5	107			Calcarenites Upper Cretaceous	**Flank margin cave**—ceiling domes
Small-gorge	140	NNW-SSE		Calcarenites Upper Cretaceous	Karstified fracture
Small-gorge	136			Calcarenites Upper Cretaceous	Karstified fracture
Grotta Rumena 6	83			Calcarenites Upper Cretaceous	Structural cave Rock shelter
Grotta Rumena 7	115	N 90		Calcarenites Upper Cretaceous	**Sea cave**—cemented breccia
Grotta Rumena 8	131			Calcarenites Upper Cretaceous	**Sea cave**
Grotta Spada	110	N 110		Calcarenites Upper Cretaceous	**Sea cave**—notches, breccias–calcite laminations
Notch 3	120			Calcarenites Upper Cretaceous	Biogenic form
Bedding plane anastomosed solution voids	150			Calcarenites Upper Cretaceous	**Flank margin cave**—(genesis)

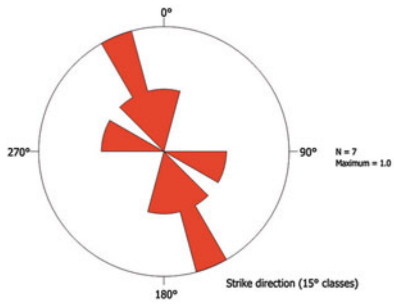

Figs. 6.332–333 Rose diagram of karstified geological structures in the cave (*left side*); Grotta Rumena 3 on a fracture (*right photo*)

Figs. 6.334–335 Grotta Rumena 4 and wall notch (*left photo*); Sea cave Grotta Rumena 8 (*right photo*)

Figs. 6.336–337 Anastomosed solution voids along a bedding plane in the Rocca Rumena relict sea-cliffs (*left side*); Small domes in the ceiling of *flank margin cave* Grotta Rumena 5 (*right side*)

6.7.3.1 The Rumena Flank Margin Cave

In this general context of the Rocca Rumena relict marine cliff, the Grotta Rumena 1 assumes a great interest for the presence of a series of both marine encrusting organisms and speleothems, which show evidences of paleoclimatic events and changes in sea level that occurred during the Pleistocene age. The cave, which was found, explored and surveyed by CIRS Ragusa in 2002 (Ruggieri and Messina Panfalone 2011) is located at 95 m asl, at the footslope of the Rocca Rumena cliff (Fig. 6.338). It extends for about 80 m in the Upper Cretaceous limestone in an ENE-SSW direction, parallel to the vertical slope of the cliff, along a bedding plane with a dip to N 260 at 27° (Figs. 6.338 and 6.340–341).

From the morphological point of view, the cave develops with a series of low merging hemispheric chambers. The walls and ceilings appear smooth and polished, except where calcite crusts cover them and where, in some parts, small phreatic notches, rock pillars and small domes have broken the surfaces (Figs. 6.342–343). This general aspect is almost labyrinthic due to presence of

Figs. 6.338–339 Rocca Rumena relict sea-cliff (*left photo*); Map location of the cave parallel to the cliff (*right photo*)

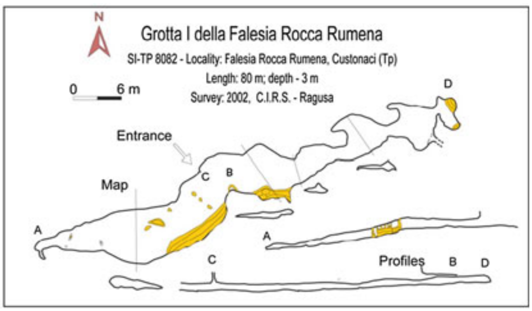

Figs. 6.340–341 Section of the cave along the dip of a bedding plane (*left photo*); Cave plan and profile (*right side*)


Figs. 6.342–343 Rock pillars and pendants with lithophaga borings (*left photo*); Small domes in the smooth ceiling (*right photo*)


Figs. 6.344–345 Cave conduit with low passage (*left photo*); Chamber with ceiling channel passage (*right photo*)


Figs. 6.346–347 Stalactite with hiatuses and lithophaga borings (*left photo*); Cave wall diffusely interested by lithophaga borings (*right photo*)

small low interconnected conduits, which open at both ends of the main chambers. These latter are partially to completely filled by red-brown detrital clay-sand soil which appears to be considerably thick, as in some parts of the cave it has reached the ceiling of some conduits occluding them (Fig. 6.344).

Calcite deposits are also present covering both the floor and the walls and in the left conduit rock pillars and pendants are present too. The right part is composed of three chambers connected by very low passages with some lateral low conduits occluded by soil. In the first chamber a phreatic morphology *ceiling channel* type (Pasini 1973) can also be observed (Ruggieri et al. 2012) (Fig. 6.345). During the survey carried out inside the cave in the course of this research, some stalactites, which showed hiatuses have been observed. The sections of these speleothems clearly show the presence of hiatuses in subaerial precipitation (Fig. 6.346). Particularly the marine events are highlighted by the presence of widespread lithophagous borings and organogenic (mostly coral) crusts on walls and the ceiling of the cave (Fig. 6.347). For the study of the above mentioned features a collaboration has been carried out with the Dipartimento di Scienze Biologiche, Geologiche e Ambientali of the University of Catania, for the paleontological aspects, and with ENEA of Casaccia (Roma, Italy) and ISMAR-CNR of Bologna (Italy) for the dating of the speleothems. The results of these investigations are reported below.

6.7.3.2 The Rumena Cave Hard Surface Palaeocommunity

Large areas, mostly along the paleo-seaward wall, and some sectors of the ceiling of the Rumena cave are discontinuously covered with a 1–4 cm thick crust largely formed by encrusting marine organisms, locally hidden under a thin-to-thick karstic draping of calcite crystals (Fig. 6.348). The preservation state is not optimal as skeletons are often decalcified, partly-to-completely dissolved, or recrystallized, and their small internal cavities draped by very thin coatings of microcrystalline calcite. This bad state very often hampers the identification at species level, as fine morphologies and even original skeletons have not been preserved.

Scleractinian corals are dominant, and corallites can be easily recognized, even at naked eye (Figs. 6.349 and 6.350), usually well separated each other and level to the exposed surface, often coated by calcite concretions. A few large sized, hardly recognizable cirriped specimens are scattered within corals. All other encrusters are barely visible in place and only photos reveal restricted sectors where large colonies of the bryozoan *Hippaliosina depressa* (Fig. 6.351) forms crusts as well as tubes of the serpulid *Spiraserpula massiliensis* (Fig. 6.352), growing close to each other and locally forming dense aggregates. Photos also show specimens of cirripeds grouped at places, and largely coated by the crust, which leaves free only the widely diamond-shaped coronal apertures. Along nearly all the walls and the vault also *Gastrochaenolites* are very abundant, mostly seemingly produced by *Lithophaga lithophaga* (Fig. 6.353). Further borings are barely visible, some referable to *Meandropolidora* sp. and *Entobia* sp.

The analysis of small crust samples allow further species to be recognized. Corals are mostly represented by Dendrophyllids belonging to *Leptosammia* *pruvoti* and *Cladopsammia rolandi*. Cirripeds are largely referable to *Balanus perforatus*, but a single plate of *Verruca spengleri* has been also discovered. Cheilostome bryozoans are relatively common and diversified. Two species *H. depressa* and *Trypostega* cf. *venusta* whereas some other species *Escharina dutertrei protecta*, *Puellina venusta*, *Celleporina* sp. and *Turbicellepora* sp., have been recognized through single specimens. Cyclostome bryozoans are present at least with six taxa, mostly represented by single young or fragmentary colonies not identifiable at species level, apart for one colony referable to a Lichenoporidae representative and one specimen belonging to *Annectocyma major*. All the species found are encrusting, either forming large sheet-like colonies, or narrow running ribbons or small, spot-like colonies. They usually colonize the corallite external surfaces, often forming superimposed layers. Among serpuloideans the serpulid *S. massiliensis* and the spirorbid *Pileolaria militaris* are the most abundant species. In contrast, *Serpula concharum*, an unedifiable species of the genus *Vermiliopsisim* and the spirorbids *Vinearia koehleri*, *Spirorbis cuneatus* and *Janua pagenstecheri* are present with single to few specimens. The two scleractinian species can be quantitatively important in present-day communities of both walls and roofs of marine caves which are not too shallow and not located in high energy settings. Consequently, a relatively deep location of the Rumena cave at the time of its last colonization can be hypothesized (Rosso et al. 2012).

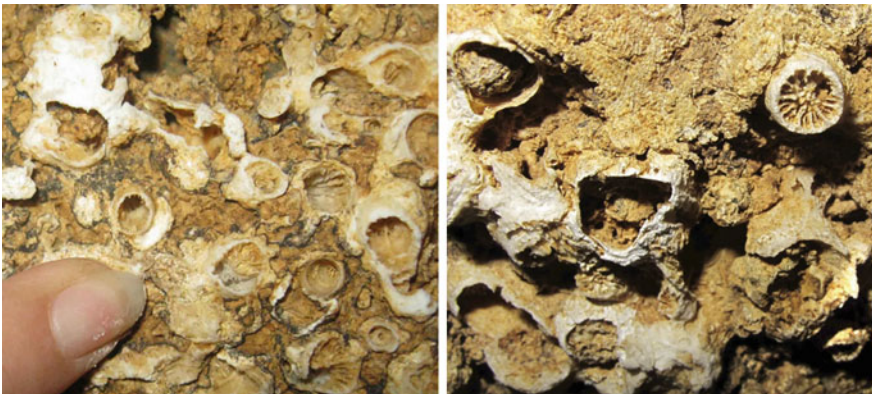

Figs. 6.348–349 Encrusting marine organisms (*left photo*): Scleractinian corals and *Balanus perforatus* (*right photo*)

Fig. 6.350 Lithophaga borings and colonies of corals on the walls and the ceiling channel of the cave

Fig. 6.351 Sheet like bryozoan balanids

Fig. 6.352 Gregarious serpulids (*Spiraserpula massiliensis*)

Fig. 6.353 Lithophaga borings

6.7.3.3 The Rumena Cave Speleothem Dating

A stalactite overgrown by Scleractinian corals was collected in the left chamber of the Rumena cave. The speleothem section shows four hiatuses that are considered to represent four different sea level transgressions older than the coral overgrowth (Fig. 6.354).

Several pieces of the continental layers of the stalactite were analyzed for ^{230}Th/U using a multi-collector ICPMS NeptunePlus and all the ages resulted to be beyond the upper limit of the ^{230}Th age range. Small fragments (3–5 mg) of the thecal wall of three corals (Fig. 6.355) were analyzed for ^{87}Sr/^{86}Sr ratio and the strontium ages were then calculated from the regression curves LOWESS look-up Table version 4: 08/04 (revised from McArthur et al. 2001).

The age of the corals (Fig. 6.355) is 1.1 ± 0.2 M years (mean ± 2SD), in agreement with the ^{230}Th/U ages of the continental layers beyond the upper limit of the U-series chronometer. The δ^{18}O of the continental layers at 1 mm spatial resolution has been measured and the comparison with marine and continental records suggests that the calcite of the stalactite was precipitated during MIS 27–31 (Antonioli et al. 2012a, b).

From these preliminary researches it is highlithed that some of the speleothems from the Grotta Rumena 1 (Fig. 6.356) thus represent a unique paleoclimatic and paleo sea level archive together with the Bahamas flowstone (Lundberg and Ford 1994) and the Argentarola speleothems (Dutton et al. 2009).

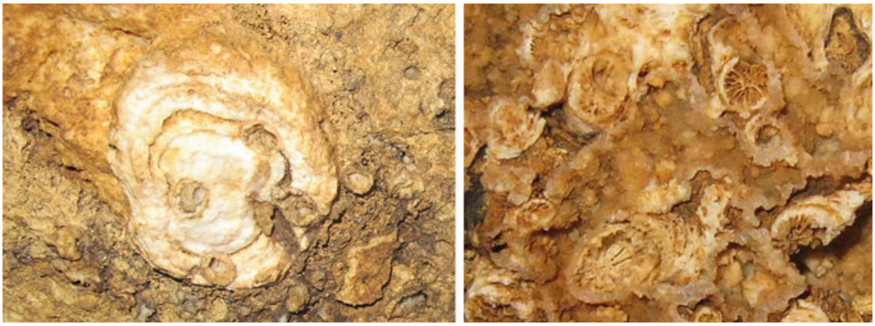

Figs. 6.354–355 Stalactite of Rumena cave showing the hiatuses of marine transgression phases (discovered during this study) (*left photo*); Scleractinian corals 1 Myrs old (*right photo*)

Fig. 6.356 Speleothems of the Grotta Rumena 1 extensively involved in some phases of sea ingressions during the Pleistocene age

6.7.4 *Caves in the Sea Paleo-Terraces of the Cornino Plain*

Two caves have been surveyed in the coastal belt of the Cornino plain (Table 6.11, Fig. 6.357), both showing the morphologies of a *flank margin cave* genesis. The first, called Grotta Cornino, is sited at 14 m asl with its narrow entrance in the internal margin of a sea paleo-terrace. It develops along a bedding plane in the Lower Pleistocene biocalcarenites with a unique chamber 10 m long and 6 m wide. From the morphological point of view, the cave shows smooth walls and ceiling without phreatic water flow forms such as scallops (Fig. 6.358).

The second cave, called Grotta della Piana San Alberto, is located at 70 m asl with its entrance on the internal margin of a sea paleo-terrace. It develops, parallel to the small scarp, for about 22 m along a bedding plane of the Lower Pleistocene biocalcarenites (Fig. 6.359).

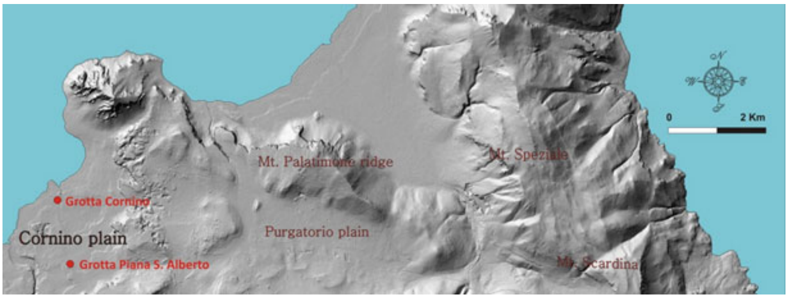

Fig. 6.357 Location of the caves surveyed in the Cornino plain (*Hillshade map from* DEM Regione Siciliana 2007–2008)

Figs. 6.358–359 Grotta Cornino with smooth ceiling (*left photo*); Grotta Piana S. Alberto along a bedding plane (*right photo*)

Table 6.11 Caves in the sea paleo-terraces of the Cornino plain

Morphology	Elevation m asl	Structure		Lithology	Cave type/Deposits
		Fracture	Bedding plane		
Grotta Cornino	14			Biocalcarenites Lower Pleistocene	**Flank margin cave**
Grotta Piana S. Alberto	70			Biocalcarenites Lower Pleistocene	**Flank margin cave**

6.7.5 The Peninsula of Capo San Vito–Mt. Monaco Relict Sea-Cliffs and Makari–Tonnara del Secco Sea Paleo-Terraces Features

The total number of morphologies surveyed in the above reported relict sea-cliffs and sea paleo-terraces amounted to 25 (Figs. 6.360, 6.361, 6.362 and Table 6.12). Of these 14 are sea caves with elevation ranging from c. 12–375 m asl of the Grotta dei Pendenti (Figs. 6.364, 6.365, 6.366, 6.367–368, 6.369–370, 6.371–372, 6.383 and 6.384–385); 6 are *flank margin caves* (Figs. 6.373–374, 6.375–376, 6.377–378, 6.379–380 and 6.381–382); 4 are structural caves and 1 is an erosive notch.

The structural data collected, illustrated in Fig. 6.363, indicated a dominant E-W trend and a secondary N-S trend.

Some other erosive notches were surveyed inside seven of the above mentioned caves. Of these one paleo notch can be observed at 42 m asl on the inner wall of the "Grotta dei Cavalli" a cave of archaeological importance (Fig. 6.365), and one other at 8 m asl on the inner edge of a Pleistocene terrace (Fig. 6.368).

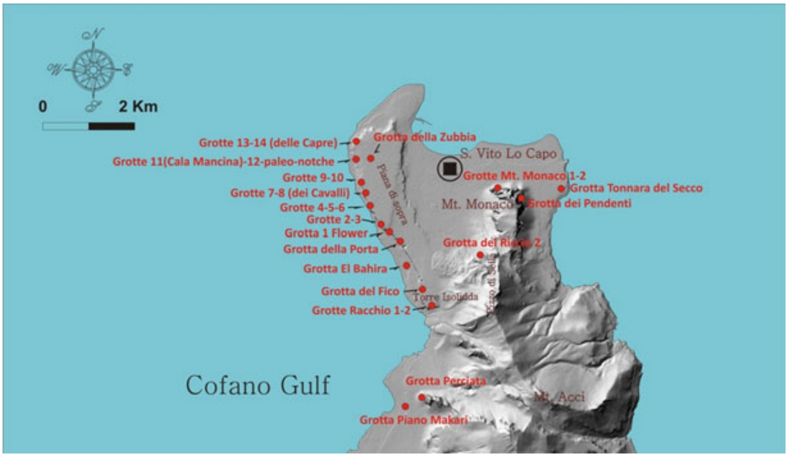

Fig. 6.360 Location of the sea caves and coastal karren surveyed in the San Vito peninsula–Mt. Monaco relict sea-cliffs and Makari–Tonnara del Secco sea paleo-terraces (*Hillshade map from* DEM Regione Siciliana 2007–2008)

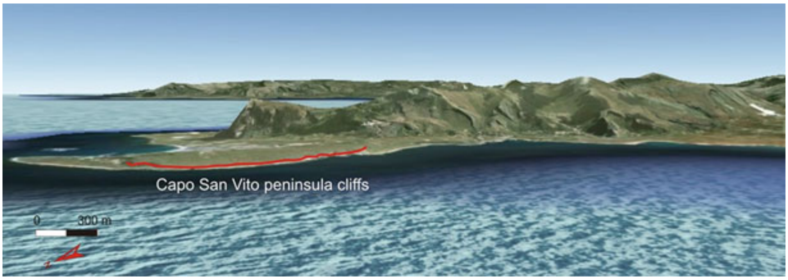

Fig. 6.361 Makari plain–San Vito peninsula coastal belt and relict sea-cliffs (*red lines*) (from Google Earth)

Fig. 6.362 Tonnara del Secco–Mt. Monaco coastal belt and relict sea-cliffs (*red line*) (from Google Earth)

Table 6.12 Caves and coastal karren in the Peninsula of Capo San Vito–Mt. Monaco relict sea-cliffs and Makari–Tonnara del Secco sea paleo-terraces

Morphology	Elevation m asl	Structure		Lithology	Cave type/Deposits
		Fracture	Bedding plane		
Cave 1 (Grotta del Fiore)	22	N 310/80°	N 240–270/75°	Biocalcarenites Upper Cretaceous	**Sea cave**—Rock steps, notches and sea fossils
Cave 2	24	N 60/70°	N 270/15°	Biocalcarenites Upper Cretaceous	**Sea cave**—with notch and sea fossils
Cave 3	36	N 30/75°	N 25/30°	Biocalcarenites Upper Cretaceous	Structural cave
Cave 4	11	N 0/75°		Biocalcarenites Upper Cretaceous	Structural cave
Cave 5	26	N 275/80° N 130/75°	N 10/15°	Biocalcarenites Upper Cretaceous	**Flank margin cave**—with notches
Cave 6	15		N 50/45°	Biocalcarenites Upper Cretaceous	**Sea cave** with notches
Cave 7	12	N 25/70°		Biocalcarenites Upper Cretaceous	**Sea cave**—contin. deposits and notches
Cave 8 (Grotta dei Cavalli)	42	N 200/75°		Biocalcarenites Upper Cretaceous	**Sea cave**—notches at +42 m asl
Cave 9	27	N 165/60°		Biocalcarenites Upper Cretaceous	**Sea cave**—Speleothems
Cave 10	40	N 255/75°		Biocalcarenites Upper Cretaceous	**Sea cave**
Cave 14 (G. delle Capre)	23		N 10/10°	Biocalcarenites Upper Cretaceous	**Flank margin cave**—bedding plane
Cave 13	24	N 160–180/50°		Biocalcarenites Upper Cretaceous	Structural cave speleothems
Notch	8			Biocalcarenites Upper Cretaceous	Inner edge of sea terrace
Cave 12	22	N 10/60°			

(continued)

Table 6.12 (continued)

Morphology	Elevation m asl	Structure		Lithology	Cave type/Deposits
		Fracture	Bedding plane		
				Biocalcarenites Upper Cretaceous	**Sea cave**—with paleo-notches
Cave 11 (Gr. di Cala Mancina)	15	N 110/80°	N 70/15°	Biocalcarenites Upper Cretaceous	**Sea cave**—continental deposits with sea fossils
Grotta della Porta	42	N 270/50°	N 4/28°	Biocalcarenites Upper Cretaceous	**Sea cave**
Grotta Racchio 1	60			Biocalcarenites Upper Cretaceous	**Flank margin cave**
Grotta Racchio 2	60			Biocalcarenites Upper Cretaceous	**Sea cave**—lithophaga borings
Grotta del Fico	75	N 250/70°		Biocalcarenites Upper Cretaceous	Structurral cave
Grotta di Piano Makari	14			Limestone Upper Triassic-Liassic	**Flank margin cave**—sea conglomerates sea fossils–mammals and human bones
Grotta El Bahira	7			Biocalcarenites Upper Cretaceous	**Flank margin cave**—linear Graffiti
Grotta Perciata	60			Limestone–Upper Triassic-Liassic	**Sea cave**
Grotta Tonnara del Secco	12	N 60/50°	N 115/20°	Calcarenites Upper Giurassic–Lower Cretaceous	**Flank margin cave**—lithophaga borings
Grotta Monaco 1	55.5	N 75/75° N 150/80°		Biocalcarenites Upper Cretaceous	**Sea cave**—lithopaga borings
Grotta Monaco 2	48	N 260/85°		Biocalcarenites Upper Cretaceous	**Sea cave**
	375	N 300°			**Sea cave**

(continued)

Table 6.12 (continued)

Morphology	Elevation m asl	Structure		Lithology	Cave type/Deposits
		Fracture	Bedding plane		
Grotta dei Pendenti				Biocalcarenites Upper Cretaceous	
Grotta del Riccio 2	224	N 0/80°/N 270/80°		Biocalcarenites Upper Cretaceous	**Sea cave**—lateral notches

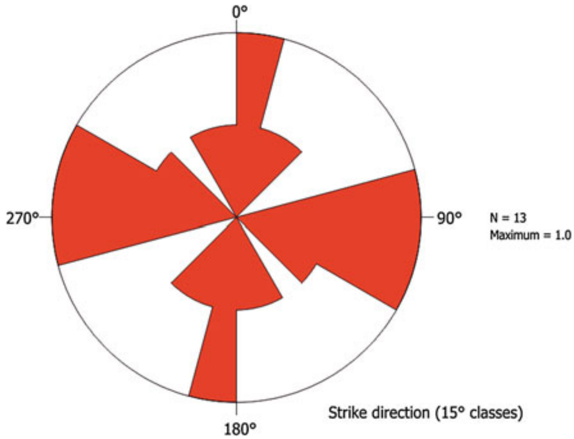

Fig. 6.363 General Rose diagram of karstified geological structures in caves

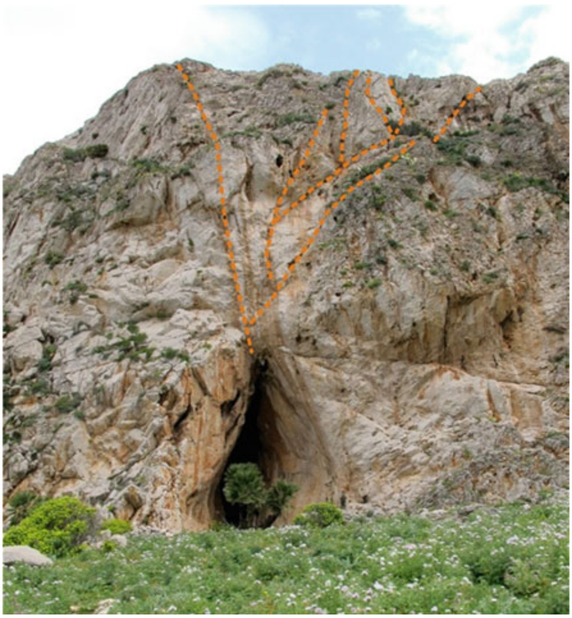

Fig. 6.364 Sea cave 1 with lateral notches and positive flower structure in the *upper part*

Fig. 6.365 Grotta dei Cavalli with notch at 42 m asl

Fig. 6.366 Torre Isolidda relict sea-cliff

Figs. 6.367–368 Notch close to Grotta Racchio 2 at 60 m asl (*left photo*); sea notches at 8 m asl and sea cave in the above terrace (*right photo*)

Fig. 6.369–370 General view of the relict sea-cliff (*left photo*) and entrance of the sea cave Grotta Perciata at 60 m asl (*right photo*) in the Pizzo Castelluzzo relief

Figs. 6.371–372 Entrance of the sea cave Grotta di Monte Monaco 1 and lithophaga borings on its wall (*right photo*)

Figs. 6.373–374 Grotta Racchio 1- Rock pillars (*left photo*); *flank margin cave* Grotta delle Capre along a bedding plane (*right photo*)

Figs. 6.375–376 *Flank margin cave* Grotta 5 (*left photo*); sea conglomerates inside Grotta Makari (*right photo*)

Figs. 6.377–378 Marine fossils in the Grotta Makari (*left photo*); mammals and human bones discovered during this study in the cave (*right photo*)


Figs. 6.379–380 Entrance and section of the Grotta El Bahira on the internal margin of a sea terrace


Figs. 6.381–382 Brackish water table and lithofaga borings inside Grotta Tonnara del Secco with entrance at 17 m asl

Figs. 6.383 Mt. Monaco 400 m high northern slope relict sea-cliff: Grotta dei Pendenti at 375 m asl, the highest and oldest sea cave in the Monti di Capo San Vito, explored and surveyed during this study

Figs. 6.384–385 Large entrance of the sea cave “Grotta dei Pendenti” with big stalactites and pendants on the ceiling (*right photo*)

6.7.6 The Zingaro Natural Reserve Relict Sea-Cliff Features

A total of 11 caves have been surveyed along the relict sea-cliffs of Zingaro Nature Reserve (Figs. 6.386, 6.387 and Table 6.13). Six of these are sea caves, formed along structural discontinuities and have originated as a result of marine erosion processes, in some cases associated with karst weathering/corrosion processes (Figs. 6.389, 6.390–391 and 6.392–393), while one is a structural cave with signs of striation on the fault wall (Figs. 6.394–395). The remaining four caves show clearly observable morphologies related to *flank margin caves* genesis (Figs. 6.396–397).

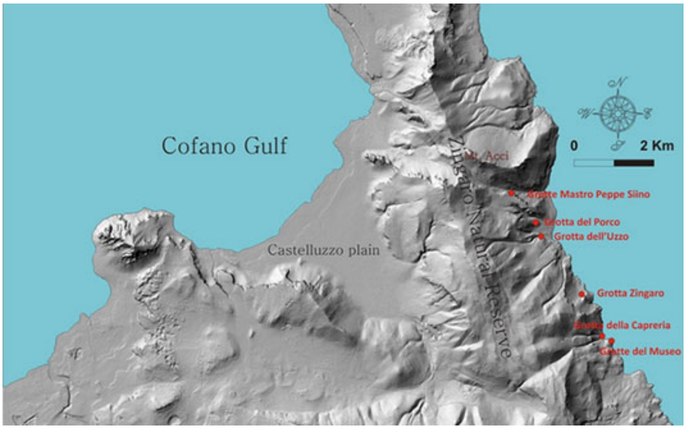

Fig. 6.386 Location of the sea caves surveyed in the coastal relict sea-cliffs of the Zingaro Natural Reserve (*Hillshade map from* DEM Regione Siciliana 2007–2008)

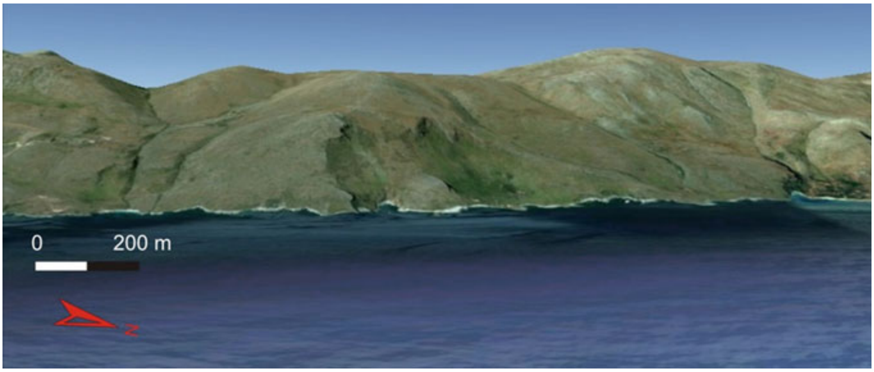

Fig. 6.387 Coastal belt and sea-cliffs of the Zingaro Natural Reserve (from Google Earth)

Table 6.13 Caves and karst morphologies in the Zingaro Natural Reserve relict sea-cliffs

Morphology	Elevation m asl	Structure		Lithology	Typology/Deposits
		Fracture	Bedding plane		
Grotta dell'Uzzo	68			Dolomites and dolomitic limestone Norian–Liassic	**Sea cave**—Archaeological site
Grotta del Porco	119	N 90/80°		Dolomites and dolomitic limestone Norian–Liassic	Tectonic cave with striation on wall fault
Grotte 1-2-3 di Mastro Peppe Siino	320–360			Dolomites and dolomitic limestone Norian–Liassic	**Sea cave**
Grotta della Capreria	5			Doloarenites and dolorudites Upper Triassic	**Sea cave**—with flowstones
Grotte 1-2-3-4 del Museo	10-15-25			Doloarenites and dolorudites Upper Triassic	**Flank Margin caves**—Flowstones and rimstones
Grotta Zingaro	130	N 270/80°		Dolomites and dolomitic limestone Norian–Liassic	**Sea cave**—with lithophaga borings

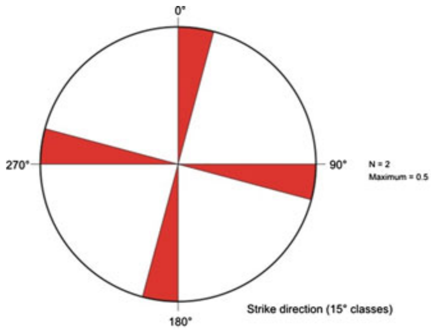

Figs. 6.388–389 General Rose diagram of karstified geological structures in caves (*left side*); Sea cave “Grotta dell’Uzzo” (*right photo*)

Figs. 6.390–391 Sea cave “Grotta della Capreria” (*left photo*); Sea cave “Grotte di Mastro Peppe Siino” (*right photo*)

Figs. 6.392–393 Sea cave “Grotta Zingaro” (*left photo*); Lithophaga borings in the external wall of the Grotta Zingaro (*right photo*)

Figs. 6.394–395 Structural cave “Grotta del Porco” (*left photo*); Striation in the wall fault of Grotta del Porco (*right photo*)

Figs. 6.396–397 *Flank margin cave* “Grotte del Museo” (*left side*); Lithophaga borings on the external cliff of the Grotte del Museo (*right side*)

In the submerged part of the present active cliffs, 15 caves were detected ranging approximately in depth from c. 5–30 m (Sottosanti 1994).

With regards to the caves of tectonic origin, the structural data collected (Fig. 6.388) indicate two equally prevailing trends: N-S and E-W.

References

Abate B, Di Maggio C, Incandela A, Renda P (1993) Carta Geologica dei Monti di Capo San Vito, scala 1:25.000 - Dip. Geologia e Geodesia dell‘Università di Palermo

Agnesi V, Macaluso T, Monteleone S, Pipitone G (1984) Fenomeni di deformazione gravitativa profonda (deep-seated gravitational slope deformations) osservati nella Sicilia occidentale. Boll Soc Geol Ital 103:671–679

Agnesi V, Macaluso T, Pipitone G (1987) Ruolo delle deformazioni gravitative profonde nell’evoluzione geomorfologica dell’area di Scopello (Trapani). Boll Soc Geol Ital 106:231–238

Agnesi V, Macaluso T, Monteleone S, Pipitone G, Sorriso-Salvo M (1989) Tipi e dinamica delle deformazioni gravitative profonde in relazione alle strutture geologiche. I casi di Monte Genuardo e di Scopello (Sicilia occidentale). Boll Soc Geol Ital 108:379–389

Agnesi V, Di Maggio C, Macaluso T (1995) Deformazioni gravitative profonde e superficiali nella penisola di Capo San Vito (Sicilia occidentale). Mem Soc Geol Ital 50:11–21

Antonioli F, Ruggieri R (2000) Geomorfologia e speleogenesi nell'area carsica di Monte Palatimone (Custonaci, Tp) ed interconnessioni con il livello di base marino. Speleologia Iblea 8:213–223

Antonioli F, Cremona G, Immordino F, Puglisi C, Romagnoli C, Silenzi S, Valpreda E, Verrubbi V (1999a) Quaternary and holocene differential movements in a mediterranean coastal area (San Vito Lo Capo, Sicily-Italy). Phys Chem Earth, 68

Antonioli F, Cremona G, Puglisi C, Silenzi S, Valpreda E, Verrubbi V (1999b) Quantitative assessment of post Tyrrenian differential crustal movements in a Mediterranean coastal area (S. Vito–Sicily-Italy). Phys Chem Earth A 24(4):343–347

Antonioli F, Montagna P, Caruso A, Ruggieri R, Lo Presti V, Silenzi S, Frank N, Douville E, Pierre C (2012a) Investigation of marine and continental layers in a stalactite older than 1 million years (Custonaci, north-western sector of Sicily). SLALOM 2012, Athens, Abstracts, 19–22 March 2012

Antonioli F, Montagna P, Caruso A, Ruggieri R, Lo Presti V, Silenzi S, Frank N, Douville E, Pierre C (2012b) Investigation of marine and continental layers in a stalactite older than 1 million years (Custonaci, north-western sector of Sicily). R Online Soc Geol Ital 21:1165–1166 (1 Fig.)

Bini A, Meneghel M, Sauro U (1986) Proposta di legenda per una cartografia geomorfologica delle aree carsiche. Atti e Mem. Comm GRotte "E Boegan" 25:21–59

Catalano F, Agate M, Basilone L, Di Maggio C, Mancuso M, Sulli A (2011) Note illustrative della Carta Geologica d'Italia alla scala 1:50.000, foglio 593 Castellammare del Golfo. ISPRA, Servizio Geologico d'Italia. Regione Siciliana Ass. Territorio Ambiente

Čalić J (2011) Karstic uvala revisited: toward a redefinition of the term. Geomorphology 134 (2011):32–42

Cucchi F, Forti F, Forti P (1983) Movimenti recenti nel Carso triestino da analisi di concrezioni stalagmitiche. Geogr Fis Dinam Quat 6(1983):43–47 (8 ff)

DEM Regione Siciliana. Modello digitale del terreno passo 2 m derivato da dati LIDAR volo ATA 2007–2008 in UTM-WGS84 fuso 33 N

Di Maggio C, Incandela A, Masini F, Petruso D, Renda P, Simonelli C, Boschian G (1999) Oscillazioni eustatiche, biocronologia dei depositi continentali quaternari e neotettonica nella Sicilia nord-occidentale (Penisola di San Vito Lo Capo-Trapani). Il Quaternario 12(1):25–49

Dutton A, Antonioli F, Bard EM, Esat T, Lambeck K, McCulloch M (2009) Phasing and amplitude of sea level and climate change during the penultimate interglacial. Nat Geosci 2:355–359

Ford DC, Williams PW (1989) Karst geomorphology and hydrology. Unwin Hyman, 601 pp

Ford DC, Williams PW (2007) Karst hydrogeology and geomorphology. Wiley, New York, 562 pp

Frank EF, Mylroie JF, Troester J, Alexander E, Carew JL (1998) Karst development and speleogenesis, Isla de Mona, Puerto Rico. J Cave Kasrt Stud 60(2):73–83

Ginés A (2009) Karren landscapes and karren landforms. In Carsologica 9 - Karst Rock features Karren sculturing. Postojna - Ljubljana

Ginés A, Lundberg J (2009) Rainpits: an outline of their characteristics and genesis. Carsologica 9—Karst Rock features Karren sculturing. Postojna, Ljubljana

Gomez-Pujol L, Fornós JJ (2009) Microrills. In: Carsologica 9—Karst Rock features Karren sculturing. Postojna, Ljubljana

Jenson JW, Keel TM, Milroye JE, Stafford KM, Taborosi D, Wexel C (2006) Karst of the Mariana Islands: The interaction of tectonics, glacio-eustasy, and freshwater/seawater mixing in island carbonates. In: Harmon RS, Wicks CM (eds) Perspectives on karst geomorphology, hydrology, and geochemistry. Geological Society of America special paper, vol 404, pp 129–138

Klimchouk AB, Sauro U, Lazzarotto M (1996) Hidden shafts at the base of the epikarstic zone: a case study from the Sette Comuni plateau, Venetian Pre-Alps, Italy. Cave and karst science, vol 23, no 3. Dec 1996

Lundberg J, Ford DC (1994) Late Pleistocene sea level change in the Bahamas from mass spectometric U-series dating of submerged speleothem. Quat Sci Rev 13:1–14

Lundberg J (2009) Coastal karren. In: Carsologica 9—Karst Rock features Karren sculturing. Postojna, Ljubljana
Macaluso T, Sauro U (1996) Weathering crust and karren on exposed gypsum surfaces. Int J Speleol 25(3–4):115–126
McArthur JM, Howarth RJ, Bailey TR (2001) Strontium Isotope Stratigraphy: LOWESS Version 3: best fit to the marine Sr-Isotope Curve for 0-509 Ma and accompanying look-up table for deriving numerical age. J Geol 109:155–170
Mylroie E, Carew L (1990) The Flank Margin Model for dissolution cave development in carbonate platform. Earth Surf Proc Land 15:413–424
Mylroie JE, Mylroie JR (2009) Caves as sea level and uplift indicators, Kangaroo island, south Australia. J Cave and Karst Stud 71:32–47
Mylroie JE, Carew JL, Vacher HL (1995) karst development in the Bahamas and Bermuda. In: Curran HA, White B (eds) Geological society of america special paper. Geological Society of America, Boulder, Colorado, pp 251–267
Mylroie JE, Jenson JW, Taborosi D, Jocson JMU, Vann DT, Wexel C (2001) Karst features of Guam in terms of a general model of carbonate island karst. J Cave Karst Stud 63:9–22
Mylroie JE, Mylroie JR, Nelson CS (2008) Flank Margin cave development in telogenetic limestones of New Zealand. Acta Carsologica 37(1):15–40
Ortofoto Regione Siciliana, Ortofoto anno 2007–2008. Realizzazione ripresa aerea digitale pixel 0.25 m. in UTM-WGS84 fuso 33 N
Otoničar B, Buziak N, Mylroie J, Mylroie J (2010) Flank Margin Cave development in carbonate talus breccia facies: an examples from Cres island, Croatia. Acta Carsologica 39:79–91
Palmer AN (2007) Cave geology. Dayton, USA, p 453
Pasini G (1973) Sull'importanza speleogenetica dell'erosione antigravitativa. Le Grotte d'Italia 4:297–326
Perna G, Sauro U (1978) Atlante delle microforme di dissoluzion carsica superficiale del Trentino e del Veneto. Memorie del Museo Tridentino di Scienze Naturali, vol XXIII, Nuova Serie, Fasc. Unico, Trento, p 1176
Rosso A, Sanfilippo R, Ruggieri R, Maniscalco R (2012) Associazioni di substrato roccioso da una grotta sottomarina del Pleistocene (Sicilia occidentale). Giornate di Paleontologia XII edizione – Catania 24–26 Maggio 2012 - Volume dei riassunti
Ruggieri R (2009) Karst Itinerary and cave discovery in the Zingaro Reserve. Azienda Foreste Demaniali. Priulla, Palermo, pp 207
Ruggieri R, Messina Panfalone D (2011) Dentro e fuori la montagna. Palermo, Priulla, p 182
Ruggieri R, De Waele J (2014) Lower to middle pleistocene flank margin caves at custonaci (Trapani, NW Sicily) and their relation with past sea levels. Acta Carsologica 43/1:11–22 (Postojna 2014)
Ruggieri R, Messina Panfalone D, Antonioli F, Rosso A, Sanfilippo R, Maniscalco R (2012) The Rumena flank margin cave and its implication in support of the evolution of the Monti di Capo San Vito (North-western Sicily). R Online Soc Geol Ital 21:632–633 (3 Figs.)
Sacchi CF (1955) Fatti ecologici e fenomeni microevolutivi nei molluschi della montagna mediterranea. Boll Zool 22:563–649
Sauro U (1979) Morfologia carsica, Cap. 9, pp 208–254. In: Geomorfologia, Castiglioni G.B., Ed. UTET
Sauro U (1995) Highlights on doline evolution. In: Barany-Kevei I (ed) Environmental effects on Karst Terrains (homage to Laszlo Jackucs). Acta geograph. Szegediensis, vol 34. University of Szeged, Szeged, pp 107–121
Sauro U (2003) The dolina: emblematic and problematic karst landform. Dela 20, 43–60. Ljubliana. ISBN 961-237-065-6
Sauro U (2012) Closed depression in karst area. In: Encyclopedia of caves. Elsevier Inc, New York
Šebela S (2008) Broken speleothems as indicators of tectonic movements. Acta Carsologica 37/1:51–62 (Postojna 2008)

Šebela S (2010) Effects of earthquakes in Postojna cave system. Acta Carsologica 39/3:597–604 (Postojna 2010)

Slabe T (1995) Cave Rocky relief and its speleogenetical significante. Karst Research Institute, Ljubliana 120 pp

Slabe T (2009) Karren simulation with platers of Paris models. In: Carsologica 9 - Karst Rock features Karren sculturing. Postojna - Ljublijans

Slabe T, Liu H (2009) Significant subsoil rock forms. In: Carsologica 9—Karst Rock features Karren sculturing. Postojna, Ljubljana

Smart PL, Beddows PA, Coke J, Doerr S, Smith S, Whitaker F (2006) Cave development on the Caribbean coast of the Yucatan Peninsula, Quintana Roo, Mexico. Geol Soc America Spec Pap 404:105–128

Sottosanti V (1994) Il patrimonio speleologico della Riserva Naturale dello “Zingaro”. Boll Acc Gioenia Sci Nat 27(348):631–639

Verres M (2009) Trittkarren. In: Carsologica 9—Karst Rock features Karren sculturing. Postojna, Ljubljana

Viles HA (1984) Biokarst: review and prospect. Prog Phys Geogr 8:523–542

Zseni A (2009) Subsoil shaping. In: Carsologica 9—Karst Rock features Karren sculturing. Postojna, Ljubljana

Chapter 7
Structural Geological Analysis of the Karst Surface Area

7.1 Aims of the Surface Structural Survey

The structural analysis and investigations being reported and which have been carried out on the above-described caves, were intended to highlight, which discontinuities have played a dominant role and which had a secondary role in the karstification processes generated in the carbonate bedrock outcropping in the various zones into which the research area was divided.

In order to investigate what type of control the Plio-Pleistocene deformational events have had on the above-mentioned speleogenetic processes, a geo-structural survey of the surface area was carried out. This consisted in the surveying of the major and minor discontinuities (faults and joints) and kinematic indicators (striations, stilolites, rock and calcite steps). In this regard, a number of structural stations from surface outcrops has been set up next to the above-described karst caves. These were located on Upper Cretaceous and Upper Jurassic—Lower Cretaceous calcarenites and calcirudites (Site *a* Mt. Bufara–Cerriolo–Piano Zubbia area) and on dolostone and dolomitic limestones of the Upper Triassic–Lower Liassic (Site *b* Monte Palatimone and Site *c* Polje di Purgatorio; Site *d* Monte Sparagio–Cocuccio. In some zones, where suitable sites for structural surveying could not be identified, orthophoto pictures were used to interpret and analyze the geological structures.

The results of the surveys conducted in the above-mentioned structural stations, located in the research area, are presented hereunder.

R. Ruggieri, *Speleological and Speleogenetic Aspects of the Monti di Capo San Vito (Sicily)*, Springer Theses, DOI 10.1007/978-3-319-21720-8_7

7.1.1 *Structural Survey of Mt. Bufara–Cerriolo–Piano Zubbia Area (Site* a*)*

The structural stations have been identified on the walls of some quarries (Figs. 7.1–2) located next to the main caves in the area (Fantasma, Clava, Maria SS. di Custonaci, Cerriolo) and on a wall of Bufara doline, the latter located in the southern zone of the Site *a* (Fig. 7.3). The recorded and plotted data are illustrated in the analysis that follows.

Figs. 7.1–2 Quarries in the area of Piano Zubbia—Scaletta (Site *a*)

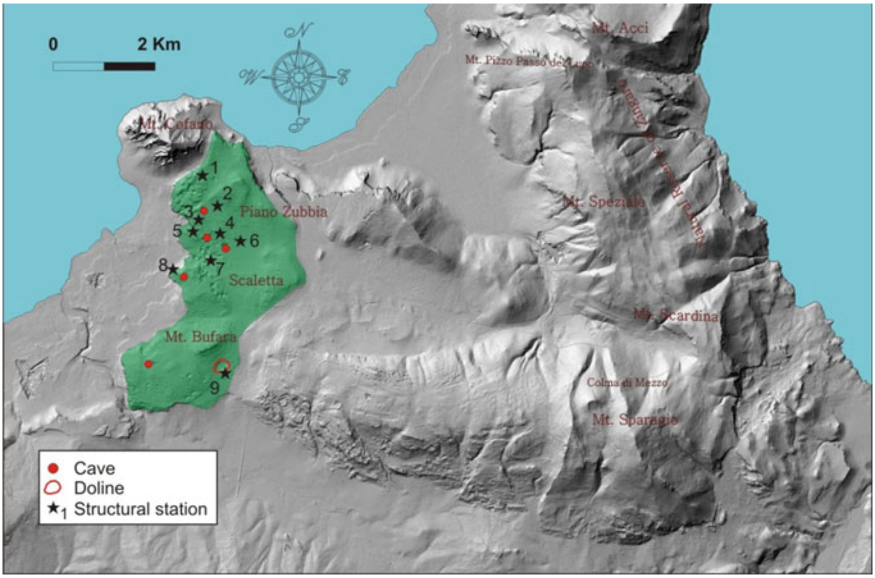

Fig. 7.3 Site *a* Locations of the geostructural surveys carried out in some quarries next to the main caves (*Hillshade map from* DEM Regione Siciliana 2007–2008)

7.1.2 Grotta del Fantasma Area

In the area next to Grotta del Fantasma three structural surveys were carried out and the collected data projected in the low hemisphere stereogram. In the station 1 of stereograms of Fig. 7.4, two systems of fractures, the NW-SE and NNE-SSW have been recorded while a single system, the NW-SE, was recorded in Stations 2 and 3. The dip directions of the strata vary from E-W, for Station 1, and S-W for Stations 2–3.

7.1.3 Grotta della Clava Area

The stereogram of Fig. 7.5 (Station 4) indicates how the deformation takes place along a preferential direction NW-SE and the direct (in red) and transcurrent dextral (orange) faults are both set along this direction. In the diagram one can note several

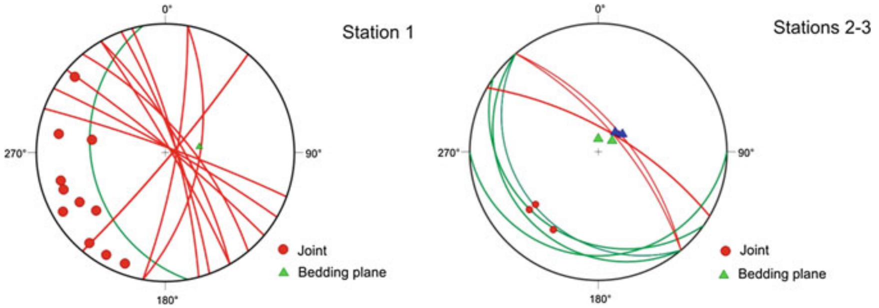

Fig. 7.4 Stereograms of structural data collected from Station 1 (*left side*) and Stations 2–3 (*right side*)

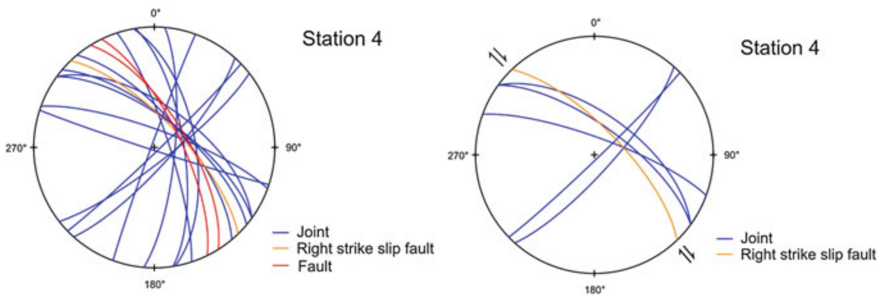

Figs. 7.5–6 Stereogram of data collected in Station 4 (*left side*); Stereogram with right strike strip fault (*right side*)

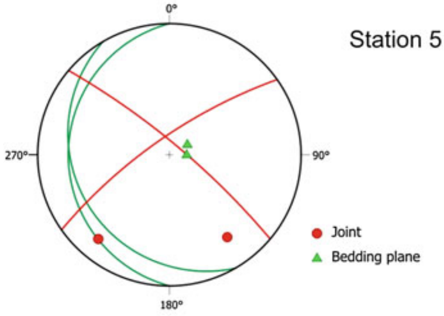

Figs. 7.7–8 Stereogram of surveyed data in the sites of Station 5 (*left side*); Fault wall near Clava cave (*right photo*)

sets of joints (blue) displaced at a high angle in relation to stratification. The diagram of Fig. 7.6 shows only the transcurrent dextral fault and two sets of joints related to it. The data surveyed in the sites of the Station 5 show joints in preferential directions NW-SE and NE-SW and bedding planes in the range N240–270 (Figs. 7.7–8).

7.1.4 *Grotta Maria SS. di Custonaci Area*

The stereogram of Fig. 7.9 illustrates a normal fault approximately oriented N 40 and a similarly oriented transcurrent sinistral fault. As a result the larger structures are formed along a preferential direction, oriented approximately NE-SW (Fig. 7.10). In the stereogram of Fig. 7.11 the data collected in the Station 7 show main structures with NW-SE/NNW-SSE orientations.

Fig. 7.9 Stereogram of data surveyed on Station 6

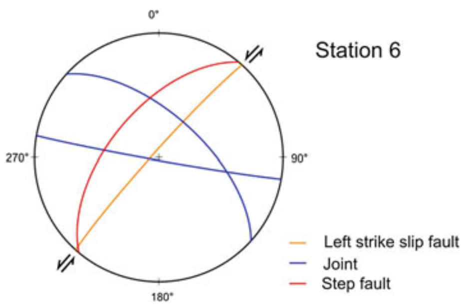

Fig. 7.10 Slip surface of a fault located in the Station 6: the kinematic indicator suggests a *left*-lateral strike-slip motion for the NE-SW trending structure

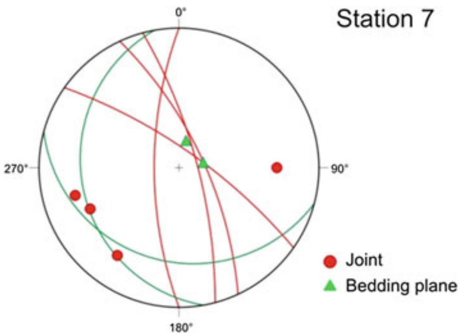

Fig. 7.11 Stereogram of the structural data collected on the Station 7

7.1.5 *Grotta Cerriolo Area*

The structural data collected in the outside wall near the Grotta Cerriolo show prevailing directions of joints in the range NNW-SSE/NW-SE, while the bedding planes show average directions around N-S (Fig. 7.12).

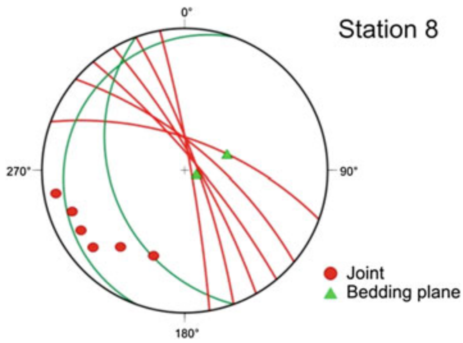

Fig. 7.12 Stereogram of the structures surveyed on the Station 8

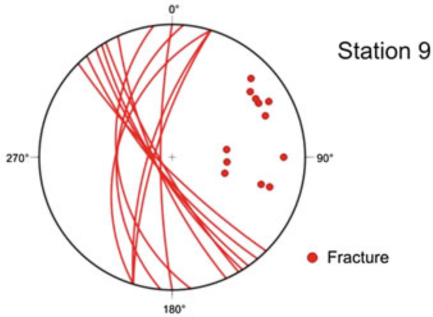

Figs. 7.13–14 Fracture on the wall of the Bufara doline (*left photo*) and stereogram of the projected data (*right side*)

7.1.6 Bufara Doline Area

In the Station 9, on the walls of the Bufara doline, the dominant structures show prevailing NW-SE directions and secondary NNE-SSW directions (Figs. 7.13–14).

7.2 Structural Survey of Mt. Palatimone Area (Site *b*)

The investigation of the area was conducted by using on-site geostructural measurements along two quarry sides located respectively in the lower (Station 1) and upper part of the western slope of the Monte Palatimone ridge (Station 2) and

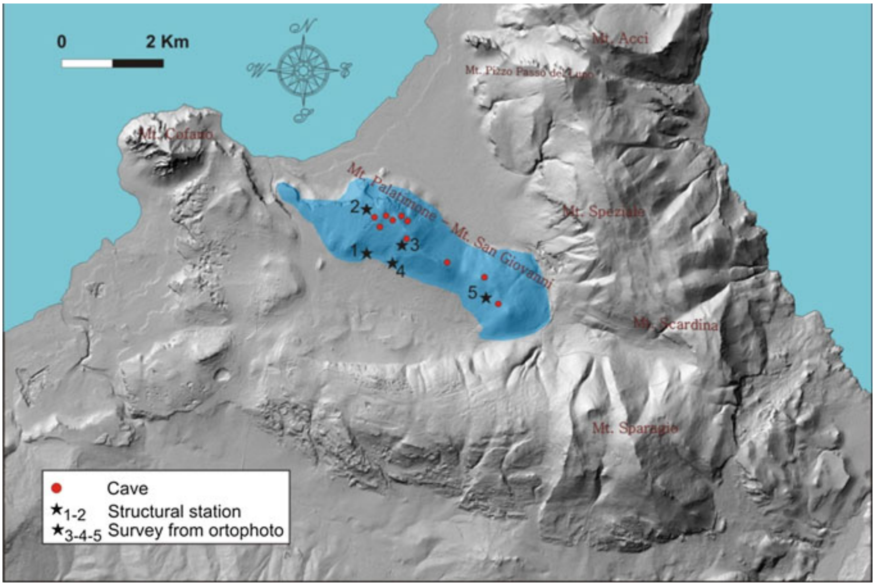

Fig. 7.15 Site *b* Locations of the structural surveys carried out on the surface in some area next to the main caves (*Hillshade map from* DEM Regione Siciliana 2007–2008)

through orthophoto images interpretation where the central and eastern areas are concerned (Stations 3–5). The data collected and plotted in these areas are discussed in the analysis that follows (Fig. 7.15).

7.2.1 Western Area (Middle Upper) Mt. Palatimone

In stereograms of Fig. 7.16 one can observe two dominant directions along, which the faults (in red) are set NW-SE and NE-SW and the minor surface shear (in green). The only group of joints detected, and probably formed due to lithostatic load, is marked in blue. On the other hand, a transcurrent dextral fault, roughly oriented NW-SE, is shown in orange. In the right side stereogram of Fig. 7.16 only the transcurrent fault (yellow) and the larger normal faults (red) are plotted.

In the stereogram of Fig. 7.17 two systems of faulting NNW-SSE and NNE-SSW can be noted, with a dip direction of the strata towards the SSW (Fig. 7.18).

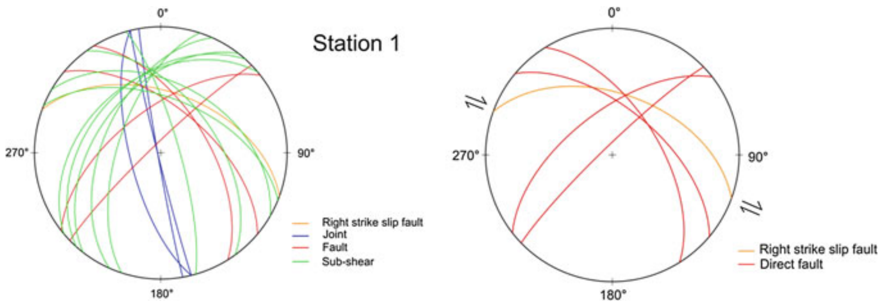

Fig. 7.16 Stereograms with projection of normal faults (*red*) and right strike slip faults (*yellow*). Station 1 in a quarry in the western foothill sector of Mt. Palatimone

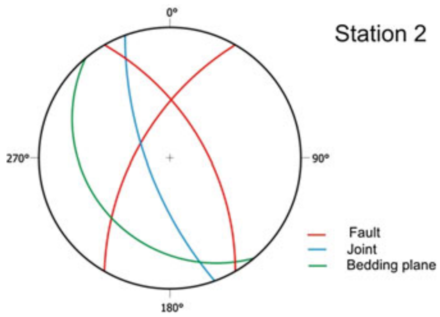

Figs. 7.17–18 Stereogram, and on the *right photo* NNE-SSW oriented wall fault dissected by a NNW-SSE fault (Station 2 in the *upper* western sector of Mt. Palatimone)

7.2.2 The Central Ridge of Mt. Palatimone

The diagram of Fig. 7.19 shows the main structural trends of a wide area of the central upper ridge of Mt. Palatimone, which is characterized by the presence of a karrenfield with extensive and wide crevasses (Fig. 7.20). The main trend along which these morphostructures are extended is NNW-SSE, with secondary structures trending NE-SW.

Moreover, in the lower part of the same central area, a less extensive karrenfield with crevasses is found. It is characterized by a main trend NW-SE with a secondary average N-S trend (Figs. 7.21–22).

7.2.3 The Eastern Ridge of Mt. Palatimone

The diagram of Fig. 7.23 shows the trends of structures that dissect the eastern sector of the ridge of Mt. Palatimone–Mt. San Giovanni. In relation to the latter, the

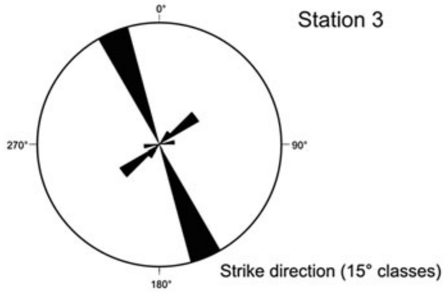

Figs. 7.19–20 Rose diagram of surface large crevasses of the *upper* central part of the structural slope of Mt. Palatimone (data extracted from orthophotos image); on the *right sector* of Mt. Palatimone with crevasses

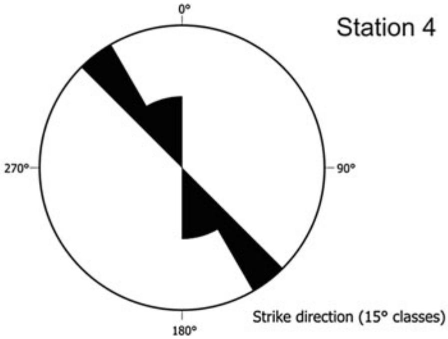

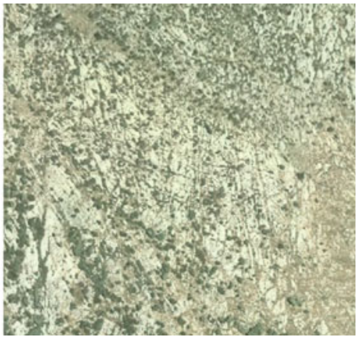

Figs. 7.21–22 Rose diagram of surface crevasses located in the pediment of the central area of Mt. Palatimone. To the *right side* orthophoto image of the area

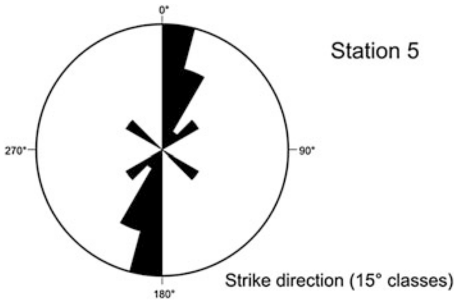

Fig. 7.23 Rose diagram of the structural slope of the *upper* eastern ridge (data extracted from orthophoto image)

data collected from orthophotos image in the Mt. San Giovanni area indicate main NNE-SSW trends and secondary NW-SE trends.

7.3 Structural Survey of Purgatorio Polje (Site *c*)

In the Site *c*, the structural data have been collected both by the analysis of lineations from orthophotos and by the survey on the walls of a road trench, both located next to the main caves of the area (Abisso del Purgatorio, Zubbia delle More, Zubbia della Palma Nana, etc.) (Fig. 7.24). The recorded and plotted data are illustrated in the analysis that follows.

7.3.1 Northern-Central Side of the Polje

In the western area of the polje, NW-SE (main) and N-S (secondary) oriented structures can be identified (Fig. 7.25). In the central area, the main structures are the NE-SW, together with the N-S, while in the eastern zone the NE-SW are still dominant, prevailing on the N-S and NW-SE (Fig. 7.26).

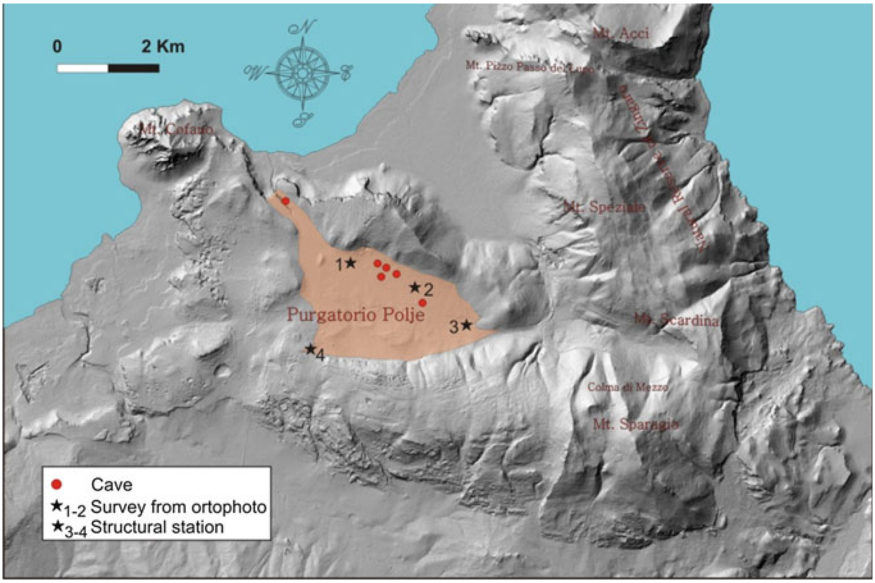

Fig. 7.24 Site *c*—Locations of the structural surveys carried out in some area next to the main caves (*Hillshade map from* DEM Regione Siciliana 2007–2008)

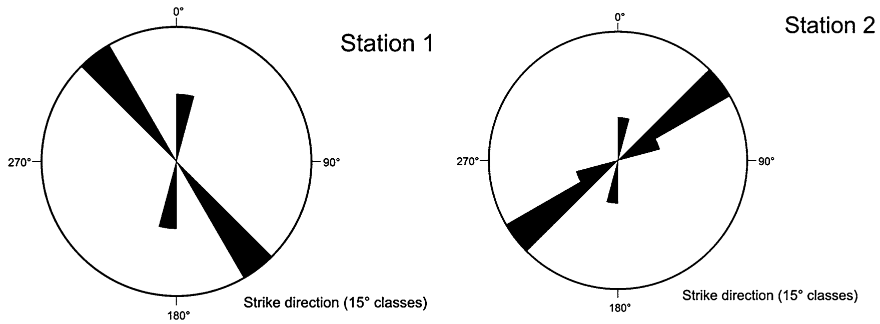

Fig. 7.25 Rose diagram of the lineations from orthophotos image in the western (*left side*) and in the central part of the polje (*right side*)

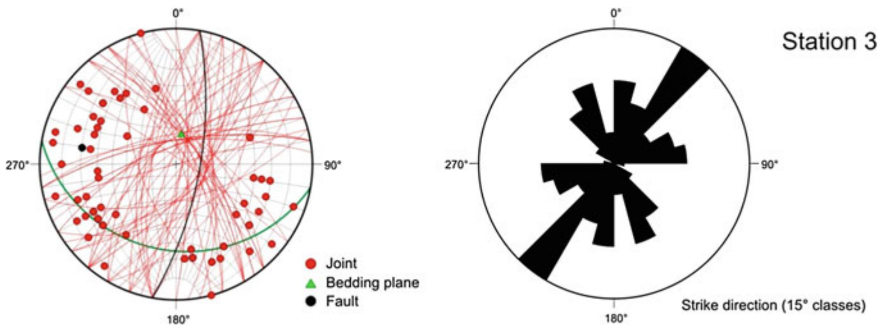

Fig. 7.26 Stereogram and rose diagram of the structural survey of the eastern part of the polje (Station 3)

7.3.2 Structural Survey of "Alto Muciara" Area in the South–Western Sector of the Purgatorio Depression (Site c*)*

The surveys that were carried out in the area referred to as "Alto Muciara" (Station 4), in the furthest western area of the Purgatorio depression (Fig. 7.27), have shown the presence of predominantly ENE-WSW and E-W oriented structures (Fig. 7.28). The study of abutting and crosscutting relationships and kinematic indicators present on the shear planes has allowed to reconstruct for this set of structures a right strike-slip movement (Figs. 7.29a, b and 7.30).

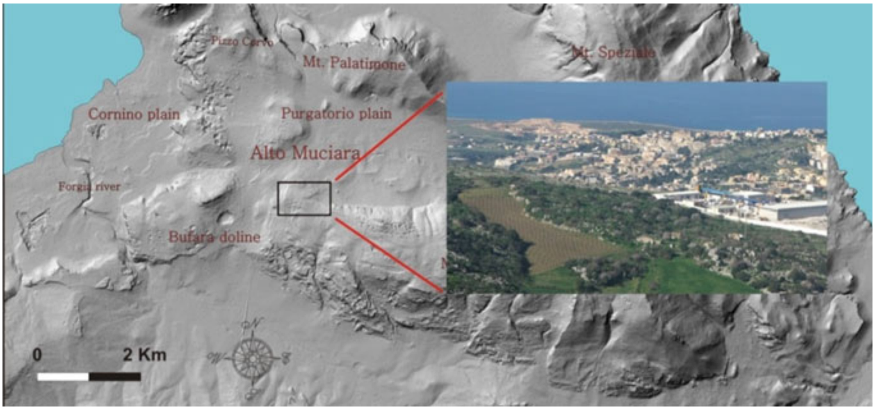

Fig. 7.27 Site *c*, Station 4: “Alto Muciara” in the south–western sector of the Purgatorio plain (*Hillshade map from* DEM Regione Siciliana 2007–2008)

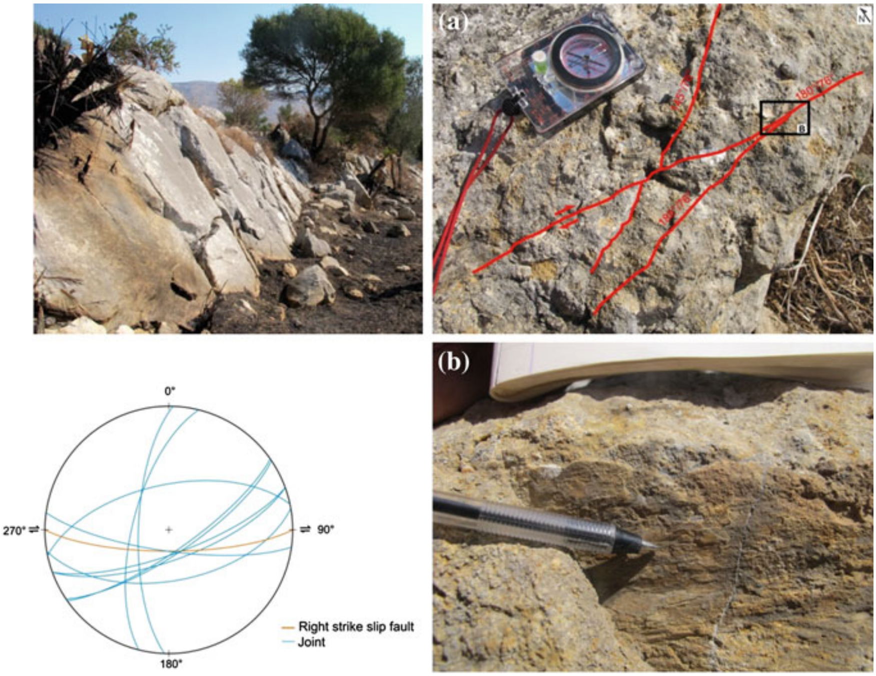

Figs. 7.28–29 Figure 7.28 *left photo up* Positive flower structure along the “Alto Muciara” dry valley. Figure 7.28 *left below* Stereogram with E-W trending right-lateral small fault. *Right photo* Fig. 7.29a crosscutting relationship between the South dipping structure and SE dipping structure; Fig. 7.29b striation and calcite fibers on the fault plane

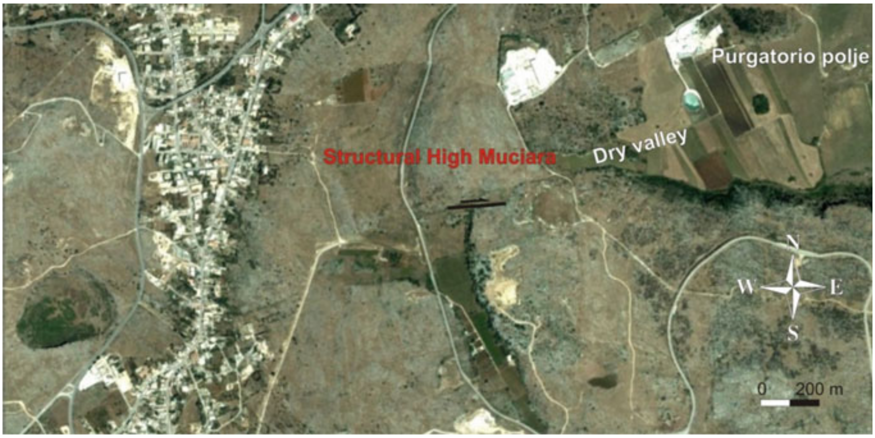

Fig. 7.30 Orthophoto image of the western sector of the Purgatorio polje with right strike slip fault, which would have created the "Alto Muciara" positive flower structures and the following closing of the valley (from Google Earth)

7.4 Structural Survey of Mt. Sparagio Area (Site *d*)

The structural investigation of the Mt. Sparagio ridge, called Site *d* (Fig. 7.31), was conducted both through surveys carried out along quarry faces located in the Cocuccio area (Figs. 7.32–33, Station 1) and also through orthophoto images and on-site surveying carried out in the Pozzo Noce (Station 2) and Giacolamaro area

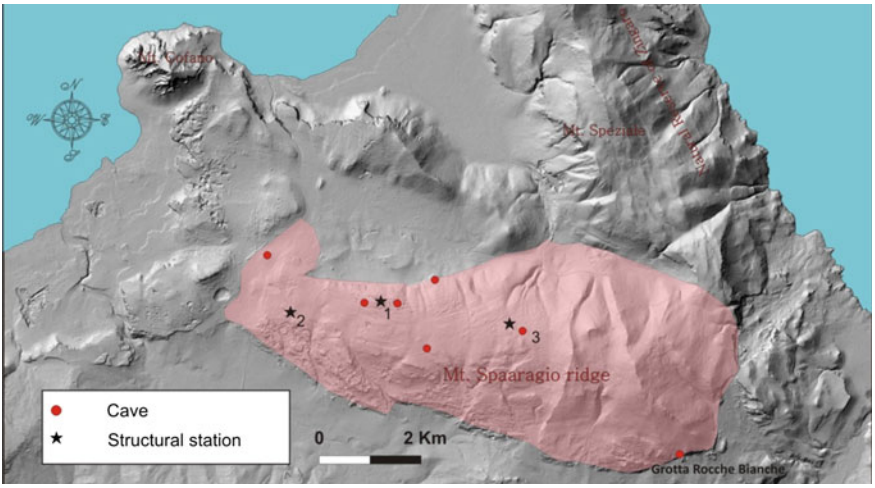

Fig. 7.31 Site *d*—Locations of the geostructural surveys carried out in some area next to the main caves (*Hillshade map from* DEM Regione Siciliana 2007–2008)

(Station 3). The former constitutes a sector of the ridge affected by extensive morphologies exhibiting crevasses. The data collected and plotted in the diagrams are discussed in the analysis that follows.

7.4.1 Cocuccio–Giocolamaro–Noce Areas

The survey carried out in the Station 1, on the wall of a quarry of Cocuccio area, shows a set of joints with N-S and NE-SW trend and a right strike slip fault oriented NW-SE (Fig. 7.34) with striation (Fig. 7.35).

The surveys of the crevasses karrenfield in the Noce area show two sets of intersected discontinuities with NE-SW predominant trend set and ESE-WSW secondary one (Figs. 7.36–37). In the Giacolamaro area the data plotted in the Rose diagram of Fig. 7.38 indicate two main trends NE-SW and NNW-SSE (Fig. 7.39).

Fig. 7.32–33 Walls of a quarry in the Cocuccio area affected by joints (*left photo*) and by a fault with striation (*right photo*)

Figs. 7.34–35 Stereogram of data surveyed in the station 1 and striation along a right strike slip fault (Cocuccio area)

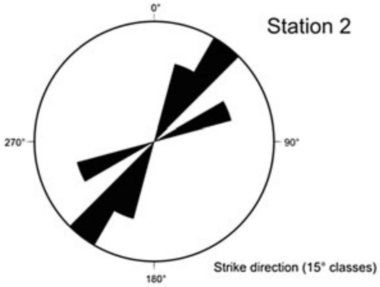

Figs. 7.36–37 Rose diagram of the data surveyed in the crevasses karrenfield (*left*) and photo of the intersected fractures in the Pozzo Noce area, Mt. Sparagio ridge (*right side*)

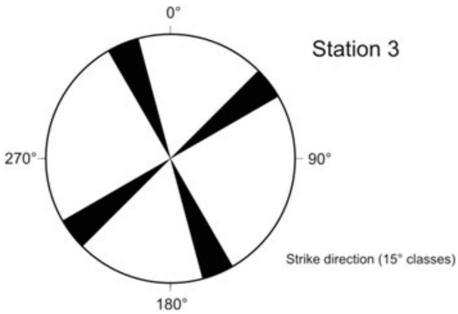

Figs. 7.38–39 Rose diagram of data surveyed in the Giacolamaro area and limestones dissected by fractures

7.5 General Analysis of the Results

The structural data collected and projected on Schmidt diagrams shows how, in all the sites under study, despite dispersion in the collected measurements, two sets of roughly NW-SE and NE-SW oriented structures (Table 7.1 and Fig. 7.40) are always present.

In Site *a* "Mt. Bufara–Cerriolo–Piano Zubbia" the analysis of the kinematic indicators present on some fault planes has allowed the reconstruction of the relative movements of some of the tectonic structures that were identified. In particular, evidence of movement to the right on the NW-SE and movement to the left on the NE-SW oriented structures was found.

Structures having a kinematic dextral strike slip component were also detected at Site *b* "Monte Palatimone" and Site *d* "Cocuccio, Mt. Sparagio." In the latter, the two sets that have been discussed so far are poorly represented, while the presence of a series of structures having a direction, which varies from N-S to NNE-SSW is

Table 7.1 Synoptic table of comparison among the structural features (faults and joints) and the main karstified cave structures surveyed in the selected areas of study

Site	Station	Main structure	Kinematic feature	Main caves/landforms	Main structure	Kinematic feature
A	1	NW-SE		Fantasma cave	NE-SW	Left strike slip
	2–3	NW-SE			WNW-ESE	Displaced speleothems
	4	NW-SE	Right strike slip	Clava cave	NW-SE	Displaced speleothems
	5	NW-SE				
	6	NE-SW	Left strike slip	Maria SS Custonaci cave	NW-SE	Displaced speleothems
	7	NW-SE				
	8	NNW-SSE		Cerriolo cave	NNW-SSE	
	9	NW-SE		Bufara doline	NW-SE	
B	1	NW-SE	Right strike slip			
	2	NNW-SSE		Zubbia Meraviglie—Zubbia Campana	NNW-SSE—NNE-SSW	
	3	NNW-SSE		Crevasses karrenfield (slope)	NNE-SSW	
	4	NW-SE		Crevasses karrenfield (pediment)	NW-SE	
	5	NNE-SSW		Zubbia S. Giovanni	NNE-SSW	
C	1	NW-SE		Gorge Abyss	NW-SE	
	2	NE-SW		Zubbia dei Rovi	NNE-SSW	
	3	NE-SW		Purgatorio Abyss	NE-SW	
	4	E-W	Right strike slip	Muciara positive flower structure		
D	1	NW-SE	Right strike slip	Zubbia Cocuccio 1–2	N-S—NW-SE	
	2	NE-SW		Crevasses karrenfield		
	3	NNW-SSE		Zubbia Tre Corna	NNW-SSE—NE-SW	

much more evident. However, for the latter structures it has not been possible to reconstruct the kinematics.

In the Station 4 of Site *c* “Alto della Muciara” a set of structures having a direction that varies from E-W to ENE-WSW with dextral transcurrent movement was detected.

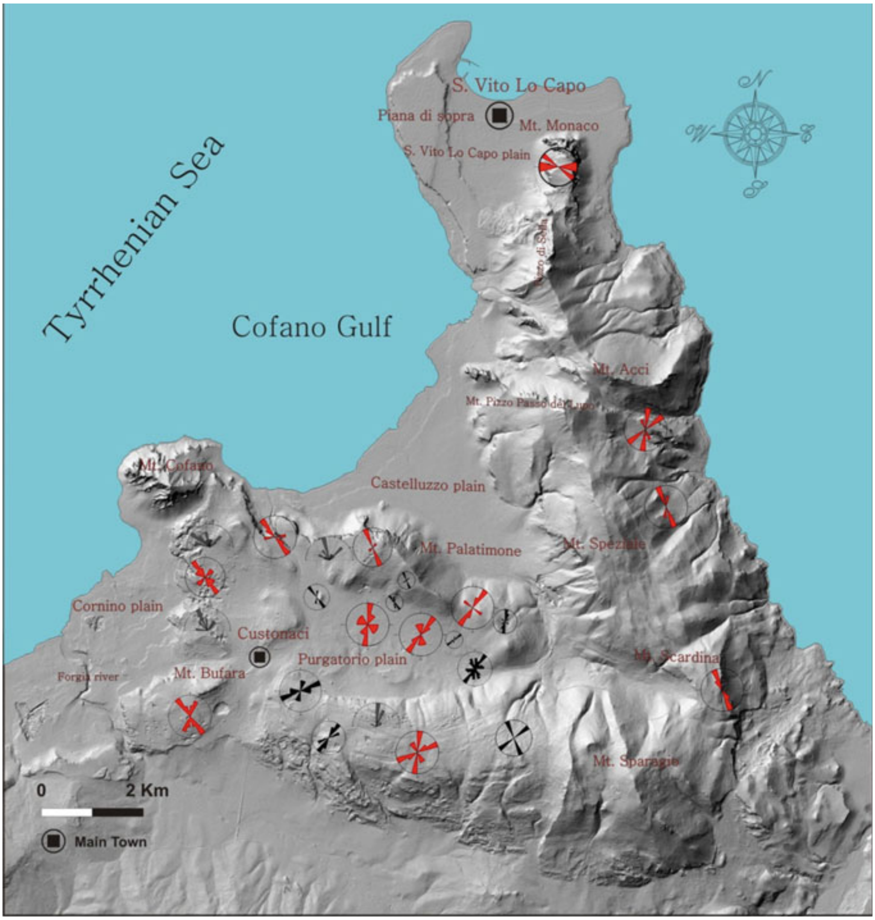

Fig. 7.40 General view of the surface structural trends (*black Rose diagrams*) and cave karstified structures (*red Rose diagrams*) surveyed in the study area (*Hillshade map from* DEM Regione Siciliana 2007–2008)

7.6 Correlation between Structures and Cave Morphostructures in Site *a*

From the above reported data surveyed in Site *a*, it can be underlined that the most intensely karstified structures, in the Mt. Bufara–Cerriolo–Piano Zubbia area, are those with NW-SE trend along, which the Clava and Maria SS. di Custonaci caves have developed. These structures have also shown, from external investigations that were conducted, characteristics of normal and dextral transcurrent faulting. In the above caves displaced speleothems were observed and probably caused by the above mentioned kinematic movements along the faults.

Along these same structures NW-SE, the Grotta del Fantasma develops downward, while in its upper part the NE-SW trending structures are dominant, the latter also detected externally with characteristics of normal and sinistral transcurrent faulting.

The latter kinematic feature has also been observed inside the cave as a result of the removal/displacement suffered by one speleothem grown between both sides of the structure (see Fig. 6.184, Sect. 6.6).

7.7 Correlation between Structures and Cave Morphostructures in Site *b*

The comparison between the karst morphostructural data and the structural surveys has resulted in the following considerations:

1. In the upper western ridge, the most important caves are mainly developed on structures trending NNW-SSE and, to a lesser extent, NE-SW, reflecting the structural pattern identified from external surveys.
2. The same trends are evident with regard to the surface crevasses and cave crevasses of the central part of the ridge: NNW-SSE dominant on NE-SW.
3. In contrast, in the eastern middle-upper ridge, the most heavily karstified structures (where the main caves that have been surveyed are located) are, on average, NE-SW oriented and, to a lesser extent, NW-SE.

7.8 Correlation between Structures and Cave Morphostructures and Karst Landforms in Site *c*

From the above reported data surveyed in Site *c*, it can be underlined that the most intensely karstified structures, in the polje, are those with NE-SW trend, in the central-eastern area, along which the Abisso del Purgatorio has developed, while in the central-western part the more karstified structures are resulted those with NW-SE trend along which the Abisso delle Gole and the Zubbia delle More have developed.

At last, the “Alto Muciara” dry valley developed along E-W structures with dextral transcurrent movement.

7.9 Correlation between Structures and Cave Morphostructures and Karst Landforms in Site *d*

Among the structures detected along the Mt. Sparagio ridge, those that have led to the formation of karst caves and karst landforms were:

1. The NNE-SSW in the eastern area (Cocuccio area).
2. The NE-SW followed by ESE-WNW in the western area (Noce area crevasses).
3. The NW-SE and the NE-SW in the Giacolamaro area.

7.10 General Observations on the Karst Landform Mt. Palatimone–Purgatorio Polje

The above discussed structural findings have revealed, in the central area of the ridge of Mt. Palatimone–Mt. San Giovanni, the presence of two areas dissected by a dense network of interconnected fractures on which medium to large crevasse morphologies and cave-crevasses have formed.

In the central middle-upper area of the structural slope, the crevasses range in width from decimeters up to several meters. Their lengths reach up to several tens of meters while depths range from a few decimeters to 5–7 m. The dominant structural trends are NNW-SSE while secondary trends are NE-SW.

In the central area of the foothills the crevasses are set along a structural slope with a gentle gradient, dissected from NW-SE trending structures (dominant) and N-S trending structures (secondary). In fact this area, being the product of the receding side of the ridge (pediment), makes up the central part of the Purgatorio polje system.

In the upper region of the eastern part of the ridge (Portella della Ronza—Monte San Giovanni) the structures exhibit an average dominant NNE-SSW trend and secondary NW-SE trends. In the lower foothills area, corresponding to the eastern part of the polje (the pediment side that has retreated as a result of erosion and corrosion), the prevailing trend of the lineations, measured both on site and from the orthophoto image analysis, is NE-SW and, to a lesser extent, N-S and NW-SE.

Therefore (see Fig. 7.40):

- The structures and karst morphostructures with NW-SE/NNW-SSE trends are dominant in the western area of the ridge;
- The structures and karst morphostructures with NNE-SSW/NE-SW trends are dominant in the eastern part of the ridge and the polje.

References

DEM Regione Siciliana Modello digitale del terreno passo 2 m derivato da dati LIDAR volo ATA 2007–2008 in UTM-WGS84 fuso 33 N

Ortofoto Regione Siciliana Ortofoto anno 2007–2008. Realizzazione ripresa aerea digitale pixel 0.25 m. in UTM-WGS84 fuso 33 N

www.google.com/intl/it/earth/index.html

Chapter 8
Results and Discussion

8.1 Structural Control in the Karst Processes

The presence of three sets of structures identified during the current research in the study area is documented by several authors (Abate et al. 1998; Renda et al. 2000; Tondi 2007). These authors attribute the three sets to a predominantly transcurrent kinematic; dextral for the sets E-W and NW-SE and sinistral for the sets N-S and NE-SW (Abate et al. 1998; Tondi et al. 2006). They set the genesis of these structures in a dextral fracture system of a Plio-Pleistocene regional transtension, which involves the southern Tyrrhenian Sea and the northernmost part of Sicily (Renda et al. 2000). In fact, as shown in Figs. 7.36–37, the most abundant features exposed in the study area may be interpreted as minor structures related to a roughly east-west-striking fault driven by a NW-oriented compression (Tondi et al. 2006).

Even in the various structural stations that were set up, surfaces which are oriented NW-SE and E-W have been detected. These show evidence of dextral transcurrent kinematics and NE-SW lineaments with sinistral transcurrent kinematics. Abate et al. (1998) and Tondi et al. (2006) recognized positive flower structures at both dextral and sinistral transcurrent lineaments in the whole area of the Monti di Capo San Vito.

The Structural high of the Muciara area (Fig. 8.1), which currently forms a barrier that separates the Purgatorio polje from the Bufara doline, is located in an area affected by some transcurrent lineaments having the same directions of the three sets encountered in the field structural stations of the study area. One can hypothesize that this area, once crossed by a valley, which allowed the flow of water from the Purgatorio plain to the area of the Bufara doline, has been tectonically uplifted during the Middle Pleistocene as a result of the transcurrent movements activated along NW-SE, NE-SW and E-W lineaments (Figs. 7.28–29, Chap. 7). These were activated as a result of the dextral transcurrent system, which controls the recent

R. Ruggieri, *Speleological and Speleogenetic Aspects of the Monti di Capo San Vito (Sicily)*, Springer Theses, DOI 10.1007/978-3-319-21720-8_8

Fig. 8.1 Structural high of Muciara dry valley

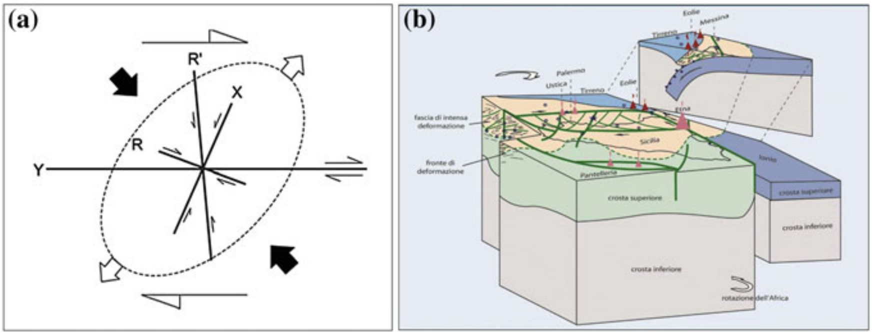

Fig. 8.2 **a** Two-dimensional geometry of today stress field acting in northwestern Sicily, and structural interpretation of the structures mapped in the studied area (modified after Tondi et al. 2006); **b** 3D model of the Sicilian area showing the most important neotectonic fault system (*green*), the chain sectors (*beige*) and the undeformed areas (*light grey*) (modified after Napoli et al. 2012)

evolution of the southern margin of the Tyrrhenian Sea (Giunta et al. 2000; Renda et al. 2000, Napoli et al. 2012) and generates the neotectonic lineaments affecting the northern part of Sicily (Fig. 8.2).

With reference to what has been reported, the following assumptions regarding the structural control on the speleogenetic processes, documented and presented in this research, have been formulated (Fig. 8.3).

1. The processes of karstification, which began with the Pliocene–Lower Pleistocene uplifting, have, in their initial phases, involved mainly N-S oriented

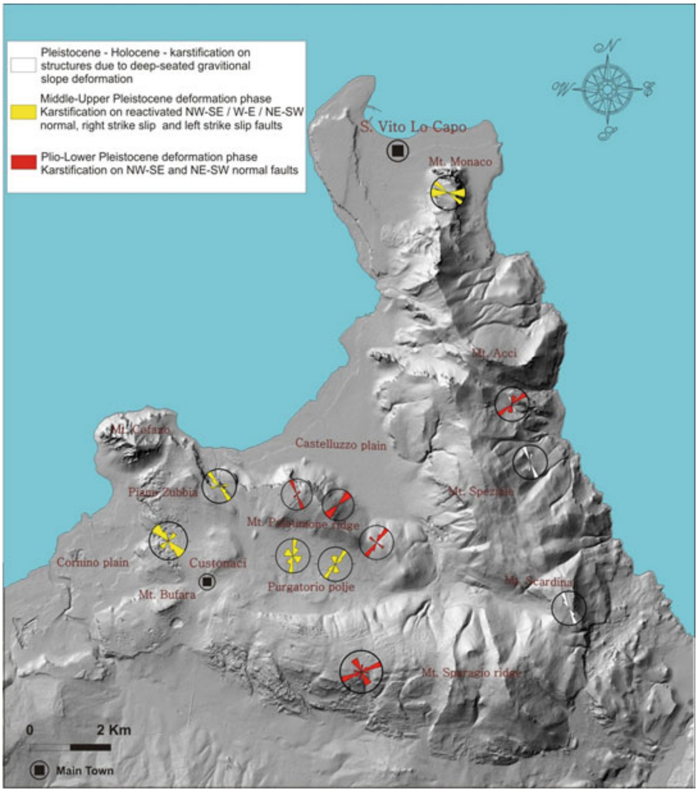

Fig. 8.3 Map of cave karstification trends linked to the Plio-Pleistocene-Holocene deformation phases in the different sectors of the study area. Red trends in the Rose diagram show karstification processes occurred in the Pliocene up to Lower Pleistocene structures, while yellow trends show karstification processes occurred in Middle and Upper Pleistocene–Holocene reactivated structures, which have deepened the main caves of the study area, present in the Purgatorio polje and in the Piano Zubbia area (*Hillshade map from* DEM Regione Siciliana 2007–2008)

extensional Mesozoic structures reactivated by transcurrent tectonics induced from the Tyrrhenian spreading. Successively NNE-SSW/NE-SW oriented structures were involved, the latter also related to the above-mentioned initial phase of deformation. The caves located in the areas of Mt. Palatimone ridge (Abisso Eolo, Zubbia della Campana, Zubbia-Crepaccio, Zubbia ru Malu Pilu, Zubbia Cucca) originated on these structures. The caves found in the Mt. Sparagio (Zubbia Cocuccio and Zubbia delle Tre Corne) also originated on such main structures.

2. The origin of new caves (Grotta della Clava, Grotta Mari SS. di Custonaci, Zubbia delle Meraviglie, Abisso del Purgatorio and Abisso delle Gole) in the western and central part of the area (Piano Zubbia and Purgatorio polje

respectively) can be attributed to the last deformation phase (Middle–Upper Pleistocene), which is still active. The deepening of caves, which were previously set on NE-SW oriented structures, with the opening or reactivation of transtensional faults, continued since the Tyrrhenian transcurrent tectonic phase with NNW-SSE/NW-SE trend (Abisso del Purgatorio, Grotta del Fantasma, Abisso delle Gole, Zubbia della Palma Nana).

3. The genesis of the main karst forms, present in the eastern part of the research area (Mt. Speziale–Mt. Scardina ridge), both superficial (uvala depressions of Pianello) and underground (Zubbie di Borgo Cusenza, Grotta del Sughero, Zubbia e Grotte di Monte Scardina) can be probably attributed to Pleistocene and Holocene deformation processes. Most of the caves, in fact, show the same structural trend (NNW-SSE) along, which the origin of deep-seated gravitational slope deformations has produced, in the southern coastal area of the Zingaro Reserve, sizeable landslide phenomena, such as the Scopello landslide, and the important fault, which runs along the eastern side of Mount Scardina.

8.2 Influences of Morphotectonic Evolution and Climate Changes on the Karst Landforms of the Study Area

On the basis of morphological and structural elements that have emerged during this study, a genetic evolution has been formulated concerning the main karst forms originating along the coastal belt and in the inland areas. This genetic evolution deals with the influence produced by tectonics of the Monti di Capo San Vito on the speleogenesis, also when linked to the climatic-eustatic episodes that took place during the Pleistocene.

8.2.1 Coastal Areas

Along the coastal plains of the study area, the presence of seven orders of marine terraces (Di Maggio et al. 1999; Antonioli et al. 1999a, b) located at different elevations and faulted in some sectors (Tondi et al. 2006) witness how from the end of the Pliocene and up to the present, the area of Monti di Capo San Vito has been subjected to differential uplifting as a consequence of tectonics with alternating phases both compressive and extensional (or combined). This activity has influenced the coastal belt speleogenesis with the formation of a series of karst morphologies, and marine erosive forms, present both in the inner edges of the paleo-terraces, on the relict sea-cliffs, and in other cases up to a certain inland distance from the latter.

The speleogenetic processes, originating in this context with the emersion of the coastal areas at the end of the Lower Pleistocene, differently from those generated in the inner sectors of the area (ridges and Purgatorio polje), have been more subject to the combined effects of the eustatic changes and the contextual tectonic uplifting. This in terms of more or less accentuated variations of the erosion base level, respectively during the phases of glacial lowstand and during the phases of the Quaternary interglacial highstand.

That said, on the basis of the surveys carried out (reported in Sect. 6.3), the main morphological and structural characteristics of the karst forms located in the coastal sector and facing the relict sea-cliffs of the study area, and the influence of the tectonic and eustatic events on their evolution, can now be described.

8.2.1.1 Cornino Plain and Scurati—Rocca Rumena Relict Sea-Cliffs

In this sector, as it has been described (see Sect. 6.3), sea caves and *flank margin caves* have been surveyed. The latter have been observed both on the internal margin of some marine terraces present in the Cornino plain and on the Scurati–Rocca Rumena relict sea-cliffs (Figs. 8.4 and 8.5). On the latter some sea paleo-notches are present too.

The structural analysis carried out on the surveyed caves has underlined N-S main trend for those located in the Scurati relict sea-cliff (Fig. 6.314, Sect. 6.7) and NNW-SSE main trends and E-W secondary trends for those located in the Rocca Rumena cliffs (Fig. 6.332, Sect. 6.7).

As for the age of the terraces the before mentioned studies (see Sect. 2.2.1, Di Maggio et al. 1999; Antonioli et al. 1999a, b) have allowed the dating of terrace VI, referred to the Eutyrrhenian (sub-stage 5e), for the presence of warm senegalese fauna with *Strombus bubonius*, while from the dating of a speleothem an age greater than 300 ka can be attributed to terrace III (Antonioli et al. 1999a, b). From this it has been calculated that the rates of uplifting for the area of Cornino would be around 0.076 mm/year.

In this context, a notable contribution derived by the exploration and study, carried out during this research, regarding the Grotta Rumena 1 (Ruggieri et al. 2012), sited on the Rocca Rumena relict sea-cliff at 95 m asl.

As described (in Sect. 6.3), the morphologies encountered inside the cave and its position with respect to the slope underline its genesis as a cave classifiable as *flank margin cave* (Mylroie et al. 2008), in as much as originating by salt-fresh mixing processes and dissolution along structural voids (bedding planes and fractures) of telogenetic limestones (with high diagenetic maturity) of Upper Cretaceous age.

Inside the cave the widespread presence of encrusting marine organisms and lithophaga borings showed the important role carried out by the cave during the Pleistocene (Sicilian) marine transgression as an ideal habitat for the colonization of several marine species (corals, bryozoans, serpulids, etc.).

Beyond this fact there is the presence of speleothems showing in Chap. 4 hiatuses that increase the importance of the cave as an extraordinary paleo-climatic archive, that underlines the cyclic nature of the eustatic variations during Quaternary.

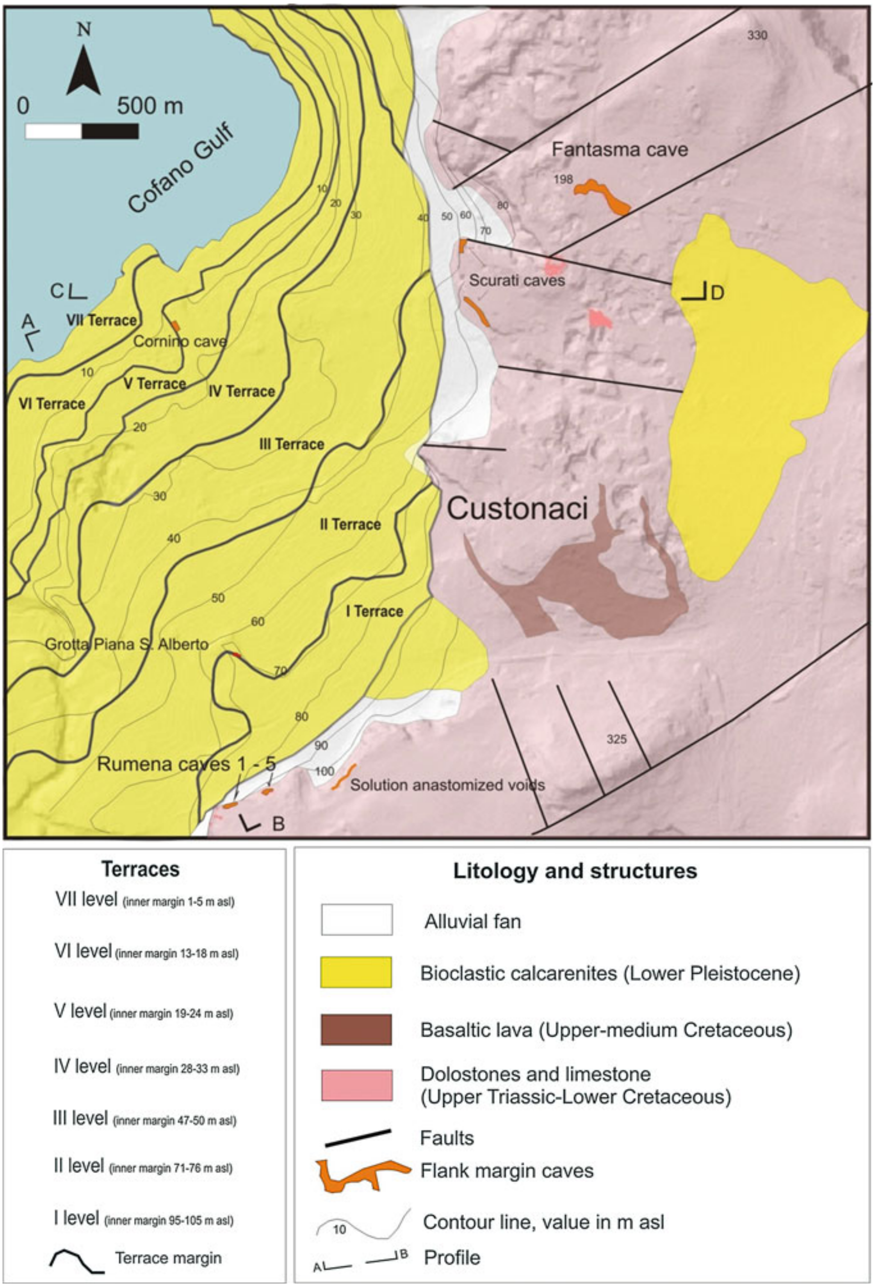

Fig. 8.4 Map of sea terraces and locations of the main *flank margin caves* in the Cornino plain and relict sea-cliffs (locations of sea terraces, after Di Maggio et al. 1999)

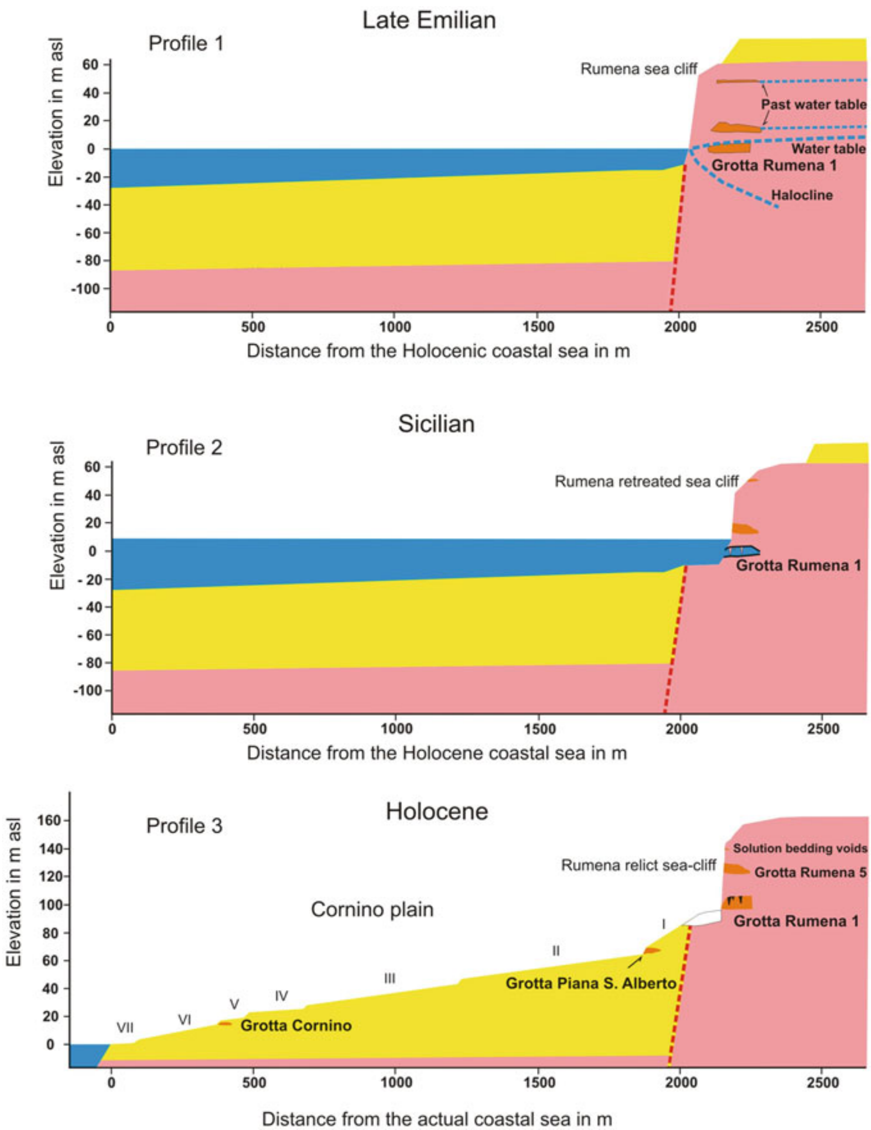

Fig. 8.5 *Profile 1* Genesis of Rumena cave as *flank margin cave* in the Lower Pleistocene (Late Emilian?); *Profile 2* The sea invades the cave and the colonization of marine organisms takes place in the Sicilian; *Profile 3* (profile A–B of Fig. 8.4) showing the seven order Pleistocene sea terrace levels (after Di Maggio et al. 1999) and the Rumena relict sea-cliff facing the Cornino plain with the locations of the surveyed *flank margin caves*. This profile also shows as the Rumena cave has been uplifted at about 95 m asl during the last Million of years, as resulted from the dating of the speleothem, collected inside the cave, and with calculated uplift rate of 0.1 mm/year (see legend of Fig. 8.4)

Table 8.1 Rumena cave speleogenetic phases

Phase	Period	Paleogeography	Cave genesis evolution	Morphologies /fillings
I	Lower Pleistocene Late Emilian (?)	Faulting and uplifting with formation of a sea cliff	*Flank margin cave*	1. Low hemispherical chambers 2. Smooth ceiling/domes
II	Lower Pleistocene Sicilian **MIS 31-37** (see Figs. 8.4 and 8.8) Compensation between Upliftings and sea transgressions (?)	1. Uplifting and retreat of the marine cliff with invasion of the sea inside the cave 2. Climate change with eustatic sea level variations	1. Submarine cave with colonization of sea organisms (in semi-dark environments below the fair weather swell zone) 2. Alternation of submarine cave and 3. Epigenetic cave (vadose/epiphreatic)	1. Biogenic encrusts/lithophaga borings 2. Speleothems with hiatuses 3. Ceiling channel
III	Middle–Upper Pleistocene **MIS 5e –** Holocene	Uplifting of the land and formation of the Rocc Rumena relict sea-cliff	Vadose karst cave	1. Debris deposits 2. Calcite speleothems 3. Ceiling and walls condensation-corrosion

The radiometric dating carried out on the corals and on the continental parts of the speleothem allowed to deduce for the cave an age of 1,000 ka, or a little more, linked with the MIS 31-37 confirming, moreover, for the sector under study a rate of uplift of around 0.1 mm/year for the before stated period between Lower Pleistocene and Holocene.

According to the above described results, the following speleogenesis evolution has been formulated for the Rumena cave summarized in the following three main phase (see synoptic Table 8.1):

- Lower Pleistocene–Late Emilian (?): genesis of the Rumena *flank margin cave*
- Lower Pleistocene–Sicilian: retreat of the cliff due to erosion, transgression of the sea with its invasion inside the cave and subsequent sea organisms colonization.

During this phase the presence of three hiatuses in the Rumena cave speleothems shows a certain compensation between tectonic upliftings and transgressions of the sea, which had to occur for a certain amount of time.

- Middle–Upper Pleistocene–Holocene: Filling of the vadose caves with continental debris and calcite deposits.

Fig. 8.6 Survey of the paleo-notch elevation on the Cerriolo relict sea-cliff by topographic GPS RPK

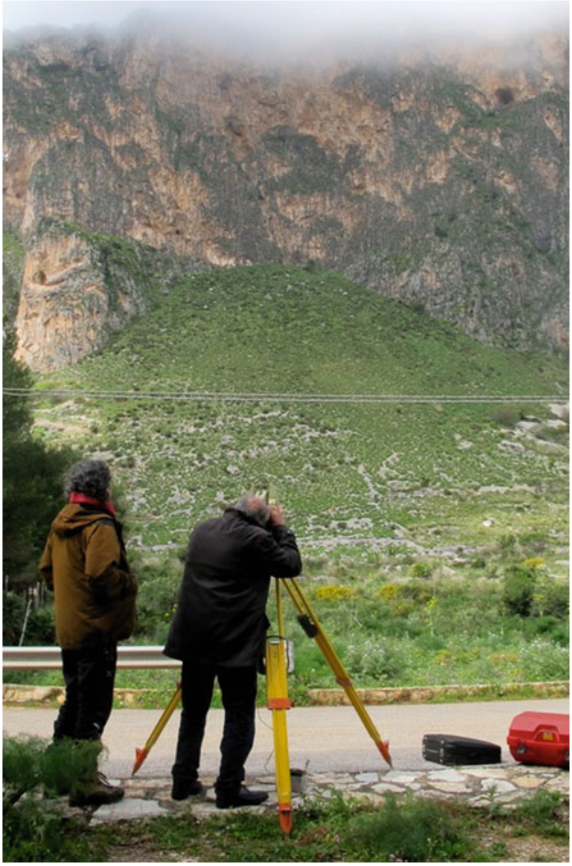

Fig. 8.7 Survey for intersection by total station Leica TC 905/L of the sea cave Grotta dei Pendenti in the Monte Monaco

Age of the Relict Sea-Cliff Karst Morphologies

In order to determine the elevations of both of the sea caves/flank margin caves and of the sea-notches on the relict sea-cliffs, several measurements have been carried out by topographic GPS RPK (Real Time Kinetic) Leica 1200 and in zones of bad reception the classic method of intersection was carried out with the use of a Leica 905/L total station (Figs. 8.6 and 8.7), while other measures have been taken from technical maps at 1: 10.000 scale.

Plotting on a diagram the elevations of above mentioned morphologies present in the relict Cofano-Scurati-Rocca Rumena sea-cliffs (Tables 6.8, 6.9 and 6.10, Sect. 6.7), three main range levels are evidenced equal to: 60–70 m asl, 90–120 m asl and 140–150 m asl (Fig. 8.8). At these three ranges using the rate of uplift of 0. 1 mm/year it could be possible to attribute sea highstand respectively ugual to MIS 15-17, MIS 31-37 and MIS 49.

In particular, using the calculated rate of uplift equal to c. 0.1 mm/year, it has therefore been possible to attribute a probable date for the formation of several surveyed caves classified as *flank margin caves,* present in the above mentioned groups of caves, whose elevation is surely correlated to a paleo-marine level. This, however, is surely not always feasible for the epigenetic caves. So, for these caves reported in the Tables 6.9, 6.10 and 6.11 of Sect. 6.7, referred to Fig. 8.4 and profile 3 of Fig. 8.5, starting from the lower levels, one can attribute a probable age of:

- c. 130 ka for Grotta Cornino, sited on the internal margin of the VI terrace at 13 m asl (MIS 5e);
- c. 700 ka for Grotta della Piana San Alberto, sited on the internal margin of the II terrace at 70 m asl (MIS 17);

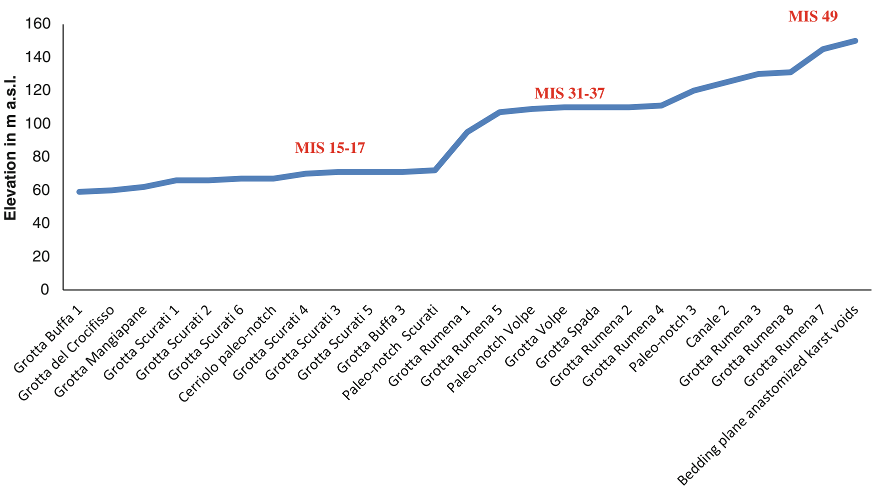

Fig. 8.8 Diagram of the caves and coastal karren elevations present in the Cofano–Scurati–Rocca Rumena relict sea-cliffs with indication of the probable relative Marine Isotopic Stage (MIS)

- c. 1,100 ka, or slightly more, for Grotte Rumena 1-4-5, located on the Rocca Rumena cliff at range 95–110 m asl (MIS 31-37);
- c. 1,500 ka, or slightly more, for the open tapering notches on the horizontal bedding plane on the Rocca Rumena cliff at 150 m asl (MIS 49).

Age of Grotta del Fantasma

The relatively short distance of the Grotta del Fantasma with respect to the actual coastal line (1,500 m) and to the relict sea-cliff (around 500 m westwards, see Figs. 6.183, 6.184, 6.185, 6.186, 6.187, 6.188, 6.189, 6.190, 6.191, 6.192, 6.193 and 6.194), constitutes a realiable sea level indicator. In this regard, on the base of tectonic uplift rates, calculated using the Rocca Rumena cave dating and the MIS 5e (terrace VI) (0.1 mm/year) and other geomorphological constraints, the horizontal maze-like chamber and conduits of the Fantasma cave might thus have been created by the mixing corrosion of fresh and salt water probably around 800 ka (c. MIS 19) (Fig. 8.9).

For the caves located on the Scurati cliff at c. 70 m asl (Table 6.9, Sect. 6.7) for correlation the same age as the Grotta di Piana San Alberto can be given of c. 700 ka (Fig. 8.5).

8.2.1.2 San Vito Lo Capo Peninsula Relict Sea-Cliffs

As before reported (see Sect. 6.7, Table 6.12), a discrete number of caves, developed both on fractures and on bedding planes, have been surveyed in the coastal belt of Piano Makari and on the Mesozoic limestone cliffs of Capo San Vito peninsula. The caves developed on fractures show entrances more or less generally

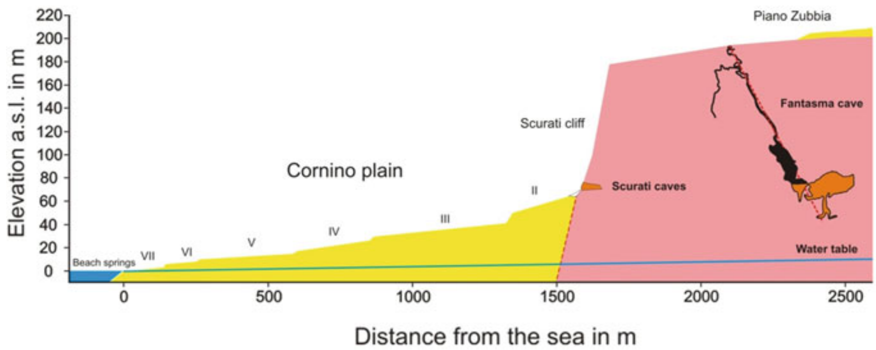

Fig. 8.9 Profile C–D of Fig. 8.4 showing the six order Pleistocene sea terrace levels (after Di Maggio et al. 1999) in the Cornino plain and the projected profiles of the Scurati–Sala del Fantasma "*Flank margin caves*" (in *orange*)

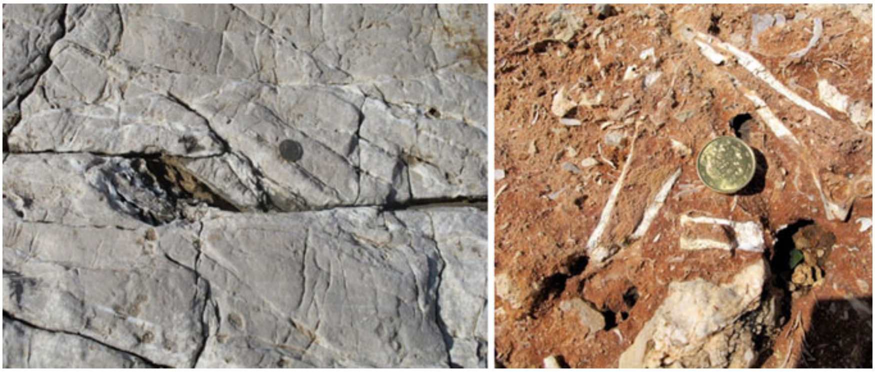

Figs. 8.10–11 Pull-apart neotectonic structure (*left photo*) and continental deposits with deer bones along the coastal belt of Castelluzzo and San Vito Lo Capo peninsula (*right photo*)

Figs. 8.12–13 Neotectonic deformations affecting both the Upper Jurassic–Lower Cretaceous calcarenites with striae outcropping along the coastal belt of the Capo San Vito peninsula (*left photo*) and the Lower Pleistocene calcarenites outcropping along the Castelluzzo coastal plain (*right photo*)

with ogival sections and with lengths from a very few to about ten meters. For these caves a mix of karst and sea erosion genesis has been recognized, this latter in some cases underlined by the presence on the wall of sea paleo-notches and of lithophaga borings (Grotta del Cavallo, Grotta di Cala Mancina, Grotta del Fiore, etc.).

The structural analysis has shown prevailing E-W trends and secondary N-S ones and in one case the development on a transpressive NE-SW structure positive flower type with a left component, in same manner probably linked to Plio-Pleistocene tectonic and actual transcurrent phases, which have affected along the coastal belt both the Mesozoic limestone basement and the Tyrrhenian and more recent continental deposits (Di Maggio et al. 1999; Nigro et al. 2000; Tondi et al. 2006) (Figs. 8.10–11 and 8.12–13).

Age of the Relict Sea-Cliff Karst Morphologies

The caves developed prevalently along bedding planes show a *flank margin cave* genesis and some are characterized by horizontal extension greater than the vertical one (Grotta delle Capre, Grotta El Bhaira, etc.). Other caves formed from the coalescing of more chambers with interspaced remains of rock pillars and pendants (Grotta Racchio). Most of the surveyed sea caves are instead developed along sub-vertical fractures and in several cases show erosion notches on the walls.

Taking into account only the two above mentioned cave typologies (*flank margin caves* and sea caves), whose elevations can be correlated, with good approximation, to a past sea level, the diagram of Fig. 8.9 points out the presence of the following four ranges of cave elevations: 8–15 m asl; 22–27 m asl; 40–42 m asl; 56–60 m asl. At these ranges, on the base of the uplift rate related to the time interval following 125 ka, equal to an average of 0.05 mm/year (Di Maggio et al. 1999), could be attributed the following sea highstand respectively equal to: MIS 7, MIS 13, MIS 19 and MIS 33-35 (Fig. 8.14).

From this, taking into account some of the more important caves from the archeological and paleontological point of view, located in the Capo San Vito peninsula cliff—Piana di Makari area, the following probable age can be attributed:

- c. 140 ka for Grotta El Bhaira (classified as *flank margin cave*) at 7 m asl (MIS 5);
- c. 250 ka for Grotta di Piana Makari (classified as *flank margin cave*) at 12.5 m asl (average elevation of the cave) (MIS 7);
- c. 300 ka for Grotta di Cala Mancina (sea cave) at 15 m asl (MIS 9);
- c. 840 ka for Grotta dei Cavalli (sea cave) with notches at 42 m asl (MIS 19-21);
- c. 1,200 ka for Grotta Racchio (classified as *flank margin cave*) at 60 m asl (MIS 35).

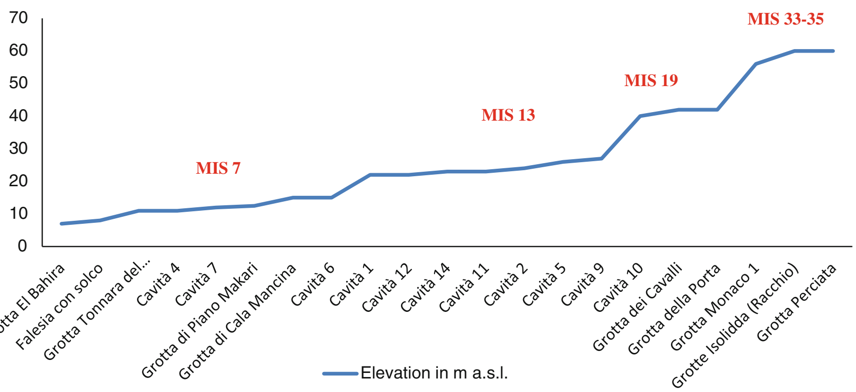

Fig. 8.14 Diagram of the cave elevations located in the Mt. Monaco–Capo San Vito peninsula relict sea-cliffs with indication of probable relative Marine Isotopic Stage (MIS)

8.2.2 *Inland Areas*

In the general context of the Mt. di Capo San Vito, the area which has underlined more the presence of significant karst morphologies, both for that which concerns the surface forms, micro and macro, and for the more specific speleological aspects, are certainly the western and central sectors characterized by the karst landforms "Purgatorio polje—Bufara doline—Muciara dry valley—Cipollazzo gorge". Moreover, in these sectors the deepest caves of the area of Mt. di Capo San Vito are present, constituted by the 194 m deep Abisso del Purgatorio, the 120 m deep Abisso delle Gole, and by the most extensive caves such as the Grotta del Fantasma (1,138 m long) and the Grotta Maria SS. di Custonaci (1,321 m long). So, on the base of morphological and structural elements surveyed in the course of this research, the karst and speleogenetical evolution of the above area has been described as being influenced by the Plio-Pleistocene tectonic events.

8.2.2.1 The Paleogeographic Context and Evolution of the Karst Processes

Late Miocene—Early Pliocene

The area probably begins to delineate in the Late Miocene and the Early Pliocene with an extensional tectonic phase characterized mainly by NW-SE trending structures that displace the Mesozoic limestones in a sequence of high and low structures (Nigro and Renda 2005). In this way, the opening of the Cornino and Castelluzzo plains and, towards N-E, of the Castelluzzo plain, is outlined. The absence of Messinian evaporitic sediments in this area leads to hypothesize the presence of sectors, probably already emerged, coinciding with the higher actual portions of the Mt. Palatimone and Mt. Sparagio ridges.

During Early Pliocene the paleogeographic context was characterized, in the central-eastern sector, by a narrow belt, bordered by the aforesaid emerging ridges, and by a more extended western sector, corresponding to the actual Cornino plain and Piano Zubbia area of open sea.

During this period, in the emerging sectors (the actual top of the ridges) the first speleogenetic processes began to take place, and the depth subsequently gradually increase due to the uplifting induced by the Middle-Pliocene tectonic phases.

The underground karst morphologies could be ascribed to the tectonic phases of the Lower and Middle Pliocene, morphologies observed in the medium-summit sectors of the Mt. Palatimone and Sparagio ridges constituted by vadose vertical caves developed on NW-SE structures (Zubbia 1-2-3, Zubbia su Filu Ferru) that were originally extensional and that resumed by the Middle Pliocene compressive tectonic phase.

The Lower Pleistocene

With the increase of the uplifting in the Lower Pleistocene, the morphology and paleogeography of the depression is redrawn, characterized by a western sector, coinciding with the present Cornino plain and Piano Zubbia—Scaletta areas still in continuity, and by an emerged central-eastern sector.

In this context there were peninsulas and small islands and landlocked submerged areas, where the Lower Pleistocene calcarenite sediments are controlled by NE-SW and NNE-SSW structures.

This emersion was caused by the tilting of the area towards the West, subject to planation with the erosion of the Lower Pliocene calcarenites and of the underlying biocalcarenites of the Lower Miocene (Mischio) and Tortonian clays.

The processes of karstification, which started during this period in the northern belt of the area bordered by the uplifting ridge of the Mt. Palatimone, also took place westwards in the present area of Piano Zubbia—Scaletta—Bufara, as an effect of the Late Lower Pleistocene uplifting that caused the erosion of the biocalcarenites. This caused the outcropping of the underlying Upper Cretaceous limestones.

Between the end of Early Pleistocene and Early Middle Pleistocene the paleogeographic context had been characterized by an emerged area, bounded on the west by sea cliffs, constituted by the present territories of Piano Zubbia—Cerriolo—Rumena—Bufara and eastwards by the adjacent plain of Purgatorio, this latter bordered by the uplifting ridges of Mt. Palatimone—Mt. Sparagio (Fig. 8.15).

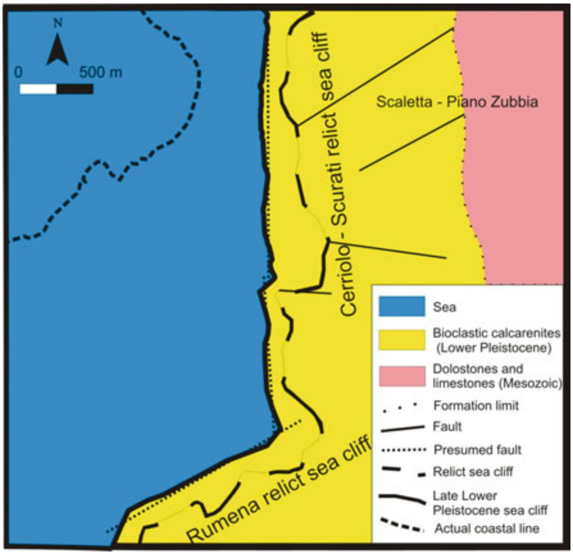

Fig. 8.15 Presumed paleogeography of the emerged area in the Lower Pleistocene (Late Emilian ?) due to faulting and contextual uplifting, which formed a sea-cliff between the actual Piano Zubbia-Cerriolo-Rumena-Purgatorio sector and the submerged Cornino plain

The karst processes in this Late Lower Pleistocene phase involve NE-SW structures, both in the Piano Zubbia—Scaletta area and in the depression of Purgatorio.

The Middle Pleistocene

At the beginning of the Middle Pleistocene the depression of Purgatorio starts to assume, to all effects, the aspect and the hydrological functions of a polje characterized, as a whole, by absorbent area with autigenic recharge bordered on the northern side by the ridge of the Mt. Palatimone, and its southern part by a clay belt bordered by the Mt. Sparagio ridge.

The phases of absorption-capture, through swallow holes, and flooding in the rainy periods, contribute to the planation of the karstified sector and to the contextual retreat of the southern slope pediment of the Mt. Palatimone—San Giovanni ridge. In this phase of activity, characterized by periods of concentrated absorption through swallow holes, and periods of overflow, two karst forms, in particular, could represent a certain importance for the evolution of the polje: the sink cave of "Abisso del Purgatorio" and the fluviokarst valley of Muciara. The first due to its function of the capturing the waters of the eastern part of the polje, to which it owes its actual principal development, the latter for its function of collecting and draining, outside the depression, the overflow of the central-western part of the area towards the Bufara doline area (Fig. 8.16).

As before reported, to this drainage would, therefore, be attributed the genesis of the actual Muciara dry paleo fluviokarst valley, developed on WSW-ENE structures, and most likely the formation of collapse doline of Bufara to which the waters were directed. In fact, the afore-mentioned doline, generated from successive collapses due to corrosion processes of a particularly fractured area, finds an explanation only with the presence of a hydrological flow from a basin of a certain size that, in this case, could only be generated by the seasonal flooding of the polje. This assumption is supported by the presence of relict forms of tributary valleys, which from the Muciara area are oriented towards the Bufara doline (Fig. 8.17).

To a Middle Pleistocene strike-slip tectonic phase (Abate et al. 1998), then could be ascribed the progressive closure of the drainage way of the fluviokarst valley of Muciara, due to the formation of high positive flower structures, surveyed with the present study.

The influences of the subsequent Pleistocene tectonic phases on the evolution of the polje can be resumed as follows:

1. The closure of the external drainage caused by the uplifted blocks of the transcurrent tectonics oriented E-W in the Muciara sector (Fig. 8.17);
2. Tectonic uplifting that progressively lowers the karst base level triggering, also, a retreat of the swallow holes of the polje and an underground drainage in the direction of the Cipollazzo fluviokarst gorge developed along a NW-SE structure, probably preexisting, that was reactivated following the Middle Pleistocene deformations (Fig. 8.18).

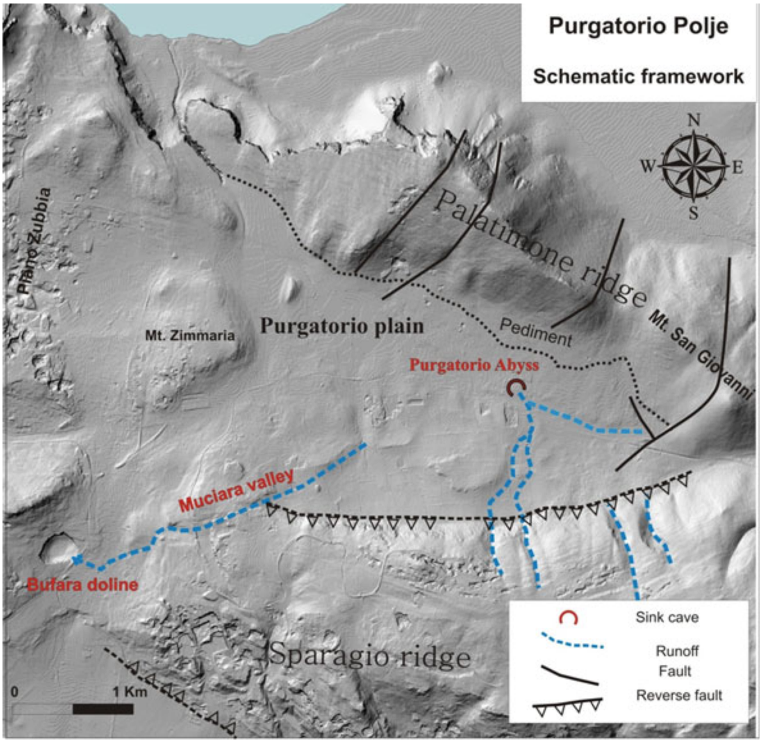

Fig. 8.16 Probable hydrographic scenery of the Purgatorio polje during the beginning of the Middle Pleistocene when the Muciara valley conveyed surface waters to the Bufara doline and the Purgatorio Abyss captured the main runoff of the eastern sector of the depression (*Hillshade map from* DEM Regione Siciliana 2007–2008)

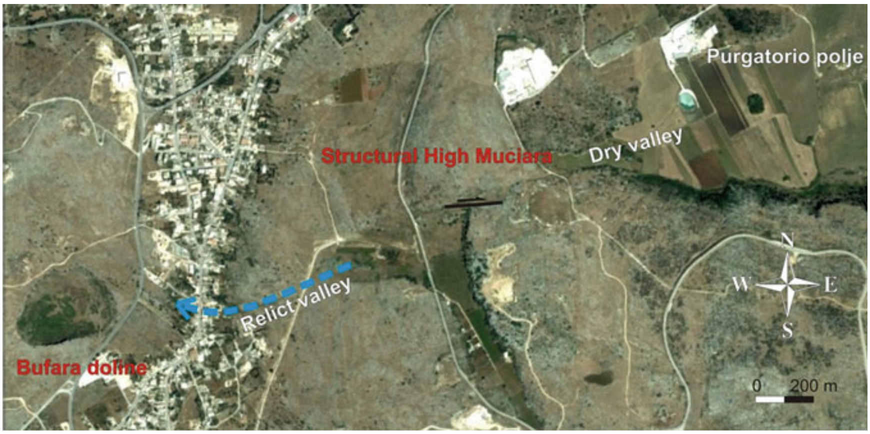

Fig. 8.17 Map of the “Structural high Muciara” with, on the *left*, the relict valley tributary of the Bufara doline and on the *right* the dry valley in the western sector of the Purgatorio polje (from Google Earth)

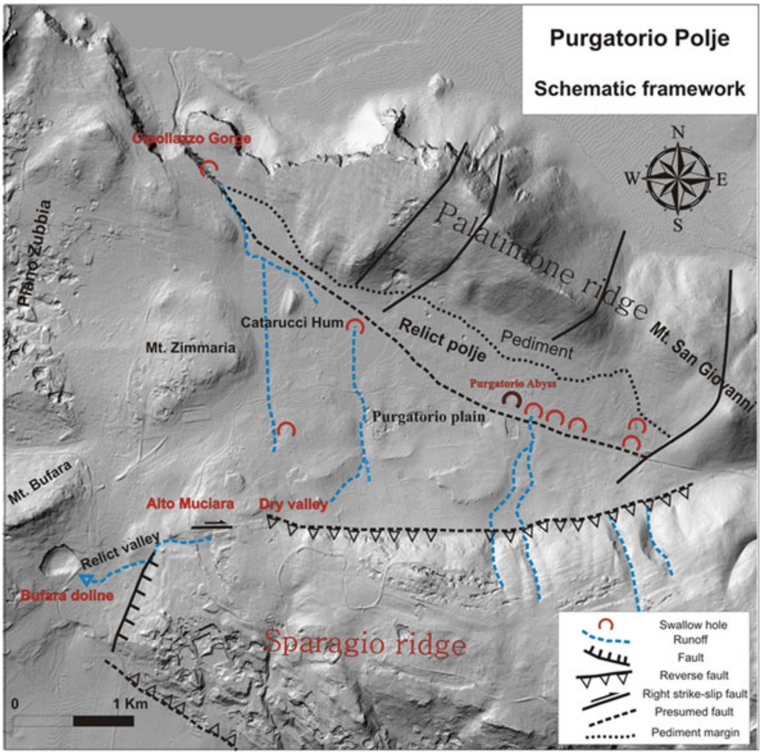

Fig. 8.18 Actual hydrographical network of the Purgatorio polje–Alto Muciara landform (*Hillshade map from* DEM Regione Siciliana 2007–2008)

The Upper Pleistocene–Holocene

As a consequence of the aforementioned tectonic phases, active from the Middle Pleistocene until today (Catalano et al. 2011; Tondi et al. 2006; Tondi 2007), the above described karst forms assumed the following characteristics in the Holocene:

- The Bufara doline appears at present time a relict form subject to erosive phenomena of weathering and secondary to corrosive processes. The evolution of the doline, considering the pile of the detritus, which occupies the bottom, shows a progressive dismantling and refilling caused by disintegration of the rocky walls.
- The Purgatorio Abyss doesn't function any more as the main sink-cave, to which it owes its past genesis and evolution. This because new swallow holes (Fig. 8.18) developed upstream in virtue of Pleistocene tectonics that caused uplifting in all the polje landform. At present, the presence of wet mud in its

explored deeper part shows that the active phreatic sector of the cave might be located at a depth greater than 200 m, at around 90 m asl.

- The Cipollazzo fluviokarst gorge, developed in the phase of reorganization of the superficial and subterranean drainage following the closure of the Muciara fluviokarst valley, is located on a pre-existing structure running NW-SE, probably reactivated by Late Pleistocene tectonics. Its condition of a suspended valley about 40 m higher respect to the below Castelluzzo plain would be justified therefore with its successive genesis and evolution respect to the area already in advanced phase of uplifting (western sector of Mt. Pignatello and Mt. Palatimone ridge).

Finally concerning the morphological and hydrological aspects, the polje system in its totality at the present state, is a relict landform in as much as the before mentioned deepening of the karst base level (to more than 200 m), linked to Pleistocene uplifting, and does not permit the alternation of flooding cycles and successive drainage responsible in time for the erosive planation processes. On the other hand the evolution of this landform on the basis of the surveyed morphologies (hums, extensive and deep crevasses area, depressions, swallow holes, deep caves, etc.), allows a forecast towards forms that are more and more coalescent, evolving in time as relict forms, such as karst corridors and small doline type depressions, with the increase of relief energy (Fig. 8.19).

Fig. 8.19 Relict polje of Purgatorio plain subject to karst processes

8.3 The Contributions of This Study

The contributions of this study to theoretical development of karstology can be resumed as follows:

8.3.1 The Contribution to the Evolution of Karst Forms in the Context of Tectonic Sheets Together with Indications of Recent Activity

The individualizations and the analysis of the structural and karst morphological elements surveyed in the main explored caves in the study area and the correlation with the structures surveyed at the surface allowed the individualization of the state of control of the processes of karstification carried out by the tectonic phases that were active during the Plio-Pleistocene upliftings. In this respect, the survey of kinematic indicators both inside of several caves and at the surface, has outlined the kinematic character of some karstified structures, which allow the hypothesis of at least two speleogenetic phases. The first is developed mainly on NE-SW structures with characteristics of left movements, linked to the Upper Pliocene (?)—Pleistocene deformation phases, the second on reactivated NW-SE structures, with characteristics of right movements, linked to successive Late Pleistocene—Holocene deformation phases.

Concerning the evolution of large forms such as the Purgatorio polje the survey and the analysis of the structural and morphological elements has permitted the formulation of a probable evolution history beginning with the uplifting occurred at the end of the Lower Pleistocene, which displaced the actual Cornino plain from the Rumena—Piano Zubbia Purgatorio plain and their successive processes of planation and karstification. This then evolved with the uplifting of the Late Pleistocene-Holocene into a relict structure with the closure of the Muciara valley drainage and the opening of the only outlet of the polje constituted by the hanging Cipollazzo gorge.

8.3.2 The Contribution that the Study of Karst Phenomena can give to the Variations of the Land-Sea Interface and of the Same Morphotectonic Evolution of the Coastal Belt, and of the Contiguous Inland Areas

The surveying of the karst forms on the relict sea-cliffs has permitted, particularly with the exceptional discoveries carried out during this research of marine and continental incrustations in the Rumena cave and their dating, to add an important element for the knowledge about the past climatic events and their influence on the evolution of the coastal belt and contiguous areas of the inland. In particular, with the dating of the speleothems of Grotta Rumena, it has been possible to put an upper limit to the series of paleo marine terraces surveyed by different authors in the course of preceding studies, equal to about 1,000–1,200 ka. From this a calculation of a rate of uplifting of about 0.1 mm/year was made for the Cornino area and with this element the attribution of the age of the formation of some caves classified as *flank margin caves* located both on the aforementioned Scurati–Rocca Rumena relict sea-cliffs and at relatively short distance from the latter. In this respect, the importance of the Grotta del Fantasma, 500 m from the Scurati relict sea-cliff, has been underlined. A particularly interesting cave for the hypercorroded morphologies as a whole, the oldest for salt-fresh mixing processes of solution due to an initial *flank margin cave* genesis, the most recents for the corrosion of strong acids probably due to old bat droppings, in a successive epigenetic phreatic/vadose phase linked to the Late Pleistocene uplifting of the area.

Therefore, in the general context of the results obtained during the research, the discoveries made in the Grotta Rumena, an exceptional and unique paleoclimatic and paleo sea level archive, must be recongnized as a significant contribution to the knowledge of the geological history of the Monti di Capo San Vito.

8.4 Open Questions

In conclusion, the results obtained, which have enlarged the geological and karstological knowledge of the study area, can be used as a starting point for the realization of further studies aimed at solving several open questions. One of these, as mentioned here before, concerns the karst hydrogeological context for the modeling of the underground hydrological flow direction towards the coastline and/or other sectors.

Another one relates to the morpho-tectonic evolution and rate of uplifting of the coastal belt in relation to climatic variations through the dating of speleothems found during this research. These latter further studies could most likely extend the results obtained in this research from the area of Monti di Capo San Vito to a wider geographical context as the central Mediterranean area.

References

Abate B, Incandela A, Nigro F, Renda P (1998) Plio-Pleistocene strike-slip tectonics in the Trapani Mts. (NW Sicily). Boll Soc Geol. It 117:555–567, 10 ff

Antonioli F, Cremona G, Immordino F, Puglisi C, Romagnoli C, Silenzi S, Valpreda E, Verrubbi V (1999a) Quaternary and holocene differential movements in a mediterranean coastal area (San Vito Lo Capo, Sicily-Italy). Phys Chem Earth 68

Antonioli F, Cremona G, Puglisi C, Silenzi S, Valpreda E, Verrubbi V (1999b) Quantitative assessment of post Tyrrenian differential crustal movements in a Mediterranean coastal area (S. Vito-Sicily-Italy). Phys Chem Earth (A) 24(4):343–347

Catalano F, Agate M, Basilone L, Di Maggio C, Mancuso M, Sulli A (2011) Note illustrative della Carta Geologica d'Italia alla scala 1:50.000, foglio 593 Castellammare del Golfo. ISPRA, Servizio Geologico d'Italia. Regione Siciliana Ass. Territorio Ambiente

DEM Regione Siciliana. Modello digitale del terreno passo 2 m derivato da dati LIDAR volo ATA 2007–2008 in UTM-WGS84 fuso 33 N

Di Maggio C, Incandela A, Masini F, Petruso D, Renda P, Simonelli C, Boschian G (1999) Oscillazioni eustatiche, biocronologia dei depositi continentali quaternari e neotettonica nella Sicilia nord-occidentale (Penisola di San Vito Lo Capo-Trapani). Il Quaternario 12(1):25–49

Giunta G, Nigro F, Renda P, Giorgianni A (2000) The Sicilian-Maghrebides Tyrrhenian Margin: a neotectonic evolutionary model. Bollettino della Società Geologica Italiana 119:553–565

Mylroie JE, Mylroie JR, Nelson CS (2008) Flank Margin cave development in telogenetic limestones of New Zealand. Acta Carsologica 37(1):15–40

Napoli G, Nigro F, Renda P (2012) The interation of compressional and extensional tectonics during the Sicily Chain building. Rend Online Soc Geol It 21:178–180

Nigro F, Renda G (2005) Transtensional/extensional fault activity from the Mesozoic rifting to Tertiary chain building in Northern Sicily (Central Mediterranean). Geol Carpath 56(3):255–271

Nigro F, Renda P, Arisco G (2000) Tettonica recente nella Sicilia nord-occidentale e nelle isole Egadi. Boll Soc Geol Ot 119:307–319, 7 ff

Renda P, Tavernelli E, Tramutoli M, Gueguen E (2000) Neogene deformations of Northern Sicily, and their implications for the geodynamics of the Southern Tyrrhenian Sea margin. Memorie della Società Geologica Italiana 55:53–59

Ruggieri R, Messina Panfalone D, Antonioli F, Rosso A, Sanfilippo R, Maniscalco R (2012) The Rumena flank margin cave and its implication in support of the evolution of the Monti di Capo San Vito (North-western Sicily). Rend Online Soc Geol It (21):632–633, 3 figs

Tondi E, Zampieri D, Alessandroni M, Giunta G, Renda P, Unti M, Giorgianni A, Cello G (2006) Active faults and inferred seismic sources in the San Vito Lo Capo peninsula, north-western Sicily, Italy, vol 262. Geological Society, London, Special Publications, pp 365–377

Tondi E (2007) Nucleation, development and petrophysical properties of faults in carbonate grainstone: Evidence from the San Vito Lo Capo peninsula (Sicily, Italy). J Struct Geol 29 (2007):614–628

www.google.com/intl/it/earth/index.html

Appendices

A.1 Geostructural Data Surveyed in the Study Area in Addition to Those Mentioned in the Text

1. Site *a*: Geostructural Stations in the Bufara–Tribli Areas

See Tables A.1, A.2 and A.3.

Table A.1 Bufara Doline—station 81 north wall

Bedding plane		Fracture		*Station: 81*
Strike	Dip dir.	Strike	Dip. dir.	
			200/70	
			125/65	
			320/75	
			177/70	
			220/80	
			105/80	
			208/80	
			65/85	
			227/80	
			180/65	
			187/70	
			155/60	
			191/80	
			247/80	
			345/50	

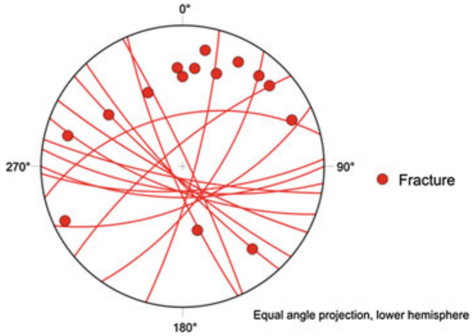

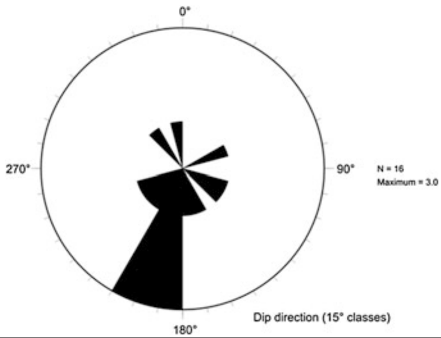

Note North wall

R. Ruggieri, *Speleological and Speleogenetic Aspects of the Monti di Capo San Vito (Sicily)*, Springer Theses, DOI 10.1007/978-3-319-21720-8

Table A.2 Bufara Doline—station 82 west wall

Bedding plane		Fracture		*Station: 82*
Strike	Dip dir.	Strike	Dip. dir.	
			287/75	
			270/80	
			238/75	
			230/75	
			246/75	
			225/80	
			235/75	
			287/70	
			275/45	
			240/80	
			287/45	
			262/45	

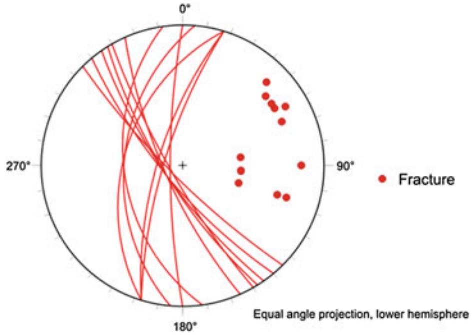

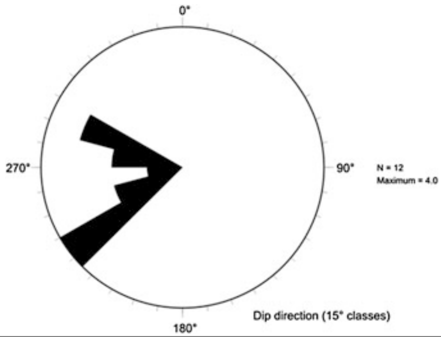

Note West wall

Table A.3 Bufara Doline—station 83 south wall

Bedding plane		Fracture	
Strike	Dip dir.	Strike	Dip. dir.
			106/40
			75/45
			57/50
			40/80
			60/55
			70/55
			40/50

Station: 83

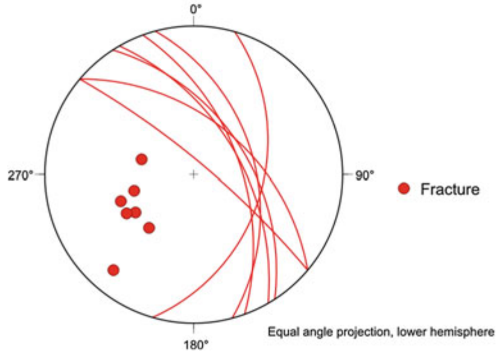

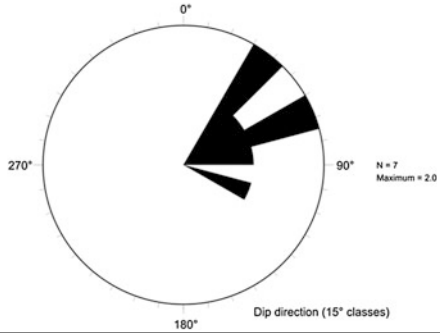

Note South wall

2. Site *a*: Geostructural Stations in the Piano Zubbia–Scaletta Area close to Grotta del Fantasma

See Tables A.4, A.5, A.6 and A.7.

Table A.4 Stations 88–89

Bedding plane		Fracture	
Strike	Dip dir.	Strike	Dip. dir.
	N 180/12*		N 30/70
	N 230/24		N 50/70
	N 230/16		
	N 215/21		

Stations: 88–89

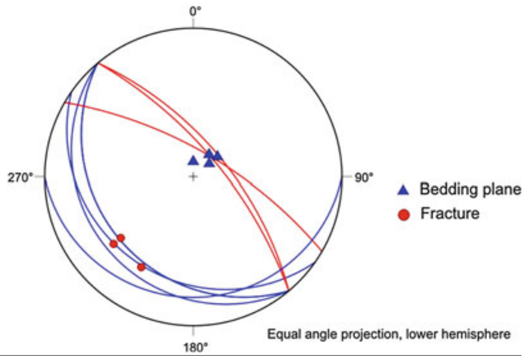

Note *S. 88

Table A.5 Stations A–B

Bedding plane		Fracture	
Strike	Dip dir.	Strike	Dip. dir.
	N 260/12*		N 100/82
	N 270/18		N 295/75
	N 260/10		

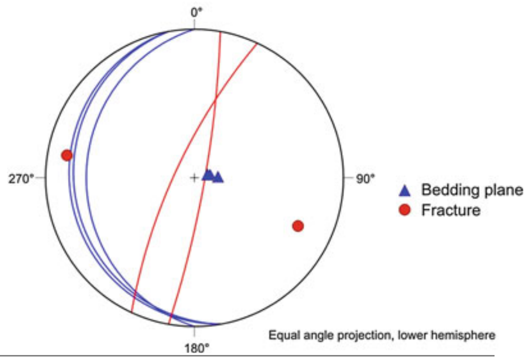

Note *S. A

Table A.6 Stations C–D

Stazione	Bedding plane	Fracture	Note
C	N 210/35		
D	N 190/17–N 210/28		

Table A.7 Station 124 (to north of Grotta del Fantasma)

Bedding plane		Fracture	
Strike	Dip dir.	Strike	Dip. dir.
	N 260/30		N 75/80
			N 100/80
			N 130/85
			N 40/85
			N 20/85
			N 60/75
			N 100/60
			N 50/70
			N 60/85
			N 30/85
			N 70/80

Station: 124

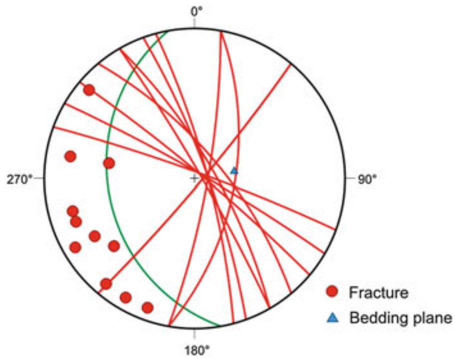

Note Quarry

3. Site *a*: Geostructural Stations in the Piano Zubbia–Scaletta Area close to Grotta della Clava

See Tables A.8, A.9 and A.10.

Table A.8 Stations 86–87

Bedding plane		Fracture	
Strike	Dip dir.	Strike	Dip. dir.
	N 90/10*		N 45/80
	N 90/21*		
	N 130/16*		
			N 10/80
			N 10/85
			N 50/85
			N 40/45
			N 20/60

Stations: 86–87

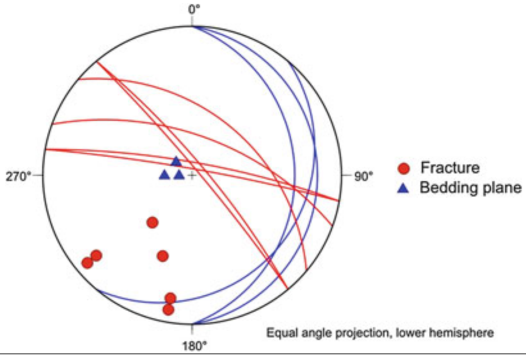

Note S 86 (Fault with encrustings calcite inside small quarry)
*S. 87

Table A.9 Station 120 (–121)

Bedding plane		Fracture	
Strike	Dip dir.	Strike	Dip. dir.
	N 270/15		N 325/75
	N 0/15		N 40/80
	N 240/30*		

Station: 120

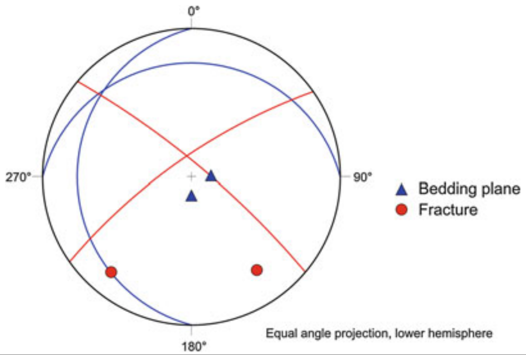

Note Quarry westwards of Grotta della Clava
*Point 121

Table A.10 Stations 122–123

Bedding plane		Fracture		Stations: 122–123
Strike	Dip dir.	Strike	Dip. dir.	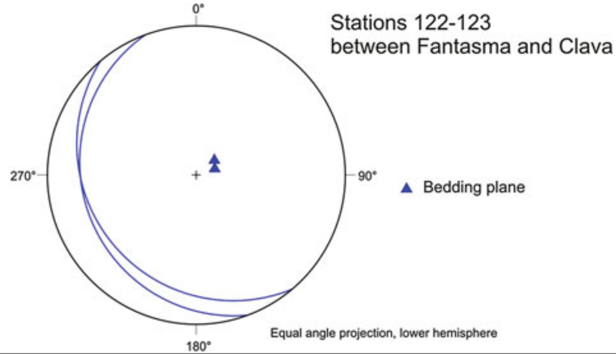
	N 250/15			
	N 230/18			

Note Stations between Clava and Fantasma caves

4. Site *a*: Geostructural Station in the Piano Zubbia–Scaletta Sector close to Grotta Maria SS. di Custonaci

See Table A.11.

Table A.11 Stations 147–150

Station	Bedding plane	Fracture
147	N 260/20	N 35/75
148		N 65/70
149		N 270/70–N 75/75
150	N 195/22	

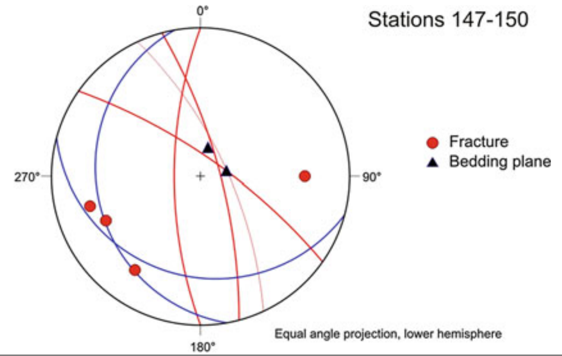

5. Site *a*: Piano Zubbia–Scaletta Sector close to Grotta del Cerriolo

See Table A.12.

Table A.12 Station 125

Station	Bedding plane	Fracture
125	290/10–250/35	
A		N 50/80–N 60/80
B		N 80/85–N 70/80
C		N 20/65–N 40/70

Station: 125

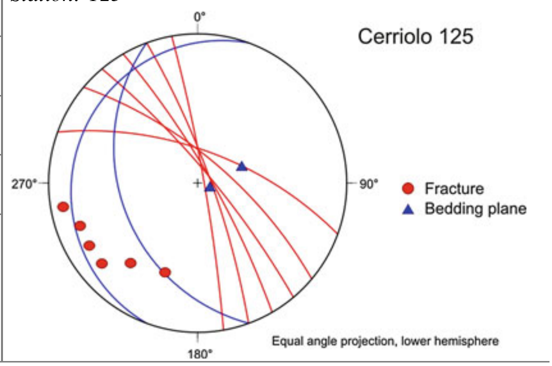

Note Small cave close to Grotta Cerriolo

6. Site *b*: Geostructural Stations in the Mt. Palatimone Area

See Tables A.13, A.14, A.15, A.16, A.17, A.18, A.19, A.20, A.21, A.22, A.23, A.24, A.25 and A.26.

Table A.13 Station 99—Mt. Palatimone pediment sector

Bedding plane		Fracture	
Strike	Dip dir.	Strike	Dip. dir.
70	160/30	90	180/50
		40	130/80
		80	170/45
		140	
		170	80/55
		140	50/55

Station: 99

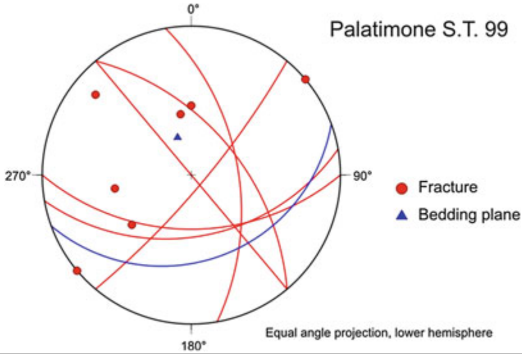

Note Big quarry

Table A.14 Station 100—Mt. Palatimone pediment sector

Bedding plane		Fracture	
Strike	Dip dir.	Strike	Dip. dir.
120	210/40	80	350/80
90	180/30	90	180/80
		100	190/70
		140	50/50
		140	50/45
		130	220/80
		130	220/85

Station: 100

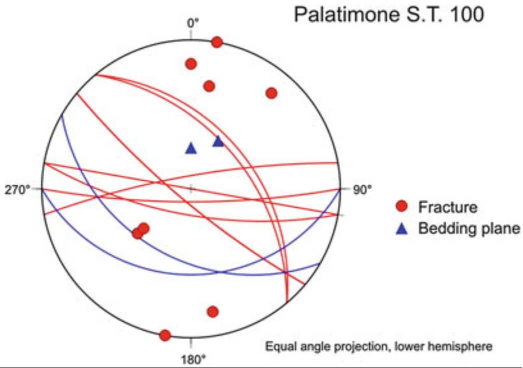

Note Small quarry

Table A.15 Station 103—Mt. Palatimone pediment sector

Bedding plane		Fracture	
Strike	Dip dir.	Strike	Dip. dir.
		7	
		170	
		140	
		170	
		132	
		144	
		138	

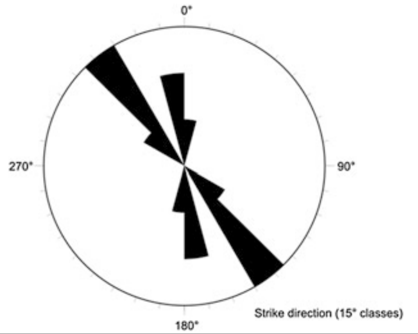

Note Crevasses area

Table A.16 Station 104—Mt. Palatimone pediment sector

Bedding plane		Fracture	
Strike	Dip dir.	Strike	Dip. dir.
		160	
		170	
		170	
		145	
		0	
		5	
		0	
		50	

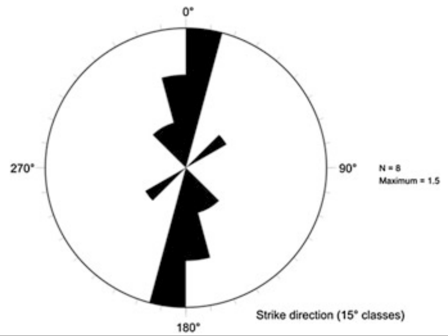

Note Crevasses area 2

Table A.17 Station 109—Mt. Palatimone—NNE-SSW oriented fault left sector

Bedding plane		Fracture	
Strike	Dip dir.	Strike	Dip. dir.
	210/20	30	300/80
		30	300/85
		30	300/75

Station: 109

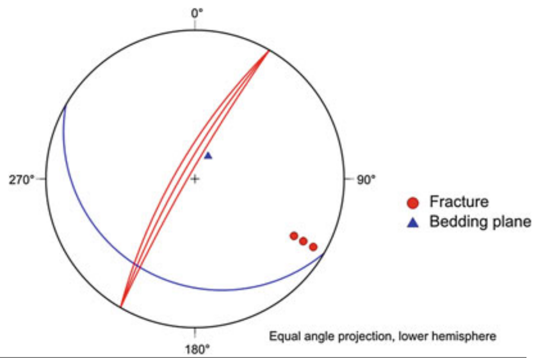

Table A.18 Station 117—Mt. Palatimone—quarry close to Zubbia delle Meraviglie

Bedding plane		Fracture		*Station: 117*
Strike	Dip dir.	Strike	Dip. dir.	
	200/35		300/85	
			30/85	
			300/80	
			300/85	
			300/85	
			330/80	

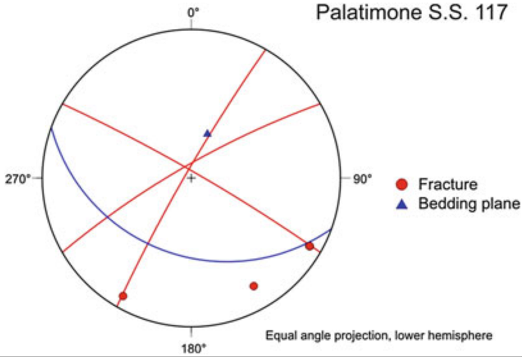

Table A.19 Station 118—Mt. Palatimone—quarry close to Zubbia delle Meraviglie

Bedding plane		Fracture		*Station: 118*
Strike	Dip dir.	Strike	Dip. dir.	
	230/20			
			300/62	
			250/75	
			60/60 karstified	

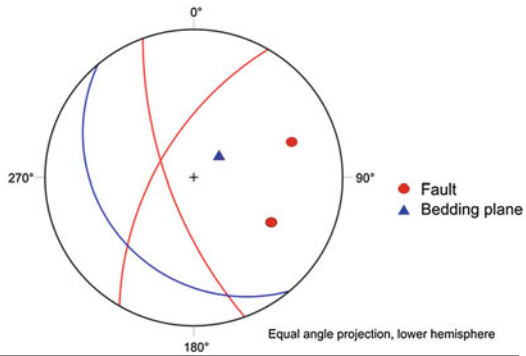

Table A.20 Station 118 bis—Mt. Palatimone—quarry close to Zubbia delle Meraviglie

Bedding plane		Fracture		*Station: 118 bis*
Strike	Dip dir.	Strike	Dip. dir.	
	190/25		310/85	
			300/85	
			250/80	
			310/85	
			65/75	

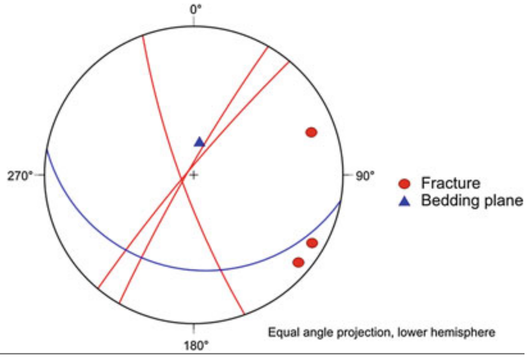

Note Scan line N 120

Table A.21 Station 118 tris—Mt. Palatimone—quarry North of the Zubbia delle Meraviglie

Bedding plane		Fracture		*Station: 118 tris*
Strike	Dip dir.	Strike	Dip. dir.	
	230/25		150/90	
			60/60	
			80/60	
			120/80	
			240/80	
			200/70	
			250/75	

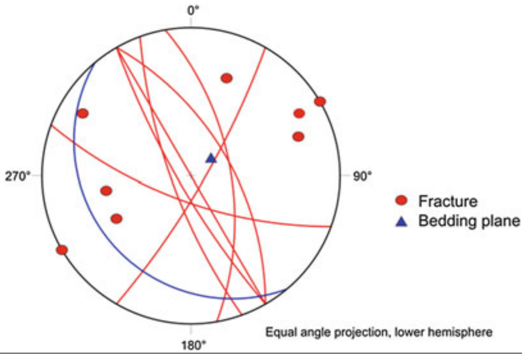

Note Scan line 60/75

Table A.22 Stations 108–119—Mt. Palatimone—quarry north of Z.M./east zubbia F.F

Bedding plane		Fracture		*Stations: 108–119*
Strike	Dip dir.	Strike	Dip. dir.	
	190/16			
	200/23			

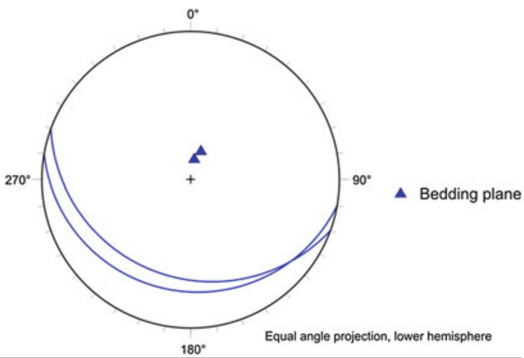

Table A.23 Scan line from station 115—Mt. Palatimone—crevasses area East of NNE-SSW oriented fault

Bedding plane		Fracture	
Strike	Dip dir.	Strike	Dip. dir.
		160	
		40	
		22	
		30	
		50	
		90	
		80	
		70	

Station: 115

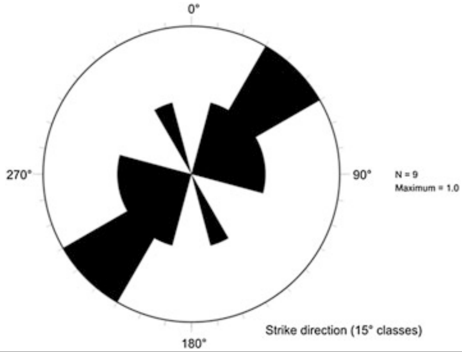

Note Scan line 90 m/N 100

Table A.24 Stations 110–117—Mt. Palatimone—crevasses sector

Bedding plane		Fracture	
Strike	Dip dir.	Strike	Dip. dir.
110	200/32	130	220/80
		100	190/80
		140	230/85
		40	310/85
		90	180/80
		40	310/80
		25	295/85
		100	190/70
		150	240/85
		110	190/85
		155	245/85
		80	170/85
		110	200/85
		150	240/85

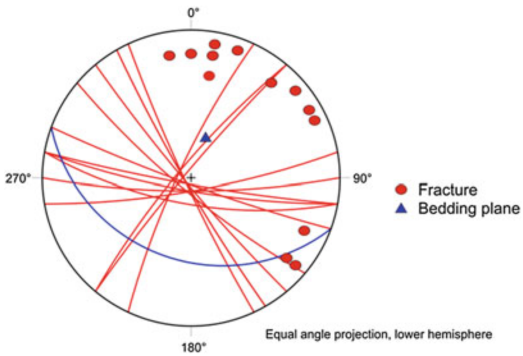

Note

- Surveys in situ and from orthophoto
- 220/80 grike/joint
- 190/80 length 100 m, width 10 m
- 230/85 crevasse/trench
- 240/85 from orthophoto

Table A.25 Mt. Palatimone—crevasse central sector (survey from orthophoto)

Bedding plane		Fracture	
Strike	Dip dir.	Strike	Dip. dir.
		45	
		150	
		150	
		45	
		40	
		155	
		80	
		160	
		45	
		160	
		150	
		155	
		150	

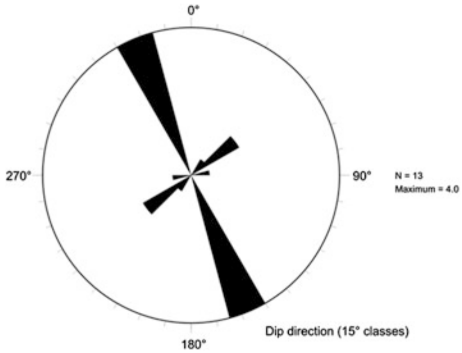

Table A.26 Mt. Palatimone–Portella della Ronza—eastern sector (survey from orthophoto)

Bedding plane		Fracture	
Strike	Dip dir.	Strike	Dip. dir.
200/28		15	
		18	
		10	
		16	
		15	
		8	
		10	
		10	
		10	
		10	
		30	
		45	
		48	
		120	
		120	

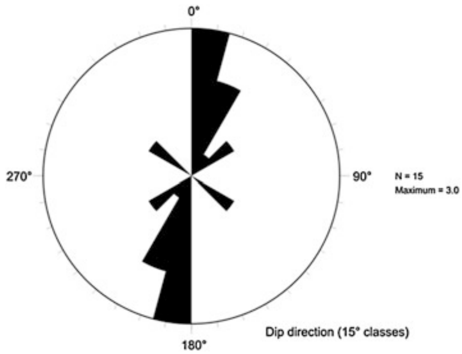

7. Site *c*: Geostructural Stations in the Purgatorio Polje

See Tables A.27, A.28 and A.29.

Table A.27 Station 128 polje

Bedding plane		Fracture	
Strike	Dip dir.	Strike	Dip. dir.
	220/15[a]		
	225/20		
	195/24		
	235/25		

Station: 128

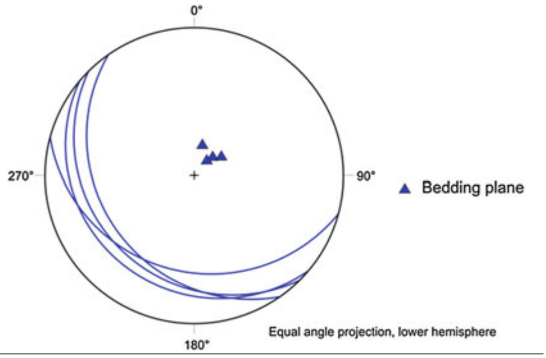

Note [a]Close to 128

Table A.28 Cucca area—road trench station

Fracture			Bedd. plane
Dip direction			
85/60	330/70	140/65	190/25
320/80	345/85	310/60	
115/65	50/80	55/70	
335/75	60/75	120/70	
355/70	105/85	100/70[a]	
350/70	110/65	130/85	
350/70	60/70	150/50	
340/75	55/70	310/70	
75/85	60/70	165/60	
140/70	60/65	280/70	
340/75	100/85	280/65	
130/80	300/60	60/80	
35/85	280/60	350/70	
50/70	145/65	330/70	
35/65	100/70	70/75	
70/70	130/70	310/85	
50/70	250/60	190/45	
290/85	110/70	80/60	
50/60	130/70	300/70	
130/70	250/60		
290/70	110/75		
310/70	350/65		
90/80	100/65		
120/65	350/70		

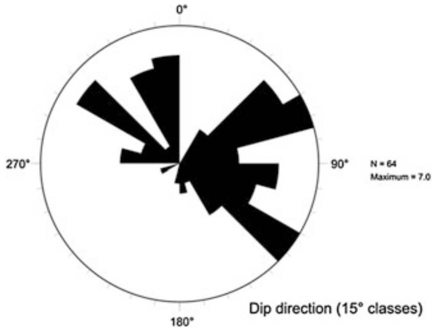

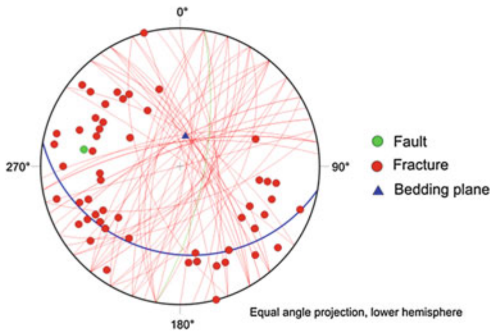

Note [a]Fault

Table A.29 Polje—area close to Purgatorio Abyss

Bedding plane		Fracture	
Strike	Dip dir.	Strike	Dip. dir.
		N 60	
		N 50	
		N 55	
		N 55	
		N 5	

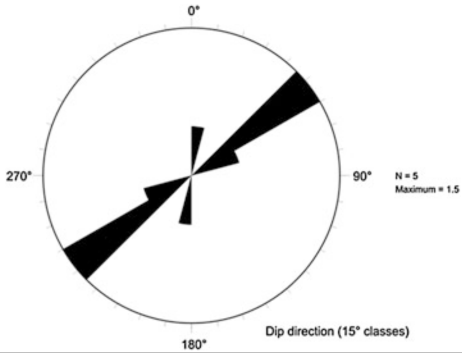

Note Surveys from orthophoto

8. Site *d*: Geostructural Stations in the Mt. Sparagio Area

See Tables A.30, A.31, A.32, A.33 and A.34.

Table A.30 Stations 78–79 bis-105—quarry close to Zubbia Cocuccio 2

Bedding plane		Fracture	
Strike	Dip dir.	Strike	Dip. dir.
	N 170/60		N 0/48
	N 170/60		N 0/48
			N 80/60
		N 20	
			N 40/50

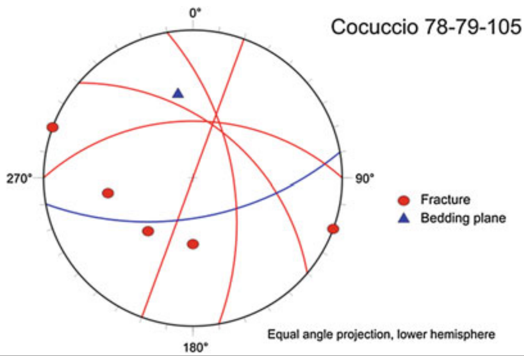

Table A.31 Station close to quarry Cocuccio 1

Bedding plane		Fracture	
Strike	Dip dir.	Strike	Dip. dir.
N 110		N 20	

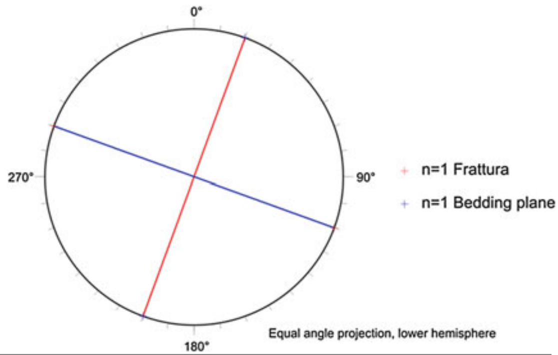

Note Survey from orthophoto

Table A.32 Stations 71–75—Pozzo Noce sector (crevasses landform)

Bedding plane		Fracture	
Strike	Dip dir.	Strike	Dip. dir.
		120	
	180/31	90	
		155	
		196	
	180/24	90	0/42

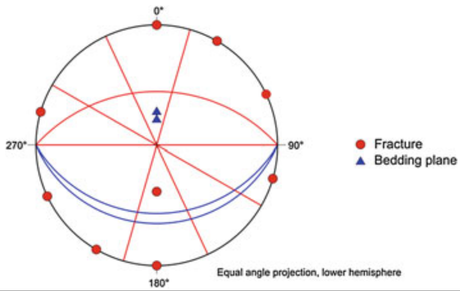

Table A.33 Pozzo Noce Crevasses area

Bedding plane		Fracture	
Strike	Dip dir.	Strike	Dip. dir.
		30	
		35	
		40	
		25	
		25	
		60	
		60	

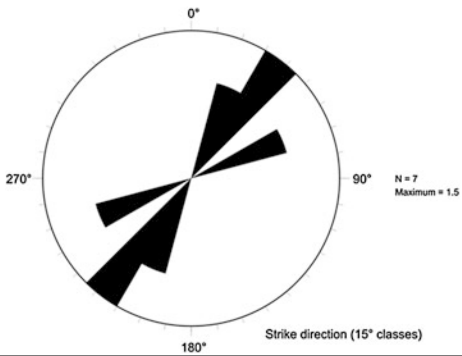

Note Survey from orthophoto

Table A.34 Station 89—Zubbia Tre Corna area

Bedding plane		Fracture		*Station: 89*
Strike	Dip dir.	Strike	Dip. dir.	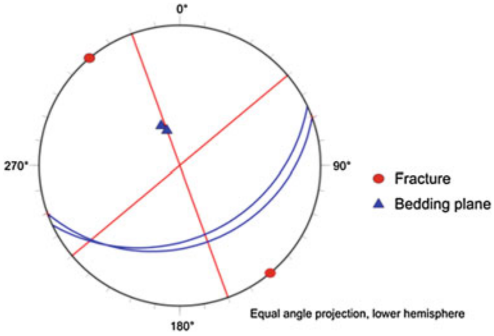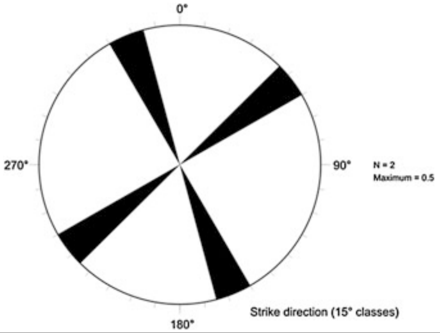
	155/35		N 50	
	160/30		N 160	

Note Survey from orthophoto